

University of Reading



**Optimal Energy Controllers of Energy
Storage Systems Based on Load
Forecasting for RTG Cranes Network.**

By:

Feras Alasali

This Thesis is submitted for the degree of
Doctor of Philosophy

School of Biological Sciences
Department of Biomedical Engineering
University of Reading
UK

December 2018

Declaration

I confirm that this is my own work and the use of all material from other sources has been properly and fully acknowledged.

Feras Alasali

Abstract

Given the increased international trading in ports around the world, there are significant challenges facing ports such as rising energy consumption and greenhouse emissions. The electrification of Rubber Tyred Gantry (RTG) cranes is one approach used to reduce gas emissions and fuel costs at port, but has also increased the electrical demand across the electrical distribution network. This will force port operators to reinforce the low voltage network to meet this increased demand and remain within the operating constraints. An energy storage system is one potential solution to increase the energy efficiency of the low voltage distribution networks whilst avoiding expensive reinforcement of the power system. This thesis aims to highlight and address the peak demand problem in the network of electrified RTG cranes and attempts to reduce peak demand and electricity costs by optimality controlling the energy storage system by utilising load forecasts. Since there is currently lack of understanding of the volatile demand behaviour, the research begins by investigating the unique characteristics of the electrical demand of the RTG crane. This understanding is a vital tool to develop an accurate forecast model and maximise the benefits of using an energy storage system through a control system. Several short-term load forecast models have been developed based on the ARIMAX and ANN models to predict accurate day-ahead electrical RTG crane demand. The forecast results show that the highly volatile demand behaviour creates a substantial prediction challenge compared to normal residential low voltage network demand. This thesis then presents the significance of forecasting the crane demand to improve the energy performance of an electrical distribution network with an ESS by employing several optimal controllers. The novel optimal control algorithms considered for the network of RTG cranes are split into: a Model Predictive Controller (MPC) with rolling forecast system and a Stochastic Model Predictive Controller (SMPC) based on a stochastic prediction demand model. The proposed MPC and SMPC control models are compared to an optimal controller based on a fixed load forecast profile and a common and standard set-point controller. Results show that the optimal controllers based on a load forecast have improved the storage device performance for the peak reduction and cost savings compared to the traditional control algorithm. Further improvements are then presented for the receding horizon controllers, MPC and SMPC, which better treat the volatility of the crane demand and the uncertainty in the forecasts. Furthermore, an economic analysis of the results for different ESS location scenarios is presented to assess their viability.

Acknowledgements

First all praise and thanks are to Allah, the Almighty, for give me the strengths, knowledge, ability and his blessing to complete this thesis. The author would like also to thank some people who have helped and guided me during my Ph.D. study.

I would like to begin by expressing my gratitude and appreciation for the support of my supervisors Prof. William Holderbaum, University of Reading, and Dr. Stephen Haben from the University of Oxford for their time, assistance, guidance, encouragement and effort in this work from inception until the completion of the research. Their guidance has been invaluable and changed my outlook on the world and my future achievements. I would also like to offer my sincere appreciation to Prof. Victro Becerra from the University of Portsmouth, Prof. William Harwin, Dr. Ben Potter and to the members of the Port of Felixstowe project including Dr. Ian Harrison, Dr. Rayner Meyer, Dr. Stefano Pietrosanti, Dr. Antonio Luque for their help and sharing their experience of research life. My thanks extend to Mr. Wayne Travis from the Port of Felixstowe team who kindly donated his time to explain daily port operations and providing me the cranes and substation data.

I gratefully acknowledge the help provided by the Hashemite University, Jordan in funding this research and the scholarship which allowed me to achieve the Ph.D. I would like also to sincerely thank my friends, who supported me during my study and they have made this journey more enjoyable. Also my thanks goes to my mother, Dalal, father, Muhieddin, brothers, sisters and my uncle, Emad, those who surrounded me with their love, care and support throughout my whole life.

Special thanks to my children Aws and Lareen for their patience and unconditional love. Thanks for them to be in my life. I am forever grateful to my beloved wife, Saja, for her support, encouragement and tolerance during the challenging times to ensure that I continued on my path. She has always been to my side, providing me the power to achieve my goals. My most sincere to Eng. Abdelrasoul Foudeh and his wife, Khadeejeh, for their inspiration and care during this long journey. Without Eng. Abdelrasoul support, I would not have been able to start and complete my PhD.

Table of Contents

| | |
|--------------------------------------------------------------|-----|
| Declaration | i |
| Abstract | ii |
| Acknowledgements | iii |
| Table of Contents | iv |
| List of Figures | ix |
| List of Table | xii |
| Abbreviations | xv |
| Chapter 1: Introduction | 1 |
| 1.1 Global Shipping Trade and Carbon Emissions | 1 |
| 1.1.1 Energy Saving Options for RTG Cranes | 4 |
| 1.2 Energy Storage Technologies | 6 |
| 1.2.1 Classification of Energy Storage Technologies | 7 |
| 1.2.2 Comparison of ESS Technologies | 8 |
| 1.2.3 Role of Energy Storage in Cranes Networks. | 10 |
| 1.3 Port of Felixstowe and RTG Crane System | 12 |
| 1.3.1 Port of Felixstowe | 12 |
| 1.3.2 RTG Cranes | 13 |
| 1.3.3 Electrified RTG Crane Network | 16 |
| 1.4 Problem Statement | 18 |
| 1.5 Research Objectives..... | 18 |
| 1.6 Contribution to the Literature | 19 |
| 1.7 Publications..... | 20 |
| 1.8 Thesis Outline | 21 |

| | |
|-----------------------------------------------------------------------------------------------------------|----|
| Chapter 2: Literature Review | 23 |
| 2.1 Introduction..... | 23 |
| 2.2 Control Algorithms of Energy Storage Systems for RTG Crane and Low Voltage Network Applications. | 23 |
| 2.2.1 Control of Energy Storage Devices for RTG Crane Systems..... | 27 |
| 2.2.2 Control Modelling Solutions to Improve ESS Benefits on LV Network. | 31 |
| 2.2.3 Optimal Energy Controller Using Receding Horizon..... | 35 |
| 2.2.3.1 Model predictive control of an ESS. | 37 |
| 2.2.3.2 Stochastic model predictive control of ESS. | 39 |
| 2.3 Load Forecasting in Power Systems. | 41 |
| 2.3.1 Overview of Load Forecasting Techniques | 42 |
| 2.3.1.1 Time or statistical series forecast techniques | 43 |
| 2.3.1.2 Artificial intelligence methods | 44 |
| 2.3.1.3 The hybrid forecast models | 44 |
| 2.3.2 Role of Load Forecasting in Low Voltage Network..... | 47 |
| 2.3.2.1 Renewable Energy..... | 47 |
| 2.3.2.2 Buildings..... | 50 |
| 2.3.2.3 Electric Vehicles..... | 53 |
| 2.4 Summary | 56 |
| Chapter 3: The Characteristics of RTG Crane Demand | 58 |
| 3.1 The RTG Crane Demand Characteristics | 59 |
| 3.1.1 Overview of the Electrified RTG Crane Demand..... | 60 |
| 3.2 Time Series Analysis | 65 |
| 3.2.1 Weekly and Daily Analysis | 66 |
| 3.2.2 Autocorrelation Analysis | 70 |
| 3.3 Cross-correlation Analysis..... | 73 |
| 3.4 Summary | 76 |

| | |
|-----------------------------------------------------------------------------------|-----|
| Chapter 4: Load Forecasting for electrical RTG crane demand | 77 |
| 4.1 Methodology..... | 79 |
| 4.1.1 ARIMAX Forecast Model..... | 80 |
| 4.1.2 ANN Forecast Model..... | 85 |
| 4.1.3 Exogenous Variables Estimation..... | 91 |
| 4.2 The RTG crane demand forecast models..... | 94 |
| 4.2.1 ANN Forecast Modelling..... | 94 |
| 4.2.2 ARIMAX Forecast Modelling..... | 100 |
| 4.3 Results and Discussion for the Forecast Models..... | 105 |
| 4.3.1 Data Collection and Analysis..... | 105 |
| 4.3.2 Load Forecasting Model Evaluation..... | 105 |
| 4.3.3 Overall Comparisons..... | 106 |
| 4.3.4 Effect of Estimating Exogenous Variables..... | 109 |
| 4.3.5 Forecast Error Analysis..... | 110 |
| 4.4 A Comparison of the Forecast Model Techniques..... | 111 |
| 4.4.1 ARIMAX Forecast Model..... | 112 |
| 4.4.2 ANN Forecast Model..... | 112 |
| 4.4.3 A Comparison Summary..... | 113 |
| 4.5 Summary..... | 113 |
| Chapter 5: MPC controller for RTG Cranes with Energy Storage Systems | 115 |
| 5.1 The ESS and RTG Crane Demand Model Topology..... | 116 |
| 5.1.1 The Energy Storage System (ESS) Model..... | 118 |
| 5.1.2 The Electrified RTG Crane Demand Data..... | 120 |
| 5.1.3 ESS Performance Evaluation..... | 121 |
| 5.2 Benchmark Control Methodology..... | 121 |
| 5.2.1 Set-point Controller..... | 122 |

| | | |
|---------------------------------------------------------------------------------------|---------------------------------------------------------------------------------------------|------------|
| 5.3 | MPC Controller..... | 123 |
| 5.4 | Optimal Energy Management Controller..... | 127 |
| 5.5 | Results and Discussion | 128 |
| 5.5.1 | RTG Crane Prediction Demand Results. | 129 |
| 5.5.2 | Case Study: a specific network of crane operation example. | 131 |
| 5.5.3 | Prediction Horizon Evolution | 133 |
| 5.5.4 | Economic Results..... | 135 |
| 5.6 | Summary..... | 136 |
| Chapter 6: Stochastic Model Predictive Control for electrified RTG cranes..... | | 138 |
| 6.1 | Stochastic Model Predictive Control. | 139 |
| 6.1.1 | Energy Prediction Model Based on an ARIMAX and Monte Carlo Method.. | 140 |
| 6.2 | Stochastic Model Predictive Control. | 142 |
| 6.3 | Results and Discussion | 145 |
| 6.3.1 | Network of RTG Cranes Prediction Demand Results. | 145 |
| 6.3.2 | Case Study: a specific network of crane operation example. | 147 |
| 6.3.3 | State of Charge (SoC) Evolution. | 150 |
| 6.3.4 | Numerical Issues of the DP for State of Charge (SoC) | 151 |
| 6.3.5 | Economic Results..... | 152 |
| 6.4 | Summary..... | 155 |
| Chapter 7: Analysis and Comparison of ESS Control Strategies..... | | 156 |
| 7.1 | Analysis of Energy Storage Control Strategies | 157 |
| 7.1.1 | A Comparison Analysis for Optimal Controllers Based on Load Forecast Profile Accuracy. | 157 |
| 7.1.2 | Results and Discussion for ESS Controllers..... | 162 |
| 7.2 | A Comparison Analysis for Different ESS Location Scenarios. | 163 |
| 7.2.1 | Peak Demand Reduction: a specific example..... | 165 |
| 7.2.2 | State of Charge (SoC) Evolution. | 167 |

| | | |
|-----------------------------------------------|----------------------------------------------------|-----|
| 7.2.3 | Economic Analysis. | 168 |
| 7.3 | A Comparison of the ESS Control Strategies | 170 |
| 7.3.1 | Set-point Controllers..... | 171 |
| 7.3.2 | Optimal Controllers Based on Load Forecasting..... | 172 |
| 7.3.3 | A Comparison Summary..... | 173 |
| 7.4 | Summary | 174 |
| Chapter 8: | Conclusions | 176 |
| 8.1 | Summary of the Thesis and Main Findings. | 176 |
| 8.2 | Contributions to Knowledge | 179 |
| 8.3 | Limitations of the Research | 180 |
| 8.4 | Future Work..... | 181 |
| References | | 184 |
| Appendix A | | 200 |
| Network of RTG cranes measurement system..... | | 200 |
| Appendix B | | 203 |
| Model Predictive Control (MPC)..... | | 203 |
| MPC controller: problem statement..... | | 205 |
| Appendix C | | 208 |
| Dynamic programming | | 208 |
| Appendix D | | 211 |
| SMPC and the computational effort | | 211 |

List of Figures

| | |
|------------------------------------------------------------------------------------------------------------------------------------------------------------------|----|
| Figure 1-1: Port of Felixstowe (PoF), United Kingdom. | 2 |
| Figure 1-2: General handling operation process of port container terminals [6]..... | 2 |
| Figure 1-3: Total fuel consumption distribution, Noatum Container Terminal Valencia [6].... | 4 |
| Figure 1-4: Comparison of fuel saving options for RTG cranes [5] [7] [8]. | 5 |
| Figure 1-5: An example of a peak shaving strategy. | 7 |
| Figure 1-6 : The classification of ESS based on categories of applications [11]. | 8 |
| Figure 1-7: The major container ports in UK from 2000 to 2014 [21]..... | 13 |
| Figure 1-8: Crane system: (a) electrified RTG crane at the Port of Felixstowe; (b) an example of the actual electrified RTG crane demand for a specific day..... | 14 |
| Figure 1-9: RTG crane system: (a) single line diagram of an RTG crane system for the main electric..... | 15 |
| Figure 1-10: Average energy consumption for an RTG crane system on a typical operation day [19]. | 16 |
| Figure 1-11: RTG crane energy in kWh for eight working days [19]. | 16 |
| Figure 1-12: Single line diagram of the network of electrified RTG cranes at the Port of Felixstowe, UK. | 17 |
| Figure 1-13: Conductor rail bar with crane connection. | 17 |
| Figure 2-1: A simple classification of ESS control techniques. | 27 |
| Figure 2-2: General schematic diagram for the receding horizon controller (MPC and SMPC). | 36 |
| Figure 2-3: The spectrum of short-term forecasting methods according to the three main technologies. | 43 |
| Figure 3-1: The half hourly RTG crane demand (blue line) with linear model fit to the data (dotted)..... | 62 |
| Figure 3-2: Illustration of RTG crane demand data in a histogram along with a normal distribution fit and lognormal. | 64 |
| Figure 3-3: Distribution of half hourly RTG crane demand. | 65 |
| Figure 3-4: Box plot of half hourly RTG crane demand by week. | 67 |
| Figure 3-5: Breakdown of half hourly RTG crane demand distribution by day type..... | 67 |

| | |
|-----------------------------------------------------------------------------------------------------------------------------------------------------------------------------------------------------------------------------------------------------------------------------------------------------|-----|
| Figure 3-6: An overlay of the weekly profile of the RTG crane demand of three consecutive weeks..... | 68 |
| Figure 3-7: An example for the daily crane demand for the same day over 4 weeks..... | 68 |
| Figure 3-8: An example for the daily crane demand over one-week (week 6)..... | 69 |
| Figure 3-9: Box plot of RTG crane demand by half hours..... | 70 |
| Figure 3-10: PACF plot for RTG crane demand time series for 500-time lags..... | 72 |
| Figure 3-11: Scatter plot for RTG crane demand, container gross weight and number of moves: (a) crane demand (kWh) with container gross. (b) container gross weight (tonne) and number of crane moves..... | 74 |
| Figure 4-1: General schematic of load forecasting procedure implemented in this chapter. .. | 79 |
| Figure 4-2: General schematic of ARIMAX forecast model..... | 81 |
| Figure 4-3: The summary of the ARIMA and ARIMAX approach [84] [87]. | 83 |
| Figure 4-4: The structure of typical artificial neuron processing in an NN unit..... | 86 |
| Figure 4-5: (a) The simplest neural network. (b) The multilayer neural network. | 87 |
| Figure 4-6: The summary of the ANN model approach [120] [121]..... | 89 |
| Figure 4-7: Electrified RTG crane demand variation for different container gross weight..... | 91 |
| Figure 4-8: Illustration of distribution of number of crane moves and container gross weight data in a 2D histogram. | 93 |
| Figure 4-9: Illustration of conditional distribution when $X_2(n)$ is 2..... | 93 |
| Figure 4-10: The proposed ANN forecast model. | 96 |
| Figure 4-11: Representation of ANN forecast models: Model A employs four input neurons while Model B uses two input neurons..... | 100 |
| Figure 4-12: ACF plot for the RTG crane demand..... | 102 |
| Figure 4-13: PACF plot for the RTG crane demand..... | 103 |
| Figure 4-14: Schematic for the various ARIMAX and ARX forecast models. | 104 |
| Figure 4-15: Daily MAPE results which presents: (a) the benchmarks and best forecast model, (b) the impact of estimating both exogenous variables on forecast models, (c) the impact of estimating one exogenous variable on forecast models (d) presents the highly accurate forecast models. | 108 |
| Figure 4-16: Illustration of error percentage data in a histogram along with a normal distribution fit..... | 111 |
| Figure 5-1: Single line diagram of the RTG crane network at the Port of Felixstowe, UK, including the ESS location scenario. | 117 |

| | |
|--------------------------------------------------------------------------------------------------------------------------------------------------------------------------------------------------------------------------------------------------------------------------------------------------------|-----|
| Figure 5-2: Histogram of daily mean absolute percentage error (MAPE) over 33 days for the ANN forecasting methodology (Model B1) from Chapter 4..... | 120 |
| Figure 5-3: An example of using ESS with set-point controller with two set-point values. .. | 123 |
| Figure 5-4: The SoC for ESS across a day period for set-point controllers, for the case study presented in the main text. | 123 |
| Figure 5-5: The scheme of MPC for the electrified RTG crane network equipped with an ESS..... | 124 |
| Figure 5-6: A simple illustration of the receding horizon used in MPC..... | 127 |
| Figure 5-7: Results of ANN forecasts for the cranes demand for the first day of the testing period. | 130 |
| Figure 5-8: Results of rolling ANN forecast model with different time step updating for the data and forecast model. | 130 |
| Figure 5-9: A specific example presenting the actual demand, and the results demand after implementing the set-point controller, the MPC and the optimal energy management controller for the substation demand in a network of RTG cranes for the given data set (Day 4 of testing period data). | 132 |
| Figure 5-10: The percentage of peak demand reduction by MPC with different horizon window sizes..... | 133 |
| Figure 6-1: General schematic of the stochastic optimal energy management procedure implemented..... | 140 |
| Figure 6-2: Illustration of the empirical distribution of the electrified RTG crane demand and container gross weight data via a 2D histogram. | 142 |
| Figure 6-3: Results of MC-ARIMAX (average), ARIMAX and ANN models for the cranes demand for the first day of the testing period. | 146 |
| Figure 6-4: Example of the MC-ARIMAX forecast model (red lines) with actual demand (black line). | 147 |
| Figure 6-5: Results of rolling MC-ARIMAX (average), with different updating rates..... | 147 |
| Figure 6-6: A specific example of the results presents the actual demand, and demand profiles from the set-point controller, the optimal management system and the SMPC for crane network for the given data set (Day 4 of testing period). | 149 |
| Figure 6-7: Box plot of the daily peak demand reduction achieved by the set-point, the optimal energy management and the SMPC controllers over the testing time period..... | 150 |

| | |
|-------------------------------------------------------------------------------------------------------------------------------------------------------------------------------------------------------------------------------------------------------------|-----|
| Figure 6-8: The network of RTG cranes demand profile with and without ESS (for day 5 of test set). | 151 |
| Figure 6-9: The State of Charge (SoC) of the ESS throughout the day (day 5 of test set). | 151 |
| Figure 6-10: The percentage of peak demand reduction resulting from the SMPC energy management controller based on a DP solution for different SoC search space resolutions (ΔC). | 152 |
| Figure 7-1: The average percentage of peak reduction for a specific case study. | 160 |
| Figure 7-2: The relationship between MAPE and the percentage of daily peak reduction for the SMPC controller. | 160 |
| Figure 7-3: Box plot of the daily peak demand reduction achieved by MPC, SMPC, optimal management system and set-point controllers over two test data sets. | 163 |
| Figure 7-4: Single line diagram of network of electrified RTG cranes at the Port of Felixstowe, UK with different ESS location scenarios. | 165 |
| Figure 7-5: (a) The network of RTG cranes demand profile with and without an Energy storage System (for day 5 of test set); (b) The State of Charge (SoC) of the ESS throughout the day (day 5 of test set) with shade area for the low tariff period. | 168 |
| Figure 7-6: The percentage of annual electric energy cost saving for different controller algorithms for a network of electrified RTG cranes equipped with an ESS. | 170 |

List of Table

| | |
|---------------------------------------------------------------------------------------------------------------------------------|----|
| Table 1-1: List of main ESS specification and criteria [11] [12] [14]. | 9 |
| Table 1-2: Comparison of energy storage technologies | 10 |
| Table 2-1: Categories of forecasts based on the prediction horizon. | 42 |
| Table 2-2: The advantages and drawbacks of some of the main short-term forecasting methods. | 46 |
| Table 3-1: Summary of the electrified RTG crane demand. | 63 |
| Table 3-2: Percentage of time that the crane daily demand is over the average value. | 65 |
| Table 3-3: The linear equation parameters and R- squared for the relationship between the current and lagged crane demand. | 72 |

| | |
|----------------------------------------------------------------------------------------------------------------------------------------------------------|-----|
| Table 3-4: The linear equation parameters and R- squared for the relationship between the current, container gross weight and number of crane moves..... | 75 |
| Table 3-5: Differences between the demand for the same number of moves and container weight..... | 75 |
| Table 4-1: The PACF and ACF behaviour to select p, q parameters [80] [107]. | 84 |
| Table 4-2: The forecast error for an ANN model with different number of hidden layers. | 97 |
| Table 4-3: Overall MAPE values for an ANN model with different numbers of neurons. | 97 |
| Table 4-4: Overall MAPE values for ANN model with different input variables. | 98 |
| Table 4-5: Statistical tests: ADF and PP. | 101 |
| Table 4-6: The BIC results for the demand series when (d = 0) for a variety of (p, q). | 103 |
| Table 4-7: Overall MAPE over each of the three testing periods. | 107 |
| Table 4-8: Performance of forecast models over 34 testing days (period 2). | 107 |
| Table 4-9: A comparison for the advantages and disadvantages of ANN and ARIMAX. | 113 |
| Table 5-1: The daily MAPE for the ANN prediction models. | 130 |
| Table 5-2: ESS parameters used in the case study. | 131 |
| Table 5-3: The percentage of peak reduction for the crane study in this chapter. | 133 |
| Table 5-4: The percentage of annual energy cost saving for the annual electricity bill. | 136 |
| Table 6-1: The SMPC controller model procedures. | 144 |
| Table 6-2: The daily MAPE for the cranes demand forecast models: ANN, ARIMAX and MC-ARIMAX prediction models. | 146 |
| Table 6-3: The energy storage system parameters. | 148 |
| Table 6-4: The average percentage of demand reduction for a specific example over the 5 day testing period. | 149 |
| Table 6-5: The percentage of annual energy cost saving to the annual electricity bill. | 153 |
| Table 6-6: The main techno-economic parameters for an ESS. | 154 |
| Table 6-7: The ESS scenarios viability results | 155 |
| Table 7-1: The average peak demand reduction for the ESS controllers with average forecast errors. | 158 |
| Table 7-2: The percentage of annual electric energy cost saving to the annual electricity energy bill. | 161 |
| Table 7-3: The percentage of annual electric energy cost saving to the annual electricity energy bill. | 162 |
| Table 7-4: The energy storage system parameters. | 166 |

Table 7-5: The percentage of peak demand reduction results for a specific case study. 167

Table 7-6: The ESS viability results for the different control strategies and all ESS location scenarios..... 170

Table 7-7: A comparison for the advantages and disadvantages of each control technique. 174

Abbreviations

| | |
|-----------------|---------------------------------------------------------------------|
| ESS | Energy storage system. |
| RTG | Rubber tyred gantry. |
| WSC | World shipping council. |
| TEU | Twenty-foot container equivalent unit. |
| PoF | Port of Felixstowe. |
| CO ₂ | Carbon dioxide. |
| NiCd | Nickel–cadmium. |
| Li | Lithium. |
| LV | Low voltage. |
| MV | Medium voltage. |
| AC | Alternating current. |
| DC | Direct current. |
| IGBT | Insulated gate bipolar transistors. |
| MPC | Model predictive control. |
| SMPC | Stochastic model predictive control. |
| ToU | Time of use. |
| PI | Proportional integral. |
| SoC | State of charge. |
| PV | Photovoltaics. |
| MILP | Mixed integer linear programming. |
| RBF-NN | Radial basis function neural network. |
| RH | Receding horizon. |
| EV | Electric vehicle. |
| GA | Genetic algorithm. |
| HVAC | Heating, ventilation, and air conditioning. |
| DP | Dynamic programming. |
| MAPE | Mean absolute percentage error. |
| AR | Auto regressive. |
| MA | Moving average. |
| ARMA | Auto regressive moving average. |
| ARIMA | Auto regressive integrated moving average. |
| ARIMAX | Auto regressive integrated moving average with exogenous variables. |
| SARIMA | Seasonal auto regressive integrated moving average. |
| ANN | Artificial neural network. |
| WT | Wavelet transform. |
| SVM | Support vector machine. |
| LSSVM | Last squares support vector machine. |
| Reg | Regression. |
| ANFIS | Adaptive network-based fuzzy inference system. |
| rRMSE | Relative root mean square error. |
| MRE | Mean relative error. |
| SMA | Simple moving average. |
| MARS | Multivariate adaptive regression splines. |
| kNN | K-Nearest neighbours. |

| | |
|----------------|---------------------------------------------------------|
| sMAPE | Symmetric mean absolute error. |
| SVR | Support vector regression. |
| RF | Random forecast. |
| ReTree | Regression tree forecasting. |
| AIMMS | Multidimensional modelling system. |
| R ² | R-squared. |
| ADF | Augmented Dickey-Fuller test. |
| PP | Philips-Perron test. |
| KPSS | Kwiatkowski-Phillips-Schmidt-Shin test. |
| ACF | Autocorrelation function. |
| PACF | Partial autocorrelation function. |
| ACF | Autocorrelation function. |
| IQR | Inter quartile range. |
| AIC | Akaike's information criterion. |
| BIC | Bayesian information criterion. |
| MLP | Multilayer perceptron. |
| SOLAS | International Convention for the Safety of Life at Sea. |
| RMSE | Root mean square error. |
| MAE | Mean absolute error. |
| MC-ARIMAX | Monte Carlo and ARIMAX. |
| MIMO | Multi-input multi-output. |
| PLC | Programming logic computer |
| CSV | Comma separated variable |

Chapter 1: Introduction

The aim of this thesis is to investigate the potential for reducing the electric energy costs and maximising the peak demand reduction at sea ports, through the use of an Energy Storage System (ESS). Specifically, it will explore the potential effects of an ESS located at the low voltage side of a network of Rubber Tyred Gantry (RTG) cranes. The ESS is a common alternative solution to avoid the expensive cost of conventional network reinforcement. In this chapter the carbon emissions and increasing electricity demand problems at ports are briefly introduced. The electrification challenges at port, energy saving options, the various ESS technologies available, and the role they can play in ports is presented. The subsequent sections describe the network of RTG cranes which will be studied in this thesis, the project objectives, the key contribution to knowledge of this work and the fully defined problem statement which motivates this research.

1.1 Global Shipping Trade and Carbon Emissions

The trend in global consumerism and the increase in worldwide population is raising the need to improve marine container transportation. According to the trade statistical data from the World Shipping Council (WSC), 127.6 million Twenty-foot container Equivalent Units (TEUs) were exported and imported globally in 2014 with a 4.3% increase from the previous year [1]. In 2015, ports worldwide issued approximately 9,000 calls for container ships and 1,000 calls for vehicle vessels per week. On average, ships respond to about two port calls per week [2]. The United Nations report (Review of maritime transport, 2016) shows that the world gross domestic product increased by 2.5% compared to 2014, with the world seaborne trade increasing by 2.1% [3].

In order to respond to the accelerated growth of world seaborne trade, ports need to improve the efficiency of their handling operations by installing suitable infrastructure. Port facilities are costly to build and operate, in order to complete the container handling process from land to sea or conversely. In port container terminals, container ships are in the berths waiting for the quay crane to load/unload the containers to lorries. Then, the cargo is transferred by yard truck from the quayside to the yard, where the port keeps the containers temporarily until transferring it to the cargo owner, by using the yard crane and vice versa, as shown in

Figures 1-1 and 1-2. These port facilities and equipment are scaled to move a specific range of container weights at a speed that allows the safe operation at the port site. Sea ports are large logistical operations that require significant engineering, technician, administration, and logistics support. Coupled with this, where ports are gateways to and from other countries, they require customs facilities.



Figure 1-1: Port of Felixstowe (PoF), United Kingdom.

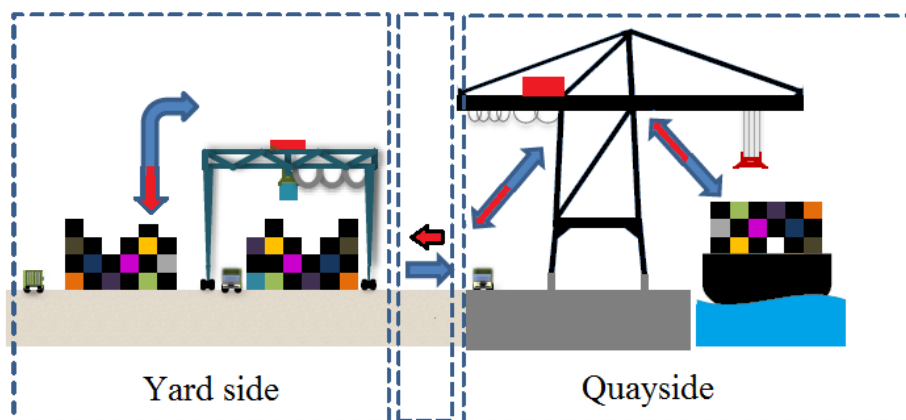


Figure 1-2: General handling operation process of port container terminals [6].

During the handling process of the container terminal, vast amounts of fuel are consumed, producing CO₂ emissions via the different handling and transfer operations. Research carried out on data released by the Port of Los Angeles to evaluate the gas emissions at container terminals, shows that 38% of the CO₂ emissions come from quay cranes and yard equipment including the RTG cranes and handlers. Furthermore, the CO₂ emissions increased by 18% in 2014 compared to the previous year [4]. The high operating costs, pollution, and

noise from the diesel yard equipment, has led sea ports to move towards replacing diesel RTG cranes with electric RTG cranes, which offer greater environmental opportunities and higher energy efficiencies. The use of electrified RTG cranes can increase the reduction in CO₂ emission by 60% - 80%, which can lead to reduction in the overall container terminal CO₂ emissions by 20% per TEU handled compared to diesel RTG cranes [5]. Another benefit of using electrified RTG cranes, is the reduction in costs for equipment repairs and maintenance by around 30% compared to diesel RTG cranes [5].

In ports, most of the electrical energy consumption comes from electrified cranes and refrigerated containers (Reefer) [6]. In an RTG crane system, most of the electricity energy or fuel consumption comes from hoisting containers with different weights to different heights. Furthermore, the peak demand increases when the RTG crane moves heavier containers [7]. As electricity demand on the ports' electrical distribution networks augments due to the electrification of RTG cranes, port operators will be forced to reinforce the network to meet this increased demand. The traditional reinforcement solutions focus on upgrading or replacing existing electrical infrastructure such as cables and substations. This solution is effective but commercially expensive [5] [7].

Reducing the electric load and peak demand on the distribution network would help to reduce the infrastructure reinforcement costs and carbon emissions at the electricity supplier side. Considering the reduction in electricity load at port buildings through, lighting and heating or cooling offer little capacity compared to other port loads. The refrigerated container loads are mandatory in order to maintain set temperature and avoid destroying the contents within the container. The electrified cranes represent the largest electric load in the port and provide the biggest opportunity for peak demand reduction and cost saving. However, the network of cranes will require smarter solutions to increase energy saving, since the RTG crane load profiles have a highly volatile and stochastic behaviour compared to other low and medium voltage loads including domestic customers. Traditionally, reducing the electric energy of the network of cranes will lead to reduced energy costs and CO₂ emissions on container terminals. One practical technology, and the subject of this thesis, is Energy Storage System (ESS). This can be significant tool for a more energy efficient ecosystem and help to decrease environmental concerns. In general, the objective of an ESS is to reduce the cost of electricity and avoid the need to upgrade the distribution network by shifting energy consumption from

peak to valley periods [7]. The next section will therefore discuss the energy saving options at ports in more details.

1.1.1 Energy Saving Options for RTG Cranes

In the previous section the carbon emission problem for sea ports was introduced and discussed. Fuel consumption by diesel RTG cranes and yard tractors is a major contribution to increase the direct CO₂ emissions of the port container terminal. The configuration of diesel RTG cranes include various functioning state combinations of large diesel engines, motors (hoist, trolley and gantry motors) and other parts that allow the crane to produce different moving modes. These moves and handing operation modes are responsible for the majority of the diesel RTG cranes contribution to total fuel consumption. For example, 62% of the total fuel consumption at Noatum Port Valencia was produced by RTG cranes and 33% was associated to the moves of yard tractors, as illustrated in Figure 1-3 [6]. It is clear from the data in [4] and [6] that not all container terminal sites have the same behaviour in terms of fuel consumption. This mainly relates to yard layout, human operator choices, yard equipment configurations and size of the yard. This section presents the technology options to reduce fuel consumption.

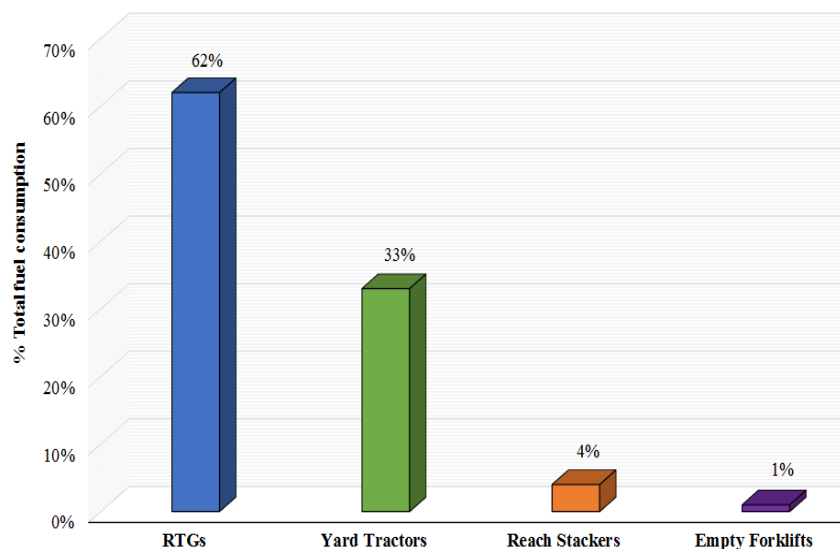


Figure 1-3: Total fuel consumption distribution, Noatum Container Terminal Valencia [6].

To reduce CO₂ emission and fuel consumption at port container terminal, there are several solutions which have been introduced as follows:

- Electrified the RTG cranes.
- ESS equipped with RTG crane.
- Variable speed generator.

The variable speed generator technology allows to run the engine at the most economical speed to increase fuel reduction and reduce carbon emission [8]. From the variable speed generator solution, a simpler option has been presented in [9] called Idle mode technology as solution to save fuel when the crane is in idle mode (not in use) by reducing the generator idle speed [9]. However, this solution can be effective only during idle mode and most of the fuel consumption comes during the active mode (hoisting the containers). Figure 1-4 presents a basic comparison of potential fuel consumption reduction technologies [5] [7] [8]. The three main categories for comparing of these options, as seen in Figure 1-4, are: the expected cost of each solution, energy saving and carbon reduction. Financially, the capital cost in Figure 1-4 is mainly presented the direct cost of the proposed solution to only convert the available diesel RTG crane to electric, variable speed generator or adding ESS. Furthermore, the electrification solution is more expensive compared to other options due to the need to upgrade the electrical infrastructure of the port and replace the diesel RTG crane. Environmentally, all solutions introduce a significant CO₂ emissions reduction compared to conventional diesel RTG cranes. Operationally, all technologies here are required to increase energy savings without interfering with the terminal operations.

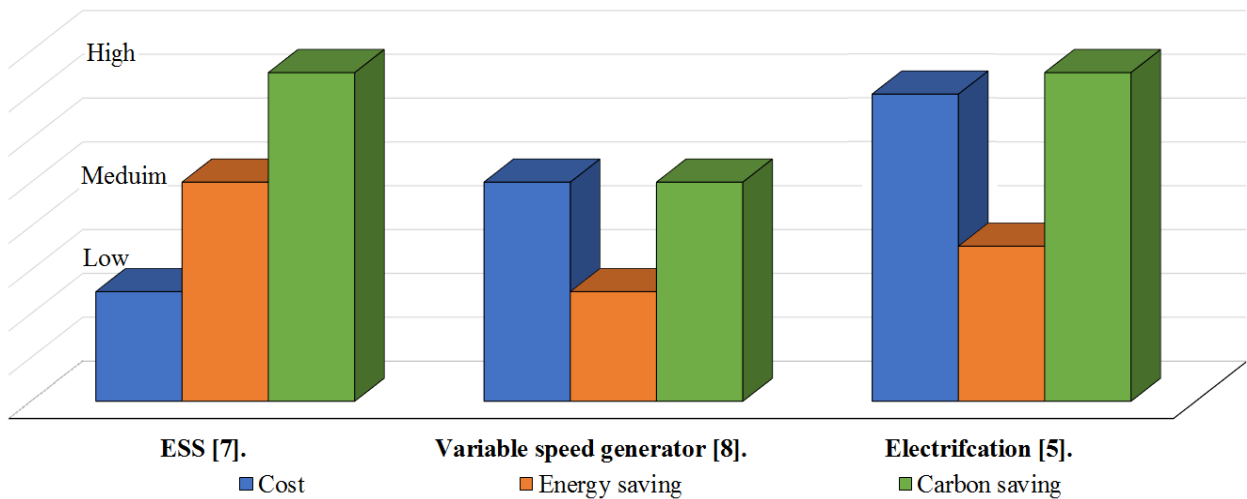


Figure 1-4: Comparison of fuel saving options for RTG cranes [5] [7] [8].

A pilot project at the Port of Felixstowe (PoF) in the UK to electrify four RTG cranes showed a reduction in CO₂ emission of 12% between 2007 and 2014 [10]. The PoF is currently moving towards electrifying more RTG cranes, and estimating that the port can achieve up to 45% energy saving and 30% carbon emission reduction by 2018. However, the electrification solution requires upgrading the electrical infrastructure, modify the RTG crane system and a new operator control system, increasing the overall cost. Therefore, an ESS can play a significant role to minimise the cost of the electrification option, increase cost saving and reduce gas emission. In addition to the cost challenge, there is lack of understanding of the ports and the RTG cranes electric energy demand behaviour. This understanding is vital for developing optimal power generation strategies to reduce the environmental effects of gas emissions, peak demand and electricity costs. In addition, none of these options currently deals with the crane demand forecast as an effective tool to understand the demand behaviour which is absolutely necessary for the optimal energy management system solutions such as load shedding, peak demand reduction, energy cost saving and electrical infrastructure development.

1.2 Energy Storage Technologies

An ESS in a power system can be defined as a unit or energy conversion method, which stores the energy for a period of time in the power system and releases it when the customers or utilities need it. This process is subject to a control system, as shown in Figure 1-5. Energy storage technologies are expected to be a significant part of the future smarter energy systems, producing a substantial contribution to power system security and flexibility. ESS's provide flexibility during times of overload, fluctuating energy generation and electricity price, and give storage devices a key role in increasing energy cost saving, building a low carbon future network and facing many of the other power system challenges [7] [11]. In many places this new demand has not been taken into consideration by planning engineers during the design stage of existing power networks. The ESS solution for RTG cranes has, up until recently, mainly focused on saving energy on a single RTG crane system by using recovered potential energy. The generated energy during the lowering of the containers is used to charge the ESS and discharge it when the crane is lifting the containers [7]. However, the highly volatile behaviour of the electrified RTG crane demand, the electricity price and the benefits of using load forecast are currently not consider in the ESS solution for the RTG crane system, which can help to increase energy savings of the network of electrified RTG cranes. In addition, a

central ESS that feeds more than a single electrified RTG crane can play a key role to reduce the peak demand at port substation and electricity bill cost.

An energy storage system has three main operation states: charge, discharge and store, which can be used to shift energy consumption from peak to valley periods, as shown in Figure 1-5. An adequate optimal energy strategy for a network of electrified RTG cranes system equipped with an ESS located on the side of the substation could be of great interest worldwide. To date no studies have considered an optimal energy management system or a central ESS which feeds more than a single electrified crane. Furthermore, an optimal energy strategy for a network of RTG cranes will help sea ports to reduce the electricity energy cost and carbon emissions; especially as RTG cranes are vital to the export and import of goods through ports around the world. Energy storage technologies have the ability to increase reliability to the existing electrical distribution network and can play many roles in energy saving and electric system security. These roles and the classification of energy storage technologies will be briefly discussed in the following section.

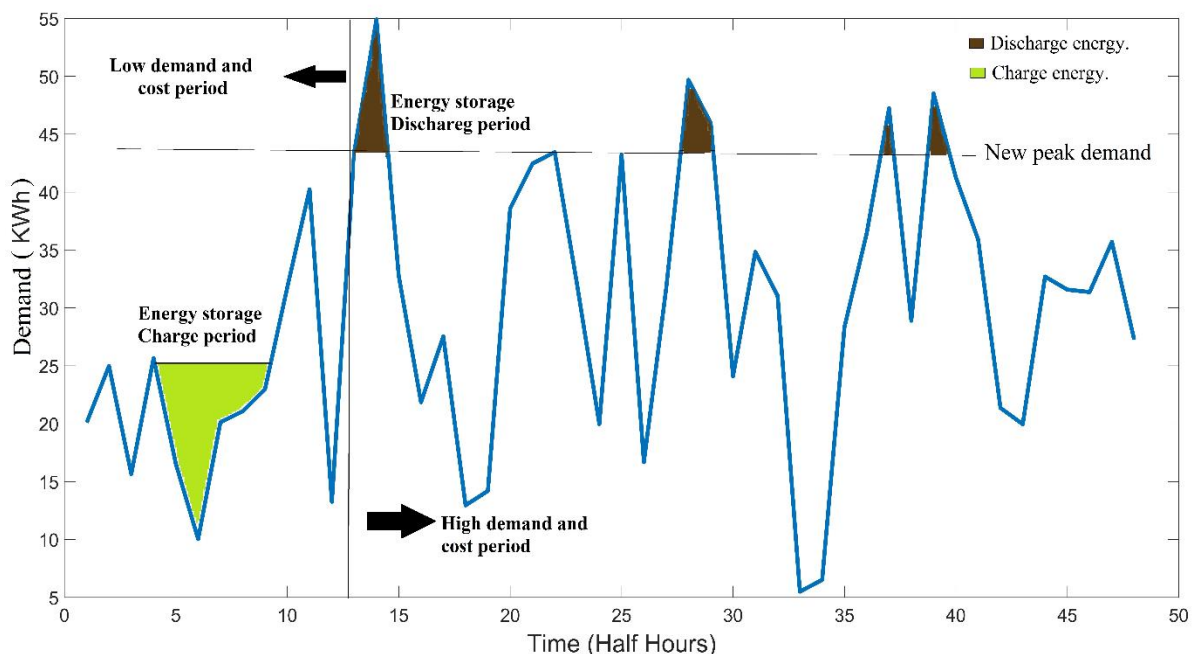


Figure 1-5: An example of a peak shaving strategy.

1.2.1 Classification of Energy Storage Technologies

In order to store energy, the energy storage system needs to convert the electrical energy into another form of energy. The topic of ESS, its classification and uses has been widely

discussed [11] [12] [13] and are briefly summarised here. The energy storage technologies that are being considered for power grid application can be classified mainly into:

- Mechanical energy storage: e.g. pumped hydro, compressed air, and Flywheel.
- Electrochemical energy storage: NiCd or Li batteries and flow batteries.
- Chemical energy storage: fuel cells.
- Electrical energy storage: supercapacitors.
- Thermal energy storage: sensible heat storage.

The diversity of energy storage technologies allows the use of ESS in a wide range of different applications. Figure 1-6 presents the classification of energy storage systems based on the scale of application: large, medium and small scale [11].

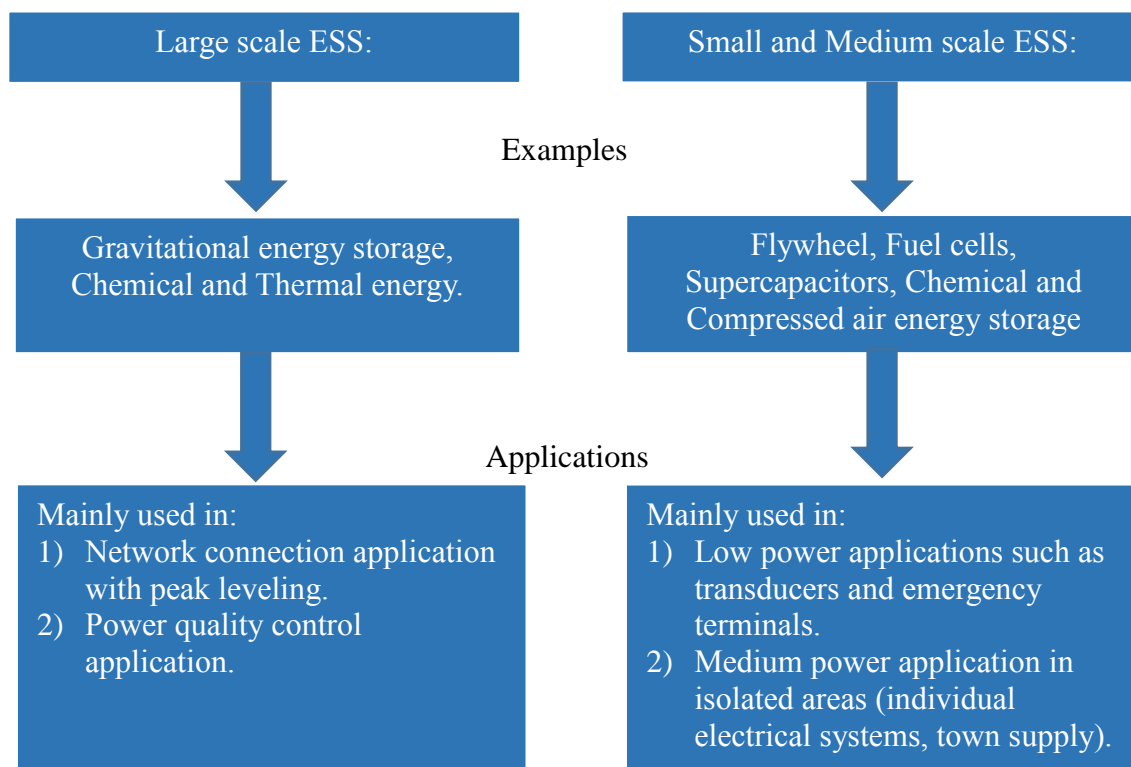


Figure 1-6 : The classification of ESS based on categories of applications [11].

1.2.2 Comparison of ESS Technologies

There is a wide range of energy storage technologies that can be used in power system networks to increase energy cost saving and reduce peak demand. This section will briefly

introduce the main advantages and disadvantages of the energy storage technologies that are used in low and medium power applications. This comparison, based on the evaluation criteria presents in Table 1-1, may help to give a clearer image why some types of ESS may be more effective than others [11] [14] [15]. Table 1-2 summarises the advantages and disadvantages for batteries, supercapacitors, and flywheel energy storage systems. The battery and supercapacitor energy storage devices have been used widely in medium and low voltage applications in power system networks. Recently there has been more research on potential improvements to Flywheel energy storage especially with applications such as RTG cranes [7].

Storage technologies have many criteria on which they can be evaluated, but it is significant to study the criteria or concept of an ESS's power and energy density, as presented in Table 1-1. The type of ESS selected for small and individual scale applications will often be recommended based on this concept. For example, batteries have high energy density and low self-discharge rate, so they are suited for applications that need slow obtains of energy (hours or half hours), especially with low power density. On the other hand, A high power density storage device such as a supercapacitor is more suitable for applications that require high releases of power during a short time period (seconds). The contrast of power and energy density in different ESSs, as shown in Table 1-2 explains why a specific ESS technology is not appropriate for every application. Other ESS criteria and specifications are described in Table 1-1. The next part of this section will present the main roles that an ESS can play in the network of RTG cranes and the main task of the energy storage that will be presented and studied throughout this research.

Table 1-1:List of main ESS specification and criteria [11] [12] [14].

| Specifications | Explanation |
|-----------------------|----------------------------------------------------------------------------------------------------------|
| Longevity | Describes the lifetime of ESS based on the number of charge and discharge cycles. |
| Response time | Shows the required time for an ESS to react to demand or control. |
| Cost | The cost of ESS including the capital and operation costs. The cost is measured as cost per energy unit. |
| Losses | Presents the losses of energy from the ESS. |
| Power density | Amount of power in a given volume an ESS can transfer to the system. |
| Energy density | Amount of energy in a given volume an ESS can hold or store. |

Table 1-2: Comparison of energy storage technologies

| | Advantages | Disadvantages | Application |
|------------------------|--------------------------------------------------------------------------------------------------------------|----------------------------------------------------------------------------------------------------------------------------------------------------------------------------------------------------------------------------|-------------------------------------------------------------------------------------------------------------------------|
| Batteries | <ul style="list-style-type: none"> • High energy density. • Low self-discharge rate. | <ul style="list-style-type: none"> • Mid to low level power density. • Short life time which may increase cost and decrease efficiency. • High environmental impact. | <ul style="list-style-type: none"> • Peak load, standing reserve, daily load shifting, renewable energy. |
| Supercapacitors | <ul style="list-style-type: none"> • High power density. • Long life time. | <ul style="list-style-type: none"> • Low energy density. • High capital cost for energy cost unit. • High self-discharge rate. | <ul style="list-style-type: none"> • Line fault, frequency and voltage control. |
| Flywheel | <ul style="list-style-type: none"> • High power density. • Long life time. | <ul style="list-style-type: none"> • Low energy density. • High capital cost for energy cost unit. • High precision requirements for designing and controlling the energy storage system. | <ul style="list-style-type: none"> • Power smoothing, spinning reserve, frequency and voltage control. |

1.2.3 Role of Energy Storage in Cranes Networks.

An ESS on the power network has the potential to support and postpone or reduce the need for traditional infrastructure reinforcement. The traditional reinforcement approaches to maintain the technical standards such as voltage and thermal limits in distribution network focus on upgrading or replacing existing electrical infrastructure such as cables and substations [15]. This solution is effective but commercially expensive, which motivates the consideration of different ESSs technologies and control methods for supporting the power grid. For RTG crane networks, this problem is very difficult and complicated, as the port operator needs to replace service cables, conductor bars and distribution and main substations assets. Recently, researchers worldwide have begun investigating industrial electrification problems that the port and RTG crane operators face. Literature is beginning to appear [16] [17] [18] which considers the potential impact of using an ESS to support the diesel and electric RTG cranes. In the following part of this section more details are presented on how ESSs can support RTG crane networks in a similar way to how they are being used in the Low Voltage (LV) network.

Power smoothing: low voltage network components such as transformer, cables and circuit breakers have a specific electrical limitation and finite thermal capacities based on the

insulation performance; demand beyond these limits causes heat problems and electrical faults. In distribution LV networks (three-phase system), individual connections or cable may be connected to one or more users (loads) which can lead to one phase carrying significantly higher current compared to the other two phases. Typically, LV networks with unbalanced loads will cause a current in the neutral cable which, when significantly high, will lead to reactive power and third harmonic problems. The traditional approach to solve this problem, peak demand and overloading problems in LV network system is to reconnect the network to distribute demand via new interconnection points. As previously discussed, these traditional solutions are effective but highly expensive. An ESS is a potential solution which will allow the power system to operate under these thermal limits by power smoothing, balancing load, reducing peak, and load levelling. In a crane system, most of the energy consumption comes from lifting containers. Typically, the ESS is located at the RTG crane side to provide a hybrid power source. In order to increase the energy savings in an electrified or diesel RTG crane systems, ESSs have been traditionally used for peak shaving and power smoothing during the lifting mode by using recovered potential energy that has accrued during the lowering mode to reduce the dissipated energy through the dump resistors [7] [16] [19]. An ESS is developed based on the type of power flow problem and the method of control. For instance, the ESS may be designed and controlled to support the electrical distribution network to maintain electrical and thermal limitation by maximising the peak demand reduction. Load levelling would require a different way to control the ESS to smooth and balance the volatile demand.

Voltage and Frequency Control: The distribution network voltage and frequency are controlled by the balance between total load and generation. The distribution grid is regulated to work under specific frequency and voltage limits with normal deviation not more than 1% for frequency and 10% for voltage. An ESS can play a significant role in supporting the network to resolve frequency and voltage problems. Storage devices can inject and absorb energy from the grid through a charging and discharging process based on the voltage and frequency level, when above or below the required limits.

Energy Markets: In this role, storage device can be used for reducing the electricity costs and creating a new option in energy markets. Charging the ESS during the low electricity price period and discharging it when it is high can minimise the costs for balancing the energy market. For example, an ESS can have a significant role in reducing energy costs and peak

demand by aiming to shift the maximum possible peak demand during the high price period and moving the demand to the low price period, as illustrated in Figure 1-5. In ports, an ESS can play a vital role in reducing peak demand, carbon gas emissions and RTG crane operation costs. Unlike previous studies, (which often use the set-point controls to increase energy saving by using regenerative energy in an RTG crane system and neglect the electricity cost and forecast algorithm as inputs to improve the ESS efficiency,) in this thesis, the main task of the energy storage is to optimise the energy flow in RTG cranes network system by using the real-time electricity price whilst targeting the greatest peak demand reduction.

As discussed in this section, different energy storage technologies have played a significant role in peak demand, cost, gas emission and energy reduction. Furthermore, the ESS specifications, mainly the energy and power density, explain why some of storage devices are not suitable for the distribution grid applications. Generally, the ESS is controlled and designed, depending on the main target or aim of the ESS. The following section introduces the Port of Felixstowe, UK and RTG crane system which will be the main project focus.

1.3 Port of Felixstowe and RTG Crane System

This section introduces Port of Felixstowe (PoF) [10], the biggest and busiest container terminal port in UK and one of the largest in Europe, located on the east coast of Britain. This port has taken a major step to reduce their energy costs and CO₂ emission by replacing a number of diesel RTG cranes with electric-powered RTG cranes. Here, the RTG crane and crane network will be briefly presented, together with operation characteristics and how the ESS would be implemented in order to reduce the electricity costs and peak demand.

1.3.1 Port of Felixstowe

This research was conducted with the support of the Port of Felixstowe (PoF), UK, shown in Figure 1-1. This port provides one of the best locations in the UK to import and export goods. The port location is close to European shipping lanes with deep waters close to the open sea and 30 shipping lines. As shown in Figure 1-7, the PoF handles and operates more than 4 million TEUs, 3000 ships a year and offers around 90 services for 400 ports worldwide [20] [21]. In 2013, the Port of Felixstowe was the first in the UK to handle the largest container vessels through Berths 8 and 9. From January to September 2017, PoF handled mega containers ships like the Madrid Maersk vessel with 20,568 TEU [22]. In order to handle and

operate more than 4 million TEUs each year, the PoF runs 31 Ship-to-Shore cranes and 85 RTG cranes continuously. They only go offline for maintenance but typically work daily up to 24 hours for 362 days a year [22]. This level of operation, with PoF planning to electrify all RTG cranes, means a significant amount of electrical energy is consumed. There is little understanding regarding the substation impact on the crane demands and energy cost. However, by improving our understanding; energy storage systems with optimal energy management controllers have significant potential to contribute to reducing electricity energy costs and peak demand.

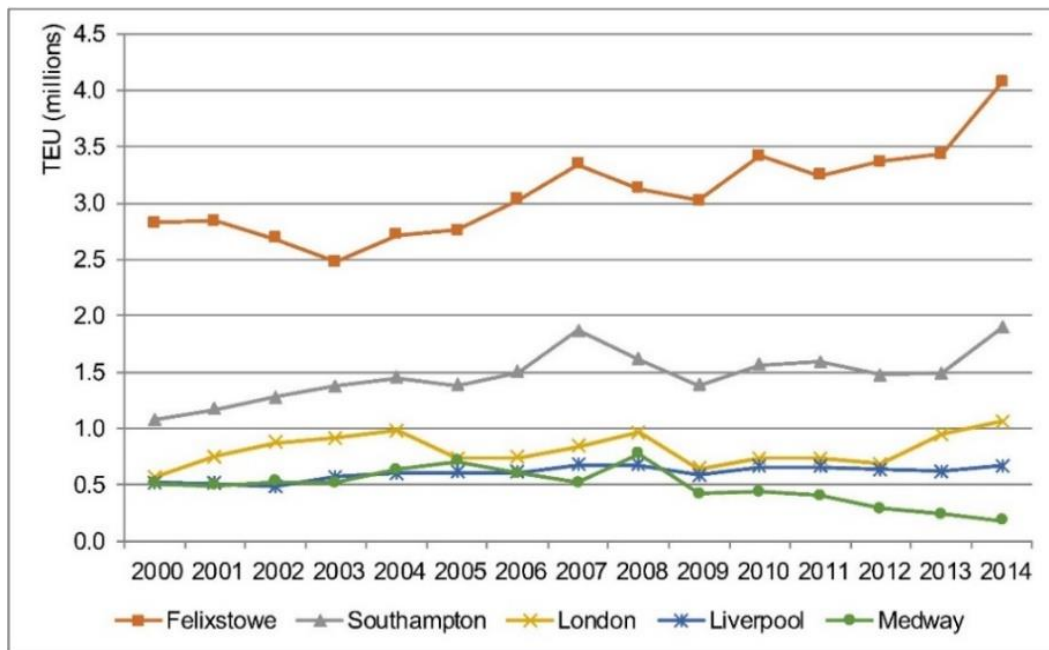
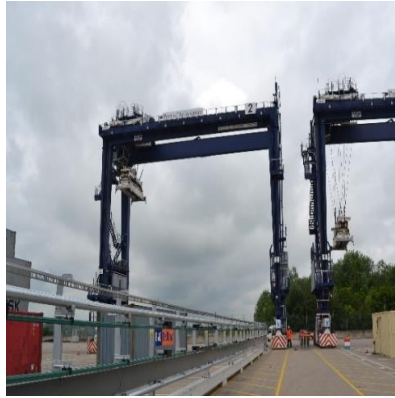


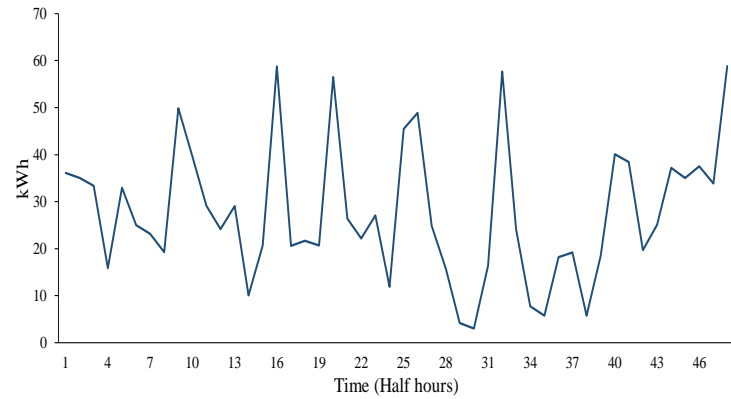
Figure 1-7: The major container ports in UK from 2000 to 2014 [21].

1.3.2 RTG Cranes

This subsection addresses the RTG crane structure and introduces the crane electric demand. The electrified RTG from PoF, used in this thesis is shown in Figure 1-8 (a) and has been retrofitted to be powered by the distribution power network at the port via a conductor bar, manufactured by Vahle (Germany), of length 217 m. This crane is manufactured by Shanghai Zhenhua Heavy Industries (ZPMC, Shanghai, China) [7].



(a)



(b)

Figure 1-8: Crane system: (a) electrified RTG crane at the Port of Felixstowe; (b) an example of the actual electrified RTG crane demand for a specific day.

The RTG cranes at the Port of Felixstowe have three main types of motors to drive the crane and move containers, as presented in Figure 1-9, as follows:

- Four electrical machines called gantry motors, move the crane around the site.
- Hoist motor raise the container. The hoist motor is capable of raising containers weighting up to 40 tonnes (fully loaded container). The hoist motor connects to a spreader through a cable reel by a gearbox, the spreader can weigh between 8 to 12 tonnes, which mean that the total hoisting weight can be 52 tons.
- Two trolley motors aim to move the cabin and hoisting unit, with or without the full loaded container, across the span of the crane.

As presented in Figure 1-9 (a), the energy source in the RTG crane system goes, through a diode rectifier that converts the Alternating Current (AC) through a uni-directional rectification process to an equivalent Direct Current (DC) and distributes it to the crane motors via the DC connections. This process aims to protect the electrical distribution side and the network auxiliaries from any damages coming from current disturbance problems. The DC bus delivers the power to the RTG crane through electronic bidirectional switches called Insulated Gate Bipolar Transistors (IGBTs). Whilst lowering the container, the crane motor works under generating conditions, which causes a reverse power in the DC network and increases the voltage above the normal operation ratings. Typically, in RTG crane system, if the DC voltage goes above 750 V, the crane dissipated the reverse energy through dump resistors and the voltage drops back to a normal level of 575 V [7].

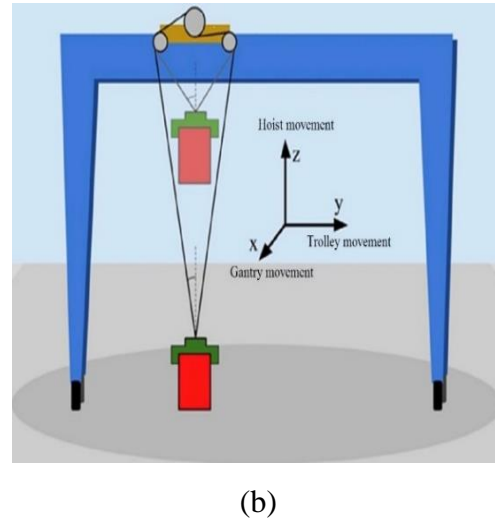
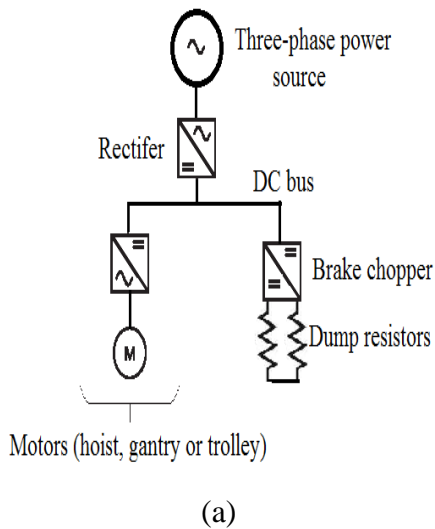


Figure 1-9: RTG crane system: (a) single line diagram of an RTG crane system for the main electric elements [7]; (b) schematic of possible RTG crane movements [19].

The power source for the RTG cranes (diesel or electricity) is sized to provide the power required to allow different moving modes and tasks. As shown in Figure 1-10, the high percentage of the energy consumed by the RTG crane systems comes from lifting containers rather than the gantry and trolley parts. Generally, the average total energy consumed by an RTG crane system for a typical operation day is approximately 530 kWh, as shown in Figure 1-11 [19]. In the literature, Papaioannou et al. [19] analysed the total daily energy usage over only eight days for diesel RTG crane. This analysis [19] does not show and investigate the daily or in a day pattern due to limited time series data. In addition, it shows that there is no day of week pattern where the total energy consumed at day 8 is not similar to day 1. An electrified RTG crane demand profile has highly stochastic and unpredictable behaviour compared to other low voltage loads such as domestic customers. The volatile nature of this load with ambiguous explanatory relationships between the RTG crane demand and exogenous variables such as temperature, and seasonality trends increases the challenges to operate and manage the energy flow in the distribution network, as shown in Figure 1-8 (b) and will be discussed in more detail in Chapter 3. Such analysis is required to operate an ESS with an optimal energy management controller, the focus of this project, to reduce the electric costs, peak demand, and make the daily energy profile smoother, (See in Figure 1-5). In addition, one of the main aims is to understand the electrical demand behaviour and improve the optimal ESS controller performance is load forecasting.

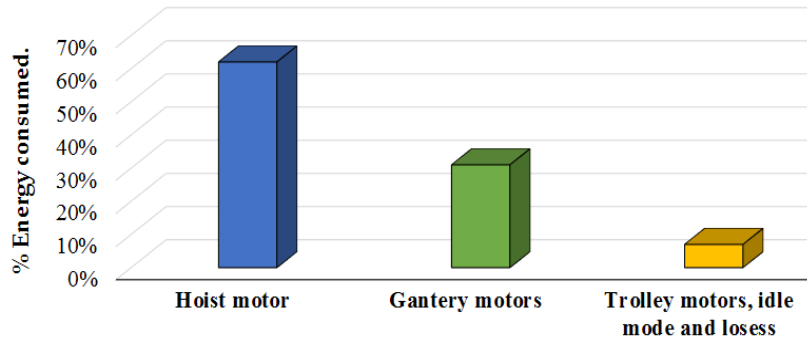


Figure 1-10: Average energy consumption for an RTG crane system on a typical operation day [19].

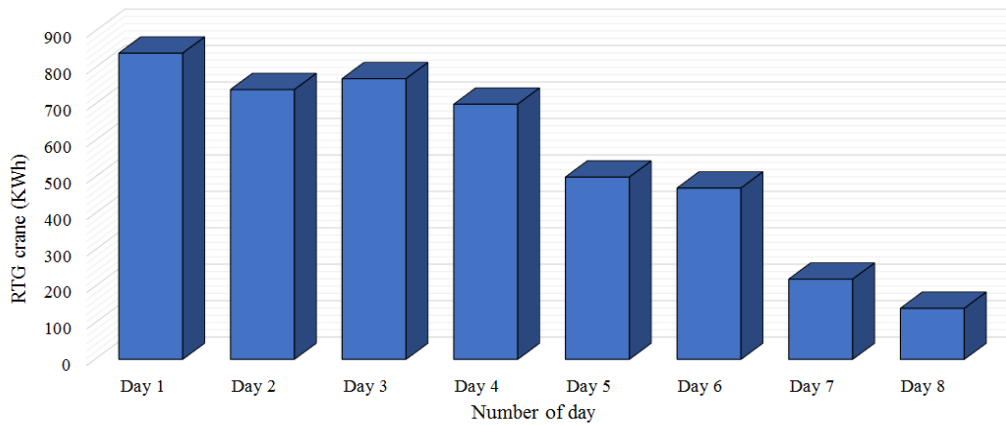


Figure 1-11: RTG crane energy in kWh for eight working days [19].

1.3.3 Electrified RTG Crane Network

The electrical grid is a hierarchal network of synchronised and interconnected power suppliers and consumers over a wide geographic area. Firstly, the power station generates the electricity and step-up the voltage to 230 kV or 400 kV (European system) to reduce the losses in the transmission stage. The electricity is distributed to consumers by the step-down voltage transformer and distribution network. In the first stage, the voltage is stepped down to 33 kV then 11 kV (medium voltage) and finally to the Low Voltage (LV) network level of, 415 V. This thesis will focus and study an ESS on the LV network for RTG cranes. Figure 1-12 represent a real single line diagram of a network of electrified RTG cranes at the Port of Felixstowe, UK, to help go through the main network terminology. The primary substation is a step-down station from 33 kV to 11 kV, and is split across the medium voltage network for the port. A secondary step-down substation with 11 kV input and 415 V output provides the cranes with the required power through the LV cables and conductor rail, as shown in Figure 1-12.

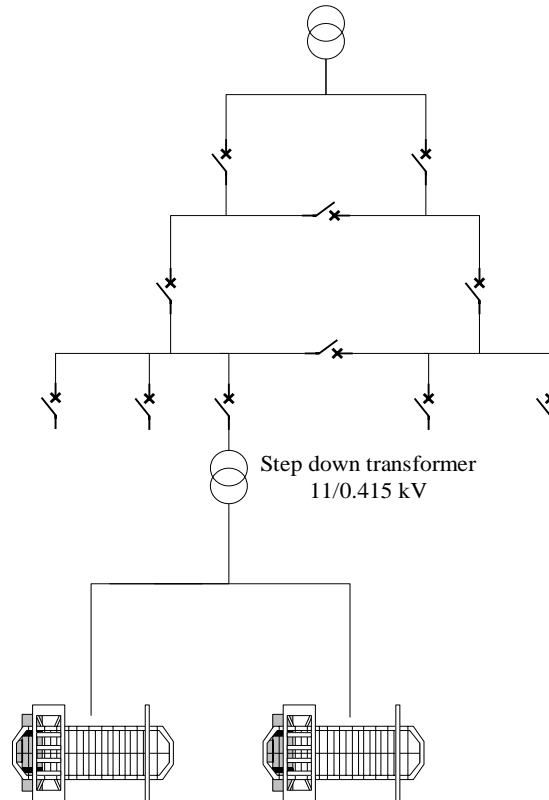


Figure 1-12: Single line diagram of the network of electrified RTG cranes at the Port of Felixstowe, UK.

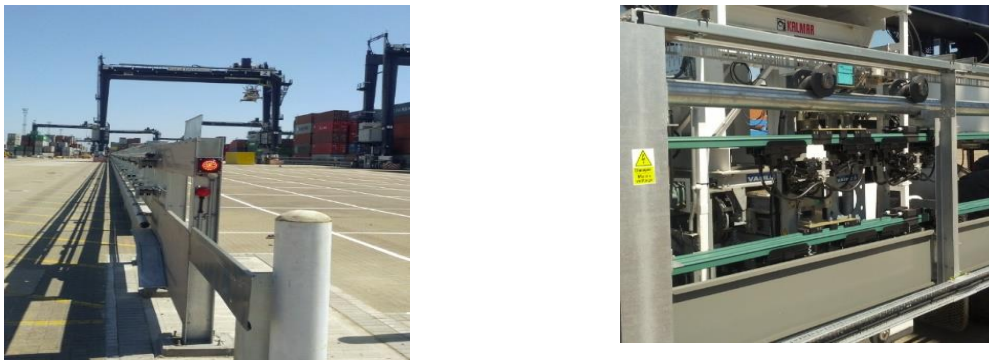


Figure 1-13: Conductor rail bar with crane connection.

In addition, unlike studies which have mainly used conventional control algorithms (set-point control) to increase energy saving in a single RTG crane system, this project investigates and analyses different ESS location scenarios with a central storage at a secondary substation to feed more than two electrified RTG cranes. This is to give sea ports an initial indicator regarding the best possible location for an ESS.

1.4 Problem Statement

As electrical loads increase across the RTG crane network due to the electrification of the cranes, port operators will be forced to reinforce the network to meet this increased demand and support the distribution network. This thesis will outline a solution to the peak demand and the energy cost problems at ports. The current literature presents the ESS as a potential significant solution to enable low voltage networks to become more energy efficient and avoid the need for expensive distribution network upgrades through the shifting of energy consumption from peak to valley periods. This thesis studies how an ESS on a network of RTG cranes can be optimally controlled, in order to reduce the electricity energy costs and achieve the maximum peak demand reduction. Understanding the port network and the RTG crane energy demand behaviour is essential to reduce the energy costs and peak demand. Therefore, this work studies the correlation between the historical crane demand and different exogenous variables in order to accurately predict the crane demand. The thesis will then investigate how the demand forecasts can be used to improve the performance of the ESS. In order to maximise the potential benefits of using an ESS in a LV network of RTG cranes, minimise the unnecessary storage device monitoring and treat the volatile and stochastic demand behaviour, the thesis investigates and studies different optimal energy management strategies for the RTG crane network equipped with an ESS.

1.5 Research Objectives

- Analyse the electrical demand of an electrified RTG crane in a period of real operation and identify the relationship between the present crane demand based on historical load, and exogenous variables (in particular number of crane moves and container gross weight). This will help to understand the ports and the RTG crane energy demand behaviour and how to develop models to predict the crane demand and control the ESS.
- Develop forecast models to generate an estimate of the future demand profile of an electrified RTG crane and cranes network (substation demand) for up to one-day ahead. Furthermore, the impact of the exogenous variables estimation as input variables on the forecast model's accuracy will also be examined. The load forecast model will be the main tool for the estimation of any financial or technical risk that may occur in the future resulting from demand volatility.

-
- Design optimal energy control strategies of the ESS based on the load forecasts of the RTG cranes network to minimise the electricity energy costs and achieving the maximum possible peak demand reduction. The optimal energy controllers aim to take into account the volatility of the crane demand behaviour and use the difference in electricity tariff during the day at the PoF to maximise the benefits of using an ESS. This control strategy is compared to standard industrial control and should demonstrate a better operation performance and higher efficiency.
 - Study and identify the effect of locating a central energy storage system at a substation feeding more than a single electrified RTG crane and analyse the storage device performance in different location scenarios.

1.6 Contribution to the Literature

The literature review, Chapter 2, presents the past and current literature for the control techniques of an ESS in the LV distribution network and RTG crane system, to support the research problem statement presented in Section 1.4. Through the present literature evaluation, a number of the gaps in the research have been identified, which have motivated the need for the research presented in this thesis and highlighted the potential benefits of the work to the industry sector and the research community. This thesis aims to fill the gap in the literature through several novel aspects that are summarised as follows:

- I. This research provides an analysis of the network of electrified RTG cranes demand under a real operation time periods and identifies the correlation between the current time electric demand, the historical demand and exogenous variables. This analysis aims to fill the gap and address the lack of understanding of energy demand behaviour at port applications and use it as a vital tool to develop power generation strategies, and reduce gas emissions, peak demand and electricity costs.
- II. Forecast models to generate a future demand profile for an electrified RTG crane and network of electrified RTG cranes (substation demand) for up to one-day ahead are developed in Chapter 4.
- III. A Model Predictive Controller (MPC) and Stochastic MPC for RTG crane network connected to an energy storage device are presented in Chapters 5 and 6. This research shows a receding horizon controller that helps to decrease the electricity energy costs

and achieve maximum possible peak reduction, taking into account the high volatile demand behaviour and uncertainty in the crane demand prediction.

- IV. This research investigates the energy storage performance for a network of two RTG cranes at different location scenarios to give sea ports an initial indicator regarding the possible location of ESS in line with economic evaluation and cost saving analysis.

1.7 Publications

The majority of the results of the research presented in this thesis have been published in peer review journals, as following:

Journals

- Alasali, F.; Haben, S.; Becerra, V.; Holderbaum, W. Day-ahead industrial load forecasting for electric RTG cranes. *Journal of Modern Power Systems and Clean Energy*, Springer, vol.6, pp. 223-234, 2018. (I.F 2.12).
- Alasali, F.; Haben, S.; Becerra, V.; Holderbaum, W. Optimal energy management and MPC strategies for electrified RTG cranes with energy storage systems. *Energies*, MDPI, vol. 10, 2017. (I.F 2.67).
- Alasali, F.; Haben, S.; Holderbaum, W. Energy management systems for a network of electrified cranes with energy storage. *International Journal of Electrical Power and Energy Systems*, Elsevier, vol. 106, pp 210-222, 2019. (I.F 3.61).
- Alasali, F.; Haben, S.; Holderbaum, W. Stochastic Optimal Energy Management System for RTG Cranes Network Using Genetic Algorithm and Ensemble Forecasts. Submitted to *Journal of Energy Storage*, Elsevier, 2018.

Book

- A book proposal with title “Energy Forecasting and Control Methods for Energy Storage Systems in Distribution Networks” has been accepted by Springer. Prof. William Holderbaum, Dr. Stephen Haben and Feras Alasali are the authors of this book that is expected to be published by March 2020.

Conference proceedings

- Alasali, F.; Haben, S.; Becerra, V.; Holderbaum, W. Analysis of RTG Crane Load Demand and Short-term Load Forecasting. *International Congress on Advances in Engineering and Technological Developments conference*, London, 2016.

-
- Luque, A.; Alasali, F.; Holderbaum, W.; Becerra, V.; et al. Energy reduction on eRTG. IEEE 16th International Conference on Environment and Electrical Engineering (EEEIC), Florence, 2016.
 - Alasali, F.; Becerra, V.; Holderbaum, W. Energy Reduction and Peak shifting on a Network of Cranes. International Conference on Energy, Environment and Economics, Edinburgh, United Kingdom, pp. 137-143, 2016.
 - Alasali, F.; Becerra, V.; Holderbaum, W. Peak power reduction for electrified Rubber-Tyred Gantry (RTG) cranes using energy storage. 8th International Symposium on Automatic Control - AUTSYM" conference, Germany, 2017.

1.8 Thesis Outline

The structure of this thesis is focussed on two main areas: firstly, data analysis and development of a load forecast model. Secondly, the optimal energy management controllers based on load forecasts that aims to minimise the electricity bill and maximise peak demand reduction. The remaining chapters of this thesis are organised as follows:

- **Chapter 2** presents the current and past research to support the problem statement. This chapter will provide an extensive literature review which focuses on load forecasting, optimal control strategies of energy storage for power distribution network and RTG cranes.
- **Chapter 3** gives a detailed analysis and understanding of the electrified RTG crane demand behaviour and characteristics by investigating the crane demand seasonality and the relationship between the demand of the crane and the exogenous variables. This understanding is a key tool to develop an accurate forecast model and more efficient optimal energy control system.
- **Chapter 4** focuses on developing different forecast models to predict the RTG crane demand for up to one-day ahead and to examine the impact of the estimation of the exogenous variables (in particular the number of crane moves and container gross weight) on the prediction model accuracy.
- **Chapter 5** introduces the receding horizon optimal energy management, Model Predictive Control (MPC), for increasing energy cost savings and reducing the greatest possible peak demand in network of RTG cranes, taking into account the electricity prices, high level of volatility of cranes demand. This chapter will present the

fundamentals of the ESS control for the RTG crane network in order to minimise electricity costs and peak demand, including a conventional technique used for benchmarking the ESS performance.

- **Chapter 6** presents a Stochastic Model Predictive Control (SMPC) model for the RTG crane network with an energy storage system. The SMPC is presented to take into account the high volatility of the crane demand and the uncertainties in the forecast estimate, in order to increase energy cost savings and improve peak reduction.
- **Chapter 7** evaluates and reviews the results of optimal control strategies of energy storage devices in the network of RTG cranes compared to benchmarking techniques. Also, this chapter presents a comparison analysis for the control algorithms presented in this thesis, including the electric energy cost saving and peak demand reduction in the RTG crane network equipped with an ESS in different location scenarios. In addition, the evolution of the economic impact of the ESS is discussed in details in this chapter.
- **Chapter 8** presents a summary of the research outcomes and detailed conclusion, related to the thesis problem statement. Furthermore, this chapter provides recommendations for potential future work based on the research presented.

Chapter 2: Literature Review.

2.1 Introduction

Oil price fluctuations, gas emissions, and increasing electricity demand have caused significant energy and environmental challenges for ports across the world. The electricity demand in ports is expected to increase significantly in the near future due to the shift towards using electrified RTG cranes. This electrification process will require port operators to upgrade the electricity distribution network to meet the new higher demand. An ESS can potential provide a viable alternative to conventional reinforcement on the LV network, which requires upgrading the existing electrical infrastructure. The previous chapter showed that an ESS control model is an important component to achieving the greatest storage device performance and increasing energy savings. With a target of investigating how load forecasting of electrified RTG cranes can be used to develop an optimum energy storage control model to reduce energy costs and achieve the maximum peak demand reductions at ports, two main categories of research are discussed and examined in this chapter:

- Control algorithms for Energy Storage Systems (ESS) in RTG crane and LV network applications.
- Load forecasting, discussing the forecast techniques and role of load forecasts in the LV network.

This chapter aims to explore the current literature of those categories and provide a critical review of the main relevant works to the research topics in this thesis.

2.2 Control Algorithms of Energy Storage Systems for RTG Crane and Low Voltage Network Applications.

Electricity demand has, and is expected to continue to, increase significantly due to high levels of electricity usage from new electricity applications such as electrical vehicles and air conditioning. This is expected to put more pressure on energy suppliers and infrastructure. However, in such situations suppliers might not be able to generate extra power or extend the existing system with generation units, transmission lines, or distribution networks. A possible solution is peak shifting by using an ESS which aims to reduce peak demand by shifting part

of the peak load to a low demand period. This has advantages, for example avoiding the need to build new electricity infrastructure and reducing overall energy costs [11]. As previously discussed in Chapter 1, an ESS can play different roles on an LV network such as power smoothing, voltage and frequency control and energy cost savings. In electrical distribution networks and port applications, an ESS could play a vital role in reducing peak demand. This process is known as load shedding. The peak demand can be defined and specified as significant peaks based on the objective of the specific research study, such as minimising energy cost, daily demand and demand over a specified period of time. In addition, the precise definition of peak demand includes the role of selecting significant peaks which can be different from one type of load to another or from low voltage to high voltage networks. For example, Gyamfi et al. [23] described the peak demand as “the highest demand that has occurred on a utility network over a specified period of time”, in this definition, the peak demand is conditioned on time and value. Furthermore, Saadat (1999) [24] defined daily peak demand as the greatest, or maximum, value of load during a 24-hour period. However, the highest demand during the 24-hour period might not be a significant peak based on the definition by Sun et al. [25], Sun et al. determined that the significant peak demand period is when demand draws above a specific value. Therefore, the highest demand during the day may not be a significant peak, that needs to be reduced. In addition, the peak period may be defined based on the peak time interval and when it occurs, so generally the peak period will be different in each case study [26]. Zhang et al. [26] specified and calculated the peak demand as the maximum average power consumption measured over each 15-minute time interval during the day. In another work, Nicholls et al. determined the peak demand period based on the Time of Use (ToU) method and specified the peak demand as the average hourly demand during the daytime from 15:00 to 21:00 [27].

Electrical load often has a significant seasonal and daily peak period for distribution power network applications, for example the residential sector. Peak demand has been investigated widely [28] [29] [30] [31] and studies have verified and defined peak demand in a variety of ways for low voltage network applications. Generally, peak demand in the residential sector occurs on hot summer days when the air conditioning starts to be used and on cold winter days when electrical heaters are used. Furthermore, there are many parameters that may affect the peak demand period such as population growth, economic situation, weather conditions, special events, and calendar dates [28] [29] [32]. In order to meet the peak demand

that occurs for a few hours during the year, electricity providers are required to increase generation capacity and manage this peak demand. The electricity utilities may face power quality problems such as voltage disturbance and frequency variation if they fail to cover the peak period. In general, the peak demand only occurs for approximately five percent of the time and one fifth of the power generation capacity is required to meet that peak demand [24]. While many papers have investigated the peak demand of LV applications such as residential demands, there is lack of understating of the electrical demand behaviour of an electrified RTG crane over a long period of time.

Typically, the ESS is controlled and designed dependent on the main target or aim of the ESS. In order to explore how controlling an ESS in the correct way can improve storage device performance and increase peak demand reduction in the LV network and RTG crane, this chapter will go through the literature of ESS control algorithms that have aimed to reduce the peak demand. This chapter will also introduce the current state of the literature studying ESS benefits for RTG cranes and LV network applications. The ESS controllers are commonly divided into two main research areas in the literature for LV network and RTG crane applications: conventional control strategies and optimal management systems [7] [33]. Figure 2-1 shows the spectrum of ESS control methods based on a literature review in this work and the study by Rowe et al. [33] and Pietrosanti et al. [7].

1. Conventional control strategies such as set-point controller and Proportional Integral (PI): this type of storage controller aims to generate a control decision based on a reference value such as frequency, voltage and power. The reference value is determined based on *a priori* network data and expert knowledge. These conventional controllers have been widely used in RTG crane systems with storage devices for reducing gas emissions and peak demand [16] [17] [34] [35]. Furthermore, the set-point controller is also used as a standard benchmark control system for an ESS in low voltage networks [33] and RTG cranes [7]. However, these controllers are principally limited for controlling volatile demands, solving complex energy problems and targeting the peak reduction and cost savings over one-day time periods, as they are sensitive to the reference value and use no knowledge of the potential future demand.

2. Optimal controllers: this control category can be further split into optimal controllers that use, and do not use, forecasts data. The optimal controller aims to find the optimal operation plan for the ESS based on the network and storage parameters and the main target of using the storage device in the network. However, they are more complex, with higher computational costs, compared to the set-point controllers. Developing an optimal controller that use the forecast data is one of the thesis objectives. Throughout the literature, this storage control algorithm can be classified into two main categories:

- Optimal controller based on full future knowledge: this type of control revolves around employing a perfect forecast with full knowledge of what the system will do in the next period of time. A planning operation schedule and optimisation controller for the energy storage systems have been developed in the literature that use perfect forecast rules to increase the energy savings. Hellendoorn et al., in [36], developed an optimal control model for diesel RTG cranes to reduce peak demand and increase cost savings by assuming a full instantaneous knowledge of the fuel consumption and costs. Similar to Hellendoorn et al., Alonso et al. created an optimal scheduling control for charging electric vehicles to reduce the peak demand in LV networks by assuming that the time of connection for charging and the initial and final state of charge are known. The literature shows that an accurate forecast model is significant to optimise the ESS operation and increase the energy savings. However, assuming full future knowledge is not practical in practice, especially for high volatile demand applications where the forecast error and the uncertainty terms are the main part of the model design.
- Optimal controllers based on load forecasting: these controllers can be designed for multiple objectives to find the optimal operation for an ESS by minimising and maximising a cost function over a specific time period using forecast data. However, forecasting errors have a significant impact on the ESS operation model and results. Therefore, receding horizon, Model Predictive Controller (MPC) and Stochastic Model Predictive Controller (SMPC), controllers have often been effectively developed within stochastic

and volatile applications such as microgrids which involve high uncertainties and volatile demand to increase peak reduction by using rolling forecasts and uncertainty estimates to improve the ESS performance without assuming the perfect demand forecast. In general, there is significant potential for using forecast profiles to feed an optimal ESS control, therefore developing a stochastic optimisation model or MPC is an ideal candidate for reducing the impact of forecast errors and increasing ESS efficacy.

The next sections will discuss the current controlling algorithms tested for ESSs that aim to reduce the peak demand and increase energy savings in RTG crane and LV applications. Firstly, Section 2.2.1 will present and review the current literature for controlling an ESS for the RTG crane systems. Secondly, due to the lack of literature for using forecast data to control an ESS in RTG cranes, Sections 2.2.2 and 2.2.3 will focus on the optimal energy management systems and receding horizon control algorithms for controlling an ESS on LV networks.

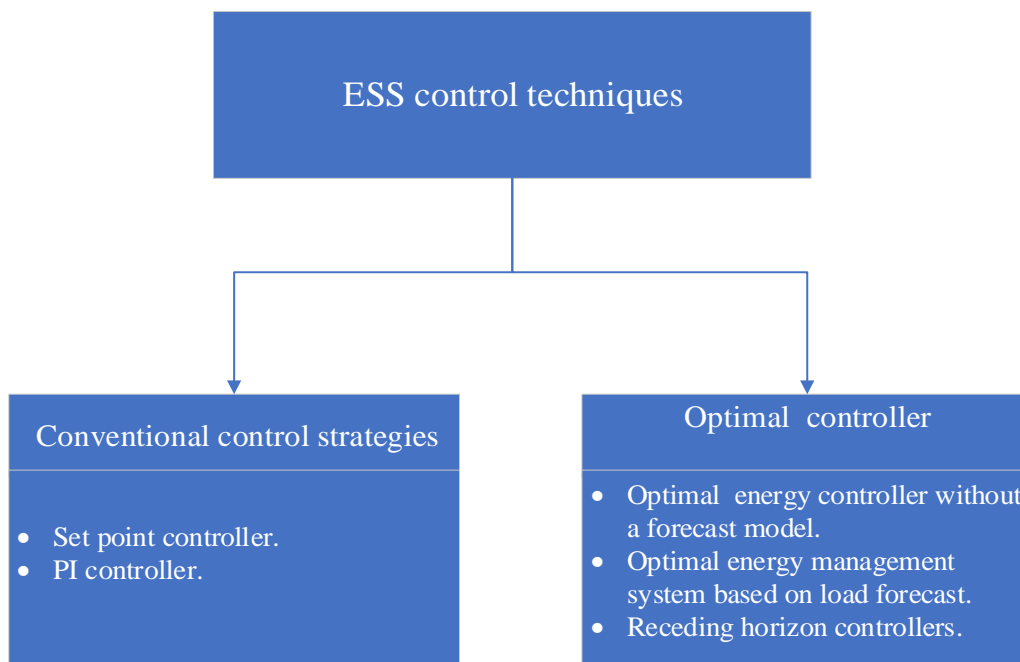


Figure 2-1: A simple classification of ESS control techniques.

2.2.1 Control of Energy Storage Devices for RTG Crane Systems.

There are two main energy sources for RTG cranes: diesel and electricity. These cranes shift containers on a shipping port platform and organise it in the yard area. The configuration

of RTG cranes include various functioning state combinations of engine, motors and other parts that allow the crane to move and complete the required tasks. In an RTG crane system, most of the electrical energy or fuel consumption comes from hoisting containers of different weights to several heights. Furthermore, the peak demand increases when the RTG crane moves heavier containers [7] [19]. In the literature, Energy Storage Systems (ESSs) have been used to increase energy savings and reduce carbon green emissions under different control algorithms. Principally, the energy saving control strategies for the RTG cranes equipped with an ESS have mainly focused on using conventional control strategies (set-point control) and there is limited literature on using optimal energy control strategies.

Conventional control strategies:

The conventional control strategies use a reference value of voltage [17] [34], power [35] or State of Charge (SoC) [16] to save energy on a single RTG crane system equipped with an ESS by using recovered potential energy that has been generated during the lowering of the containers to charge the ESS and discharge it when the crane lifts the containers. The following literature uses conventional control algorithms for the control of the ESS to increase peak demand reduction and energy savings. These studies have not considered the highly volatile behaviour of the electrified RTG crane demand, the electricity prices or the benefits of using load forecasts as inputs to control the ESS, and thus potentially have a significantly limited performance. In addition, there have been no studies which specifically consider a central ESS located at the LV network side to feed more than a single electrified RTG crane.

Kim et al. [34] developed a hybrid energy sources model for an RTG crane including a supercapacitor energy storage. The ESS is connected to the RTG crane system by a Direct Current (DC) link through a DC/DC converter. Due to the different characteristics of operating voltages for different power sources (the ESS and the crane system), the DC/DC converter matched the output voltage of the energy storage device to control the power flow. A Proportional Integral (PI) controller regulated the ESS power flow by tracking the voltage error and generating a reference value that was fed into the ESS, charging when the voltage increases via the regenerative power and discharging when the voltage is under the reference value. An RTG crane, in [34], was equipped with an ESS to reduce the fuel consumption by 30% and gas emissions by more than 40%. The simulation analysis shows that the supercapacitor energy storage is suitable for transient peaks due to the high power density [34] [17]. The high self-

discharge rate of the supercapacitor increases the challenge of using the energy storage in line with the electricity prices or daily demand reduction. Zhao et al. [17] presented a hybrid energy storage model that included battery and supercapacitor energy storage. The aim of this hybrid model was to increase the life time of the battery system by using the supercapacitors for the transient peak charging and discharging. The control strategy in this model included a double closed-loop with the PI controller in order to control the battery and supercapacitor systems. In this proposed model, supercapacitors storage was charged by the battery system or the RTG crane regenerating energy which made the supercapacitors charge sustainable. The case study, in [17], presented a simulation based on one duty cycle operation with maximum container weight (40.5 tonnes), however the results would be of more interest if real time data had been used to supply the energy for 4 hours, the suggested operation time period. Flynn et al. [35] used a flywheel energy storage to reduce gas emissions and increase energy cost savings by minimising fuel consumption. Two units of the flywheel storage system are packaged together and connected to the DC bus link in the RTG crane. The aim of this paper was to reduce the power loss and simplify the motor design and control. The flywheel system was developed to reduce the peak demand by supplying the power when the crane hoists the container and absorb power during the lowering mode [35]. The storage system control measured the primary engine power and was designed to limit the total power to 50 kW by providing the extra power in the lifting mode. In general, the crane lifted the container under constant speed after completion of the acceleration period. The ESS control then gently reduced the output power of the flywheels to 120 kW until the ESS was completely discharged, allowing the diesel generator to gradually provide the rest of the required power and avoid generating high emissions. However, the analysis of the results in this study [35] didn't show the effect of the high self-discharge rate on the flywheel behaviour or efficiency over a long term period of operation. In addition, more investigation regarding the initial and maintenance costs of the flywheel energy storage device would have helped to analysis the economic benefits of using the system.

Niu et al., in [16], used a state of charge percentage to control the battery energy storage for an RTG crane system. When the SoC of the battery energy storage was less than 50%, the diesel generator in the RTG crane system was turned on to charge the battery and turned off when the SoC was more than 80%. The hybrid energy source (battery and diesel engine) fed the crane when the SoC was between 50% and 80%, and when the SoC was greater than 80% the hybrid model operated in pure battery mode. In [16], the data was collected over specific load cycles

with an operation time of approximately 2 hours. However, this research did not investigate and analyse the load profiles of the RTG crane over a long enough time period in order to select the significant peaks and the optimal operation for the energy storage device. Furthermore, the control method reduced the peak demand based on the SoC but did not introduce or investigate how the proposed control would help to increase energy savings in an electrified RTG crane.

The research reviewed has introduced various studies on energy savings for RTG crane operation by investigating the benefits of installing different types of energy storage (batteries, supercapacitors and flywheel) to reduce fuel consumption and gas emissions. The literature shows that the conventional control algorithms (PI, set-point) are effective and simple, but are principally limited, as it takes control decisions without any knowledge of the potential future demands. In addition, it shows a gap in the literature concerning daily peak load control, electricity energy prices and centralised energy storage systems that feed more than a single RTG crane at the port substations side.

Optimal power controller

There has been limited literature on using optimal energy control strategies for increasing peak demand reduction or energy saving of RTG cranes. Pietrosanti et al. [7] introduced an optimal power management strategy device for a diesel RTG crane with an ESS located on the DC side of the crane. The goal of the optimal power strategy presented by Pietrosanti et al. was to operate a flywheel energy storage device under optimal operation conditions with uncertain stochastic power loads by charging the ESS during the lowering of the containers and discharging it during the lifting stage [7]. The simulation results were investigated over one-hour test cycles and showed that the proposed optimal power controller achieved a peak reduction of 38.47% compared to 35.9% using a set-point controller. The optimal management controller in [7] assumed that the container weight was known in advance and did not target the energy cost savings based on the differentiation in the electricity price tariffs. In another study by Hellendoorn et al [36], an optimal power control algorithm was formulated for a hybrid RTG crane system (diesel power source and supercapacitor storage) to minimise the fuel consumption. The control model had been designed to find an ESS power output that minimises fuel consumption during the crane hoisting cycle by estimating the load during this cycle. However, the proposed control algorithm required a full instantaneous knowledge of the fuel consumption and costs. This control model had been designed, exclusively, to reduce fuel

consumption and thus cannot be applied in electric RTG crane systems. The simulation results presented only the reduction in fuel consumption.

Most peak demand reduction strategies in the RTG crane and port applications equipped with an ESS mainly focused on using conventional control strategies to charge and discharge the storage device. There has been limited work produced using optimal algorithms. However, of the few available studies, they only focus on using the recovery energy to reduce peak demand or fuel consumption as the objective, in a single RTG crane system, assuming full instantaneous knowledge of the fuel and container weights. Hence there has been no consideration of a network of cranes, daily peak demand, load forecast profile or electricity bill costs as inputs to an optimal control strategy. Therefore, the following sections will investigate the benefits of using an optimal control model based on load forecasts to control ESSs on LV networks.

2.2.2 Control Modelling Solutions to Improve ESS Benefits on LV Network.

This section will explore the literature concerning situations where ESSs are used as potential solutions for peak demand and energy costs problems on the electrical distribution network. In particular, reviewed in this section discusses applications where the load is highly volatile.

Hassan et al. [37] presented a residential LV network equipped with a battery energy storage and a Photovoltaics (PV) system, using a half-hourly dataset. The optimisation model maximised the revenue streams and evaluated the impact of the battery capacity on the objective function, based on the electricity tariff. The objective function aimed to optimise the storage devices charging and discharging cycles to achieve the greatest revenue increase from an existing PV and battery system for a single residential customer. The battery system worked by storing cheap off-peak energy and excess PV power output during the peak solar period and discharging during the high tariff period. This model was formulated as a Mixed Integer Linear Programming (MILP) problem and solved by the CPLEX solver [37]. Simulations were carried out by using half-hourly residential PV generation and electricity demand profiles, and explored how the behaviour may change with different electricity tariffs. Three case studies were investigated for a network system equipped with a PV system: one without battery storage under a flat tariff, another with a battery under two daily energy tariff (ToU) and one on a wholesale tariff which is determined based on the electricity costs purchased by energy suppliers. The research also introduced the impact of the using of an energy storage device on

energy cost savings under different electricity tariffs. The analysis results in [37], showed that the battery increased the proposed system's revenue but economically the system will only be profitable when the cost of the storage device falls below £138/kWh. However, the impact of the renewable (PV) generation uncertainty and demand forecast were not investigated in this paper. In 2017, Pena-Bello et al., presented an optimisation operation algorithm for a battery storage system for grid-connected housing with a PV system [38]. The optimal energy operation control model used a genetic algorithm to optimise the economic impacts in three case studies: load shifting based on the differences in electrical tariff, PV self-consumption, and a combination of the previous two cases. The researchers collected 1 minute PV generation and electricity demand data from a single-family house in Switzerland, that was then converted to 1-hour resolution data. The optimal control model generated a 24-hour ahead battery framework that aimed to minimise the daily electricity bill by assuming a perfect day ahead forecast profile for the electricity, PV power output and electricity prices. The results showed the potential impact from of using a forecast profile to maximise the profit of using PV and battery systems. The economic analysis results for the optimisation control model showed that the battery storage system can be economically profitable in cases with a battery price of 157£/kWh with a 2% annual increase in the electricity tariff. The model in [38] assumed a perfect forecast for the residential load and PV generation which is unrealistic in practice. The research does not consider the impact of forecast error or the variability of the PV generation on the operational model and results.

As previously discussed, load forecasting is an important tool for increasing energy savings, and is essential for volatile LV demand behaviour, variable renewable energy and electric vehicle demands [39]. Wu et al., in [39] developed a stochastic dynamic programming control method for an energy storage device (Tesla Model) for a grid-connected smart home equipped with PV and a plug-in electric vehicle system. The control model aimed to minimise the energy costs under a ToU tariff and meet the home electricity and electric vehicle charging demand. In this control model, the Radial Basis Function Neural Network (RBF-NN) forecast method was selected to generate a future daily demand profile on an hourly basis for PV power output and home electricity demand. To predict the PV power output, the time of day and ambient temperature are used as input variables, while time of day, next day of the week, and temperature are used for the home demand forecast model. The stochastic energy management model was designed to handle the uncertainties that come from electric vehicle charging time,

variability of PV power and the home forecast demand by using a Markov chain and dynamic programming modelling framework [39]. However, to generate the forecast profiles and run the energy management control, the authors assumed that the charged energy was fixed and equal to a specific magnitude (12 kWh). They also assumed a specific hour for plugging in and unplugging the electric vehicle. The simulation results show a significant energy cost saving using the stochastic dynamic programming control compared to the same model without the proposed optimal control model.

The previous literature [37] [38] [39] has shown that accurate forecasts are important to optimise the control of an ESS. This literature has introduced the optimal control of ESS based on load forecast as a key feature for improving the peak reduction and the cost savings. However, it has widely focused on developing different planning, operation schedules based on full future knowledge to increase the energy savings by assuming a perfect forecast for the residential load and PV generation [38] which is unrealistic in practice and assuming that the charged energy was fixed and equal to a specific magnitude in [39]. The literature has shown that an ESS model can achieve a higher performance when the demand is accurately predicted. For example, Riesen et al., [40], presented a comparison analysis of using a real versus a perfect forecast models for LV networks connected to a residential battery storage and a PV system. The linear optimisation control model used 15-minute resolution PV and load data, to increase peak reduction and energy cost savings and minimise losses. Furthermore, the study investigated the effect of using a centralised storage system for an aggregated load of 44 households on an LV network. The results showed a reduction in the overall energy between 0.4% and 1% when the centralised storage is used compared to a local storage device. The perfect forecast model improved the control algorithm performance by 37% compared to the real forecast model [40]. This is mainly related to the weak forecast performance during the days that included low temperature. However, by introducing rolling forecasts and including additional external variables to the prediction model the performance of the ESS using a real forecast can be improved. Continuing this trend, Vieira et al. studied the impact of forecasts on minimising energy costs and matching generation and consumption for residential buildings connected to an ESS and PV system [41]. The lithium-ion battery system was used to store, and discharge energy based on the mismatch between the PV generation and the residential building's energy consumption [41]. The objective of the ESS control model was to reduce the energy bills by minimising the power flows between the residential building and the LV

network. A simple forecast model was developed to forecast the net energy demand for up to a day ahead. The forecast model generated a future net demand profile based on only the previous day, so the forecast profile matched the actual net demand of the previous day [41]. The analysis of the results of the proposed management strategy showed that the power flow between the grid and householder was reduced by 76% and there was an 84% reduction in the energy bill. The economic assessment shows that the proposed ESS solution can be cost-effective in cases where the price of the battery system is under 166£/kWh. The inaccurate forecast model was the main limitation of the control strategy, where it does not take in account any external variables such as temperature or seasonality terms in the demand that can help the model to improve the forecast performance and the ESS efficacy. The non-smooth demand behaviour of the LV network applications with regards to ESS optimal controlling based on load forecasting is a difficult problem to solve, as discussed in [37] [40] [41].

Due to the high stochastic and volatile nature of renewable energy sources and LV demand, it has been predicted that the need for a more flexible energy management systems including different economic, energy saving and ESS charging scenarios will play a significant role in future LV network systems. Mohamed and Koivo presented an optimal operating strategy for a microgrid system to reduce the energy and gas emission costs and meet the required demand [42]. The proposed dispatch energy management model [42], was based on a genetic algorithm and used the historical data and previous solution scenarios to improve the control model performance. The energy management response was affected by the weather conditions and the actual demand load. By considering rolling load forecasts and real-time weather forecasts, the performance of the energy management system in [42] could potentially be improved. Hu et al. developed an optimal controller for an LV network system connected to a battery energy storage device and a wind turbine power source [43]. The optimal controller used a rolling load forecast profile to solve the optimisation problem, and showed that the proposed control model was more effective compared to a fixed forecast horizon controller. However, no demand forecast error or wind generation uncertainty terms were considered in the optimisation problem. The following section will present the literature which shows the benefits of using the receding horizon controllers to improve the ESS performance.

The literature discussed in this section has introduced the optimal control of ESS as key feature for improving the peak reduction and the cost savings. The literature has shown that an ESS

model can achieve a higher performance when the demand is accurately predicted. Therefore, the research has widely focused on developing different planning operation schedules and optimisation controllers for ESSs based on full future knowledge to increase the energy savings. As previously discussed, very accurate forecasts are not typically possible on the distribution network, where the electrical demand is highly volatile. However, it is clear that demand forecast models, even in LV applications, have the potential to optimise the storage device control performance for peak reduction and cost savings by using realistic prediction models. In general, there is limited literature on using actual forecast data to feed optimal controllers or investigate the impact of the forecast error on the ESS control performance in LV applications. The parameters of each forecast model in the literature were chosen based on specific research needs and availability of the data. The exogenous variables play a key role in improving the forecast model's performance and different assumptions have been made to reduce the forecast error or fill the gap in the data available. In the previous literature, the specific assumptions of each work helped the researchers to classify the data and forecast the demand. However, they do not show the impact of these assumptions on the forecast model accuracy. In addition, the exogenous variables such as the weather conditions or traffic information can minimise the errors in the model and help to improve the forecast performance. Overall, choosing a suitable exogenous variable plays a significant role in improving the forecast performance and these variables are mainly selected based on model targets and data availability. Yet, the literature does not show in enough detail the impact of the exogenous variables for LV applications on the forecast model accuracy. The following section will investigate how receding horizon control method can help to minimise the impact of the forecast error on the ESS control performance. In the optimal control algorithms for the LV network application with an ESS, deterministic forecasts or stochastic processes have been used to support optimal control solutions. The translation of these control techniques to optimise the energy flow in an RTG crane system and the electrical port networks for minimum electricity energy costs and peak demand have not been established before in the literature and this is one of the focuses of this thesis.

2.2.3 Optimal Energy Controller Using Receding Horizon

As previously discussed, load forecasting accuracy is the main challenge to the development of a highly effective real time controller for an energy storage system. The controller may be affected by the forecast error and cause a suboptimal or detrimental discharging and charging

schedule. However, an accurate load forecast is still a key tool for improving the control sequences decisions. The energy storage optimisation problem can be improved by updating the control schedule for each time interval in advance based on the actual load measurements. This is mainly to reduce the impact of the forecast error on the control system. A Receding Horizon (RH), as described in Figure 2-2, is used in different areas of research as a control method that computes the control decision over the load forecast profile based on the optimisation rule, then implements the first control based on the forecast data. Before starting the next time interval, the model updates the model information based on the first control action and repeats the control operation for each subsequent time period. A RH controller, such as Model Predictive Control (MPC), generates an optimal decision by solving a chosen cost function under a number of model constraints. The MPC controller uses the forecast profile, over a finite horizon, to compute an optimal control decision at the current time [28] [44]. In general, a RH optimal controller is an ideal method of reducing the impact of forecast errors and optimising the control solution for an ESS.

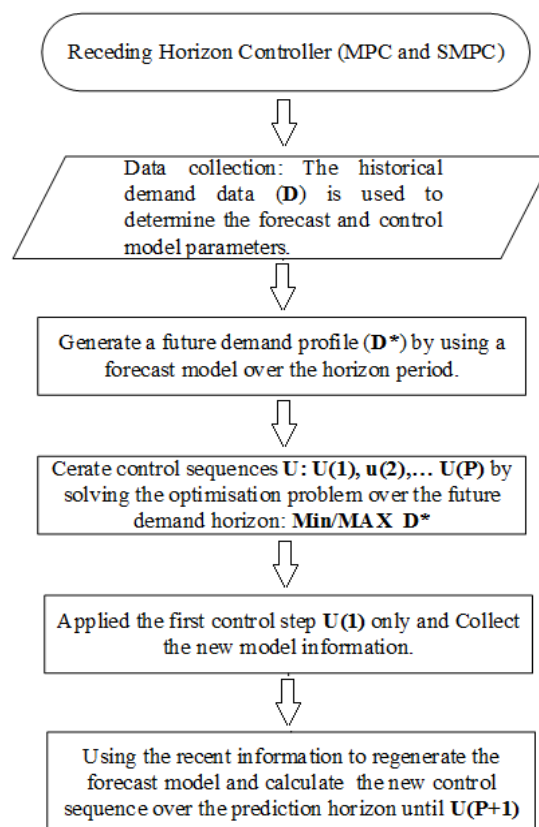


Figure 2-2: General schematic diagram for the receding horizon controller (MPC and SMPC).

2.2.3.1 Model predictive control of an ESS.

MPC controllers are commonly used within microgrids and low voltage network applications that involve high uncertainties in demand applications, to decrease the operation costs and increase system efficiency. For example, Rowe et al. [33] presented an MPC controller that allows distribution network operators to control the energy storage systems under operational constraints on a low voltage network that feeds domestic customers. The MPC controller integrates a deterministic forecast with the objective of maximising the peak reduction of the distribution network [33]. The simulation results show that the MPC controller, on average, outperformed the set-point controller for a LV model of the domestic customers demand profiles (aggregation demand). An MPC technique with an application in microgrid systems has been discussed [45]. As in the study of Rowe et al., Oh et al. [45] developed an optimisation scheme for an islanded microgrid, using an MPC strategy. The use of an MPC in controlling diesel power sources and renewable sources with an ESS successfully manage to minimise the operational cost [45].

Stochastic load forecast with a scenario-based MPC model of a microgrid system with Electric Vehicle (EV) integration was presented in [46]. The aim of the optimal management controller presented by Ji et al. was to optimise the economic performance of the electricity demand and the EV charging demand. However, one forecast model [46], was developed based on having knowledge of the EVs charging schedules in advance, so they assumed that they would know when the electric vehicle needed charging. In cases where the charging requests are unknown, the MPC controller applied the worst-case scenario and set the boundary at the greatest possible charging load. Zhang et al. [28], also presented a Model Predictive Control (MPC) strategy for microgrid systems. The objective of the control model was to minimise the electricity energy costs in a microgrid system with renewable energy resources and an ESS. The optimisation time interval for the proposed model was one-hour resolution for a one-day time horizon and the battery efficiency was assumed to be one (no power losses). In order to explore the forecast error impact on the energy management system, the MPC controller was tested under different levels of forecast errors. The analysis of the results showed that increasing the forecast errors, increased the energy costs. The MPC helped to reduce the energy cost compared to a fixed day-ahead programming control model that does not consider any update for control and prediction data variables. The research in [28] did not focus on the forecast methods or use actual forecast data, and instead, they used a simulation model to

generate different levels of forecast errors. As previously discussed, ESSs play a key role in LV network support such as power levelling and load shifting. To meet the demand scheduling of the grid, Xiong et al. [47] presented a real-time MPC to optimise the power flow for a wind farm system equipped with an ESS. The objective function of the MPC controller contained three sub-objectives with control and prediction horizon size equal to 24 hours: firstly, it aimed to reduce the impact of a wind curtailment factor; secondly, to increase the ratio of generated wind power fed to the power grid; thirdly, to maintain the generation of power to the grid. The MPC controller successfully followed the power plan of the electrical power grid system [47]. Instead of using real forecast data, the research in [47] added a random noise to actual demand data. In other work, MPC controllers have been used for large scale ESSs located at wind power plants to improve the energy dispatchability [48]. The simulation results have shown that an ESS with model predictive control (MPC) can reduce the generation plan errors to meet the power grid needs by approximately 80% [48]. The proposed MPC model tested by using 7 days of data and the forecast wind farm generation demand was provided by a third-party, the Bonneville Power Administration. In general, these sets of studies show the potential effectiveness and capabilities of using MPC as an ESS control technique.

Uncertainty in MPC system

The volatile and stochastic demand behaviour on electrical distribution network applications increase the challenge of accurately predicting the LV demand. As discussed in the previous section, forecast error and uncertainty have a significant impact on MPC energy storage control algorithms. Uncertainty and forecast error impacts on MPC solutions have been discussed in the literature [28] [46] [49]. The research, in [50], formulated a hybrid renewable energy system with battery energy storage in a family residential home, using an optimal energy operation strategy based on an MPC algorithm to minimise the energy costs and meet the electricity demand. Due to the high level of uncertainty regarding weather conditions that effect the renewable sources output, Wang et al. [50] used real time hourly weather forecast data to reduce the impact of uncertainty. For customer energy demand side, a day-ahead demand scheduling algorithm was used to generate the energy consumption for a single-family house. This schedule aimed to shift the flexible loads, such as washing machines, to match renewable generation output. Both the real time weather forecast, demand response schedule, and rolling updates helped the MPC control model to handle the uncertainties and increase the overall

system performance. This is showed the significant of using rolling forecast model to minimise the error impact of the optimal control performance. Wang et al. [50] assumed that the electricity consumption of a residential home was perfectly forecast in order to match the renewable output. In the research presented in this thesis, an imperfect forecast model for highly volatile demand is considered, unlike the study of Wang et al. [50]. Forecast errors in the prediction demand model used in an MPC controller are discussed in [51]. Holjevac et al. presented a microgrid system including electricity demand and energy storage that operated to meet consumer needs and minimise costs by using a receding horizon controller. The Holjevac et al. work [51], showed that the efficiency of the energy operation model depends on demand and generation prediction output, and daily correction of the MPC controller schedule. The operating horizon size for the MPC model was one day ahead with 48-time steps similar to [49]. The corrective schedule aimed to update the initial operation points, this helped to reduce the impact of the forecast errors by updating the demand and control model data at successive time steps. However, the receding horizon controller was designed to minimise the energy costs only based on the energy and balancing prices and did not investigate the peak demand reduction for the households in the network.

The previous set of literature, discussed in this section, presents the impact of uncertainty and forecast error in RH controller and shows the significance of studying this impact. Furthermore, it showed a considerable evidence supporting the capability of forecasts to improve optimal energy management controller performance [49] [50]. There are a limited number of studies that have discussed the impact of uncertainty in LV applications or electrical industrial demands with regards to ESS performance.

2.2.3.2 Stochastic model predictive control of ESS.

The difficulty in forecasting the LV demand due to highly volatility adds a significant uncertainty to the control of the ESS. The energy model output will be contingent on the forecast model's accuracy [28] [50]. The majority of the literature for MPC controllers have considered the load forecast as a deterministic process [51]. However, the electricity demand forecast can also be modelled as a stochastic process. Stochastic optimisation techniques are a special subset of mathematical programming algorithms that use objective function problems which take into account uncertainty to improve the system performance. Additionally, as previously discussed the receding horizon controller can increase the efficiency of ESS control.

Hence the research presented in this thesis will consider the Stochastic Model Predictive Control (SMPC) to treat the both uncertainty in the load forecast and update the control at successive time steps. In general, the SMPC problems in LV applications are solved by general optimisation solvers such demand scenario trees [33] and dynamic programming [53].

Rowe et al. [33] presented a stochastic receding horizon controller, SMPC, for ESS's in several LV distribution networks. The objective function for SMPC, aimed to achieve the maximum possible peak demand reduction under high levels of forecast demand uncertainty. The SMPC treats the uncertainty term by minimising the expected performance for a given cost function. In [33], a scenario tree, which comprised of potential future scenarios, was developed to present possible scenarios for electricity demand based on the historical data in line with their associated probabilities. The future demand scenarios, combined with the MPC to develop a SMPC, rapidly increased the size of the optimisation problem in every time step and thus increased computational costs. Hence, Rowe et al. [33] introduced an algorithm to select the number of nodes and reduce the tree scenario branches. The results in [33], showed that the SMPC algorithm outperforms set-point and MPC controllers of ESS. The objective function, in this study [33], only included the peak demand reduction, without taking into account the energy cost. D. Zhu, and G. Hug [52] presented a SMPC to optimally operate generation demand, renewable energy and an ESS, in a microgrid system. The cost function aimed to reduce the energy costs and meet the required demand for one step ahead. To solve the SMPC problem, [52] employed a decomposition technique to reduce the overall computation time by decomposing the scenarios into subproblems and solve in parallel. The work successfully shows that the computation time for SMPC can be reduced by dividing the main objective into subproblems [52]. In the proposed SMPC, the load profile was assumed to be deterministic over the horizon, and hence did not consider the forecast load uncertainty. The previous set of literature showed the significant of treating the forecast uncertainty term in LV network by creating number of customers [33] or generation [52] demand scenarios.

Stochastic energy management controller based on Dynamic programming (DP) have been effectively used to increase energy saving in buildings [53] [54], microgrid applications [55] [56] and electric vehicles [57] [58]. For example, Xie et al. [58] explored how, by using stochastic optimisation based on SMPC with Dynamic programming (DP), it was possible to minimise the fuel consumption in hybrid electric buses. An energy management strategy

considered the uncertainties of the bus velocity and prediction error. The analysis of the results shows that the proposed energy management strategy (SMPC) based on a Markov Chain Monte Carlo forecast method and DP can smooth the volatile power and reduce the fuel consumption by finding the optimal operation for the bus batteries. Recently, He et al. [59] presented a predictive energy management, MPC, strategy for an electric bus, using a DP and Monte Carlo prediction. The energy management targets were to improve the air-conditioners energy efficiency and reduce the energy consumption in the electric bus. The study successfully shows that the predictive control management can reduce the energy consumption by 5.8% compared to bang-bang (set-point) control on the electric bus [59]. The energy management system in [59] uses a prediction model to predict the number of passengers and heat load in the bus, however, they assumed that heat load was equal to the average value for all passengers and the bus follow a fixed driving pattern.

In this section, a Receding Horizon (RH) control methodologies for LV network applications and ESSs have been presented and reviewed. In different cases, the literature has introduced the significance of using RH controllers with forecast models compared to single step control algorithms. ESS control algorithms and energy management strategies for LV network utilising receding horizons have been the focus of most research recently. In these receding horizon algorithms, the deterministic forecasts or stochastic process has been used to estimate the demand. The transition of these control algorithms to a network of RTG cranes specifically for electricity energy cost savings and peak demand reduction has not been discussed before in the literature, therefore this is one of the focuses of this thesis. The literature discussed in this section has introduced the optimal control of ESS based on load forecast as a key methodology for increasing peak reduction and cost savings. In addition, an ESS model can achieve a higher performance when the demand is accurately predicted. Therefore, the following section will explore the literature for short-term load forecasts for LV applications.

2.3 Load Forecasting in Power Systems.

This section will explore the current literature of relevant load forecasting algorithms that have been used to predict demand and utilised in optimal controllers to achieve the greatest energy cost savings and peak reduction on the electrical distribution network. In Section 2.3.1, an overview of load forecasting techniques will be introduced and compared. While many papers have discussed and investigated load forecasting concepts for buildings, industrial loads,

renewable energy and electrical vehicles, load forecasting for RTG cranes and port substations has not been previously considered. Hence, section 2.3.2 presents the load forecasting algorithms in the current literature surrounding low voltage network applications as closet surrogate problem to RTG crane forecasting.

2.3.1 Overview of Load Forecasting Techniques

Load forecasting is an important tool used to estimate the future energy or power consumption and in general aims to minimise utility risks and power costs in power planning, operation, and traditional power control [60] [61]. An accurate forecast is the basis for reducing operational costs and using different energy sources to create a secure power system. Furthermore, accurate forecasts are an effective tool for energy management system problems such as load shedding, peak demand reduction and electrical infrastructure development by providing the necessary information for making informed decisions. Electrical load forecasting is a complex procedure, due to the volatility and potential number of factors affecting the forecast model accuracy. The historical load values, weather factors (temperature, humidity and wind speed), season, economic situation and demographic data are some of the major factors considered in most of the load forecasting models [61] [62]. This section will introduce and compare a selection of load forecasting methods that have been used to predict electrical and peak demand, especially for highly volatile load situations. Finally, the literature will be reviewed to present the role of load forecasting in low voltage network applications and how they are used with an optimal controller to increase energy savings. Load forecasting algorithms have been discussed and investigated extensively in the recent literature, for example [60] [61]. These researchers divided load forecasts into four different categories based on the prediction horizon as described in Table 2-1.

Table 2-1:Categories of forecasts based on the prediction horizon.

| Forecast categories | Explanation |
|----------------------------|---------------------------------------|
| Very short-term forecasts | From a few minutes to one hour ahead. |
| Short-term forecasts | From one hour to several days ahead. |
| Medium term forecasts | From one week to one year ahead. |
| Long-term forecasts | From one year or more ahead. |

In power system applications, short-term load forecasting has been used widely for operation scheduling, power system stability and economic operations. A large variety of methodologies

and models have been employed in order to achieve an accurate load forecast. These models are mainly divided into three main technologies: traditional or statistical methods, artificial intelligence methods and hybrid systems [62] [63], as shown in Figure 2-3. Figure 2-3 shows the spectrum of short-term load forecasting methods categorised according to the three main technologies based on a literature review in this work and the study by Papaioannou et al. [62]. The procedure of designing a forecasting model does not usually use a single-pass. It may be required to visit previous steps before finalising the model, especially between the training model, model parameters and variable selection steps. Therefore, it will require to split the data set into training, validation, and testing sets. In general, the training set is used to train the model and find the demand patterns and model parameters and the validation set is used to find the best model. The data size should give a trade-off between finding the best model parameters and model accuracy and avoid overfitting.

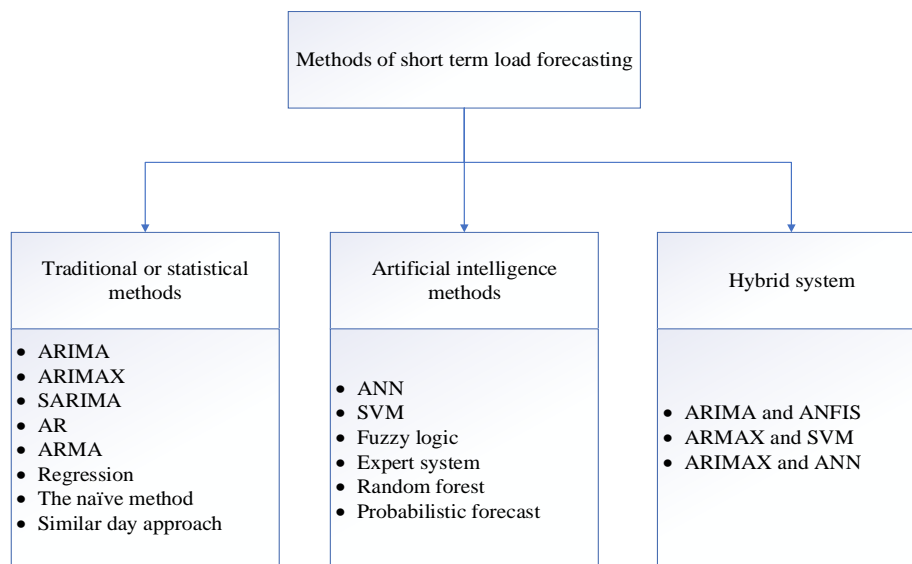


Figure 2-3: The spectrum of short-term forecasting methods according to the three main technologies.

2.3.1.1 Time or statistical series forecast techniques

These techniques are prediction methods that aim to present the data as a function of time and often used to forecast electrical load demand. In general, the traditional methods such as the naïve method [61] and linear and multilinear regression methods [60] may have problems modelling complex nonlinear time series [63]. However, the statistical methods are simple and easy to implement compared to other categories. Time series models have been developed based on the analysis of seasonal trends or patterns to forecast the time objectives ahead in many research areas such as weather, rainfall [64] [65], electric load demand [66] [67] [68],

and price forecasting [69] [70]. Generally, time series approaches include the following techniques: Auto Regressive (AR), Moving Average (MA) and Auto Regressive Moving Average (ARMA), and linear regression methods. The Auto Regressive Integrated Moving Average with exogenous variables (ARIMAX) method is a nonlinear model with the ability to work for linear models as well [67] [71]. Usually, ARIMA models are referred to as Box-Jenkins models due to ARIMA being more popular after 1970 when Box and Jenkins applied this method in their studies [72] [73]. ARIMA and ARIMAX models are two of the most popular time series models and have been widely used to forecast electrical load demand and other research areas that have highly stochastic load behaviour [67] [71]. However, using ARIMA and ARIMAX load forecasting models for RTG cranes and port substations has not been previously reported and investigated in the literature.

2.3.1.2 Artificial intelligence methods

The artificial intelligent forecast methods are mainly used to model complex and unknown nonlinear relationships for example the Artificial Neural Networks (ANN) model does not require any predetermined functional relationship between load and predictor variables [63] [74]. However, many of the intelligence forecast techniques such as ANN are described as black-box due to the lack of transparency of the results or models. The intelligence methods include mainly ANN [66], fuzzy logic methods [75] and support vector regression [76]. Generally, electrical load time series show stochastic and volatile behaviour in the low voltage distribution side of power networks. The nonlinear system of load behaviour, which has many exogenous variables such as temperature, wind speed and time period of-the-day, make short-term load forecasting more complicated [77] [78]. In order to solve these complex relationship and increase forecasting accuracy, many ANN models have been developed to predict LV demand [79] [80]. ANN forecasting models have been discussed and developed for a wide range of LV network applications such as microgrid systems and buildings that have a highly volatile and stochastic load behavior, as will be discussed in the following section. ANN techniques to forecast RTG crane and port substation demands have not been previously reported in the literature.

2.3.1.3 The hybrid forecast models

Recently, hybrid systems have been applied to increase forecast accuracy by combining two or more methods. Hybrid systems have mainly been developed to utilise the advantages of

each approach and ameliorate any weakness or disadvantages of any single method [60] [81]. The hybrid model may combine statistical methods and artificial intelligence methods such as ARIMAX and ANN [66], statistical techniques for pre-processing of data, neural network and price spike detection [81], Wavelet Transform (WT) and Least Squares Support Vector Machines (LSSVM) [82]. In order to compare the main short-term load forecasting methods and techniques, Table 2-2 illustrates the advantages and drawbacks of the main short-term load forecasting models based on the literature reviewed in the previous sections and [83] [84] [85]. In addition, ARIMAX and ANN forecasting models for Low voltage network demand such as Electric Vehicles (EVs), building and industrial load for peak shaving and energy cost saving will be discussed in more detail in Section 2.3.2.

Table 2-2: The advantages and drawbacks of some of the main short-term forecasting methods.

| Model | Advantages | Drawbacks |
|-------------------|------------------------------------------------------------------------------------------------------------------------------------------------------------------------------------------------------------------------------------------------------------|----------------------------------------------------------------------------------------------------------------------------------------------------------------------------------------------------------------------------------------------------------------------------------------------------------------------------------------------------------------------------------------------------------------------------------------------------------------------|
| Linear regression | <ul style="list-style-type: none"> • Simple method and easy to use because this method analyses the basic relationship between two sets of data. | <ul style="list-style-type: none"> • Analyses only the linear relationship between two sets of data. • Assumes that the historical linear relationship will continue in the future. |
| ARIMAX | <ul style="list-style-type: none"> • Widely used to forecast electrical demand which gives sufficient information about how this method can be used. • The exogenous variables help to decrease the forecast model error. | <ul style="list-style-type: none"> • Historical data is the main source of data for ARIMAX as a time series method. • Require extensive data analysis and large amount of data to determine the seasonal patterns. |
| ANN | <ul style="list-style-type: none"> • Does not require any functional relationship between the load and predictor variables. • Able to detect complex nonlinear relationships. • More flexible. | <ul style="list-style-type: none"> • ANN has been described as a “black box” because it is difficult to explain the model. • Increasing the number of layers in an ANN model will lead to increased costs of the model and training time. • Tends to overfit and it requires large amounts of data to determine the model parameters. • Difficult to generalise the forecast model and identify the best model parameters. |
| SVM | <ul style="list-style-type: none"> • This method avoids overfitting. • This method provides expert knowledge about the forecast target. | <ul style="list-style-type: none"> • Choosing the correct kernel is one of the main difficulties and limitations of this method. |
| ANFIS | <ul style="list-style-type: none"> • The adaptability of algorithms in this model help to avoid the fuzzy system problem by eliminating the need to generate a set of fuzzy rules and use ANN to create an automatic fuzzy rule generation. | <ul style="list-style-type: none"> • This model is very sensitive to a number of fuzzy rules and the model’s complexity will increase when the number of fuzzy rules increase. • This model described as “black box” because it is difficult to understand the nature of the ANN model. • High complexity and it requires large amounts of data to determine the model parameters. |

2.3.2 Role of Load Forecasting in Low Voltage Network

The previous section explored and compared a number of load forecasting techniques and suggested ARIMAX and ANN forecast models as important approaches to develop within this research. The forecast algorithms are key to improving the energy performance of distribution network applications such as storage systems. In LV networks, the number of customers serviced by transformer are few compared with customers serviced by medium or high voltage substation. This increases the variability of a time series for electricity demand, especially over short time periods (days or weeks). Electricity demand in the short-term has been observed to have a greater degree of volatility, and random behaviour, and shown to be sensitive to customer's behaviour, weather conditions, special events and other factors [86] [87]. In ESS applications, accurate information regarding the level of peak or base demand estimated for the next day can lead to more efficient charging and discharging schedules [86]. Furthermore, in the electric power system industry, generating companies require an accurate forecast models to predict the power system load demand and the congruent price in order to make the best market decisions for a competitive price [87].

The ARIMAX and ANN forecasting methods have been widely used with different applications and studies such as electricity price forecasting, energy in buildings and electric vehicle demand, which have a high stochastic load behaviour [83] [84] [85]. The ARIMAX a forecast model has been investigated in the literature to predict LV demand due to its simplicity and ease of implementation compared to many other techniques and has the ability to work as a nonlinear model [67] [71]. The ANN forecast method is commonly applied to complex nonlinear relationships and energy problems because it does not require determining any explicit functional relationships between the LV demand and their predictor variables [63] [74]. This section aims to critically review the key forecast approaches, especially ARIMAX and ANN, reported for LV network applications due to their potential to forecast port substation and electrified RTG crane demand. The forecast models are divided into three main categories: renewable energy; building demand; and electric vehicles.

2.3.2.1 Renewable Energy.

Several studies have used ARIMA, ARIMAX or ANN forecast models to predict renewable energy generation for LV network and energy price applications. They have also been used to investigate the benefits of predicting renewable energy sources to develop more efficient

energy management systems. Considering the forecasting of wind speed, Yuan et al. [88] developed operating strategies for energy storage to reduce the diesel fuel consumption in an isolated grid system. The ARIMA algorithm was applied to generate a one-hour ahead wind speed profile on a rolling horizon basis. The moving window for the one-hour prediction model facilitated the reduction of forecast errors within the system. The prediction profile was used to create 100 yearly scenarios from the hourly mean using a Monte Carlo method. These simulated scenarios were used to evaluate four wind farm operating strategies for an hour ahead by using the following data: ARIMA forecast results, the persistence model for the previous hour profile, a minimum of the previous six-hour values and the average of the previous six-hour profiles. The analysis of the results shows that an ARIMA forecast with an ESS outperformed the other operating strategy and increased diesel fuel savings by 7.6%. However, the forecasting model demonstrated a low performance with a MAPE of 11% in summer time when there is low wind speed, compared to 6% during the rest of the year. This is presented the significant of analysis the seasonality and find any specific patterns in the time series for LV demand which can improve the forecast model performance [61] [62]. For example, the day of the year was used as an external variable in the ARX model [96] and in another paper the time of day and day type (weekday, weekend, holiday) were chosen as the seasonal input parameters for ANN model [99]. In addition, the forecast model [88] did not consider any external predictors such as temperature and forecast weather conditions, which could help to reduce the forecast error and increase the energy savings. Klingler and Teichtmann [89] presented an optimal operation strategy for a LV network (single house-holds) connected to photovoltaic (PV) system and storage device by forecasting the hourly electricity and PV demand. To find the optimal operation for the battery system, two modules were developed. The first module forecast the household's electricity demand and PV demand using an ANN model; then the forecast outputs were fed to a second module which has been designed to calculate the optimal energy flows in the system and generate an optimal operation schedule for storage devices by using the forecast results and day-ahead electricity prices. A feed-forward ANN model with three layers (input, hidden and output) was developed to generate hourly forecast profiles for a day ahead. Three input neurons were set to forecast the PV demand: air temperature, global irradiance and relative air humidity. Only one input neuron was chosen for the electricity demand forecast model from the previous weekday data. The forecast model helped to increase the stored energy in a battery system by 23% compared to

the relay-based system model. The relay-based model starts charging the battery when the PV generation demand exceeds the household's demand without considering any information about the potential future load. The battery was often fully charged before midday. The error in the proposed forecast module was concentrated during peak periods and had values with a relative Root Mean Square Error (RMSE) of 9.3%. However, the optimal operation strategy in [89] failed to minimise the energy costs every month due to the inaccurate peak forecast which caused unnecessary charging and discharging for the battery system. It would be significant if the forecast model for the household demand included more input variables related to the electricity demand such as previous hour data to improve the forecast results.

As discussed renewable energy forecasting has a potential role in improving the storage efficiency and increasing energy savings. The renewable energy sources are highly stochastic, which is mainly related to weather conditions. An accurate forecast model is essential for optimal unit operation and economic dispatch. The following literature uses different exogenous variables to improve forecast model performance. Hossain et al. [90] used an ANN method to forecast the power output of a photovoltaic system for one hour and day ahead. The highly volatile nature of the power output is mainly related to solar irradiance due to cloud cover. To generate day ahead load profiles, [90] a feed-forward ANN model was developed with one hidden layer and four input variables (daily average solar radiation, wind speed, ambient and module temperature, and photovoltaic power output). The data was collected at a 5-minute time interval, then converted to hourly and daily averages to generate hourly and daily load forecasts. The results in [90] show that the ANN forecast model provides higher accuracy compared to time series models such as ARIMA especially under unstable weather conditions due to the ability to solve the complex and nonlinear relationship between the power and the external variables for the photovoltaic system model such as wind speed and temperature. However, increasing the number of neurons in the hidden layers leads to a reduction in the learning speed and makes the model perform more slowly. Another paper used a feed-forward neural network model with one hidden layer and different input variables compared to Hossain et al. [90]. In this study [91], Bi et al. used power output, temperature values (high, low, average) from similar days and forecast temperature values to predict the photovoltaic system power output with a half hourly time interval [91]. The proposed ANN model [91] showed acceptable forecast errors during the sunny day with a Mean Absolute

Percentage Error (MAPE) of 10.06%. However, the prediction model demonstrated a weak performance during unstable weather situations and rainy days compared to sunny days, where the output power of the PV system is more stable during sunny days with less fluctuation compared to rainy days. Therefore, adding more external variables that related to weather conditions such as wind speed and solar radiation can help to improve the performance of the model. The research in [92], used the forecast of global irradiance, as a single exogenous variable, to develop an ARX model, which aimed to forecast the hourly PV power output that was generated from solar system located on household rooftop. The exogenous variable allowed the ARX model to outperform the AR model and improve the prediction performance [92]. However, including other exogenous variables can help to achieve more accurate forecast model. In their paper Feuerriegel et al. developed two models, ARMAX and ANN, to predict the electricity prices through estimations of wind and solar power generation as exogenous variables. The two forecast models determined the expected exogenous variables value by using the forecast renewable energy data published by the European Energy Exchange [93]. Due to the highly volatile nature of electricity price profiles, which have negative or positive price spikes, the estimation data of the renewable power generation as an exogenous predictor minimises the forecast error compared to the same models that do not include the exogenous variables. Furthermore, the ANN model with the exogenous variables outperformed the ARMA and ARMAX models. However, for electricity market forecasting it is important to investigate additional external predictors such as expected and current demand, power source availability. The expected prices of these sources can help to improve the forecast performance.

Overall, choosing a suitable exogenous variable plays a significant role in improving the forecast performance and these variables are mainly selected based on model targets and data availability. Yet, the literature does not show in enough detail the impact of the exogenous variables for renewable energy applications on the forecast model accuracy. In addition, the literature showed that the input features (exogenous variable) are often more important than the chosen model. In microgrid systems, the literature focused on forecasting the renewable system output and assuming the household demands are perfectly accurate.

2.3.2.2 Buildings

This section will introduce studies where forecast models have been used in energy planning and optimisation of buildings, where energy forecasting has become a key to providing greater

energy efficiency and sustainability in a building system. Energy consumption forecasting for commercial and residential buildings is challenging due to the stochastic nature of low voltage demands and increasing requirements for building energy efficiency. For example, weather and electrical demand predictions at building sites have been used to feed Model Predictive Control (MPC) for air conditioning (HVAC) systems in order to increase the overall energy efficiency by reducing the electric energy consumption [94] [95]. Furthermore, Labidi et al. developed a forecast model including ANN and wavelet forecast methods to forecast the building boiler demand [96]. The forecast model was built separately in [96] to generate a 24-hour ahead demand profile, then fed to an MPC controller. The main objective of the MPC was to minimise the energy consumption. The analysis of the results show that the MPC reduced the demand consumptions and CO₂ emissions successfully [96]. The proposed ANN model was compared to AR and ARX forecast models, where the day of the years was used as an external variable in the ARX model. The ANN model outperformed other models with Mean Relative Error (MRE) of 6% compared to 9.8% for the ARX and 10.7% for the AR models [96]. However, the forecast results show that the exogenous predictor in this paper did not significantly improve the forecast performance. The forecasting errors in ARX and ANN models could also have been further reduced by considering additional exogenous variables such as forecast temperature, a key driver of the heating system as presented in [49] [50]. The research by Zhang et al. [97] investigated the impact of forecast error on the MPC for a residential microgrid system. The goal of the MPC controller, introduced by Zhang et al., was to reduce the impact of the forecast errors (wind, PV, electricity price and electric demand forecast error) on the energy flow schedule, energy costs and peak power price. However, the forecast error term in this research was modelled using an assumed Gaussian distribution and did not consider any external variables such as weather that could have helped to improve the forecast output. In other research, Chae et al. [98] also presented a short-term load forecasting model based on an ANN model for the electricity consumption of a commercial building complex. In [98], different input variables were investigated to improve the forecast performance. The feed-forward ANN model was developed with three layers: input, hidden and output, to generate a forecast profile for a day ahead with 15-minute time resolution. Data from the previous 6 time steps (weather condition variables, HVAC operation schedule, demand and time of electricity usage) were chosen as significant exogenous variables and input neurons for this ANN model. The results showed it was important to determine an ideal number

of neurons in the hidden layers that give the best model performance, as when the number of neurons is too few the model cannot capture the non-linear dynamics of the system and when the number of neurons is large the model can be easily overfitted. The overall results show a good performance in predicting the weekdays demand, but the forecast accuracy falls in weekends. However, the commercial buildings usually have a significant pattern of demand during the weekend, it could be beneficial if the model treated the weekend period as a separate cluster to improve the forecast performance.

As in the research of Chae et al., Grant et al. [99] developed an ANN short-term load forecasting model to predict the hourly electrical demand for a large government building over a two-week testing period. The ANN model was developed with four layers: 1 input, 2 hidden and 1 output. In this model, the time of day, day type (weekday, weekend, holiday), humidity, outside temperature and HVAC load were chosen as five input variables in an ANN forecast model. The authors compared the proposed ANN model with another forecast technique for the same data set. The ANN performed well with a 3.9% MAPE against a Simple Moving Average (SMA) of 7.7%, linear regression of 17.3% and Multivariate Adaptive Regression Splines (MARS) of 7.0%. The forecast model [99] was only tested over two weeks period without considering and investigating the effect of the seasonal demand on the forecast model, where energy consumption in buildings is usually affect by the season and weather conditions. The research by Deb et al. [100] used an ANN model to forecast the energy consumption for a diurnal cooling load in three different institutional buildings. The input data was divided into five energy classes based on the day of energy usage, and were taken as input variables for the forecast model. The aim of this process step was to reduce the highly variable energy consumption effect on the load forecasting model. A Feed-forward ANN with three layers was developed to forecast the next day's energy consumption based on the previous five days' data [100]. The number of neurons in the hidden layer was chosen by testing different design parameters. The chosen input features for the proposed ANN were limited to the day of energy usage cluster without considering any of the external variables that have been discussed previously in the literature for the same application.

The sets of research discussed in the forecast building section show the significance of developing an accurate forecast model when designing and implementing an optimal energy management controller such as an MPC controller. The researchers have currently introduced

the significance of choosing the exogenous predictor and the model forecast parameters to reduce the level of forecast errors and uncertainty that can be found in low voltage applications such as buildings. However, there is a limited literature on investigating the impact of the estimation these exogenous variables have on forecast model accuracy.

2.3.2.3 Electric Vehicles.

This section will explore load forecasting algorithms used in the control applications for minimising the energy consumption on LV grids with electric vehicles. Due to the electrification of transportation, electric vehicles are becoming key to achieving a sustainable transportation sector. Large-scale utilisation of the electric vehicles will affect the future power system by increasing the magnitude and uncertainty of LV electricity demand [101] [102] [103]. Therefore, electric vehicles charging demand scheduling and optimal modelling have been recently investigated in the literature.

Liu et al. [101] presented day ahead charging schemes for one-hour time resolution for 100% electric vehicles in a Nordic region electrical network. The objective function of charging schemes is to minimise charging costs and reduce peak demand. Five charging schemes have been developed based on the charging time and location. In all scenarios, Liu et al. assumed a specific average of charging demand (150 Wh/km) to calculate the energy consumption based on the assumption of knowing the detailed driving distance and charging availability in advance. In similar work related to electric vehicles charging demand forecast, Galván-López et al. [102] designed a demand side management system by setting an overnight charging schedule to maximise the charge of electric vehicles whilst balancing the load on the LV transformer side with the aim of reducing the electricity costs. However, the authors [102] assumed that all customers are willing to submit electric vehicle charging schedules in advance to calculate the electricity demand aggregator. Alonso et al. [103] used a Genetic Algorithm (GA) to develop a day-ahead optimal power charging schedule for electric vehicles. The aim of this schedule was to reduce peak demand in low voltage systems. In this study the electrical vehicle battery was assumed to be fully charged during a fixed time duration and it did not consider any flexibility and volatility in behaviour. Furthermore, the optimal scheduling in [103] assumed that the time of connection for charging and the initial and final state of charge were known in advance. The aforementioned research has only concentrated on developing day ahead electric vehicle charging demand and assumed that the charging schedules are

deterministic. It has not focused on forecasting the demand or taking the uncertainty of charging demand forecasting into account. Utilisation of the electric vehicles will increase electricity demand and the uncertainty of demand forecast, therefore, an accurate electricity demand forecasting method for an LV network that considers the electric vehicle charging demand is required to simulate realistic power system performance. Amini et al. [71] developed an ARIMA model to generate hourly day-ahead electric load profiles including the charging demand of electric vehicle parking lots and conventional electrical loads. Firstly, the forecast model parameters were determined based on the optimum Root Mean Square Error (RMSE) over the historical load data as a decoupled forecaster. Then, to calculate the charging demand of electric vehicles for large scale integration, the historical daily driven distances data, and fuel consumption data were included. The charging demand model in [71] was developed based on a parking lot case to reduce the demand volatility nature. Finally, to predict the aggregate of the LV network demand [71], including the connected electric vehicles, the charging demand was estimated by finding the expected value of the distance driven and the charging duration. A probability density function was developed based on historical data and the charging demand model to find the estimated values of distance driven and charging duration [71]. The number of electric vehicles in each parking lot was fixed, which helps to generate an accurate forecast profile, especially with the daily driving patterns.

Arias and Bae [104], discussed the effect of traffic volume and weather conditions on the accuracy of a charging demand forecast. Their research focused on using real and historical data of traffic volume and weather conditions to determine traffic patterns and thus required charging demand by using a cluster analysis technique. In order to run the proposed forecast model from their study [104], the number of input variables needed to be determined. These input variables are month, day, and total number of electric vehicles. The model used this data to find the weather and day type data from the historical data and determine the charging starting times based on a clustering analysis and a gaussian distribution of the historical data. The model, then calculated the electric vehicles charging demand to generate an hourly day-ahead load profile. To calculate the charging demand, the authors assumed that the electric vehicles can be charged only once per day at home or in a work place based on assuming that the daily driven distance for a fully charged battery is more than the average daily travelled distance. Furthermore, they also assumed that the charging time is fixed and known in advance.

The analysis of [104] shows how a forecast can play a significant role in understanding electric vehicle charging demand on small and large scales. Majidpour et al. [105] developed a k-Nearest Neighbour (kNN) forecast model to predict the hourly electric vehicle charging load a day in advance for a parking lot case study. The main objective of this research was to predict the electric vehicle energy consumption based on two different data sets: the electric vehicle charging record and parking station record. The paper's analysis shows that there is a difference between the two data sets, where the charging record includes the electric vehicle user profile data for each charging event compared to the station record, which includes direct measurements for the charging points. To determine the charging demand, it was assumed that the electric vehicle was charged by 1 kWh in every hour of the charging mode. In [105], 18% of the outlet numbers for the kNN model's results for charging station recorded data exceeded the 30% error, while the average was around 10% and the highest error was 48%. Finally, Poghosyan et al. [106] presented an agent-based model to forecast the aggregate half hourly electric vehicle demand for the LV substation level based on four future electric vehicle energy consumption scenarios that have different rates of low carbon technologies. The proposed forecast model and load demand data was updated on a yearly basis where the model targets long-term load forecast. This work [106] presented a forecast model for the increase in electric vehicle charging load over 10 years based on various scenarios, taking into account the rate of electric vehicle uptake.

To conclude, the literature reviewed shows the significance of developing an accurate load forecast to increase energy savings. As discussed, recent applications such as the LV network demand and EV are highly volatile and stochastic. This demand behaviour will increase the difficulties of creating an accurate forecast model. The parameters of each forecast model for EV demand in the literature was chosen based on specific research needs and availability of the data. The exogenous variables play a key role in improving the forecast model's performance and different assumptions have been made to reduce the forecast error or fill the gap in the data available. In the previous literature [104] [105], the specific assumptions of each work helped the researchers to classify the data and forecast the demand. However, they do not show the impact of these assumptions on the forecast model accuracy. In addition, the exogenous variables such as the weather conditions or traffic information can minimise the errors in the model and help to improve the forecast performance.

The literature studied in section 2.3.2 has introduced ARIMAX and ANN forecast models with exogenous variables as a very common forecast methods for LV level demands. The literature has shown the improvement in forecast performance which can be achieved when using appropriate exogenous variables compared to models which do not include these variables. Recently, forecast researchers have begun to investigate the benefits and impact of using different exogenous variables for LV application forecasts. The implantation of these algorithms, ARIMAX and ANN, to RTG crane network or port applications has not been considered in the literature to date and is one of the objectives of this thesis.

2.4 Summary

This chapter has reviewed and outlined the current literature on peak demand reduction problems and control of energy storage strategies based on load forecasting, to support and motivate the aims and objectives in this research. The research into RTG cranes has focussed on using the conventional control strategy, set-point control, to store recovered potential energy and regenerate it during the lifting of containers, which helps to increase energy savings and reduce gas emissions. It is clear from the literature that diesel cranes are the main focus, and there are no studies on energy saving for a network of electrified RTG cranes using optimal power management strategies. Discussions have shown that low voltage network demand and their applications are stochastic, and much more volatile compared to medium or high voltage networks, and this situation increases the challenge of controlling an ESS. The increase irregularity in LV demand behaviour based on customer numbers and behaviour has caused a serious management problem for the operation of microgrids and makes demand prediction very difficult [86] [87]. It is clear then that storage device can achieve a higher performance when the demand is accurately predicted. Pena-Bello et al. explored how optimisation operation algorithms with perfect day ahead forecast profiles can minimise the energy operation costs for a battery storage system in grid-connected housing with a PV system [38]. Riesen et al. [40], then discussed the impact of using real forecast and perfect forecast models on optimal control algorithms for an LV network connected with residential battery storage and a PV system, which show the significance of using receding horizon controllers compared to those with fixed forecast horizons, as also has been discussed by Rowe et al. [33].

The load forecasting strategies have shown that the parameters of each forecast model in the literature was chosen based on specific research needs and the availability of data. The

exogenous variables play a significant role in improving the forecasts and creating more accurate future demand profiles. It is important to note, to date there have been no studies that discuss the prediction of RTG crane electric demand. Load forecasting will help ports to understand the RTG crane energy demand behaviour and provide ports with an important tool for the estimation of any financial or technical risks that may occur in the future resulting from demand inconsistency and the electrification process of RTG cranes. This will be the core of Chapters 3 and 4 in this thesis, which will mainly analyse the demand of an electrified RTG crane from real operation data and identify the key relationship determining the future demand profile of an electrified RTG crane. Furthermore, Chapter 4 will examine the impact of the exogenous variables estimation as input variables on the forecast model accuracy.

Motivated by the limited number of studies on using different optimisation methods, and the lack of studies on using load forecasting to select the peak demand and control the energy storage in an RTG crane system, this research will develop novel optimal energy management strategies using forecasted electrified RTG crane demand profiles to control the ESS in order to reduce electricity energy costs and increase peak demand reduction. The literature reviewed in this chapter has presented a set of potential optimal controllers that have used the deterministic forecasts or a stochastic process to control the demand within particular optimisation problems. These potential techniques, such as receding horizons controllers, can be suitable and helpful for the control of an ESS in an RTG crane network. The comprehensive review shows that there is a gap and need for investigation of the energy cost saving and peak demand reduction in the electrified RTG crane network equipped with ESS, by taking into account the highly volatile demand behaviour and challenges in generating an accurate future load profile. Novel optimal energy management strategies (MPC and SMPC) for the RTG crane network are presented in Chapters 5 and 6. In receding horizon controllers, the objective function is to minimise the electric energy cost and increase the peak demand reduction, considering the electricity price and high levels of uncertainty in the crane demand forecast. Finally, the contribution in this research includes the investigation on using a central ESS feeding more than a single RTG crane, there are currently no studies which explores the potential energy cost savings and peak demand reduction in a network of RTG cranes with central or individual ESSs. This will be the core of Chapter 7, which will present a further comparison and analysis for the proposed optimal controllers.

Chapter 3: The Characteristics of RTG Crane

Demand.

The previous chapters introduced the problem of high peak demand and energy costs on the LV network system, in particular on ports with electrified RTG cranes. Load forecasting was highlighted as a potential solution for supporting the network by facilitating the control of the energy storage system. In addition, Chapter 2 presented how load forecasting accuracy is dependent on different external variables and how more accurate forecast can increase the benefits of using an ESS to reduce peak demand and energy costs. To develop an accurate forecast model for LV applications, it is significant to understand the electrical demand behaviour and investigate the correlation between the demand and any exogenous variables. Due to the lack of understanding of the ports and the RTG crane energy demand behaviour, this chapter will analysis the demand characteristics of RTG cranes and explore the relationship between crane electrical demand and different exogenous variables such as the demand seasonality, the number of crane moves, and container gross weight. The detailed background and key findings in this chapter will be used in the following chapters in this research to develop and determine the most appropriate parameters for an accurate forecast model.

Generally, the LV demands have strong explanatory relationships with external variables, such as temperature and seasonality trends, that can help to generate accurate forecast profiles. An electrified RTG crane demand profile has highly volatile and less predictable behaviour compared to many other low voltage loads such as residential customers, as will be presented in this chapter. The volatile nature of the RTG crane demand and the ambiguous explanatory relationships between the RTG crane demand and the exogenous variables increases the challenges for creating accurate crane prediction profiles compared to say, low voltage demands. Motivated by the highly volatile behaviour of the RTG crane demand and the lack of understanding of the energy demand behaviour for port applications, this chapter aims to investigate the characteristics of the demand of RTG cranes and explore the relationship between crane electrical demand and different exogenous variables. This understanding is vital

for developing an accurate forecast model and optimal control strategies to reduce the environmental effects of gas emissions and peak demand problems. Furthermore, to the authors knowledge, there are no studies found which specifically consider investigating the characteristics of electrified RTG crane demand in order to forecast the crane demand or control the ESS. The findings in this chapter will be used in Chapter 4, to determine the key exogenous variables for developing an accurate forecast model. In addition, the output of this chapter will help to find the optimal operation schedule for the ESS modelling based on the better understanding of the crane demand behaviour, in Chapters 5 and 6.

3.1 The RTG Crane Demand Characteristics

The previous chapters introduced the RTG crane demand as a more volatile, and less predictable time series compared to Medium Voltage (MV) and LV demands. This section and Section 3.2 will further elaborate and provide evidence on the characteristics of the electrified RTG crane demand and identify the different seasonalities in the crane demand profile. Then in Section 3.3, the correlation between the crane demand and the exogenous variables (number of crane moves, and gross container weight) is investigated.

In this chapter, the smart meter data for a single RTG crane was collected over a period of three months from January to March 2016 at the Port of Felixstowe in the UK. This port handles and operates more than 4 million twenty-foot container equivalent units (TEUs) every year, by running 85 RTG cranes continuously, it is only non-operational for maintenance, and work up to 24 hours daily as two work shifts for 362 days a year [22]. The collected RTG cranes data, cranes demand, number of moves and container gross weight, (data with half hourly time resolution over 24 hours) represent the crane behaviour over the data period during different work and operation days. In this chapter, we analysed the real RTG crane demands, corresponding to all time intervals of the day (24 hours) based on half hour data resolution. The collected data has been used to operate and generate the results presented in this research. This work has presented and tested control algorithms on half hourly data. The half hourly RTG crane's electric demand represents the average demand over the half-hour period. In general, the cranes demand behaviour on the electrical distribution network changes at a sub-second resolution. Therefore, in practice the actual performance of the ESS control and forecast algorithms will be likely reduced. However, the high resolution of the RTG cranes demand profiles used is expected to have a significant effect on the performance of the ESS control

algorithm especially for the power and frequency investigation criteria. However, the high data resolution will include a larger number of time steps within the same window size in the real-time algorithms, which will introduce more computational costs in the forecast and control algorithms. Furthermore, it is expected that sea ports will have smart meters with half hourly resolution for electricity billing purposes, therefore without additional costs for high-resolution substation monitoring, the prediction will remain at a half hour resolution. In this thesis, the energy price parameter at the Port of Felixstowe (PoF), will require a horizon size equal to 24 hours (48 half hours) to utilise the deviation of electricity energy price over a full day. For the ESS topology, the resolution of the demand profiles is likely to be dependent on the main role and aim of the ESS. For instance, an ESS being used to reduce the voltage fluctuation as a voltage supporter device will require a higher resolution demand profile, where the small voltage deviation can have a high impact on the distribution network. On the other hand, an ESS being used for electricity cost and peak demand reduction, similar to our case, will only require lower resolution data as the peak demand will have less impact on the thermal constraints of the distribution network, where the distribution network infrastructure (cables and substation) are able to work outside the operating specifications for a short period. Furthermore, the electricity bills are normally calculated based at a relatively low resolution (half or one hour). The resolution of the RTG cranes demand profiles used are expected to have a significant effect on the performance of the ESS control algorithm. For the ESS topology, the resolution of the demand profiles is likely to be dependent on the main role and aim of the ESS. For instance, an ESS used to reduce voltage fluctuations will require a higher resolution demand profile, since the small voltage deviation can have a high impact on the distribution network. On the other hand, an ESS used for electricity costs and peak demand reduction, similar to our case, will use lower resolution data as the peak demand will have less impact on the thermal constraints of the distribution network, where the distribution network infrastructure (cables and substation) can work outside the operating specifications for a longer period. Furthermore, electricity bills are typically calculated based on a low resolution (half or one hour).

3.1.1 Overview of the Electrified RTG Crane Demand.

The literature discussed in Section 2.3 is on the load forecasting in LV network applications and how choosing the forecast model variables can affect the prediction model performance.

The literature shows that there are no studies which specifically forecast RTG cranes and there is only one study that analyses the daily diesel RTG crane demand over only eight days period [19]. However, the study in [19] does not investigate the peak demand, the volatility nature of the demand or the correlation between the demand and external variables, so a significant part of this thesis is on the study of the RTG crane electrical demand and forecast. This section introduces an overview of the electrified RTG crane demand in order to investigate the non-smooth and stochastic demand behaviour of the crane. In order to show the behaviour of the RTG crane demand over a long period of time, the half hourly demand has been plotted in Figure 3-1 for the 3-month data set. This plot for a long period of time aims to highlight any possible seasonal trends. A line has been plotted in Figure 3-1 to examine the linear long-term trend in the data, as described in Equation (3-1).

$$\widehat{D}_L(n) = a + b n, \quad (3-1)$$

where $\widehat{D}_L \in \mathbb{R}^N$ is the RTG crane demand, N is the total length of analysed data and n is a half hour time step over the data set period and $a, b \in \mathbb{R}$ ($a = 21.1$ and $b = -0.0003$). In this study, the R-squared (R^2) statistics have been used to measure the goodness of the data fit with the regression line, as described in Equation (3-2).

$$R^2 = 1 - \frac{e_r}{e_b} \quad (3-2)$$

where e_r is the sum of squared errors of the proposed regression line trend and e_b is the sum of squared errors of the baseline model, as described in Equations (3-3) and (3-4), respectively.

$$e_r = \sum_{n=1}^N \left(D_L(n) - \widehat{D}_L(n) \right)^2, \quad (3-3)$$

$$e_b = \sum_{n=1}^N \left(D_L(n) - \mu \right)^2, \quad (3-4)$$

where the RTG crane demand, D_L , data set has N values can be specified as $D_L = (D_L(1), D_L(2), \dots, D_L(N))^T$, $\widehat{D}_L(n)$ the predicted demand value based on the regression line trend at n and μ is the mean of the crane demand data, as described in Equation (3-5).

$$\mu = \frac{1}{N} \sum_{n=1}^N D_L(n). \quad (3-5)$$

The plotted trend line in Figure 3-1 show that the average demand (21.1 kWh) exhibits verily little linear trend and is quite flat from the start to the end of the data. The linear fit gives an R^2 value of 0.017. In other words, the linear model only explains 1.7% of the load variability and is an insufficient for explaining the majority of the demand behaviour. As seen in Figure 3-1, the distribution of the base or average demand and peak demand values show volatile behaviour and there is no strong seasonalites or patterns from month-to-month or week to week without a clear sign of patterns. This irregular behaviour is likely due to the effect of operator behaviour decisions. The work activity inside ports will also depend on the occurrence or the movement of shipments which may have annual seasonalites but they are not obvious on our time scale considered. For example, a port may have many ships berthed at the same time and this requires increased crane activity.

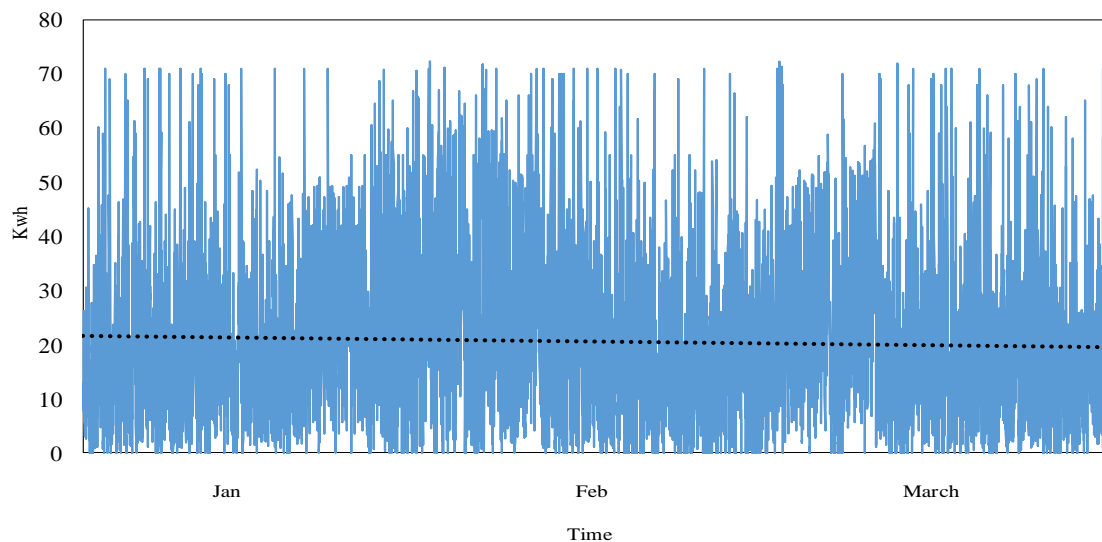


Figure 3-1: The half hourly RTG crane demand (blue line) with linear model fit to the data (dotted).

Analysis of the RTG crane demand data is shown in Table 3-1 to present various statistics of D_L including the average values and variability at half hourly and daily resolutions. The equations of average demand, μ , and standard deviation, σ , used in this section are presented in (3-5) and (3-6). In addition, to show the extent of variability between standard deviation and mean, the coefficient of variation, CV, also known as the relative standard deviation is

expressed in Equation (3-7). Furthermore, the total daily crane demand is also presented in Table 3-1.

$$\sigma = \sqrt{\frac{\sum_{n=1}^N (D_L(n) - \mu)^2}{N - 1}} \quad (3-6)$$

$$CV = 100 \frac{\sigma}{\mu} \quad (3-7)$$

Table 3-1: Summary of the electrified RTG crane demand.

| The RTG crane demand resolutions | μ | σ | CV | Maximum demand (kWh) | Minimum demand (kWh) |
|----------------------------------|--------|----------|--------|----------------------|----------------------|
| Half hourly | 21.10 | 14.85 | 70.38% | 72.3 | 0.0 |
| Daily | 516.65 | 294.02 | 56.90% | 865.6 | 120.9 |

Table 3-1 shows the standard deviation, σ , for the half hourly demand profile is 14.85 kWh and 294.02 kWh for the daily crane demand. This shows a significant sign that the crane demand data is volatile and varies significantly around the mean value with 70.38% and 56.90% coefficients of variation for half hourly and daily demand, respectively. In general, the high standard deviation and coefficient of variation values are due to the diversity in the container weight (5 to 40 tonnes per container) and number of crane moves, as will be shown later. Furthermore, the histogram of the half hourly crane demand is plotted and fitted with a normal distribution line and lognormal fit in Figure 3-2 to present the relation between the D_L , μ and σ . However, the data is clearly not normally distributed which complicates analysis.

The half hourly RTG crane demand values are distributed between 0 kWh and 73 kWh, which gives a wide range of possible crane demand values and illustrate the uncertainty in the crane demand. It is observed that a high number of instances are clustered between 0 kWh to 15 kWh and not around the μ value, leading to further emphasise that the normal distribution is not able to accurately describe the distribution of the crane data. Furthermore, the lognormal gives a better fit compared to the normal distribution but still does not completely explain the data. The histogram distribution has a long tail compared to that expressed by a normal distribution better describing the large values of demand which are more likely to occur. The high number of occurrences for the low demand, as presented Figure 3-2, is mainly related to the large

amount of low activity at the port including maintenance periods. In the literature, Papaioannou et al. [19] analysed and studied the energy usage by the various RTG crane motors. On average an RTG crane is in idle mode (waiting mode without lifting activity) about 30% of the day time [19], which explains the high number of instances for the low demand values.

In addition, Figure 3-3 shows an alternative visualisation of the distribution of crane demand for the demand data at Port of Felixstowe. Based on the average half hourly crane demand, in Table 3-1, the RTG crane demand is divided into four main categories: low demand (0-10 kWh), normal demand (10-30 kWh), high demand (30-50 kWh) and high peak demand (above 50 kWh). As seen in Figure 3-3, the low demand values occur about 27% of the time while about 21% and 5% of the time the electrical crane demand is high or has high peak demand, respectively. The remaining 47% of the time crane remains consumed around the average demand value.

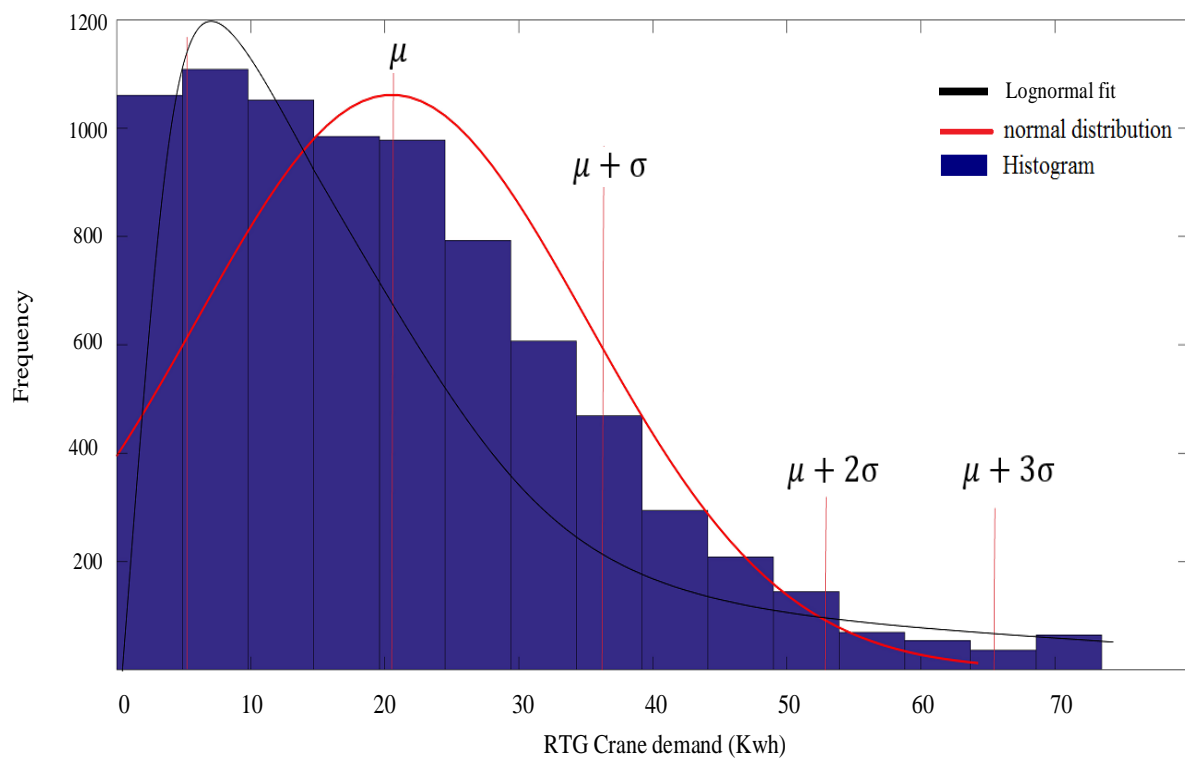


Figure 3-2: Illustration of RTG crane demand data in a histogram along with a normal distribution fit and lognormal.

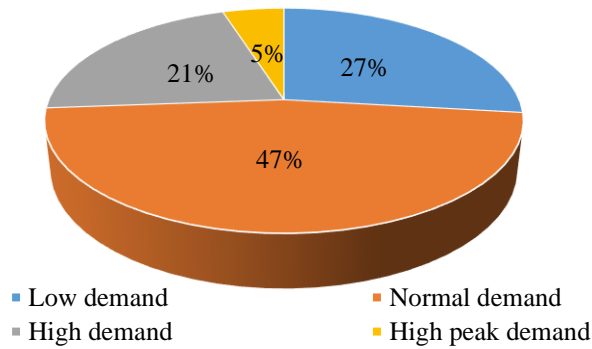


Figure 3-3: Distribution of half hourly RTG crane demand.

In the literature, Papaioannou et al. [19] analysed the energy usage for diesel RTG crane over eight days only with average daily demand equal to 518.75 kWh. In [19], the analysis showed that the RTG crane works about 50% and 12.5 % of the testing days with high demand above 700 and 800 kWh, respectively. In this thesis, to investigate the distribution of peak demand on a daily level over 3 months, Table 3-2 presents the percentage of time that the daily crane demand is over the average value. On average an RTG crane is working 9.8% of the time at a high demand level (above 800 kWh) and 31.6% of the time above 700 kWh. Furthermore, an important aim of the research is to reduce the percentage of time that that crane demand exceeded the average demand, as shown in Figure 3-3 and Table 3-2. This will be tested using an optimal ESS controller based on the future knowledge of the demand. In the following sections, the analysis of the RTG crane demand time series patterns, demand characteristics and demand correlation with external variables are presented.

Table 3-2:Percentage of time that the crane daily demand is over the average value.

| | Percentage of time | Daily average demand |
|--------------|--------------------|----------------------|
| Over 700 kWh | 31.6% | 516.6 kWh |
| Over 800 kWh | 9.8% | |

3.2 Time Series Analysis

As discussed in Chapter 2, time series analysis of LV network demand typically shows a significant weekly and daily seasonality [86] [87]. This section investigates and analyses the energy consumption of the electrified RTG crane using demand profiles usage over 3 months in order to identify if there is any significant seasonality or patterns in the demand curves. The previous section presented general analysis of the RTG crane demand and showed that the

demand values are distributed over several months without obvious patterns. The time series analysis in this section will be focused on finding patterns or cycles in crane demand based on the following:

- Weekly and daily analysis: to investigate if there are any cycles in the half hourly crane demand from week to week or day to day.
- Autocorrelation analysis: to study the half hourly demand by considering seasonal patterns in energy consumption which are not at daily or weekly cycles.

3.2.1 Weekly and Daily Analysis

In this section, the energy consumption of RTG crane profiles has been presented to investigate and explore weekly and daily patterns. In Figures 3-4 and 3-5, the overall breakdown of half hourly RTG crane demand distribution by week and day type are presented. Firstly, in order to investigate the half hourly RTG crane demand over 24 weeks, Figures 3-4 shows box plots representing the demand over each week of the data set. In this section, an extra data collected (crane demand) by the port operator has been used to analysis the seasonality by covering higher number of weeks. In Figure 3-4, the median for the 24-week points sits between 12 kWh and 27.5 kWh across the data set. The median values show a 129.2% increase in the maximum median value compared to the minimum median value. Furthermore, the Interquartile Range (IQR) value from one week also varies significantly, for example the lower and upper IQR values for week 8 is between 16 kWh and 39 kWh with median 27.5 kWh compared to 6 kWh and 18 kWh with median 12 kWh for week number 23. This introduce the non-smooth behaviour of RTG crane demand with no clear sign of weekly seasonality or consistency from week to week.

Secondly, the day of the week (daily) patterns for the energy consumption of electrified RTG crane is investigated by plotting the distribution of the half hourly crane demand based on the day type, as seen in Figure 3-5. As discussed in Section 3.1, 74% of the half hourly crane demand data set is under 30 kWh and 5% above 50 kWh, which is similarly displayed in the demand distribution by day type. However, only on Saturday is the number of observations for low demand vales (0-10 kWh) smaller than other days. In addition, the breakdown of RTG crane demand by day type shows that all days have a wide range of demand records and there is no particular day with clear low or peak demand values. The daily distribution of the crane

demand does not show a clear pattern or behaviour where the low and peak crane demand values in specific days are similarly distributed. The RTG cranes that work up to 24 hours a day in the Port of Felixstowe are able to handle container weight up to 40 tonnes in each move [19]: with a mix of heavy and light goods. As seen in Figure 3-5, the highest number of crane demand loads are low demand values under 10 kWh. This is due to the frequency of cranes operation for low container weight under 15 tonnes [19].

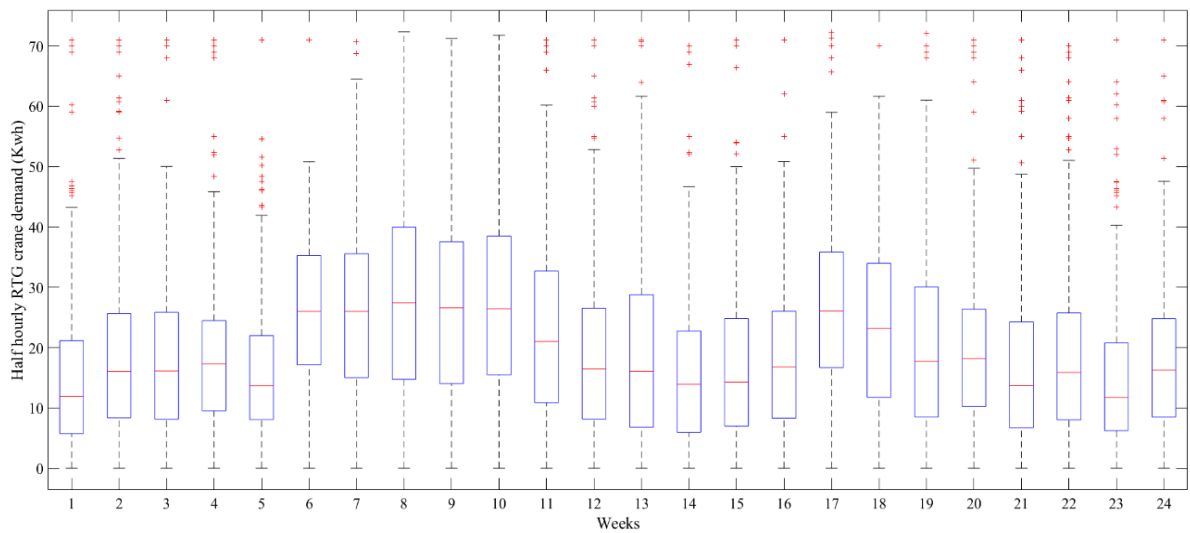


Figure 3-4: Box plot of half hourly RTG crane demand by week.

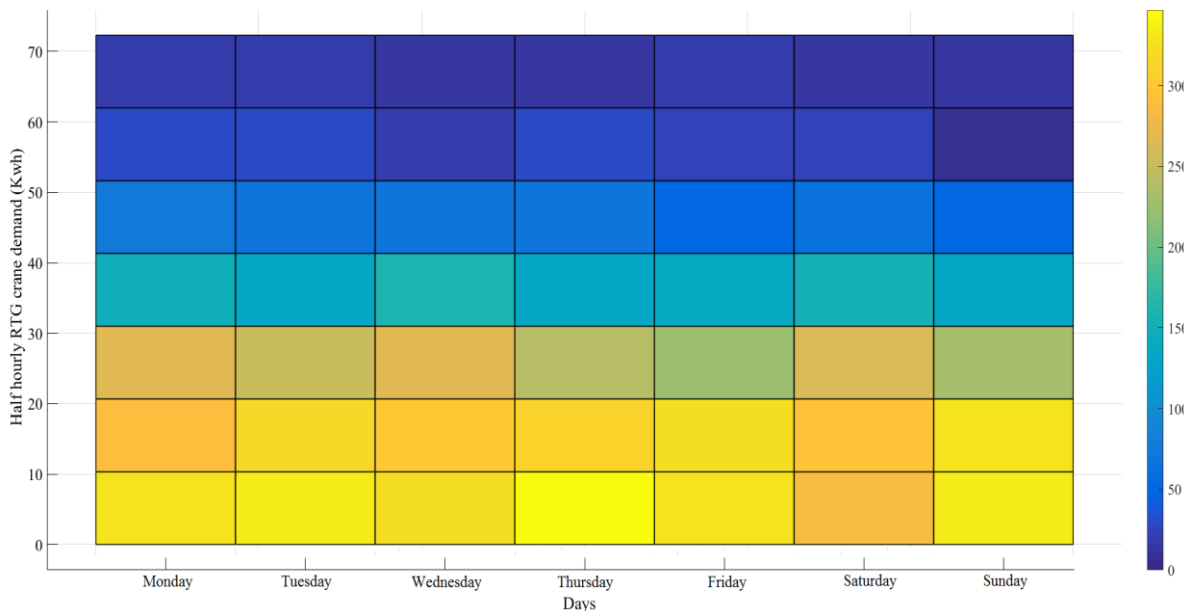


Figure 3-5: Breakdown of half hourly RTG crane demand distribution by day type.

Weekly shifts are a common cycle in LV applications [86] [87], Figures 3-6 and 3-7 show the RTG crane demand of three consecutive weeks overlapping each other and an example for the energy consumption curves for the same day over four different weeks. As seen in Figure 3-6, no clear weekly patterns are visible. For instance, the demand curve in week 8 at half hour number 20 (10 am) shows that the crane demand was 13 kWh, but it was 38 kWh in week 9 and 21 kWh in week 10. In addition, there is no clear sign that the peak demand occurs at the same time of the week, as seen in Figure 3-7. The peak demand in week 6 was 64 kWh at half hour number 2, but it was 38 kWh in week 7 at half hour number 33, as seen in Figure 3-7. This results support that the crane demand is clearly very volatile due to the lack of weekly or daily patterns or demand repetition.

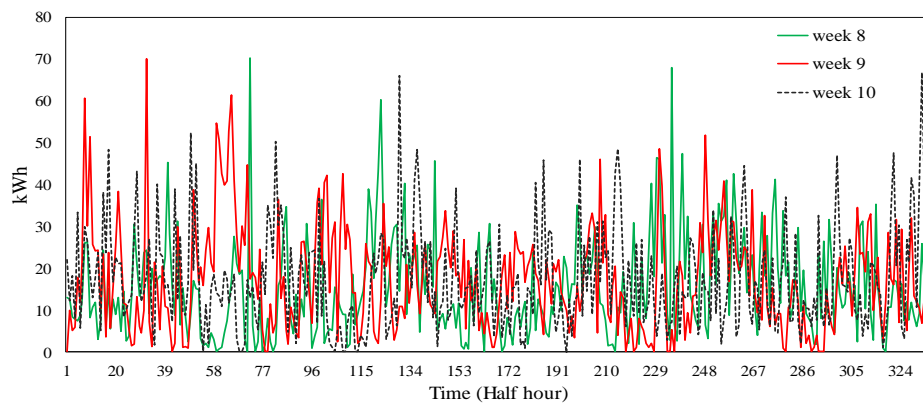


Figure 3-6: An overlay of the weekly profile of the RTG crane demand of three consecutive weeks.

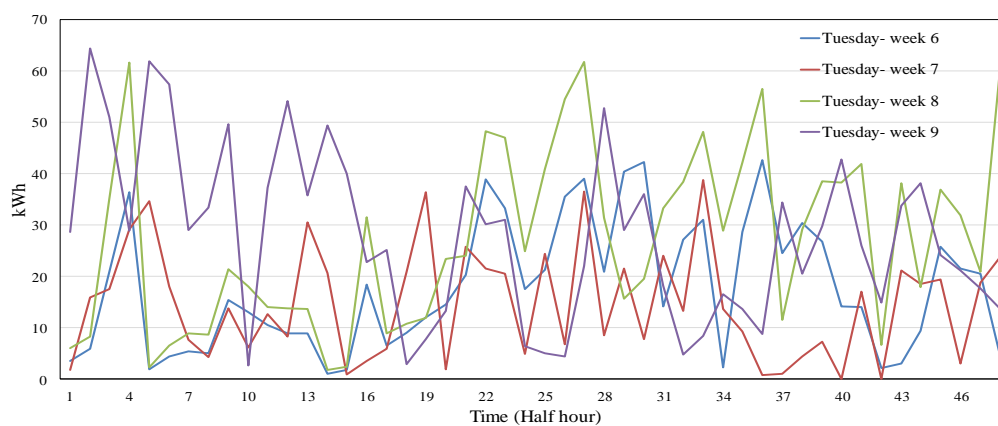


Figure 3-7: An example for the daily crane demand for the same day over 4 weeks.

Furthermore, the current literature has shown that there are mainly two peak periods in the LV network applications related to the householder demand behaviour: morning 7:00 to 9:00 and evening 17:00 to 19:00, these periods can change based on the seasons, day of the week and weather conditions [86] [87]. Figure 3-8 presents an example for the RTG crane demand profile over one week, the daily crane demand profiles are different from day to day and unlike the LV demand the weekend days do not have a clear distinction to weekday demand. It is evident that the daily activity of the electrified of RTG crane is highly changeable with no obvious matches between the demand curves that can help to design load forecasts or for the development of ESS control algorithms. In particular, even the majority of the daily peak points do not match.

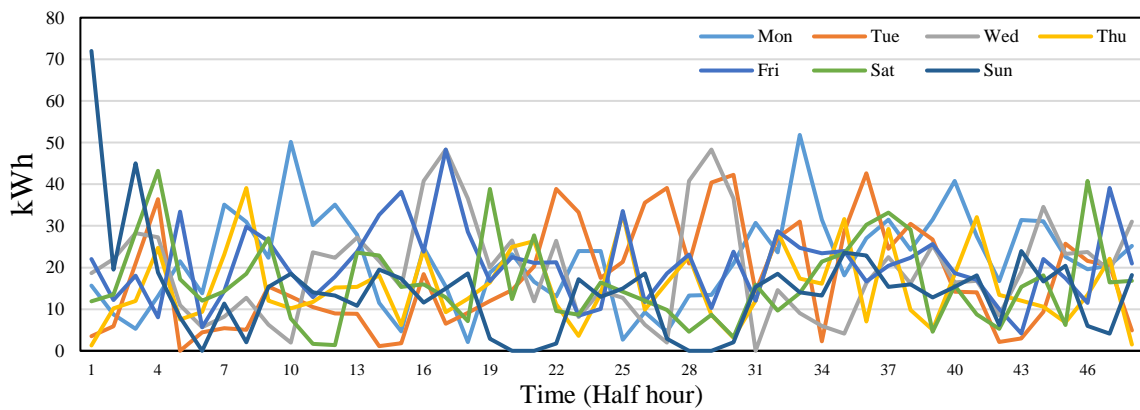


Figure 3-8: An example for the daily crane demand over one-week (week 6).

In order to investigate the RTG crane demand behaviour and patterns based on the half hour time of the day. Figures 3-9 presents the breakdown of RTG crane demand by half hours and shows that during the day every half hour has a wide range of demand records ranging from 0 kWh to over 72 kWh. The blue boxes, in Figure 3-9, show the inter-quartile range and the red line shows the median of the crane demand for the data set. The breakdown of the crane demand shows that the demand has volatile behaviour with similar distribution of demand over all 48 half hour time periods. As an example, the mean value of crane demand for the first half hour time is 15 kWh compared to 20.5 kWh in the following half hour. The median for the 48-half hour demand points sits between 14 kWh and 23 kWh across the day time, which presents 64.3% increment between the minimum and maximum median values. In addition, it's clear that the peak or low demand values are not concentrated within a specific time period during the day and any half hourly features are not obvious. This conclusion and analysis are supported

by the fact that the RTG cranes work up to 24 hours daily [22] and indicates that there is no organisation of the cranes as a function of time of day. Furthermore, Figure 3-9 shows that a few energy consumption observations were above 50 kWh and the majority of observations were below 30 kWh. This signifies that it may be very difficult to find half hourly or hourly usage patterns for this set of data.

The analysis results of this section shows the crane demand is clearly very volatile and, as expected, increases difficulty in forecasting the same day for different weeks due to the lack of weekly or daily patterns or demand repetition. Hence the LV forecast models are likely not valid on the RTG crane network.

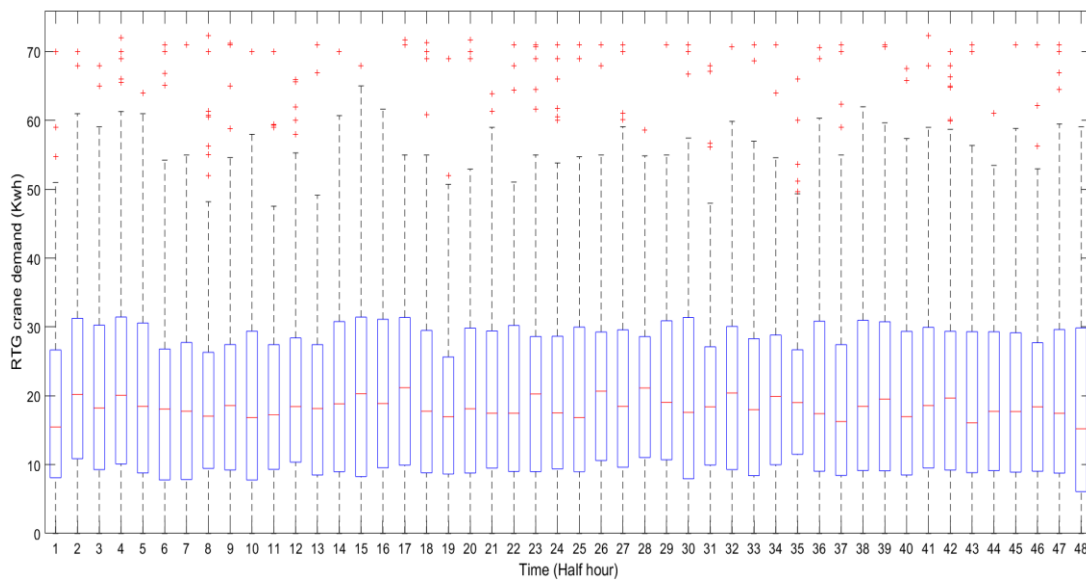


Figure 3-9: Box plot of RTG crane demand by half hours.

3.2.2 Autocorrelation Analysis

The previous analysis shows a lack of weekly and daily seasonality over the demand time series, therefore, this section aims to find if there is any special demand behaviour which are not a weekly or daily patterns. To find any correlation or patterns between the time series points, the Partial Autocorrelation Function (PACF) was calculated over 500-time lags, this is shown in in Figure 3-10. The PACF can help to find intraday and longer correlations which repeatedly occur. The PACF plot, Figure 3-10, shows the relationship between the RTG crane demand time series at $D_L(n)$ for up to 500 half hourly lags. The PACF can be defined as follows:

$$\text{PACF}(i) = \text{corr} \left(\left(D_L(n), D_L(n-i) \mid D_L(n-1), \dots, D_L(n-i-1) \right) \right). \quad (3-8)$$

In general, the PACF analysis, Equation 3-8, helps to find the correlation, corr , between the two direct variables relation without taking into account the effect of all lags in between [107]. The PACF plot shows the correlation relationship between the time series and the lagged time series, at say lag i , after removing the time effects lags $(1, 2, \dots, i-1)$ between them. The PACF coefficient is considered as significant if it is larger than a particular magnitude. The confidence interval line for PACF plot in Figure 3-10 has critical threshold of $\pm 1.96/\sqrt{n}$ where n is the number of observations [107], hence more observations reduce the size of critical value. The values of the partial autocorrelation sequence outside the ± 0.088 confidence boundary occur at lags 1 to 5, which have values under 0.25 except for the first lag which is above 0.5. The PACF plot shows a cut off after lag number 5 and it shows other significant PACF lags between lag 450 and lag 500. The distribution of the significant lags in the PACF plot does not show a clear pattern or seasonalities in compared other LV demand which typically shows significant lags at 48, multiply. However, the significant lags between lag 450 and lag 500, as shown in Figure 3-10 were distributed with no large main spike that decreased after a few lags or was followed by a damped wave which can present a moving average term. These lags are likely random salience, difficult to understand, and they are likely an artifact due to the small size of the time series. Furthermore, the early correlation lags could be due to the crane driver tasks that take more than a single time step to complete it. Hence the distribution of these significant lags in the PACF plot do not show a clear auto correlation behaviour for the RTG crane demand time series. To investigate the small lags between the $D_L(n)$ and $D_L(n-i)$ for $i = \{1, 2, 3, 4\}$ in more details, a linear regression model is considered. The regression examines the linear relationship between the variables in order to find a line of best fit. In this section, the R-squared (R^2) is calculated to find how well the linear model fits the lagged crane demand to the current demand, as described by Equation (3-9).

$$\hat{D}_L(n) = a + b D_L(n-i); i = \{1, 2, 3, 4\}. \quad (3-9)$$

Table 3-3 summarises the equation's parameters ($a, b \in \mathbb{R}$) and R-squared value for the relationship between the $\hat{D}_L(n)$ and the demand time series with lag i ($D_L(n-i)$). The calculation results show that the highest R^2 value is 0.16. In other words, the linear model explains only 16% of the load variability. The R^2 decreased gradually from 0.16 to 0.04 in line with the increase in the i value for the crane demand from the previous time step. Due to the

low R^2 values, the linear model based on the correlation between the current and historical crane demand is not an effective estimate to forecast the crane's demand behaviour. This shows that there are other factors that must be considered to understand the true data volatility as will be discussed in Section 3.3. In addition, the RTG crane demand time series analysis in this section with lack of large correlations at lag 48 (daily patterns) or 336 (weekly patterns) support the conclusion that there is no clear sign of any daily or weekly patterns over the time series.

Table 3-3: The linear equation parameters and R- squared for the relationship between the current and lagged crane demand.

| Correlated variables | Linear model equations parameters | | R^2 |
|--------------------------|-----------------------------------|------|--------|
| | a | b | |
| $D_L(n)$ vs $D_L(n - 1)$ | 12.62 | 0.40 | 16.06% |
| $D_L(n)$ vs $D_L(n - 2)$ | 14.96 | 0.29 | 8.37% |
| $D_L(n)$ vs $D_L(n - 3)$ | 15.76 | 0.25 | 6.32% |
| $D_L(n)$ vs $D_L(n - 4)$ | 16.54 | 0.21 | 4.59% |

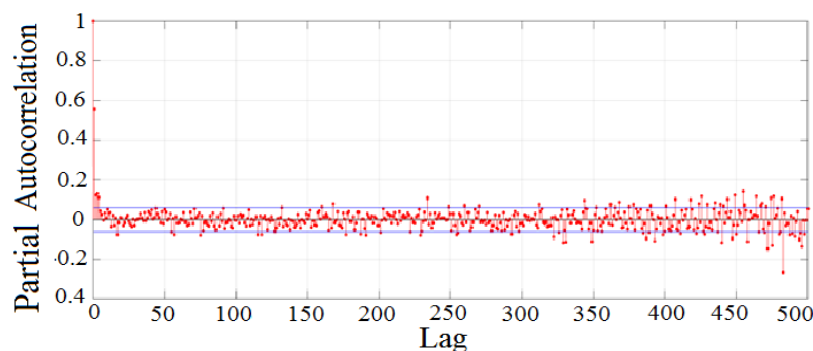


Figure 3-10: PACF plot for RTG crane demand time series for 500-time lags.

Overall, the collected data set for the electric RTG crane demand depicts random and volatile behaviour. The time series analysis shows that the crane demand does not have a clear half hourly, daily or weekly seasonality. This increases the difficulties of forecasting the crane demand compared to, say, LV demand. The non-smooth behaviour of RTG crane demand is mainly due to the effects of human and work environmental behaviour factors during the crane and port operation time. The work activity inside ports mainly depends on the volatile occurrence and movement of shipments [6] [20]. For example, a port may have many ships berthed at the same time and this requires increased crane activity. The term volatile or stochastic has been defined as the variables that change rapidly with low regularity, these terms

are used throughout the thesis to qualitatively define and describe the difficulty of predicting RTG crane demand. In the following sections, the analysis of the RTG crane demand time series patterns, demand characteristics and correlation with external variables are presented.

3.3 Cross-correlation Analysis

Due to the highly volatile and irregular behaviour of the electrified RTG crane demand compared to LV demand and the difficulties in finding seasonality patterns, the analysis in this section aims to investigate the correlation between the crane demand and some exogenous variables. In general, there are two key pieces of information that affect the energy consumption in the RTG crane: container weight and the number of crane moves [19]. In this section, the correlation between the current crane demand, number of crane moves, and container gross weight will be examined. This investigation can help to determine the forecast model inputs and develop an accurate forecast model. Furthermore, to the author knowledge, there are no studies which consider studying the relation between the previous exogenous variables to forecast the RTG crane demand.

In general, the RTG crane demand increases when the RTG crane moves heavier containers, as shown in Figure 3-11. The relationship between the current crane demand and the external variables is considered based on a linear regression. In this section, the R^2 statistics have been used to measure the goodness of the data fit with the regression line and the three data sets. This linear relationship is described based on the regression Equation (3-11).

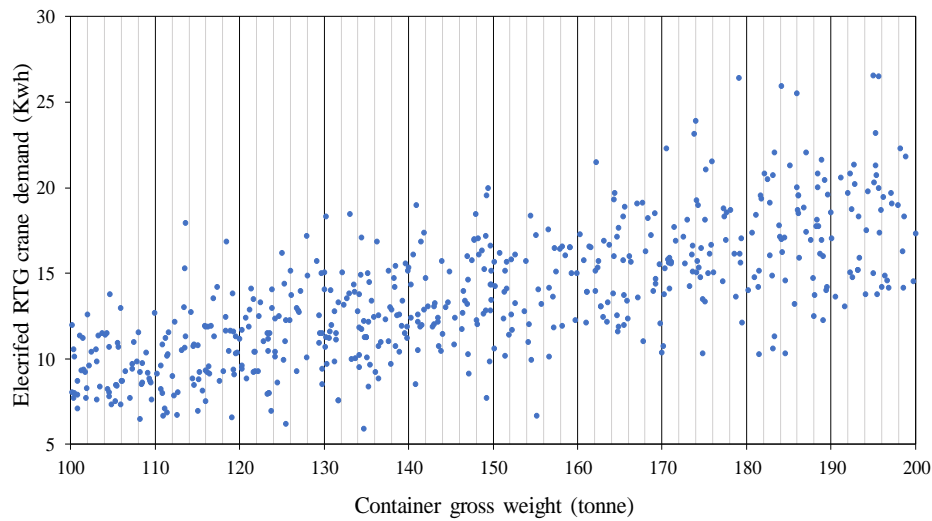
$$\hat{D}_L(n) = a + b X(n), \quad (3-10)$$

where n is a half hour time, $X(n)$ is the external variables: either $X_1(n)$ for container gross weight or $X_2(n)$ for number of crane moves, and $a, b \in \mathbb{R}$.

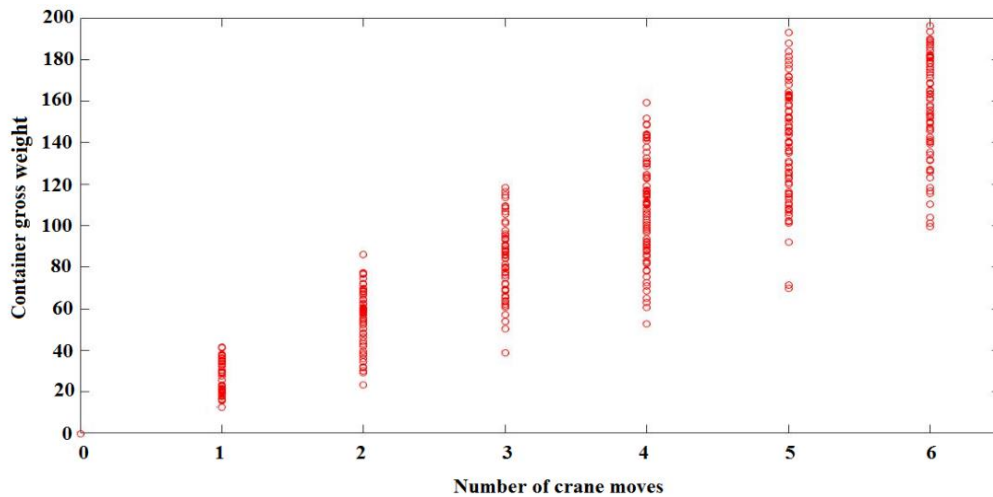
Figure 3-11 shows the relationship between the three data sets and present good evidence of the correlation between all the data sets which may be used to create a predictors terms for a load forecasting model. In addition, Figure 3-11 presents the linear line trend for the relationship between the $\hat{D}_L(n)$ and both external variables, $X_1(n)$ and $X_2(n)$, as described by Equation (3-11).

$$\widehat{D}_L(n) = a + b X_1(n) + c X_2(n) \quad (3-11)$$

Table 3-4 summarises the equation's parameters ($a, b, c \in \mathbb{R}$) for Equations (3-10) and (3-11), the R^2 measurement for checking the quality of each relationship. The data in Table 3-4 shows that the demand fits nicely with the regression line with R-squared values of 0.80, 0.78 and 0.85. However, the plot, in Figure 3-11, shows that larger uncertainty and outlier points are associated with larger container weights and larger number of moves which increases the difficulties in forecasting the RTG crane demand for the situations.



(a)



(b)

Figure 3-11: Scatter plot for RTG crane demand, container gross weight and number of moves: (a) crane demand (kWh) with container gross. (b) container gross weight (tonne) and number of crane moves.

Table 3-4: The linear equation parameters and R- squared for the relationship between the current, container gross weight and number of crane moves.

| Correlation | Linear model equation parameters | | | R ² | Equation |
|---------------------------------------------------------------|----------------------------------|--------|-------|----------------|----------|
| | a | b | c | | |
| D _L (n) and X ₁ (n) | 15.61 | 11.213 | 0 | 80.42% | (3-10) |
| D _L (n) and X ₂ (n) | 15.65 | 11.195 | 0 | 78.37% | (3-10) |
| D _L (n), X ₁ (n) and X ₂ (n) | 15.74 | 5.568 | 5.539 | 85.32% | (3-11) |

In this thesis, the exogenous variables have been investigated and utilised within the forecast models, as described in Chapter 4, in order to generate an accurate day ahead demand profile. To achieve a satisfactory load forecast for RTG crane loads, the forecast model must be able to capture the correlation between the load in the time series, the number of crane moves and container gross weight. The linear model describing the RTG crane power demand, as a function of number of crane moves, and container gross weight is significant with a high R² value, but the effect of human unpredictability on the demand is still present as can be seen in Table 3-5. The path for the crane move is decided by the crane drivers as they may choose to move the container through either an arc, square or oscillatory path which means variations in the amount of energy used for the same number of moves and container weight. The crane driver decides the type of move based on their experience in order to make the job easier and faster and every driver has a different level of experience to complete the required task. For example, on the 11th and 15th of February 2016, the electrified RTG crane consumed 30.9 kWh and 21.2 kWh for the same number of moves and container weight.

Table 3-5: Differences between the demand for the same number of moves and container weight.

| Moves | Weight (ton) | Time | Demand (kWh) |
|-------|--------------|-----------------------------------|--------------|
| 7 | 173 | 11 th of Feb (05:00) | 30.9 |
| | | 15 th of Feb (17:00) | 21.2 |
| 4 | 102 | 19 th of Feb (14:00) | 8.3 |
| | | 4 th of March (21:00) | 12.4 |
| | | 21 th of March (06:00) | 15.2 |

3.4 Summary

This chapter has introduced and investigated the electrical demand characteristics of the network of RTG cranes that are significant for the understanding of the demand behaviour in order to develop a load forecast model and the ESS control algorithms later in this thesis. The key contribution of Chapter 3 is to fill the gap in the literature and address the lack of understanding of the energy demand behaviour in port applications. This understanding is vital for developing load forecasting algorithms, in Chapter 4, and then feeding the accurate forecast profile to optimal control strategies, Chapters 5 and 6, to reduce the energy costs, and peak demand. This chapter presented a time series analysis for the RTG crane demand to investigate any patterns and trends in the demand profiles and the correlation with exogenous variables. The results of this chapter showed there is no clear sign of patterns or trends on the crane demand profiles but there is a strong correlation between the demand, number of crane moves and container weight. However, the effect of human unpredictability nature on the demand is still present with different demand for the same container weight and moves, as seen in Table 3-3. Hence some properties of the RTG crane load behaviour will always be difficult to predict.

The time series and cross-correlation analysis in this chapter will have a direct implication on the development of the forecast models in Chapter 4. To achieve a satisfactory load forecast for the RTG crane loads, the best parameters must be identified. For example, to identify and choose the best orders of the ARIMA parameters (p , d , q), the PACF plot and the time series analysis are required to be considered. In addition, the cross-correlation analysis shows it is important to include the number of crane moves and container gross weight, for any accurate forecast model.

Chapter 4: Load Forecasting for electrical RTG crane demand.

The previous chapter investigated the RTG crane demand characteristics that are significant for understanding the crane demand behaviour and developing an accurate load forecast model to feed into the ESS control algorithms. Short-term load forecasting plays a vital role in many electrical power system applications, such as planning, energy markets, power generation, and ESS operation [60] [61]. However, the highly volatile behaviour of the RTG crane demand creates a substantial prediction challenge. This work is the first extensive investigations into short term load forecasts for electrified RTG crane demand. In this chapter, two main load forecasting models, ARIMAX and ANN, are developed to predict the electrical RTG crane demand for up to a day ahead. The forecast methodologies in this chapter use the RTG crane demand analysis, from Chapter 3, to inform the inputs to the prediction model. The chapter also examines the impact of the estimations of the exogenous variables on the forecast model performance. In particular, results in this chapter demonstrate the forecast model's accuracy when the model is used with different input variables that help to identify which of the exogenous variables are the most suitable variable for the final forecast models.

It should be noted that the forecast models presented in the literature for buildings and smart grids use the strong seasonal correlation and other exogenous variables that have a clear relationship with the load demand. In contrast, the crane demand is highly volatile; and does not possess clear seasonality. To the author knowledge, there are no studies found which specifically consider forecasting of loads for electrified RTG cranes.

As discussed in Chapter 2, a large variety of methodologies and models have been employed in order to achieve an accurate short-term load forecast. ARIMAX and ANN forecasting concepts have been applied widely in different energy applications such as buildings and renewable energy [108] [109]. The overview of load forecasting techniques in Section 2.3 presents the advantages and drawbacks of using ARIMAX and ANN techniques to predict the LV demand. There are many publications that have discussed and developed load

forecasting models in the literature, which successfully predict the volatile targets such as wind speed [110], solar energy [111], microgrid systems and building demand by using ANN and ARIMAX techniques. These systems in the literature have clear physical explanatory relationships with exogenous variables. For example, Torr  [112] proposed an ARIMAX model to forecast the electrical power prices at Nord Pool, the model included exogenous variables such as temperature, wind speed, and reservoir level which mainly reflect seasonal trends in the weekly spot price and helped to reduce the forecast error. In addition, Chapter 2 presented the significance of generating an accurate forecast model to feed the optimal controller to improve the storage device performance in an electrical distribution network. Several papers in the literature that consider highly volatile demand, such as electric vehicles, assume that the forecast model is perfect or include particular assumptions which guarantee optimal conditions. For example, Galv n-L pez et al. [102] supposed that all electric vehicle customers in an LV network are willing to submit the charging schedules in advance to calculate the electricity demand aggregation and generate the future load. Furthermore, Alonso et al. [103] assumed that the time of connection for charging and the initial and final State of Charge (SoC) value would be known when developing day ahead optimal power charging schedule for electric vehicles.

This chapter aims to fill the gap in the literature and address the lack of understanding of the energy demand behaviour at port applications. This research attempts to develop short-term forecast models to predict the electrified RTG crane load one-day ahead. The forecast models are used with estimation techniques to select the number of crane moves and container gross weight. The key finding in this chapter and the forecast model outputs are used in Chapters 5 and 6, to feed the optimal control strategies for energy storage systems in RTG crane network. The sections of this chapter are structured as follows: Section 4.1 presents and discusses the methodology of the proposed forecast models. Section 4.2 presents the RTG crane demand forecast model based on the estimation approach for the exogenous variables. In Section 4.3, introduces the RTG crane demand data, forecast evolution methods, and the results of the RTG crane demand forecast models. Finally, the conclusions of the research presented in this chapter are discussed in Section 4.4.

4.1 Methodology

This research adopts the ARIMAX and ANN methodologies presented and previously discussed in Section 2.3.2. In the literature, these methods have been used to predict volatile demand and can help to achieve a high energy storage control performance in LV applications [71] [88] [96]. This chapter will develop various time series and ANN forecast models, including an estimation approach for the exogenous forecast model input variables. As described in Chapter 3, due to the highly volatile behaviour of the RTG crane network demand compared to the LV demand, the crane forecast problem presented in this work is particularly challenging. Furthermore, the time series and cross-correlation analysis in Chapter 3 have a direct implication on identifying the best parameters for a more accurate load forecast model. The analysis of the results in the previous chapter showed there is no clear sign of patterns or trends in the crane demand data but there is a strong correlation between the crane demand $D_L(n)$, container weight $X_1(n)$ and number of crane moves $X_2(n)$. Hence the using of volatility and stochasticity terms in this thesis is mainly related to the lack of seasonality and patterns in the crane demand time series and the effect of human unpredictability nature on the crane demand, as presented and discussed in Chapter 3.

The forecasts models have been developed in this chapter to predict half hourly day ahead RTG crane demand $\hat{D}_L(n)$, i.e from $n+1$ to $n + 48$ where n is the current half hour. In this thesis, the forecast and historical data are presented in equations with and without (^) notation, respectively. A general schematic of the proposed load forecasting procedure in this work is presented in Figure 4-1. The following sections develop different forecast models, ARIMAX in Section 4.1.1 and ANN in Section 4.1.2. Then, Section 4.1.3 investigates the impact of the exogenous variables on the prediction system by adapting ARIMAX and ANN forecast models.

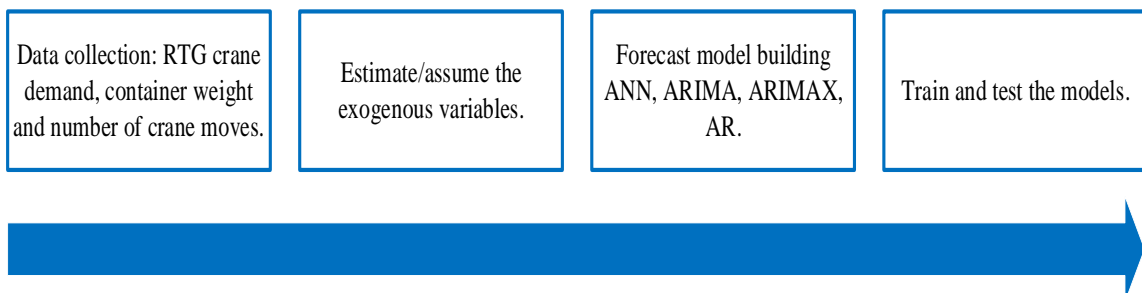


Figure 4-1: General schematic of load forecasting procedure implemented in this chapter.

4.1.1 ARIMAX Forecast Model

The ARIMAX technique is a statistical method for time series that formulates the historical data as a function of time to predict the future value. Generally, time series approaches are among the simplest forecast methods that include the following models: Auto Regressive (AR), Moving Average (MA), Auto Regressive Moving Average (ARMA) and Auto Regressive Integrated Moving Average (ARIMA) as linear forecasting methods. The ARIMA forecast as linear model is a simple method and easy to implement where it requires only historical time series data. Furthermore, it is widely used to forecast electrical load demand. The Auto Regressive Integrated Moving Average with exogenous variables (ARIMAX) is an updated version of ARIMA which can include exogenous variables and non linear relations. The advantage of the exogenous variable is the creation of new parameters that help to decrease the forecast errors and increase the utilisation of available data [67] [71]. ARIMA and ARIMAX models are popular time series models for forecasting LV demand [67] [71]. The ARIMA technique consists of the following main components [66] [71]:

- Autoregressive model (AR) (p): is the order, p, of the AR component for when there is a significant relationship between historical observations (previous time lags) and the current time.
- Integrated component (d): is the number, d, of discrete differences that can be applied in order to change the status of forecast data from non-stationary to stationary and remove seasonality, as described in Equation (4-2).
- Moving average model (MA) (q): is the order, q, of the MA component and model significant relationship between historical errors.

The combination of the differencing component with the ARMAX model, will generate a non-seasonal ARIMAX model with (p,d,q) parameters, seen in Equation (4-1) and Figure 4-2. In addition, the differencing may be applied more than once in order to make the series stationary [66] [67]:

$$\widehat{D}_L^{(d)}(n) = \sum_{j=0}^h \varphi_j X_j(n) + \sum_{i=1}^p \phi_i D_L^{(d)}(n-i) + \sum_{i=1}^q \theta_i Z(n-i) + C, \quad (4-1)$$

$$D_L^{(d)}(n) = D_L(n) - D_L(n-d), \quad (4-2)$$

where the $\widehat{D}_L^{(d)}(n)$ is the d differenced cranes estimated demand at time n with $D_L^{(0)} = D_L$, as defined in Equation (4-2); $\sum_{i=1}^p \phi_i D_L^{(d)}(n-i)$ is the p^{th} order autoregressive polynomial lag (AR(p) model); $\sum_{i=1}^q \theta_i Z(n-i)$ is the q^{th} order moving average polynomial lag (MA (q)); $\sum_{j=0}^h \varphi_j X_j(n)$ is the h^{th} exogenous variables term; φ_j, ϕ_i and θ_i are the coefficient of the exogenous variables, and the AR(p) and MA (q) terms, respectively; $Z(n)$ is the past forecast error term (assumed to be normally distributed) and C is a constant term. As previously discussed in Chapter 3, $X_j(n)$ is the exogenous variables: $X_1(n)$ is the container gross weight and $X_2(n)$ is the number of crane moves.

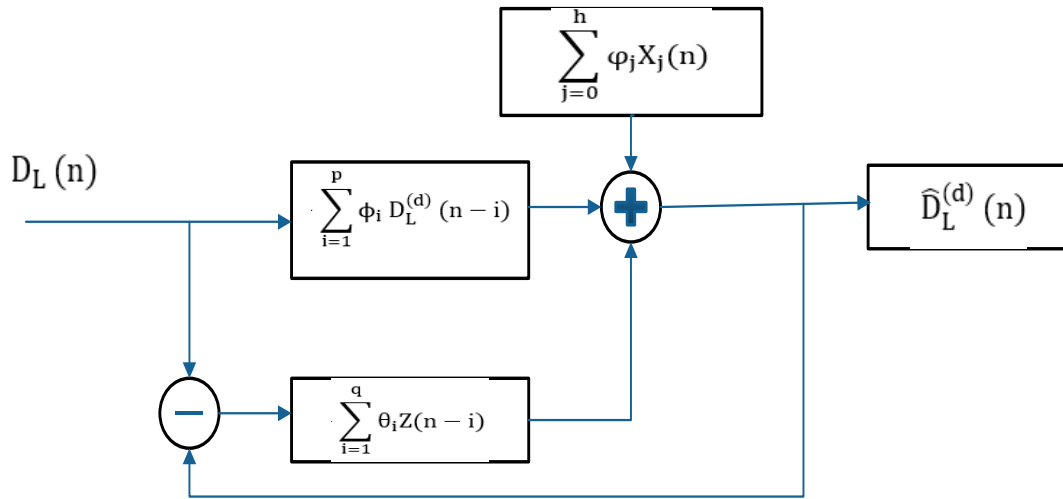


Figure 4-2: General schematic of ARIMAX forecast model.

To determine the exogenous variables in an ARIMAX model is important to investigate the relationship between the current and any external variables [66] [67] [71]. In this chapter, each individual exogenous variable, $X_1(n)$ and $X_2(n)$, has been included in the ARIMA model to develop a new ARIMAX model, as will be described in section 4.1.3. The variables that have been calculated as significant are used only if they reduce the forecast error [66]. Overall, to develop an ARIMA or ARIMAX model, there are seven iterative steps that need to be followed. Figure 4-3 shows and summarises the general approach of developing the ARIMA and ARIMAX models.

- 1- The first step is collecting and pre-processing the demand data and then checking the stationarity of the time series. The stationary time series is defined as a series

signal where the distribution of the random variables is invariant to time [66] [113]. For example, the time series with trends or seasonality are not stationary, whereas, a white noise series is considered stationary. Thus, the stationary is important for an ARIMA model. To determine if the time series is stationary, a unit root tests can be used. A number of methodological tests can be carried out such as the Augmented Dickey-Fuller test, Phillips-Perron (PP) test, and Kwiatkowski-Phillips-Schmidt-Shin (KPSS) test for stationary trends [80] [113].

- 2- If the data is not stationary, the first, second or more order differences need to be applied until the data become stationary. In this step the (d) differenced parameter value (d) is determined. Given the final stationary signal, we can select the appropriate (p, q) parameters of the ARIMA model.
- 3- The data is divided into training, validation and testing data sets in order to select the model and validate it. Typically, the training and validation are used in the forecast model selection phase and then the testing set is used to compare the models. This process aims to provide an unbiased evaluation of the forecast model [80] [107].
 - In general, the training set is the largest data set and it is used to fit the parameters of the model, train the forecast model and find the patterns. The training sets needs to be large enough to represent the data characteristics. This data set is mainly used to select the potential models. Then the validation set is used to try and find the best of these by training each of the models parameters in the training set and then testing the errors for forecasts in the validation set. The validation set is used as a final performance check for the trained network before testing the model with around 10% to 15% of the training set. The reason for this structure is to avoid a specific good forecast on the training set which turns out to be inaccurate in the test set. In addition, this way aims to avoid “overfitting”, by selecting a forecast that is over trained on the training set.
 - Finally, the testing set is used to provide an unbiased evaluation of the final forecast model and is typically 10% to 30% of the training set.

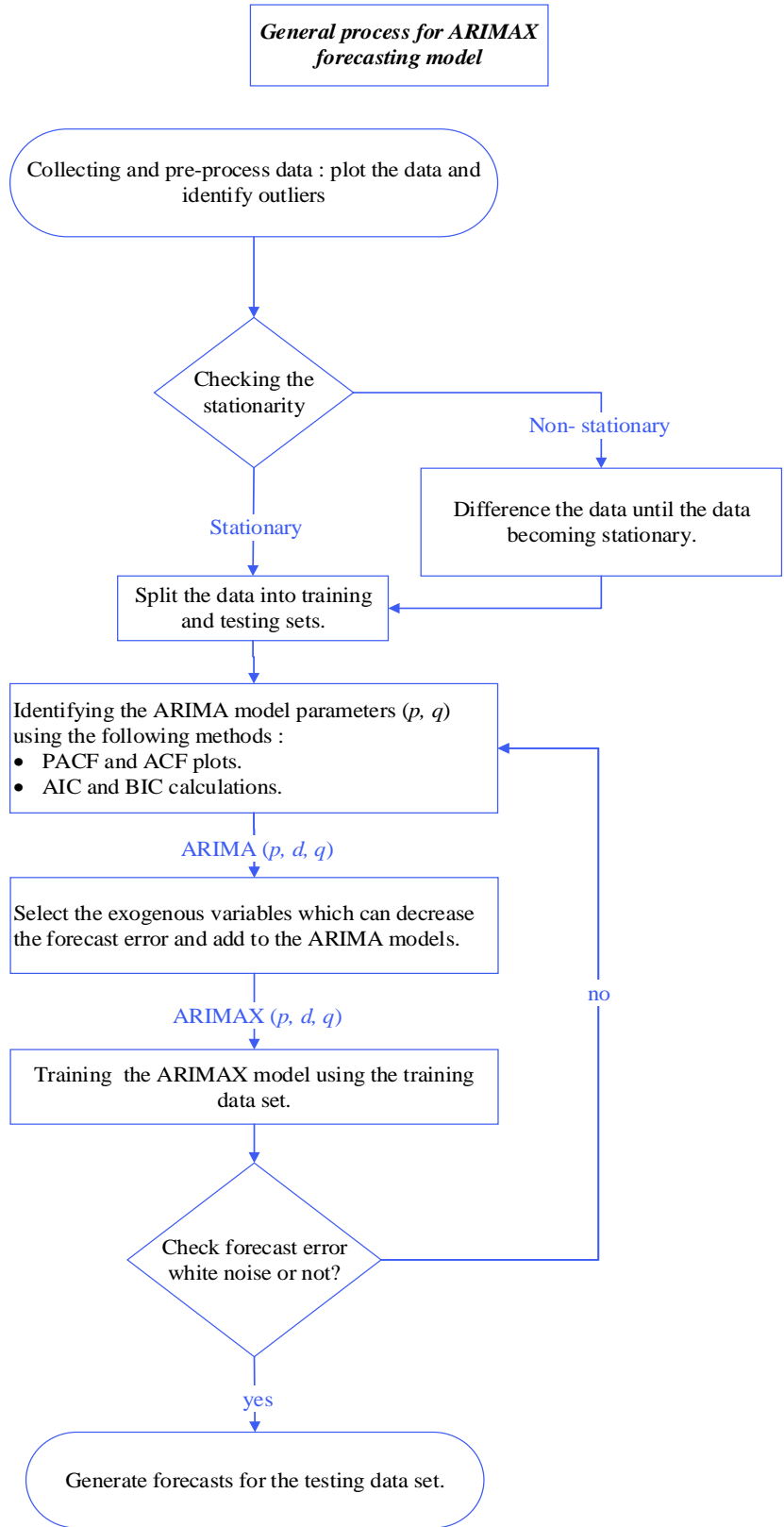


Figure 4-3: The summary of the ARIMA and ARIMAX approach [84] [87].

4- The autoregressive and moving average parameters (p, q) in ARIMA or ARIMAX models are often identified by firstly plotting the ACF and PACF of the stationary series to find the approximate (p, q) values. Then a selection of (p, q) values are test using Akaike’s Information Criterion (AIC) or Bayesian Information Criterion (BIC) to find the best parameter values in close proximity to the initial (p, q) guess. The procedure for using the ACF and PACF to find the approximate (p, q) values in ARIMA is also well known as the “Box-Jenkins” method [80] [107]. The ACF is a function used to measure the relationship between the historical observations and how the series is correlated. The ACF plot shows the correlation relationship between the time series and lagged time series for different lags. Furthermore, the ACF is an important tool for identifying the order of an MA(q) process, because it is expected to be effectively zero after lag q . In general, at least 50 observations are required to give a reliable estimate of the ACF. In contrast, the PACF plot shows the correlation relationship between the time series and the lagged time series, at say lag i , after removing the time effects lags $(1, 2, \dots, i - 1)$ between them. In order to select the ARIMA parameters (p, q), Table 4-1 outlines the procedures to select these parameters by using the ACF and PACF plots.

Table 4-1: The PACF and ACF behaviour to select p, q parameters [80] [107].

| Model | ACF | PACF |
|-----------------|----------------------------------------------------|----------------------------------------------------|
| MA (q) | Cuts off after lag q , and zero beyond lag q . | Exponential decay and/or damped sinusoid |
| AR (p) | Exponential decay and/or damped sinusoid | Cuts off after lag p , and zero beyond lag p . |
| ARMA (p, q) | Exponential decay and/or damped sinusoid | Exponential decay and/or damped sinusoid |

However, in some cases it is very difficult to determine the ARIMA or ARIMAX model parameters (p, q) through the ACF and PACF plot. For example, if both p and q are positive or there are significant spikes in both PACF and ACF plots. In this situation, another method is required to determine the ARIMA and ARIMAX parameters such as AIC or BIC [80] [107]. The AIC and BIC are useful tools for determining and selecting the best parameters or order of ARIMA and ARIMAX models in close proximity to initial (p, q) guess. The AIC and BIC give a trade-off between finding the maximum

likelihood estimate while penalizing the number of model parameters. This way helps to avoid overfitting and attempts to find a parsimonious model. In general, the best model parameter values are obtained from the minimum BIC or AIC value. The equations below describe the BIC and the AIC [80] [107] [114].

$$\text{AIC} = -2\log(L) + 2(p + q + r + 1), \quad (4-3)$$

$$\text{BIC} = \text{AIC} + (\log(F) - 2)(p + q + r + 1), \quad (4-4)$$

$$r = \begin{cases} 1 & \text{if } C \neq 0 \\ 0 & \text{if } C = 0 \end{cases}, \quad (4-5)$$

where L is the likelihood of the data, F is number of observations and C is a constant term and refers to Equation (4-1).

- 5- The selected exogenous variable are added to the ARIMA model to develop the ARIMAX model in terms of their ability to improve the forecast model performance and reduce the forecast error.
- 6- In this step, the proposed model uses the training data set to train the model and re-select the model parameters if the forecast error does not appear to be white noise.
- 7- Finally, the forecast is generated for the testing data set and the forecast error and the model performance are evaluated.

In general, the RTG crane demand shows a lack of seasonality and pattern in the demand time series where there is not a strong correlation between the current and historical demand. The ARIMAX model will rely more on the exogenous variables to generate and improve the forecast profile.

4.1.2 ANN Forecast Model

Energy demand forecasting is a challenging and complex problem which can involve different nonlinear relationships such as temperature and wind speed for renewable energy applications. Energy forecasting has used a variety of artificial intelligence techniques because they are highly flexible and can handle complex nonlinear relationships to develop accurate forecast models [67] [78]. One of the most popular artificial intelligence methods is ANN, this technique is a mathematical model with a wide range of applications including control systems [115] and forecasting [82]. Artificial neural network models were designed to mimic how biological NNs of the central nervous system operate and learn [62] [116]. The ANN is one of

the most popular short-term electricity load forecasting techniques and is widely used to forecast microgrid demand [78] [82].

Neural networks are mathematical models constructed by multiple layers of artificial neurons interconnected by a synaptic weight, W_{ij} , between each individual neuron, X_j , in one layer to each neuron in the next layer X_i [62] [86]. Figure 4-4 shows the structure of a typical individual artificial neuron where the summation of input signals (previous layer's outputs multiplied by the synapse) are processed through an activation function [62] [78] [86]. The activation function is used in the hidden units to modify the input to produce an output which is then used as an input for the next layer [107] [117]. The activation function for ANNs typically use either functions such as a sigmoid [107] or a hyperbolic tangent (tanh) function [118]. The activation function is a scalar to scalar function which aims to model non-linearity in complex behaviours and relationships and limit the neuron output [78] [107] [118].

The simplest neural network, as shown in Figure 4-5 (a), is equivalent to a linear regression containing one input layer and output layer with no hidden layers [107]. To model a nonlinearity system from the network, one or more intermediate layers with hidden neurons needs to be added to the network [62] [78] [107]. This type of network is called a multilayer feed-forward network or Multilayer Perceptron (MLP) and is popular network that is widely used in energy load forecasting [78] [107]. Figure 4-5 (b) shows the typical structure of an ANN model consisting of three layers (input, hidden, output), where the output of neurons in each layer becomes the input for the next layer [107]. Each of these layers includes a number of neurons that are fully weighted and modified by a nonlinear function and connected to the next layer [62] [78] [86].

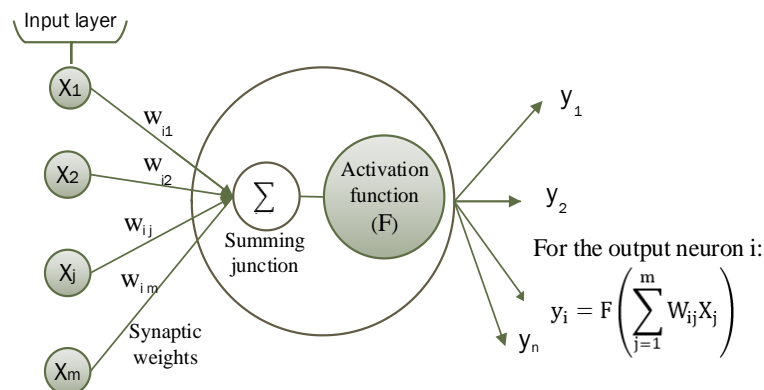


Figure 4-4: The structure of typical artificial neuron processing in an NN unit.

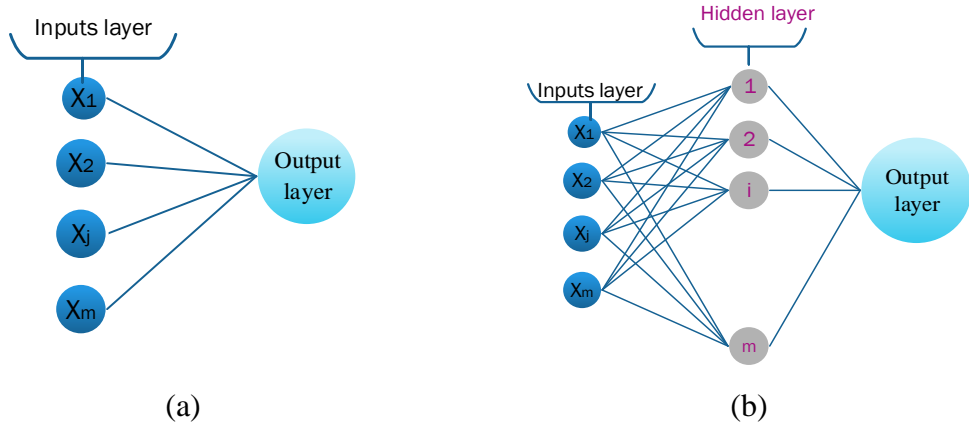


Figure 4-5: (a) The simplest neural network. (b) The multilayer neural network.

The output of each neuron, as seen in Figure 4-4, can be mathematically represented in Equations (4-6) and (4-7):

$$y_i = F\left(\sum_{j=1}^m W_{ij}X_j\right), \quad (4-6)$$

$$F(Q) = \frac{1}{1 + e^{-Q}} \quad (4-7)$$

where y_i is the summation of synaptic weights W_{ij} (between the input neuron j and the hidden neuron i) multiplied by the outputs of each individual neuron X_j (from the previous layer) and m is the number of neurons from the previous layer which are connected to the neuron i . In the structure of a typical individual artificial neuron, the summation of input signals from several synapses, as seen in Figure 4-4, are transferred through an activation function F for hidden layers described by Equation (4-7) for the sigmoid activation function, the most common nonlinear activation function, where $Q = \sum_{j=1}^m W_{ij}X_j$. The majority of the current ANN models for electrical load forecasting use sigmoid functions [62] [107] [119] [120], due to its differentiability which make it computationally easy to calculate.

Once the ANN model parameters are determined, the ANN needs to be properly trained to learn the relationship between the input and output nodes [117] [119]. This training will allow the modification of the node weights based on the training stage in order to achieve the most accurate estimation of any nonlinear forecasting model given by the output target values [78] [119]. Also, it will allow the modification of the weights of each input throughout all the network layers until the neural network model identifies the optimal model. The training stage

shows the main benefit of using the ANN technique, which is the effectiveness at fitting non-linear or complex relationships between the output target and input variables [62] [78]. However, this also means ANN models require large amounts of data to be accurate and could cause overfitting. The weights are selected in the neural network framework by using a learning algorithm. The back-propagation algorithms are the most popular and powerful learning tools in ANNs and these have been widely used as learning methods in electrical load forecasting problems [100] [120] [121]. A back-propagation algorithm aims to improve the performance of the ANN model and reduce the total error by updating the synaptic weights.

The back-propagation algorithm modifies the weights by calculating the error in a backward order, from the output layer to the input layer. In general, the ANNs use the training set to learn the key patterns between the input and output information by suitable synaptic weights. When each pattern is read, and the training reaches a satisfactory level, as described in the ANN procedures (step 5), the ANN holds the synaptic weights and uses the trained network to predict the future or make decisions. The network trains over a range of patterns, by using the back-propagation algorithm. This training process aims to improve the performance of the ANN model by minimizing the total squared error, Err , as described by Equation (4-8). Furthermore, the training process will stop, when there is no further reduction in the error function.

$$Err = \frac{1}{2} \sum_{k=1}^K \sum_i |D_{ki} - \hat{D}_{ki}|^2 \quad (4-8)$$

where D_k is the desired or target output and \hat{D}_k is the actual output vectors of the network model for a training data set on pattern k , and i refers to the i th output neuron. Furthermore, to develop an ANN model, there are three main iterative steps that need to be followed. Figure 4-6 shows and summarises the ANN model's procedures and presents the general approach of ANN [62] [120] [121].

- 1- Variable selection: the variables of the ANN are selected based on the clear understanding of the forecast target or problem and based on the relationships between predictor variables and output variables. There is no optimum or favourite method for selecting the ANN parameters. However, the trial and error method is one method that can be used to choose suitable ANN model parameters [69] [122] [123].
- 2- Data collection and pre-processing: after the variable selection step, the data base needs to be built by collecting all necessary data. In this step, all data need to be

checked to avoid any data errors or missing data. The missing observation may be handled by removal or estimating, say as the average of nearby data. This step includes analysing the data to minimise noise, detect trends and finding any significant relationships.

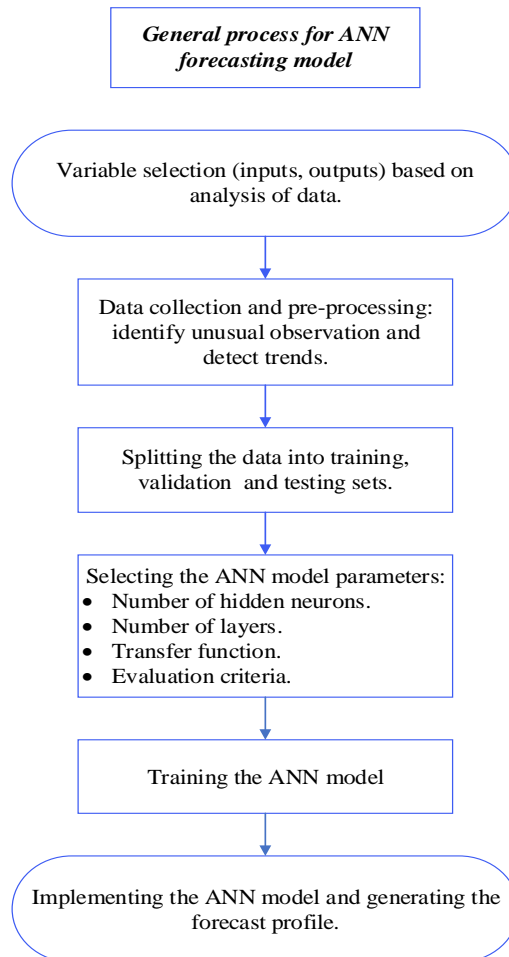


Figure 4-6: The summary of the ANN model approach [120] [121].

- 3- Splitting the data set: the time series data set will be divided into training, validation, and testing sets. In general, the training set is used to train the ANN model and find the network patterns and parameters and the validation set is used to find the best model.
- 4- ANN parameters selection: there is an infinite number of options and methods to develop an ANN model. In general, the trial and error method has been used to select the main parameters of the ANN model including the number of neurons, training functions and number of layers by creating different ANN models and calculating the

forecast error on the validation set for these models in order to choose the best model.

The below recommendation may help to select the suitable parameters [78] [115]:

- Number of hidden neurons: There is no specific or accurate formula to select the number of hidden neurons. However, there are approximation techniques in addition to the trial and test method:
 - Geometric pyramid rule: number of neurons equals the square root of the number of inputs multiplied by the number of outputs.
 - Rule of thumb: One of the most common rules of thumb is to select a number of hidden neurons between one and three times the number of inputs.
 - Number of hidden layers: in general, one or two hidden layers is able to handle a wide range of forecasting applications. In practice, increasing the number of layers may lead to the problem of overfitting and increase the learning time [62] [78] [121].
 - Transfer function: the majority of the current ANN models for electrical load forecasting use sigmoid functions [107] [121] but there are also other functions that can be used such as step function and tanh functions. There is not a specific method to select the best transfer function and in general trial and error is used [62] [78] [120].
 - Evaluation criteria in the training process: The most common evaluation methods is total squared errors [120] [121].
- 5- ANN model training stage: this step aims to learn patterns in the data and find the weight between the neurons that generates the minimum error for each model chosen, as described in Step 4. Furthermore, there are two main opinions of view about when we can stop the training:
- The training process should only be stopped if there is no improvement in the error function.
 - Training is to stop after a predetermined number of iterations.
- 6- Implementation: this step is considered the last step to generate the output forecast but in fact, it is used during the data selection, training times, and the evaluation of the model.

The procedure of designing an ANN forecasting model does not usually use a single-pass. It may be required to visit previous steps before finalising the model especially between the training model, model parameters and variable selection steps.

4.1.3 Exogenous Variables Estimation.

As previously discussed in Chapter 3, to achieve a satisfactory load forecast for RTG crane loads, the model must include the most correlated historical demand, the number of crane moves, and container gross weight. In this study, the container weight, $X_1(n)$, and the number of moves, $X_2(n)$, are the main exogenous variables to be included in the ANN and ARIMAX forecast models, due to the high correlation between these variables and the RTG crane demand, $D_L(n)$ (at half hour n). However, the future exogenous variables at $n+i$ ($i = 1, 2, \dots, 48$) are typically unknown and the highly volatile behaviour of the RTG crane demand for a fixed number of moves and container weight, as seen in Table 3-1 and Figure 4-7, increases the difficulty of achieving an accurate forecast model even when assuming the $X_1(n+i)$ and $X_2(n+i)$ are known in advance. Estimation techniques based on different distribution methods have been used widely for estimating the exogenous variables of forecast models [124] [125]. This chapter aims to examine the impact of the exogenous variables on the ARIMAX and ANN forecasts output. Here we develop models for:

- Estimating both exogenous variables $X_1(n)$ and $X_2(n)$.
- Estimating only one exogenous variable, for example $X_1(n)$ and assume that the second variable $X_2(n)$ is known in advance.

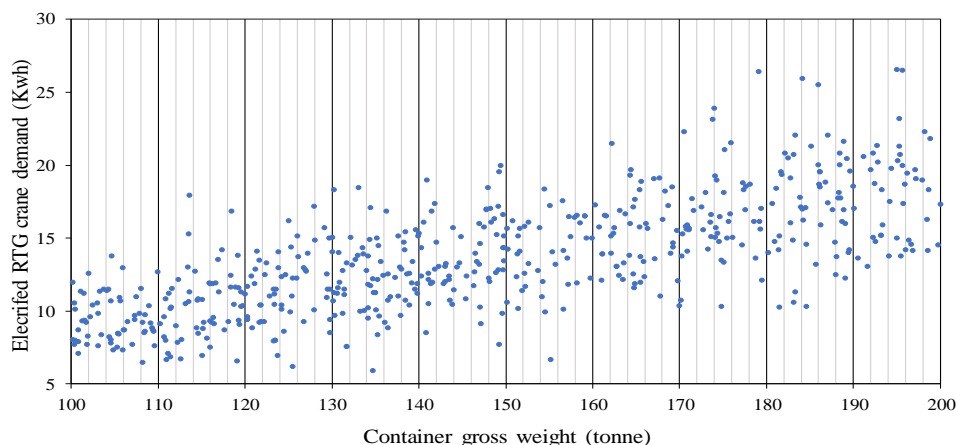


Figure 4-7: Electrified RTG crane demand variation for different container gross weight.

The proposed forecast models with these estimation methods are compared to the case when assuming the exact values of the $X_1(n)$ and $X_2(n)$ are known in advance. The variables are estimated by randomly sampling from the constructed distribution functions for these variables. When one variable is known, the other is sampled from conditional probability distribution. The estimation model utilises the empirical distribution of the crane demand, number of moves and container gross weight to improve the prediction performance. Figure 4-8 displays the 2D histogram of the exogenous variables data sets. Each of the histogram bins (bars) presents the joint distribution of the exogenous variables (container gross weight and number of crane moves). In Figure 4-8, the numbers of bins help to estimate the distribution where there is only a relatively small number of observations.

In this section, a Monte Carlo method is proposed to sample and estimate the future $X_1(n)$ and $X_2(n)$ from the probability empirical distribution as displayed in Figure 4-8. Monte Carlo is a computational algorithm which uses repeated random sampling to model the range of possible events for many scenarios [59]. The basic steps for using the Monte Carlo method to generate the future $X_1(n)$ and $X_2(n)$ are summarised as follows [59]:

- 1) Identify the problem variables and specify the presample data. In this work, the training data set is used as the presample data.
- 2) Specify the empirical joint distribution of the number of crane moves and container gross weight by using the histogram bins (bars), as seen in Figure 4-8.
- 3) Generating stochastic samples from the joint distribution of the container weight and number of moves.

On the other hand, if one of the exogenous variables is known, the conditional distribution is used to determine the other variable. From Figure 4-9 if $X_2(n)$ is 2, the conditional distribution (sampling) is defined by the dots with the red box for which $X_2(n) = 2$.

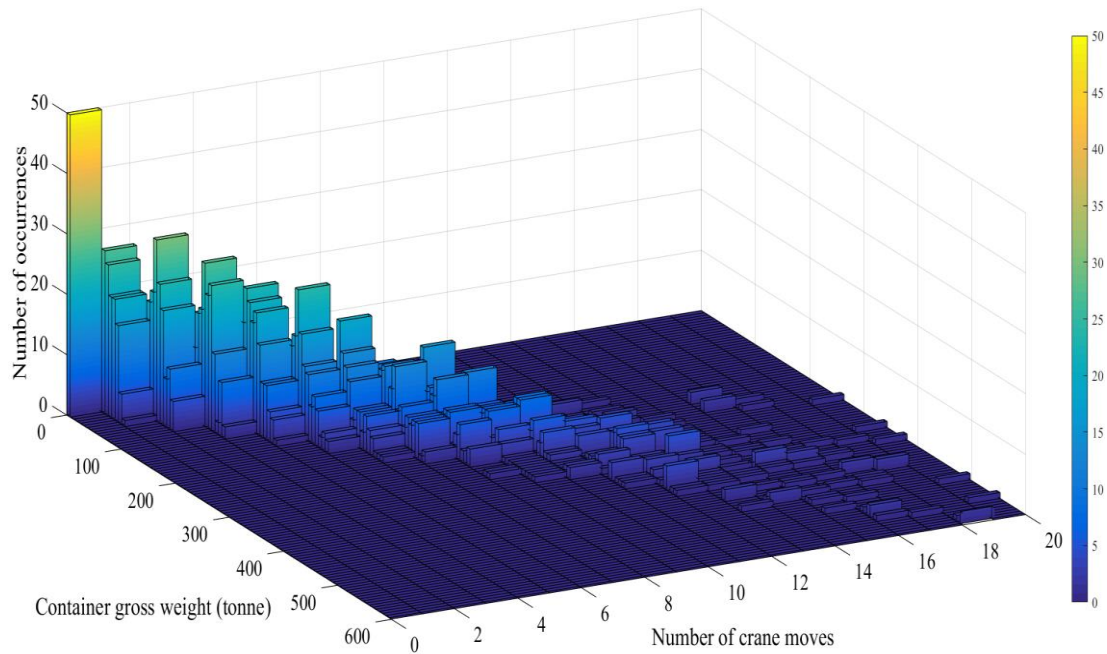


Figure 4-8: Illustration of distribution of number of crane moves and container gross weight data in a 2D histogram.

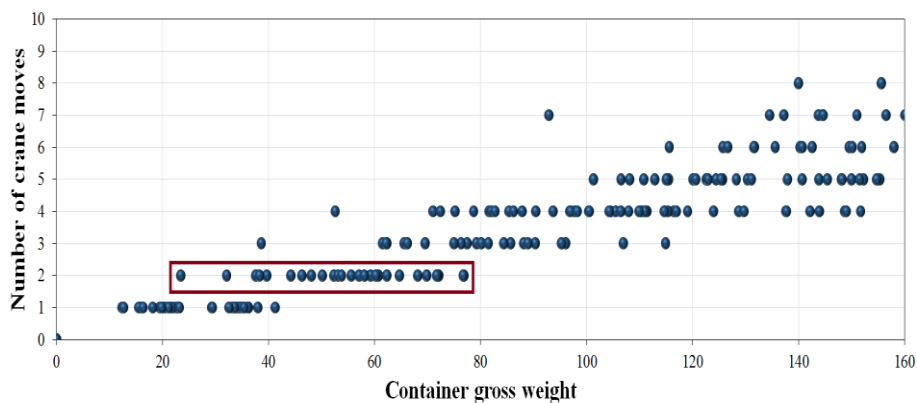


Figure 4-9: Illustration of conditional distribution when $X_2(n)$ is 2.

Ports worldwide are converting from diesel to electrified RTG cranes with fully automated work solutions to achieve the gas emissions and safety of life at sea convention (SOLAS) requirements. From 1st of July 2016 all shippers, freight forwarders and ports around the world are required to follow the new SOLAS requirements. This requires the gross weight of each container to be recorded when leaving and arriving at any port [126] [127]. These new international requirements and rules will help ports around the world to know the exact weight of the container in advance. Furthermore, this makes the assumption of knowing the container gross weight and number of crane moves in advance achievable and realistic in the future

especially at fully automated ports. To test the effect of estimating the container weight and number of moves on the accuracy of the forecast, in the following section, we have developed ANN and ARIMAX forecast models to predict RTG crane demand 24 hours ahead using variations on the input variables. The proposed forecast models developed include the following four exogenous variables variations:

- Estimating the future exogenous variables $X_1(n)$ and $X_2(n)$.
- Estimating one of the exogenous variables and assuming the other variable is known in advance.
- Assuming both exogenous variables are known in advance.
- Generating the forecast models without the exogenous variables $X_1(n)$ and $X_2(n)$.

4.2 The RTG crane demand forecast models.

As described in previous section, developing accurate ANN and ARIMAX forecast models is a critical challenge. In addition, studies on forecasting the LV demand are sparse in the literature and none present a prediction model that generates forecast profile of electrified RTG crane demands. This section will present the forecast models that are used to predict the half hourly electrified RTG crane demand for the next 24 hours. Section 4.2.1 will develop an ANN forecast model and go on to describe the process to determine the neural network parameters. Section 4.2.2 will present the ARIMAX forecast model and develop a number of time series forecast models. The ANN and ARIMAX forecast models are developed using variations on the input exogenous variables, to investigate the effect of estimating these variables on the accuracy of the forecast.

4.2.1 ANN Forecast Modelling.

The ANN feedforward model aims to forecast the electrified RTG crane $\widehat{D}_L(n+i)$, where n is the current time step and $i = 1, 2, \dots, 48$. As presented in Section 4.1.2, the ANN model procedure in Figure 4-5 was followed in order to select the suitable parameters models, as follows:

1- Variable selection:

- Output variables: the main target of this chapter, the future electrified RTG crane demand $\widehat{D}_L(n+i)$.

-
- Input variables: firstly, the exogenous variables $X_1(n)$ and $X_2(n)$ has been selected as main input variables, due to the strong relationship between them and $D_L(n)$. Secondly, the trial and error method were used to choose addition input variables based on the relation between current demand $D_L(n)$ and historical demand. The analysis of the results for the trial and error tests is presented in the selection parameters step (step 4).
- 2- Data collection and pre-processing: the measured data (RTG crane demand, container gross weight and number of moves) were collected at the Port of Felixstowe in the UK from two electrified RTG cranes over three different periods during normal operation days.
- The first data set was collected from 15th of April to 10th of May 2016.
 - The second data set from 7th of September to 10th of October 2016. The first and second data sets originating from the same crane.
 - The third data set was collected from another RTG crane over seven days from the 7th to the 13th of December 2016.

The three data sets that has been used in this chapter are different from those used in Chapter 3 to develop the forecast models.

- 3- Dividing data set: The first data set is divided into 21 days of training and validation data sets and five days of testing data. The second and third data sets are used as testing data sets.
- 4- ANN model parameters selection: the following parameters functions have been used in this section, due to their ability to successfully solve complex relationships, its computationally ease perform and the common set of parameters in this majority of the current ANN models for short-term electricity load forecasting [62] [78] [86].
- Training function: Levenberg-Marquardt backpropagation.
 - Transfer function: sigmoid function.
 - Evaluation criteria: The total squared errors.
 - The stopping criteria: when no further improvement in the error function.
 - Final forecast model evaluation: in this section the MAPE is used to evaluate the forecast performance. The forecast model evaluation methods

will be described in further details in Section 4.3. The MAPE with other evaluation forecast methods are defined in Section 4.3.2.

Furthermore, in order to select suitable model remaining parameters, the trial and error test is used to select the number of hidden layers and number of neurons in the hidden layers.

The trial and error test analysis for ANN forecast model

The analysis in this test aims to check the ANN forecast model's performance using the training and validation data sets for different ANN parameters in order to select the suitable model parameters. The number of hidden layers, number of neurons and input variables are tested to select the ANN model parameters. Firstly, we developed a reference model with the following parameters, as seen in Figure 4-10.

- Input variables: $X_1(n)$ and $X_2(n)$.
- Number of hidden layers: the proposed model includes two hidden layers.
- Number of hidden neurons: there are 20 neurons in each hidden layer.

Then, the model performance has been investigated by changing one parameter in every trial, to select and best model parameter.

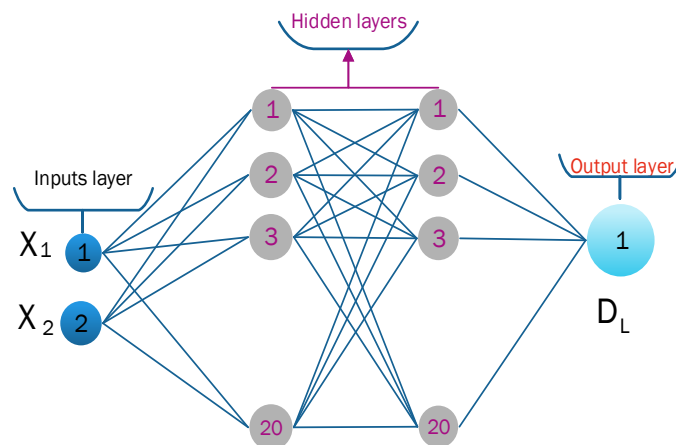


Figure 4-10: The proposed ANN forecast model.

The number of hidden layers: the reference ANN model, as seen in Figure 4-10, is tested here by changing the number of layers from one to four hidden layers. Table 4-2 shows the MAPE results during the training period for models with one to four hidden layers to avoid overfitting and increase the learning time problems [62] [123]. The minimum MAPE was 9.7% for the two hidden layers model and the maximum MAPE value was 10.9% for the four-hidden layer model. However, all the MAPE results for

every number of layer option had values of around 10% and the difference was only around 1% between the maximum and minimum MAPE values. The mean value of the daily MAPE for the two-layer model was also the lowest compared to other models. As a result, the most suitable number of layers for this data set is two hidden layers.

Table 4-2: The forecast error for an ANN model with different number of hidden layers.

| Number of layers | Overall MAPE | Mean of the daily MAPE |
|------------------|--------------|------------------------|
| 1 | 10.3% | 10.2% |
| 2 | 9.7% | 9.6% |
| 3 | 10.7% | 10.5% |
| 4 | 10.9% | 10.8% |

The number of neurons in each hidden layers: the literature review has shown that for the load forecasting problems, the number of neurons mainly used was between 5 and 20 to avoid the overfitting problem due to an unnecessary increase in the number of neurons [78] [123]. In order to compare how the number of neurons can affect the ANN model in this project, the proposed ANN model parameters are fixed except for the number of neurons which were varied from 5 to 25. Table 4-3 presents the overall MAPE results for the ANN models with 5, 10, 15, 20 and 25 neurons in each of the two layers. The table results show that the minimum MAPE was 9.7% for the (20 20) neurons model. The maximum MAPE value was 12.3% for the system with 5 and 25 neurons. Furthermore, most ANN of the models recorded MAPE values between 10% and 11%.

Table 4-3: Overall MAPE values for an ANN model with different numbers of neurons.

| Number of neurons | 5 | 10 | 15 | 20 | 25 |
|-------------------|-------|-------|-------|-------------|--------|
| 5 | 11.9% | 11.5% | 11% | 10.9% | 11.3% |
| 10 | 11.5% | 10.8% | 10.4% | 10.2% | 11.1 % |
| 15 | 11.3% | 10.9% | 10.3% | 9.9% | 10.7% |
| 20 | 11.1% | 10.6% | 10.1% | 9.7% | 10.5% |
| 25 | 12.3% | 11.9% | 11.7% | 10.9% | 11.8% |

The input variable: the reference ANN forecast model with X_1 and X_2 as input variables are used to test the impact of adding other variables. As previously discussed in Chapter 3, the RTG crane demand analysis shows a weak relation to the historical load. However, to check the effect of the different input variables on the above proposed ANN model, and then choose the most suitable new input variables, from variable X_3 to X_7 , that improves the performance of the forecast model. In this test, we added one new variable (from the below variables) each time to the reference ANN forecast model with X_1 and X_2 . The exogenous variables (X_3 to X_7) are used in the literature to minimise the errors in the model and help to improve the forecast performance for LV demand application [92] [104] [105]. Overall, choosing a suitable exogenous variable plays a significant role in improving the forecast performance and these variables are mainly selected based on model targets and data availability.

- X_3 : Hour of the day.
- X_4 : Previous half hour load.
- X_5 : The average of previous two hours.
- X_6 : Previous day load in same half hour.
- X_7 : Previous week load in same half hour.

Table 4-4 shows that the proposed model with only the two input variables X_1 and X_2 is the best model with the lowest overall MAPE (9.7%) and mean daily MAPE (9.6%). All input variables from X_3 to X_7 had MAPE values of more than 10% and the highest overall MAPE (11.7%) was for the model with X_6 as an input variable. Furthermore, the ANN models with X_3 to X_7 input variables recorded MAPE values between 10.5% and 11.7%.

Table 4-4: Overall MAPE values for ANN model with different input variables.

| Item | The proposed ANN model | X_3 | X_4 | X_5 | X_6 | X_7 |
|--------------|------------------------|-------|-------|-------|-------|-------|
| Overall MAPE | 9.7% | 10.6% | 10.7% | 10.5% | 11.7% | 11.4% |
| Daily MAPE | 9.6% | 10.5% | 10.6% | 10.5% | 11.6% | 11.1% |

5- Implementation of ANN forecast models with various inputs.

The trial and error analysis in line with the correlation analysis from the previous steps helped to estimate the best model parameters. For summary, the ANN proposed models in this work are the feedforward ANN activated by a sigmoid function and trained by the Levenberg-Marquardt with 2 hidden layers; 20 neurons in each hidden and 1 output layer referring to the RTG crane demand in order to simplify the model network, as seen in Figure 4-9. In addition, the following modified ANN forecast models are to test the effect of estimating the future exogenous variables $X_1(n)$ and $X_2(n)$, as described in Section 4.1.3, on the accuracy of the forecast.

- Model A

The objective of Model A is to investigate the performance of a forecast model that does not include any of the exogenous variables $X_1(n)$ and $X_2(n)$. The RTG crane demand data analysis in Chapter 3 shows that the autocorrelation over the time series is weak. However, for this model, the lags with the highest correlation are chosen. The following values have been used as input neurons for Model A: the average of the previous day's demand; the average of the previous week's demand; the same half hour demand for the previous day (X_6); the previous half hour's demand (X_4). In this model, the parameters of Model A has been modified to include 4 input neurons, as presented in Figure 4-11. In this chapter, we have used Model A as a benchmark to compare against the other ANN forecast models.

- Model B

Model B has been structured to generate the forecast models using the exogenous variables, $X_1(n)$ and $X_2(n)$, as presented in Figure 4-11. The exogenous variables have been selected based on the correlation analysis in Chapter 3 and the trial and error test results. Model B has been divided into four sub models based on the exogenous variables that are known or estimated, as described in Section 4.1.3:

- Model B1: assuming both exogenous variables are known.
- Model B2: estimating the number of crane moves while assuming the container gross weight is known by using the Monte Carlo method to sample the future variable, as described in Section 4.1.3.

- Model B3: estimating the container gross weight while assuming the number of crane moves is known.
- Model B4: estimating both of the exogenous variables by using the Monte Carlo method to sample the future variables, as described in Section 4.1.3.

Model B aims to utilise the correlation between exogenous inputs and RTG crane demand to improve the ANN forecast performance. Throughout this chapter, we refer to the container gross weight as the exogenous variables, $X_1(n)$, and number of crane moves, as the exogenous variables, $X_2(n)$.

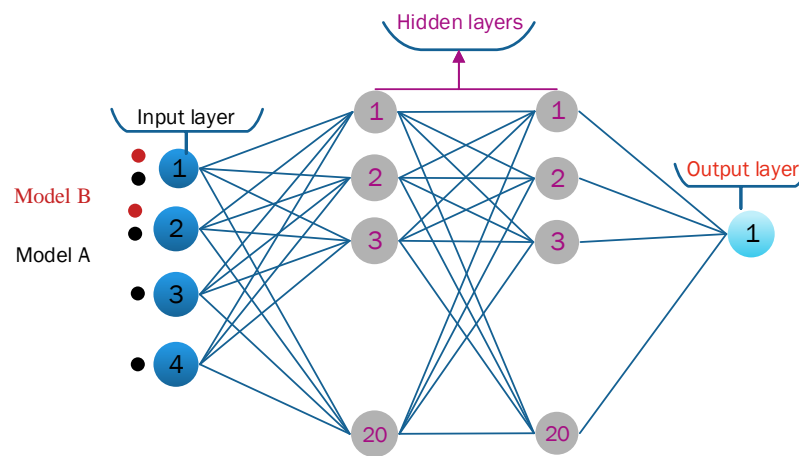


Figure 4-11: Representation of ANN forecast models: Model A employs four input neurons while Model B uses two input neurons.

4.2.2 ARIMAX Forecast Modelling

This section presents the ARIMAX model used to forecast the electrical demand of an electrified RTG crane. After the data collection stage, the general process flowchart in Figure 4-3 was used to develop the ARIMAX forecast model as follows:

- 1- The preparation and pre-processing of the electrified RTG crane data including the correlation analysis and plotting of the load curve were presented and discussed in Chapter 3. The splitting of data into training and test data sets were conducted, see Section 4.2.1.
- 2- The stationarity of the RTG crane demand: in this stage, it is necessary to make sure that the demand curve is stationary. In order to check for the stationarity and stability, the Augmented Dickey-Fuller test (ADF) and Phillips-Perron test (PP) were carried out, as the most popular unit root tests [113] [118] [128]. In general, ADF tests to see

if the time series is stationary around a linear trend that includes the lagged value. Unlike the ADF, PP test does not require selection of the level of correlation with lagged values and runs a variance estimation. However, the PP test requires a large number of samples. The null hypotheses of ADF and PP tests aim to see if the time series is non stationary [118] [128]. Table 4-5 shows the statistical tests with null hypothesis (H_0) applied to the demand time series. The null hypothesis (H_0) is rejected when the p-value goes below the significance level 0.01. The ADF and PP tests investigate the unit-root hypothesis and shows that the series is stationary due to the rejection of the null hypothesis.

Table 4-5: Statistical tests: ADF and PP.

| Test | Null Hypothesis: H_0 | Result in respect to H_0 |
|-------------------------------|--------------------------|----------------------------|
| Augmented Dickey-Fuller (ADF) | Series is non-stationary | Reject |
| Phillips-Perron (PP) | Series is non-stationary | Reject |

- 3- In case the demand series is non-stationary, it is necessary to apply the differencing method for the first, second or more order until the series becomes stationary. In our case the series was stationary, so could move to the next step and set the ARIMA difference parameter, (d) equal to 0 as no differences were required.
- 4- The identification of suitable ARIMA parameters (p, d, q): to determine the (p) and (q) parameters, the ACF and PACF for the crane demand series are plotted in Figures 4-12 and 4-13 for 120 lags in order to give the approximate (p) and (q) parameters. In this work, the demand series shows highly volatile behaviour where the significant lags of PACF and ACF did not show any signs of repetition or seasonality, as discussed in Section 3.2.1. Secondly, the Bayesian Information Criterion (BIC) was used to select the best parameters of an ARIMA model in close proximity to the initial guess. The literature review [67] [80] [107] showed that the popular forecasting ARIMA models parameters (p, d, q) are mainly between 1 to 2 for (p, q) and between 0 to 2 for (d) and these parameters have been widely applied in different electricity applications. However, this thesis extends the parameters in order to increase the opportunity to obtain the best ARIMA model based on the following:

- Covering all significant lags in the ACF plot (14 lags) and PACF plot (4 lags) especially as there is no trend or repetition for the significant lag (Figure 4-12).
- Covering a large number of p and q possibilities.

The BIC matrix was calculated and tested based on the following parameter values: (p) from 1 to 24, (q) from 0 to 24, and (d) from 0 to 2 in order to select the ARIMAX model parameters. In this work for the data given, the best ARIMAX model parameters were obtained from the minimum BIC value. Table 4-6 shows the BIC matrix results and presents the best ARIMA model parameters (p, d, q) based on the available data for the electric RTG crane demand with the minimum BIC given by (p, d, q) = (1,0,2).

- 5- The selection of the exogenous variables, which may increase the efficiency of the forecast model's performance. The correlation analysis, in Chapter 3, between the crane demand, number of crane moves, and container gross weight presents significant signs of a strong relationship that can be used to create an exogenous variable. In this chapter, the number of crane moves, and container gross weight are the exogenous variable for the ARIMAX model. In addition, the following subsection presents ARIMAX modified models based on different exogenous variables options to present the impact of the exogenous variables on forecast performance similar to the ANN model in Section 4.2.1.
- 6- The training of the model ARIMAX (1,0,2) carried out by using the training data.
- 7- The forecast error is evaluated over the testing period by using different evaluation methods such as MAPE, as presented in Section 4.3.

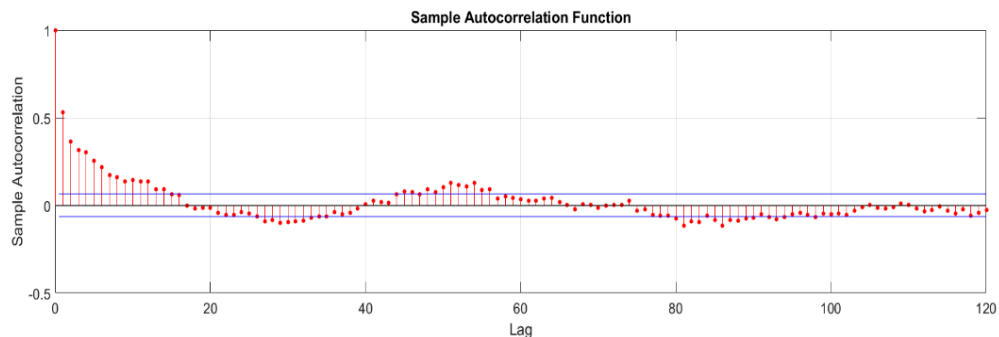


Figure 4-12: ACF plot for the RTG crane demand.

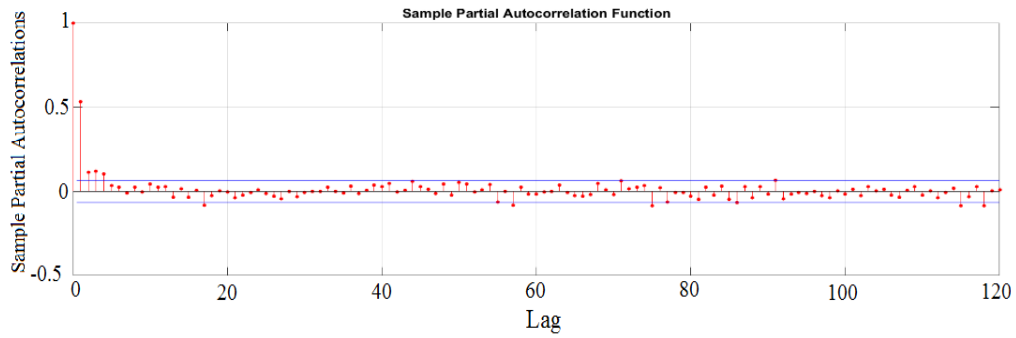


Figure 4-13: PACF plot for the RTG crane demand.

Table 4-6: The BIC results for the demand series when ($d = 0$) for a variety of (p, q).

| | | number of q | | | | | | | | | |
|-------------|---------|-------------|----------------|---------|---------|---------|---------|---------|---------|---------|---------|
| | | 1 | 2 | 4 | 8 | 10 | 16 | 18 | 20 | 22 | 24 |
| number of P | 1 | 11945.6 | 11906.1 | 11936.8 | 11943.5 | 11950.3 | 11950.2 | 11953.1 | 11956.5 | 11950.7 | 11962.4 |
| | 2 | 11964.7 | 11921.0 | 11938.7 | 11940.5 | 11938.1 | 11951.6 | 11955.1 | 11955.3 | 11959.1 | 11963.3 |
| | 4 | 11936.8 | 11916.0 | 11937.3 | 11939.3 | 11940.8 | 11948.5 | 11952.2 | 11955.0 | 11957.4 | 11948.0 |
| | 5 | 11938.6 | 11913.5 | 11944.3 | 11938.5 | 11940.9 | 11951.4 | 11952.3 | 11955.5 | 11958.8 | 11962.7 |
| | 6 | 11937.7 | 11911.0 | 11935.0 | 11940.9 | 11943.0 | 11952.2 | 11954.0 | 11952.7 | 11960.7 | 11964.7 |
| | 8 | 11944.0 | 11921.7 | 11938.4 | 11940.4 | 11939.5 | 11943.6 | 11944.2 | 11947.8 | 11939.4 | 11961.9 |
| | 10 | 11945.4 | 11946.0 | 11944.0 | 11946.2 | 11930.7 | 11938.5 | 11939.9 | 11943.2 | 11946.0 | 11949.1 |
| | 12 | 11944.8 | 11946.8 | 11944.2 | 11947.4 | 11929.2 | 11938.4 | 11948.4 | 11940.5 | 11943.0 | 11952.0 |
| | 14 | 11966.6 | 11945.2 | 11949.0 | 11942.7 | 11934.6 | 11935.6 | 11936.6 | 11936.9 | 11940.0 | 11950.5 |
| | 16 | 11976.6 | 11952.1 | 11950.2 | 11941.6 | 11938.7 | 11931.6 | 11933.7 | 11933.3 | 11937.1 | 11949.0 |
| | 18 | 11950.2 | 11947.7 | 11949.7 | 11949.4 | 11934.6 | 11928.5 | 11930.8 | 11929.6 | 11934.1 | 11947.5 |
| | 20 | 11955.2 | 11956.6 | 11952.6 | 11959.1 | 11947.4 | 11925.3 | 11927.9 | 11926.0 | 11931.1 | 11945.9 |
| | 22 | 11956.6 | 11955.1 | 11964.1 | 11955.6 | 11947.3 | 11922.1 | 11925.0 | 11922.4 | 11928.2 | 11944.4 |
| 24 | 12005.4 | 11965.4 | 11967.0 | 11952.2 | 11958.4 | 11919.0 | 11922.2 | 11918.7 | 11925.2 | 11942.9 | |

Implementation of ARIMAX forecast models

The ARIMAX model is an extension of the ARIMA (p, d, q) model, with exogenous variables. The BIC matrix calculations, as seen in Table 4-3, show that the best ARIMAX model order is equal to (1, 0, 2). The $X_1(n)$ and $X_2(n)$ are the exogenous variables in the proposed ARIMAX model. This subsection presents ARIMAX modified models based on different input variable options, as presented in Figure 4-14, to present the impact of the exogenous variables and the models parameters on the forecast model performance. The following forecast model models are mainly time series forecast models that are deduced from the ARIMAX.

- Model C

Model C is the ARIMAX (1, 0, 2) forecast model which includes the exogenous variables. This model aims to examine the exogenous variables as input parameters similar to Model B. In addition, the ARIMAX model has been divided into four models: Model C1, Model C2, Model C3, and Model C4 analogous to Model B in Section 4.2.1.

- Model D

Model D (ARX) is a subclass of the ARIMAX model. The main advantage of an ARX model is its speed at calculating the forecast and the model coefficients. The ARX(p) order based on the BIC calculations for the available data sets gives $p = 1$. The BIC matrix was calculated and tested for p values from 1 to 24 in order to: cover all significant lags in ACF and PACF plots especially when there is no trend or repeating values for the significant lags; cover a large number of lags compared to the literature. Furthermore, to evaluate the effect of exogenous variables on the forecast model, the ARX model is divided into four models (Model D1, Model D2, Model D3 and Model D4) similar to Model B and Model C.

- Model E and Model F

In this section, Model E (AR) and Model F (ARIMA) are as in Model D and Model C, respectively but without the proposed exogenous variables, $X_1(n)$ and $X_2(n)$. The ARIMA and AR forecast model order parameters are equal to (1,0,2) and (1) respectively based on the BIC calculations. In addition to Model A, Model E, and Model F are used as benchmarks.

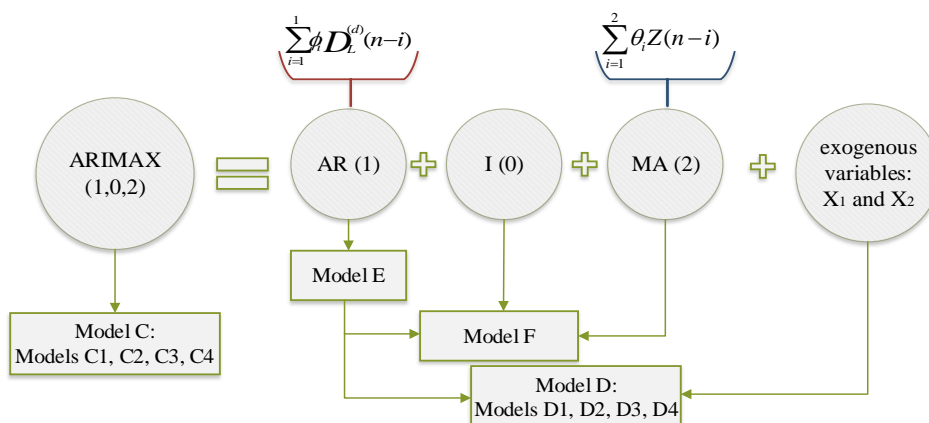


Figure 4-14: Schematic for the various ARIMAX and ARX forecast models.

4.3 Results and Discussion for the Forecast Models.

The forecast models: Model A, Model B, Model C, Model D, Model E, and Model F, as described in the previous section, present the ARIMAX and ANN with and without different exogenous variables to investigate the impact of these variables on the forecast performance for RTG crane demand. This section will present and discuss the forecast results from the previous ARIMAX and ANN models. First, the collected data for a specific example is presented, then the load forecasting model evaluation tools are introduced. Throughout Section 4.3 the forecast models are compared and the effect of estimating exogenous variables is discussed. Then, the forecast error is analysed to evaluate the best forecast model performance. Finally, a comparison of the forecast model techniques is presented.

4.3.1 Data Collection and Analysis

As discussed previously, the collected data at the Port of Felixstowe in the UK has been divided into training, validation and testing data sets. The RTG crane demand, container gross weight and number of moves data were collected from two electrified RTG cranes over three different periods during normal operation days. The measurement system at PoF is described in Appendix A. Due to the non-smooth behaviour of the RTG crane load and the lack of seasonality or trends over the time series (as described in the Chapter 3), we assume that the gap in the time series will have negligible effect on the forecast results. In this section, the testing period with 46 days data set allows us to evaluate the forecast model over three different time periods and test the transferability of the model trained on one crane to the other crane with the same specifications.

4.3.2 Load Forecasting Model Evaluation

To assess the performance of the forecasting model or compare different forecasting techniques for a specific time series or a particular application, it is important to define the performance evaluation method. The forecast accuracy or forecast error can be measured by using different techniques [80]. Reference [80] shows that there are four main performance evaluation techniques that have been used to evaluate the accuracy of load forecasting models. In this chapter, the Mean Absolute Percentage Error (MAPE), Root Mean Square Error (RMSE) and Mean Absolute Error (MAE) have been used to evaluate the models performance.

$$\text{MAPE} = \frac{100}{N} \sum_{n=1}^N \left| \frac{D_L(n) - \widehat{D}_L(n)}{D_L(n)} \right|, \quad (4-9)$$

where D_n is the demand of an electrified RTG crane; \widehat{D}_n is the forecasted load; n is the time step and N is the number of observations in the test period. The MAPE is one of most common load forecasting evaluation methods, due to its scale-independency and its ease of interpretation as a percentage [80]. However, MAPE cannot be used if the actual value is zero because it produces infinite or undefined values. In order to avoid this problem, the RMSE and MAE are also used in this section to evaluate the forecast model results. However, these evaluation methods focus on the mean of the error and does not present the forecast performance at every time step. Furthermore, in some cases the peak magnitude in the forecast and actual profiles are closed, but the error is very high which is related to the time shift between the two profiles. In future work, the evaluation method will be updated to investigate these criteria by using an energy score model.

$$\text{RMSE} = \sqrt{\frac{\sum_{n=1}^N (D_L(n) - \widehat{D}_L(n))^2}{N}} \quad (4-10)$$

$$\text{MAE} = \frac{\sum_{n=1}^N |D_L(n) - \widehat{D}_L(n)|}{N} \quad (4-11)$$

4.3.3 Overall Comparisons

The MAPE was calculated for each day of the three testing periods and plotted for each model in Figure 4-15. In addition, the overall MAPE for each model is presented in Table 4-7. From Figure 4-15 and Table 4-7, Model B1 provided the highest prediction accuracy over the three testing periods in terms of the overall performance. For all three testing periods, the Model A benchmark outperformed the other two benchmarks Model E and Model F. The MAPE for Model A was 21.9%, 27.8% and 19.6% for testing periods 1, 2 and 3, respectively. From Figure 4-15 (a) and Table 4-7, it is seen that by using the both exogenous variables in Model B1, the performance is clearly much better compared to the benchmark Models A, E, F, which only use the RTG crane historical load data with MAPE decreased by 18.7%, 27.8% and 27.4, respectively. The MAPE curve of Model B1 in Figure 4-15 (a) shows a sign of stability over the testing period compared to the benchmark models that exhibit large peaks. This is due to the weak daily and weekly trends in the data. Furthermore, the high error peaks in Figure 4-15 correspond to low demand values and can be explained by the disturbance introduced by

the human operator and the large uncertainty of the exogenous variables. The following section will present the impact of choosing each of the exogenous variables, X_1 and X_2 , on the forecast models accuracy in more details. Furthermore, to extend the forecast performance analysis, the RMSE and MAE methods were used to evaluate the forecast models' performance over the crane data set from 7th of September to 10th of October 2016 (testing period 2). Table 4-8 shows that the Model B1 outperformed all other models and provided the minimum RMSE and MAE values of 3.8 kWh and 5.3 kWh, respectively. Model E generated the highest RMSE and MAE values over the testing period of 19.1 kWh and 25.5 kWh.

Table 4-7: Overall MAPE over each of the three testing periods.

| Testing period | MAPE (%) | | | | | | | |
|----------------|----------|-------------|----------|----------|----------|----------|----------|----------|
| | Model A | Model B1 | Model B2 | Model B3 | Model B4 | Model C1 | Model C2 | Model C3 |
| Period 1 | 21.9% | 8.1% | 10.7% | 10.8% | 31.1% | 9.8% | 11.9% | 12.7% |
| Period 2 | 27.8% | 9.1% | 11.4% | 12.5% | 32.6% | 10.6% | 10.7% | 14.6% |
| Period 3 | 19.6% | 7.7% | 8.7% | 16.3% | 18.1% | 9.1% | 8.9% | 24.1% |

| Testing period | MAPE (%) | | | | | | |
|----------------|----------|----------|----------|----------|----------|---------|---------|
| | Model C4 | Model D1 | Model D2 | Model D3 | Model D4 | Model E | Model F |
| Period 1 | 43.1% | 9.8% | 9.5% | 13.6% | 49.1% | 36.3% | 36.1% |
| Period 2 | 31.2% | 10.9% | 10.9% | 13.9% | 32.5% | 36.9% | 36.5% |
| Period 3 | 43.5% | 9.7% | 10.3% | 27.8% | 42.9% | 21.3% | 23.8% |

Table 4-8: Performance of forecast models over 34 testing days (period 2).

| Model | MAE value (kWh) | RMSE value (kWh) | Model | MAE value (kWh) | RMSE value (kWh) |
|----------|--------------------|---------------------|----------|--------------------|---------------------|
| Model A | 15.2 | 16.7 | Model C4 | 17.2 | 21.1 |
| Model B1 | 3.8 | 5.3 | Model D1 | 4.4 | 6.4 |
| Model B2 | 4.6 | 6.2 | Model D2 | 4.5 | 5.7 |
| Model B3 | 5.7 | 6.7 | Model D3 | 6.1 | 7.2 |
| Model B4 | 17.9 | 21.5 | Model D4 | 17.3 | 21.3 |
| Model C1 | 4.1 | 6.3 | Model E | 19.1 | 25.5 |
| Model C2 | 4.3 | 5.6 | Model F | 18.1 | 23.3 |
| Model C3 | 5.9 | 6.9 | | | |

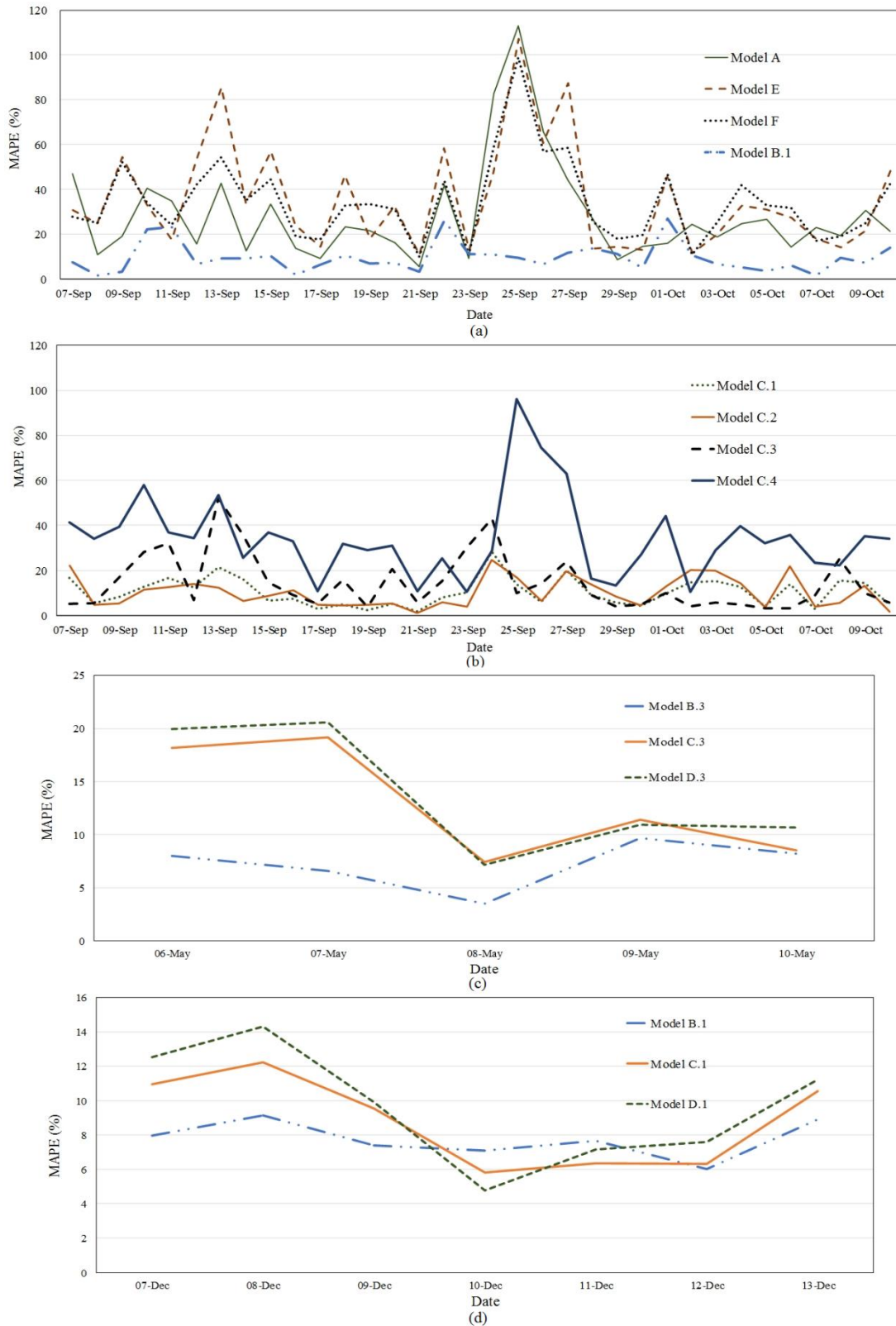


Figure 4-15: Daily MAPE results which presents: (a) the benchmarks and best forecast model, (b) the impact of estimating both exogenous variables on forecast models, (c) the impact of estimating one exogenous variable on forecast models (d) presents the highly accurate forecast models.

4.3.4 Effect of Estimating Exogenous Variables

To improve the forecast performance and reduce the error peaks, the exogenous variables have been used in the models. Tables 4-7 and 4-8 show that the proposed forecast models that estimate one of the exogenous variables (for example Model C2) or know both of them (for example Model D1) give significant improvements in the MAPE compared to the benchmark models (for example Model E) with MAPE decreased by 26.2% and 26%, respectively, over the second testing period. Furthermore, the RMSE and MAE values of Model C2 decreased by 14.8 kWh and 19.2 kWh, respectively, compared to Model E for the same testing period. In addition, Model C2 and Model D1 outperform the best models that estimate both exogenous variables (Model B4) with 11.9% and 9.8% compared to 31.1% over the first data set. Overall, models that used estimates for both exogenous variables exhibited very large errors. This indicates that, with the current data set, using the historical electrified RTG crane power demand and the estimation of both exogenous variables, X_1 and X_2 , as inputs is not recommended.

To evaluate the impact of estimating the exogenous variables, we compared models that assuming the X_1 and X_2 are known to models that estimate these variables, as shown in Figure 4-15 (b). The ARIMAX model that estimates the number of crane moves only (and assume weight is known), Model C2, and Model C1 (the ARIMAX model with the assumption that the exogenous variables are known) performed in a similar way. Furthermore, the MAPE curves of Model C2 and Model C1 show a better performance and stability compared to Model C4 (the ARIMAX model that estimates both the container gross weight and crane moves). Table 4-7 shows that the forecast models with the assumption that the crane weight is known (for example Model B2) are slightly more accurate compared to models with the assumption that the number of crane moves are known (for example Model B3). This leads to the conclusion that accurate information on container gross weight has a more significant impact on the forecast performance than the number of crane moves. In addition, the daily MAPE results in Figure 4-15 (b) show that the forecast models that estimate either one of the exogenous variables (Model C2 and Model C3) outperform Model C4, which estimates both variables. Figure 4-15 (b) shows that each of the prediction models with an uncertain estimation of the exogenous variables performs differently based on the type of variable. Figure 4-15 (c) presents the daily MAPE results over the first testing period for the ANN, ARIMAX and ARX models

that estimate the container gross weight (Model B3, Model C3, Model D3). During this testing period the ANN model (Model B3) shows a better performance compared to Model C3 and Model D3. However, the MAPE results of Models B3, C3 and D3 on the 9th of May were roughly equal with 10%. To generalise and examine the forecast models, all models in this chapter have been tested using a data set collected from another RTG crane (testing period 3), as seen in Figure 4-15 (d) and Table 4-7. The ARIMAX and ARX models with the assumption that both exogenous variables are known (Model C1 and Model D1) performed relatively similarly over this testing period. However, the ANN model (Model B1) shows more accurate results especially from 7th to 9th of December but after that all the models performed to similar degree. In Figure 4-15 (d), the lowest MAPE values for Model B1, Model C1 and Model D1 are 6%, 5.8% and 5%, respectively. Furthermore, the lowest MAPE values for all models in Figure 4-14 (d) occurred on the 10th of December.

Based on the data set, the forecast models require both the number of crane moves and container gross weight as exogenous variables. Estimation of one helps to reduce the high error peaks, outliers and avoids the impact of low or zero load values during ideal and off operation modes compared to estimation both variables. Moreover, the ANN forecast models show that the significant factor is the type of inputs that are used not the number of inputs. In this chapter, our main target is to forecast the RTG crane demand for a day ahead and compare different structures of the ANN, ARIMAX and ARX models. The analysis of results in this section shows that it is preferable to use the exogenous variables to decrease the forecast errors. On the other hand, the evaluation methods (MAPE, RMSE, MAE) used in this thesis are the most common load forecasting evaluation methods. However, these evaluation methods focus on the mean of the error and does not present the forecast performance at every time step. In addition, in some cases the peak magnitude in forecast and actual profiles are closed but the error is very high which is related to the time shift between the two profiles. In future, the evaluation method will be updated to investigate these criteria.

4.3.5 Forecast Error Analysis

Table 4-7 and Figure 4-15 present Model B1 as the most suitable and accurate model over three different testing periods. Model B1, Model C1, and Model D1 are further analysed as follows. The histogram of the forecast error percentage for these prediction models over the third testing periods has been plotted and fitted with a normal distribution line in Figure 4-16.

The error percentage values were distributed between the -60% and 60% range. By investigating the histogram plot, it is observed that a high number of instances are clustered around 0% while many instances are distributed between -15% and 15%. In Figure 4-15 the normal distribution seems to accurately describe the error. As result, the forecast models (Model B1, Model C1, and Model D1) shows no bias distribution with the normal distribution centralised around zero error and it indicates if may be difficult to improve the forecast accuracy further.

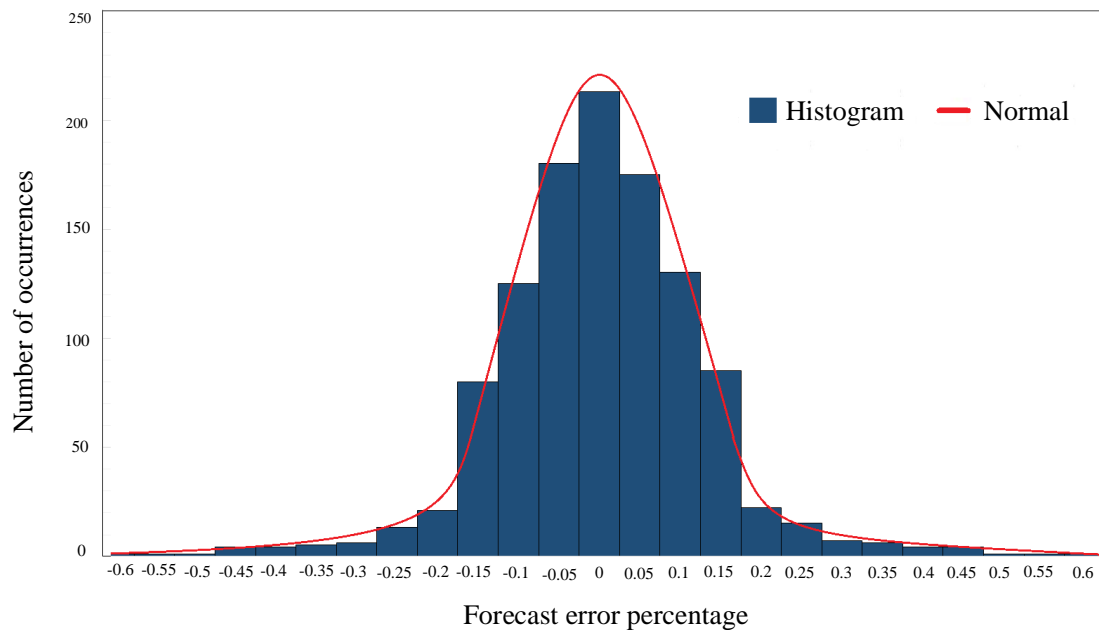


Figure 4-16: Illustration of error percentage data in a histogram along with a normal distribution fit.

As previously discussed, the electrified RTG crane demand profile is highly volatile and less predictable compared to other low voltage loads such as residential customers and renewable energy sources. Bi et al. [91] presented a 10.06% and 18.9 % MAPE forecast error for the power output of photovoltaic system in sunny and rainy day, respectively, with half hour time interval by developing ANN model. The proposed ANN model [91] used power output, temperature values (high, low, average) from similar days and forecast temperature values to generate the forecast profile. The RTG crane and L.V demands aren't directly comparable since the RTG crane has very different behaviour. However, the load forecast results illustrate a similar performance of the model forecast examples presented in the literature.

4.4 A Comparison of the Forecast Model Techniques

The forecast model strategies results, in the previous section, present and compare the

potential benefits of using the exogenous variables in terms of accuracy. In this section, other criteria will be analysed, that relate to the main characteristics of the ARIMAX and ANN model and the sensitivity to change in model parameters. In addition, to compare the proposed forecast models, in this chapter, the difficulties of design and implementation of the forecasts are presented.

4.4.1 ARIMAX Forecast Model

Section 4.2.2 presented and described how difficult time series forecast models are to develop and implement to predict day ahead RTG crane demand due to the demand volatility and irregularity. Generally, time series approaches include the following techniques: AR and ARIMA are linear forecasting methods that describe the relation between the current and historical demand. However, the ARIMAX can be a nonlinear model through the adding of exogenous variables to the ARIMA model. The ARIMA and ARIMAX parameters (p,d,q) are determined based on this correlation between $D_L(n)$ and $D_L(n - i)$. These parameters (p,d,q) are typically specified based on the PACF and ACF plots and BIC calculations. It is significant to determine the model parameters accurately where the ARIMAX forecast model is susceptible to variations in (p,d,q) parameters. Generally, the inaccurate number of lags for (p,q) will increase the forecast error and the computational costs in case the model includes more lagged values.

In section 4.4.3, the impact of choosing the exogenous variables on an ARIMAX forecast model is presented. The analysis of results showed that Model C1, which uses the actual exogenous values $(X_1(n)$ and $X_2(n))$ outperformed Models A, E, F, which only use the RTG crane historical load data. However, increasing or adding exogenous variables into the ARIMAX forecast model will increase the computational costs and difficulties of implementation compared to the ARIMA model.

4.4.2 ANN Forecast Model

The ANN forecast models are mainly used to solve complex nonlinear relationships without requiring any functional relationship between the demand and the predictor variables [63] [74]. However, the ANN is described as a black-box algorithm due to the lack of transparently of the relationship prediction values. As described in Sections 4.1.2 and 4.2.1, the developing of ANN forecast model is required to determine the number of parameters:

number of hidden layers, number of neurons in each layer, transfer function and evaluation criteria.

There is no optimum or favourite method for selecting the ANN parameters and the trial and error method is usually used to choose suitable parameters in short term load forecasting. Due to the high number of model parameters, ANN typically require large amount of data to be accurate and can cause overfitting. Therefore, the ANN forecast model requires more effort to develop and implement compared to ARIMAX model. Furthermore, the results of the trial and error test in Section 4.2.1 shows that ANN is highly susceptible to variations in ANN model parameters. Typically, increasing the number of neurons in each layer and number of layers may lead to the problem of overfitting and increase the learning time and computational costs.

4.4.3 A Comparison Summary

A summary table of the main advantages and disadvantages of the proposed forecast models in this thesis, taking into consideration the characteristics of each model discussed in this chapter are presented in Table 4-9.

Table 4-9: A comparison for the advantages and disadvantages of ANN and ARIMAX.

| Forecast model | Advantages | Disadvantages |
|----------------|------------------------------------------------------------------------------------------------------------------------------------------------------------------------------------------------------------------------------------------------------------------------------------------|------------------------------------------------------------------------------------------------------------------------------------------------------------------------------------------------------------------------------------------------------------------|
| ARIMAX | <ul style="list-style-type: none"> • Widely used in short electrical load forecasting. • Low complexity. • The exogenous variables help to decrease the forecast model error compared to ARIMA. | <ul style="list-style-type: none"> • Difficult to identify the model. • Require extensive data analysis. |
| ANN | <ul style="list-style-type: none"> • Does not need to determine any functional relationship between the load and predictor variables. • Best forecast accuracy compared to ARIMAX and ARIMA models. • Widely used in short electrical load forecasting. | <ul style="list-style-type: none"> • It's a "black box" system because it is difficult to understand the nature of the ANN model. • High computational cost. • More effort to develop. • Require large amount of data. |

4.5 Summary

Electrical load forecasting has become a significant evaluation tool for power consumers and producers. The importance of effective and accurate prediction models is to minimise utility risks and power costs and increase competitiveness. Since there is no research discussing

the RTG crane demand forecasting problem which are complex compared to typical LV distribution loads, this chapter presented two main forecast models ARIMAX and ANN. There are a number of challenges facing the load forecasting of RTG cranes. These challenges can be attributed to three factors. First, there are no clear annual, weekly or daily seasonality trends over the historical load data. Second, there are outliers in the correlation between the exogenous variable and crane demand due to the effect of the human factor. Third, there is highly stochastic, volatile and nonsmooth load behaviour especially for low demand values. In this research a number of models have been implemented and tested to forecast the day ahead RTG crane demand. After the RTG crane demand series and the exogenous variables were analysed, we examined different options for forecast model inputs. In this chapter, each model has been trained separately using 21 days of historical data. To verify the prediction ability of the forecast models they have been applied to two different cranes over three testing periods. The evaluation method results for each model, which has different input variables discussed in this chapter show that the ANN model (Model B1) outperforms all other models. Although there are some extreme error peaks, the proposed Model B, Model C, and Model D, which exclude the estimation of both input variables achieved an acceptable level of prediction accuracy. Moreover, the prediction models achieve an acceptable performance, up to 15% MPAE similar to the literature, when estimating only one exogenous variable with a more significant impact on forecast performance with accurate container gross weight measurements. This result is very encouraging for those ports that are following the SOLAS requirements and recording the container weight before moving them, which will help them to forecast and understand the RTG crane demand. The analysis of the results show that it is not recommended to estimate both exogenous variables in the models. The forecast models' results and RTG crane demand data analysis forms the contribution to knowledge as presented in Section 1.5, contribution I and II. The load forecasting model is a key tool for understanding the port electrical demand and ports gain considerable technical and economic benefits from the crane data analysis and the forecast model.

Chapter 5: MPC controller for RTG Cranes with Energy Storage Systems.

The literature review showed the significance of forecasting the LV demand to improve the energy performance of an electrical distribution network with an ESS by employing optimal and receding horizon controllers. This chapter presents three Energy Storage System (ESS) controllers for a network of RTG crane to increase the peak demand reduction and energy cost saving. Firstly, throughout this work the set-point controller is used as a benchmark ESS controller, it is commonly and standardly used in LV and RTG crane applications, as discussed in Section 2.2. Secondly, Model Predictive Controller (MPC) is developed as a receding horizon control solution. Finally, an optimal energy management system based on fixed load forecast is developed. The MPC and optimal management system are presented to investigate the benefit of using a prediction demand profile in an ESS control model. A specific case study for the network of RTG cranes equipped with an ESS is presented and the results of each algorithm compared. The optimal controllers in this chapter use the forecast model outputs developed in the previous chapter to generate the optimal ESS operation plan. The analysis of the results shows that the performance of the MPC controller is dependent on the forecast model's accuracy. The results of the MPC management strategy shows increased energy cost savings and peak demand reduction, compared to the benchmark control strategy and the optimal energy management system. This chapter uses control algorithms with actual data available from the network of RTG cranes and the storage device to update the forecast model and generate the ESS control decisions. The MPC, a receding horizon control algorithm, introduces the rolling crane demand forecasts into the ESS control, whereas the optimal energy management system uses a fixed forecast profile. This is the first study to consider a load forecast profile and electricity costs in the objective function to optimise the energy flow in the RTG crane network system with an ESS using MPC.

Model predictive controllers have been used effectively within microgrids and LV network applications that involve high uncertainties in demand applications to decrease the energy costs and increase the peak reduction. The literature has shown that an ESS can be

beneficial for decreasing the energy costs and peak demand [33] [46] [47]; accordingly, it is important to develop an optimal control strategy that maximises the advantages of the ESS and minimises the costs. These sets of studies show the usefulness and capabilities of using an MPC as an ESS control technique. An electrified RTG crane demand profile has highly stochastic and less predictable behaviour compared to other low voltage loads such as domestic customers. Challenges in developing accurate crane demand forecasts make it substantially more difficult to control the ESS and increase energy systems' efficiency by using the actual prediction data. Therefore, this chapter has key novel contributions, compared to the limited literature, which has only focused on energy savings for a single RTG crane by using the regenerative power and conventional or optimal control algorithms and neglected prediction algorithms and the electricity price terms as key inputs. In particular, the MPC with a rolling forecast model and optimal energy management controller based on a fixed load forecast are developed to decrease the electricity bills and achieve maximum possible peak reduction for a network of RTG cranes. This chapter is organised as follows: the next section, Section 5.1 describes the topology of the energy storage system and the RTG crane network demand model. Then, Section 5.2 present the set-point control model as a benchmark controller. Section 5.3 and 5.4 illustrate the methodology of an optimal energy management strategy based on the MPC controllers and optimal energy management system, respectively. Finally, Section 5.5 presents a set of results including the RTG crane network demand prediction results, the MPC and optimal controllers result (Case study: a specific network of crane operation example), and the prediction horizon evolution and the economic results of using ESS. Finally, the conclusion and work summary are presented in Section 5.6.

5.1 The ESS and RTG Crane Demand Model Topology

The previous Chapters addressed the RTG crane demand characteristics in order to understand the demand behaviour. This understanding is important for developing optimal control strategies for the ESS to reduce the peak demand and energy cost problems. This section will introduce the energy storage system and the electrified RTG crane topology. The ESS aims to reduce the electricity energy costs and peak demand. This target is achieved by minimising the substation peak demand and energy consumption during the high electricity price period. The storage device for the network of RTG crane within this thesis will be located at the low voltage side of a substation rated 11kV/ 0.415 kV, as previously presented in Chapter 1. In

cases where the ESS is located at the 11kV side of the primary substation, the storage device is able to support the 11kV zone of the electrical network to solve thermal and voltage problems, however, it is not capable of mitigating thermal or voltage challenges in low voltage zones. To use an ESS to reduce the LV network problems, the ESS needs to be connected on the 0.415 kV side. Therefore, studying the RTG cranes network connected ESS is important to understand the key role it can play in reinforcing the LV network at ports. In this chapter, two RTG cranes connected to a central ESS in the distribution network are used. Figure 5-1 shows the significance of locating the ESS in the LV network to support and solve several type of crane network problems. Unlike the literature that have studied and analysed the energy saving for a single RTG crane, this ESS location scenario has been chosen to investigate the benefits of using a central ESS to feed more than a single crane, motivated by using a central storage device in a low voltage network for residential customers [33]. This location is close to the substation and can give extra support to the secondary substation and mitigate operational constraints and help to resolve thermal issues in this zone. Furthermore, the ESS here will have limited impact on solving voltage drop problem at the load side (end of the feeder).

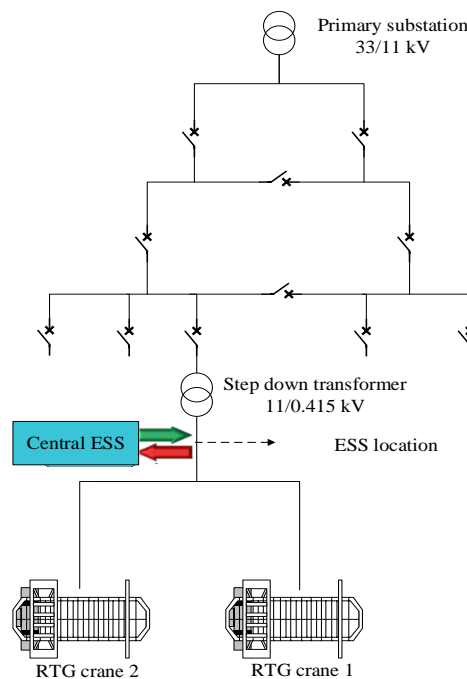


Figure 5-1: Single line diagram of the RTG crane network at the Port of Felixstowe, UK, including the ESS location scenario.

Overall, there is a significant relationship between the ESS location and voltage and thermal problem in the LV network, and by controlling the ESS effectively, the performance of an ESS on the network can be improved. A detailed comparison analysis for the ESS locations will be presented in Chapter 7 in line with the proposed optimal control strategies of the ESS presented in this work. In this thesis, the voltage and current performance based on the ESS location have not been studied, the location scenarios analysis will focus solely on peak reduction and energy cost saving performance.

5.1.1 The Energy Storage System (ESS) Model

In this section, the ESS system is described. The data has been collected from two RTG cranes manufactured by Shanghai Zhenhua Heavy Industries, China. The RTG cranes have been retrofitted to be powered by the step-down transformer (11KV/415V) via a conductor bar of length 217m [10]. The aggregation power source feeds all the required demand consumption to operate the network of RTG cranes and the changes in the ESS energy, as illustrated in Figure 5-1. Further, the half hourly RTG crane energy data over H days is considered in this section.

Let

$$D_L = (D_L(1), \dots, D_L(48H))^T \in \mathbb{R}^{48H}, \quad (5-1)$$

be the complete historical data set. The ESS controllers have been developed to find the optimal ESS operation plan over a day time period. Therefore, the half hourly crane demand in day k can describe as $L_k(n)$, where n is half-hourly time step over the day ($n = 1, 2, 3, \dots, 48$). The research objective of this chapter is to minimise the electricity cost and peak demand using an ESS connected to a network of cranes. Equation (5-2) simulates the crane network demand with the ESS.

$$S(n) = \left(\sum_{i=1}^{N_c} L_k^{(i)}(n) \right) + \left(\sum_{q=1}^{N_s} \Delta E^{(q)}(n) \right), \quad (5-2)$$

where $S(n)$ is the total substation demand at half hour n of day k, $\sum_{i=1}^{N_c} L_k^{(i)}(n)$ is the aggregation of the individual crane demand ($L_k(n) = (L_k^{(1)}(n), \dots, L_k^{(N_c)}(n))^T \in \mathbb{R}^{N_c}$), $N_c = 2$ is the number of cranes, $\sum_{q=1}^{N_s} \Delta E^{(q)}(n)$ is the aggregation of the charged or discharged energy in the ESSs at half hour n of day k ($\Delta E(n) = (\Delta E^{(1)}(n), \dots, \Delta E^{(N_s)}(n))^T \in \mathbb{R}^{N_s}$), and $N_s = 1$ is the number of ESSs in the network.

The Energy Storage System (ESS) used in this research, as shown in Figure 5-1, is described by Equations (5-3) – (5-6) and is similar to models found in the literature [33] [58]. Typically, the ΔE_s represent the increase or decrease of energy stored in the ESS, respectively. The energy stored in the ESS is increased and decreased, and is described as $\Delta E(n) = \text{SoC}(n) - \text{SoC}(n - 1)$. The change in stored energy, ΔE , in every time step, can be taken as a positive/negative change to reflect the increase/decrease of the energy in the ESS. The negative value of ΔE means that the energy in the ESS has decreased (the storage system is in discharging mode) and when it is positive it means the energy in the ESS has increased (the storage system is in charging mode). Furthermore, the stored energy $\text{SoC}(n)$ at the end of each time step n ($n=1, 2, \dots, 48$) is calculated and updated based on the previous value, $\text{SoC}(n - 1)$, described by Equation (5-3), and the change in energy $\Delta E(n)$ [33] [58].

$$\text{SoC}(n) = \text{SoC}(n - 1) + \theta \cdot \Delta E(n). \quad (5-3)$$

The ESS is subject to maintaining an upper and lower limit, SoC^{\min} and SoC^{\max} , respectively, and a minimum and maximum change in energy $\Delta E(n)$ between, ΔE^{\min} and ΔE^{\max} , respectively.

$$\left. \begin{aligned} \text{SoC}^{\min} &\leq \text{SoC}(n) \leq \text{SoC}^{\max} \\ \Delta E^{\min} &\leq \Delta E(n) \leq \Delta E^{\max} \end{aligned} \right\}, \quad \forall n. \quad (5-4)$$

$$(5-5)$$

The storage system model considers the ESS efficiency [33] [58] by combining the change in the stored energy in each time step ΔE into a variable describing the storage efficiency $\theta \in [0,1]$, Equation (5-3). When the changed energy is $\Delta E < 0$, the efficiency of the ESS is equal to $\frac{1}{\tilde{\eta}}$ and when $\Delta E \geq 0$, the storage efficiency is $\tilde{\eta}$, as described by Equation (5-6).

$$\theta = \begin{cases} \tilde{\eta} & \text{if } \Delta E \geq 0 ; \text{ charging period} \\ \frac{1}{\tilde{\eta}} & \text{if } \Delta E < 0 ; \text{ discharging period} \end{cases} \quad (5-6)$$

In this work, the ESS control aims to determine an optimal value of $\Delta E(n)$ to minimise the peak demand and energy costs. Typically, the control and operation constraints of the ESS are given in terms of the average power flow, P_s in kW, and the energy stored: as $P_s \Delta \tau$ is in kWh, where $\Delta \tau$ is the duration of the time period in hours. However, in this work, the control of the ESS aims to determine an optimal value of the increase or decrease of the stored energy, ΔE .

5.1.2 The Electrified RTG Crane Demand Data

The electrified RTG crane demand increases and decreases based on variables such as container gross weight, number of crane moves and the crane driver behaviour. These variables explain the wide variety of errors, that increase the challenge of controlling the ESS. Figure 5-2 presents the daily MAPE error for the forecast of over 33 days of electrified RTG crane demand, the highest number of occurrences is concentrated between 6% and 12%. Furthermore, the largest MAPE values (above 15%) are only repeated twice for MAPE errors equal to 24% and 27%. As seen in Figure 5-2, around 30% of the MAPE errors over one month are equal to 12% and around 80% of the MAPE values are under or equal 12%. However, the MAPE results in Figure 5-2 show a wide range of values up to 27%. Which increase the challenge of developing a regular load forecast demand controller. As discussed in Chapter 4, due to the highly volatile and stationary nature of electrified RTG crane demand, which has no clear relation with seasonal exogenous variables, forecasts are required to use the correlation between the crane demand, the container gross weight and number of crane moves to generate a more accurate model. In addition, the impact of human unpredictability on the demand has shown that different crane electricity demands can be achieved for the same container gross weight, which also it more challenging to control the ESS based on a prediction system.

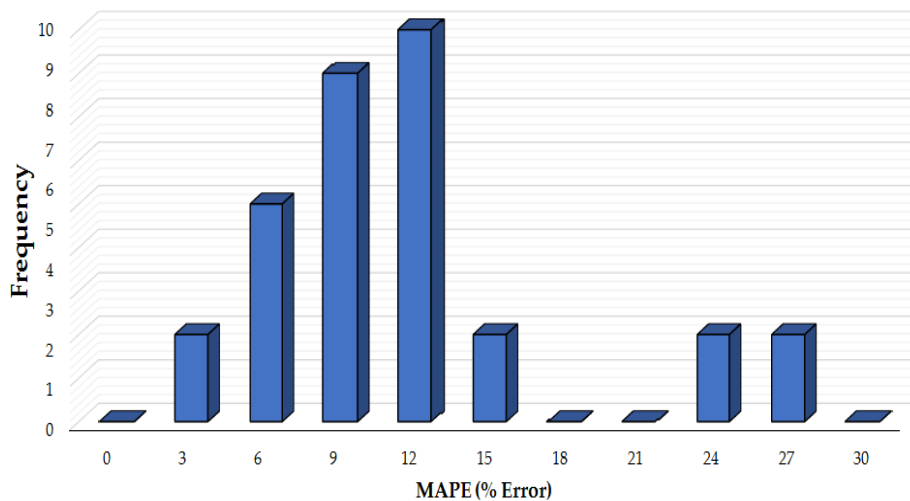


Figure 5-2: Histogram of daily mean absolute percentage error (MAPE) over 33 days for the ANN forecasting methodology (Model B1) from Chapter 4.

In this section, two electrified RTG cranes in the Port of Felixstowe (PoF), were selected to collect demand and container gross weight data. The measurement system at PoF is described

in Appendix A. The data set was collected between 1st of March and 30th of April 2017. The collected data is divided into two sets: (1) Training data set with 56 days of collected data (2) Testing data set with 5 days of collected data. In particular, the real RTG crane demands over a month is analysed, considering all time intervals of the day (24 hours) based on half hour resolution. The testing period data represent the crane behaviour on different work and operation days.

5.1.3 ESS Performance Evaluation.

The peak demand reduction and electric energy costs saving are used as a metric to evaluate ESS performance of peak demand. To understand the thermal constraints that are usually caused by peak demand values, this metric has been applied throughout this thesis to provide a sufficient understanding for the thermal problem [32] [33]. The percentage of peak demand reduction, P_R , in this work has been calculated as described in Equation (5-7).

$$P_R = 100 \left(1 - \frac{\max(S)}{\max(S_w)} \right), \quad (5-7)$$

where S_w is the RTG crane network demand profile without using an ESS and S is the demand profile including the ESS effect. In addition, the electricity cost saving, C_{saving} , is used to evaluate the economic benefits of using the ESS and is given by Equation (5-8), where D_{sh} is the amount of shifted demand from high to low electricity price tariff and ΔC is the difference between the high and low electricity tariff.

$$C_{\text{saving}} = D_{\text{sh}} \cdot \Delta C. \quad (5-8)$$

5.2 Benchmark Control Methodology.

The literature review in Chapter 2 demonstrated the potential benefits of using an ESS with low voltage networks and RTG crane systems, including the significance of developing an accurate forecast model to improve the control storage device performance. Throughout the literature review, the set-point controller is used as a typical benchmark control system for an ESS on a low voltage network [33] and with a RTG crane [7], where the set-point algorithm is effective and simple. However, set-point control is limited with respect to peak reduction and cost savings over a one-day time period, as it takes the control decisions without any future knowledge. In this chapter, a set-point controller has been used due to being a common and standard ESS control model used in the literature. This allows to create a comparison analysis

and evaluation of the performance of the proposed optimisation controllers based on the load forecast.

5.2.1 Set-point Controller

The operational principle of set-point control is well established, the controller is widely used in industry and is a standard technique to control ESSs on LV network. The set-point controller compares the storage or the network measurement to a reference value such as voltage, demand, frequency and SoC, to determine when to charge and discharge the storage device. If the RTG crane demand value is under the reference value, the set-point, the ESS will charge and when the crane demand is above the reference value the ESS will discharge and result in a reduction in the peak demand. The reference value in a set-point controller is typically chosen based on the historical data or the network constraints [7] [33]. Figure 5-3 presents the RTG crane demand profile for one day with and without an ESS controlled via set-point control. To show the impact of selecting the set-point value on the peak demand, an example model has been presented in Figure 5-3. In this test, an ESS with capacity 75 kWh and charge/discharge rate equal to the maximum energy is considered. Two set-points have been used: 30 kWh for set-point (1) and 40 kWh for setpoint (2). In the first case with reference value equal to 30 kWh, the ESS achieves a peak reduction of 15%. When the reference value in the set-point controller is 40 kWh, the ESS is able to increase the peak reduction to 23%.

As seen in Figure 5-4, the ESS with set-point (1) runs out of energy at the 3rd and 16th time step, resulting in a decrease in the peak demand reduction by 8% compared to an ESS with set-point (2). Figure 5-4 presents the cumulative sum of the charge/discharge amount, SoC, for the ESS with different set-point controllers. Determining the reference value for a set-point controller is difficult and challenging for RTG crane demand, due to the high volatility and lack of seasonality or trend to predict the behaviour of the demand. As presented in Figure 5-3, any change in the set-point value has a large potential impact on the peak reduction results. The set-point controller has the advantage of being simple and well established as a routine control system in industrial applications but is principally limited as it works without any knowledge about the future scenarios. Furthermore, the set-point controller can reduce any demand above the set value (not a significant peak) if the ESS is large enough. The ESS preference can improve by using a demand forecast, which can help to maximise the peak

reduction by having knowledge of when and how long to store energy in the ESS and using this to increase the energy cost saving.

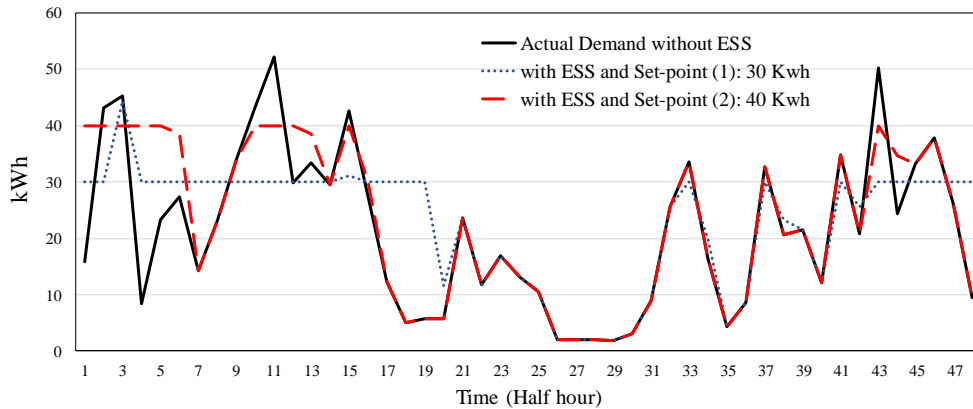


Figure 5-3: An example of using ESS with set-point controller with two set-point values.

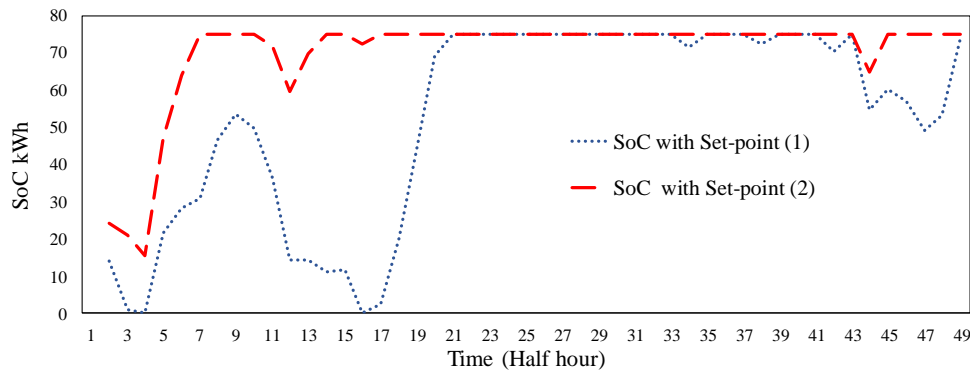


Figure 5-4: The SoC for ESS across a day period for set-point controllers, for the case study presented in the main text.

5.3 MPC Controller.

In this section, the MPC controller is formulated as a controller that creates a sequence of decision-variables to maximise or minimise a cost function over a future time horizon under adjustments with every time step [33]. The MPC controller, also known as the generalised predictive control or receding horizon control, is a time horizon optimisation model that determines a series of optimal control decisions over a specific future time period [33] [129]. Furthermore, the receding horizon controller is widely used nowadays in smart grids and energy applications. Generally, the cost function for energy, peak demand and costs in a real application is usually pre-defined and commonly known [33]. In the first control action, the MPC controller computes the decision for the first-time period based on the demand forecast

and updates of other variables. In the subsequent time intervals, the predictive control uses updates of the forecast data and other operation variables to adjust the optimal control signal at every future time step and solve the optimisation defined by the cost function. This is then repeated for all time steps [130].

Figure 5-5 presents the exemplified control scheme of the MPC system for a network of electrified RTG cranes with an ESS. The crane’s measurements, updated demand forecast data, the electricity price term and storage measurements are fed to the MPC controller in order to generate a control signal. The control decision uses the cost function in Equation (5-9) to minimise the electricity energy cost and peak demand. The demand prediction of the crane network was developed in Chapter 4. The energy prediction model, (ANN, Model B.2) has been used to predict the future crane network demand, as the Model B.2 only uses one known external variable ($X_1(n)$, container gross weight) and was shown to be an accurate forecast model with MAPEs 12%, as discussed in Chapter 4 (see Section 4.3.3). The optimal energy controllers based on load forecasting in this research will be evaluated and compared with perfect and worst case forecast scenarios as will be shown in Chapter 7.

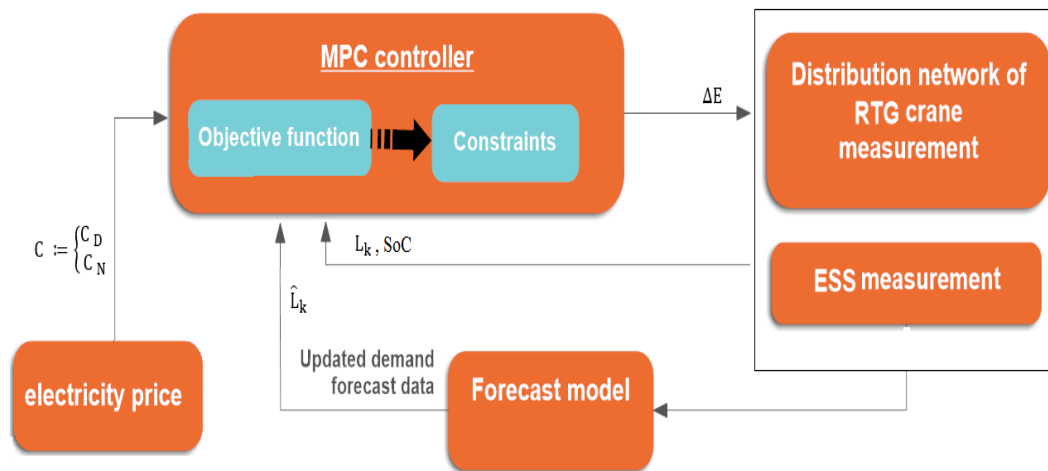


Figure 5-5: The scheme of MPC for the electrified RTG crane network equipped with an ESS.

In this section, the cost function in Equation (5-9) is optimised by generating a control signal to the ESS that aims to minimise the peak demand. The Matlab optimisation solver has been used to minimise the cost function. This cost formulation is subject to the constraints presented in Section 5.1.1 for the crane and ESS models. Recall from the previous chapter, in this thesis,

the forecast and historical or actual data are presented in the equations with and without ($\hat{\ }^{\wedge}$) notation, respectively.

$$\arg \min_{\Delta E} \sum_{n=1}^N \max \left(\hat{L}_k(n) + \Delta E(n) \right)^2, \quad (5-9)$$

The cost function in Equation (5-9) is optimised by generating a control signal to the ESS that aims to minimise the peak demand over the prediction horizon period subject to ESS and RTG model Equations (5-3) to (5-6), where $\Delta E(n)$ is the change in the ESS energy, $\hat{L}_k(n)$ is an estimated of the RTG crane demand future (forecast) at the current time step, n , for day k , and N is the number of half the hour time steps in one day ($N = 48$). In this thesis, the reduction in the energy cost of the network of cranes is achieved by finding the optimal operation of the ESS that minimise the peak demand under the following constraints:

$$\text{SoC}(n_{\text{set}}) = \text{SoC}^{\text{max}} \quad (5-10)$$

$$\text{SoC}(N) = \text{SoC}^{\text{min}} \quad (5-11)$$

The constraints, Equations (5-10) and (5-11), aims to fully charge the ESS during the low tariff period and fully discharge during the high tariff period in order to achieve the maximum energy cost saving based on the electricity price term, $C(n)$, at Port of Felixstowe, as described in Equation (5-12). The MPC controller as a real time controller is computationally expensive and the above control procedure help to achieve the maximum cost saving and reduce the computational cost by simplifying the cost function. However, this procedure could affect the peak reduction term in order to satisfy the cost constraints.

$$C(n) := \begin{cases} C_D & \forall n \geq n_{\text{set}} \\ C_N & \forall n < n_{\text{set}} \end{cases}, \quad (5-12)$$

where $n \in \{1, 2, \dots, 48\}$ is the half hour period, the high electricity tariff (C_D) is between $n_{\text{set}} = 14$ (7:00 am) and midnight, and the lower price is during the rest of the day (C_N).

The controller model obtains the updated demand prediction data for the period between the current time interval (n), and $n + i$, where i is the prediction horizon and $n + i \leq N$ and N is the one-day ahead forecast period ($N = 48$). The forecast model is designed to predict the load for one day ahead and then updates the MPC plan. After each time step the forecast model will use the actual data for this step and the forecast error to recalculate and update the forecast model. The MPC controller then calculates the optimal control decision by calculating the ESS

energy in Equation (5-9) to minimise the cost function and sends the control signal to the network system. These steps are repeated at every time step $n + 1$ by updating the forecast data and other system variables and using the updated forecast data $n + 1 + i$ to compute the control signal, as illustrated in Figure 5-6. This control process is mainly referred to as the receding horizon controller [33] [131] and it is described in more detail in Appendix B. The results section discusses the size of the horizon for an MPC as a significant parameter for the selection of this algorithm and evaluates the ESS performance using an MPC controller compared to a single time step control algorithm without future knowledge (the set-point control). The current literature on LV network applications and microgrids [33] [52] is beginning to investigate the benefits of treating the volatile demand as a stochastic element and develop a stochastic control in order to increase the efficiency performance of the ESS on the distribution network. The following chapter will extend the method by upgrading the control to a stochastic model predictive controller.

Algorithm 5-1: Basic concept of MPC for network electrified RTG crane system model with ESS.

1. Select the time horizon step and prediction horizon.
 2. Determine the control objective and constraints.
 3. Initialise: the crane, forecast data and ESS data.
 4. For $n= 1$ to N (daily demand operation), do
 - a. Solve optimal Equation (5-9),
subject to:
 - RTG crane model Equation (5-2).
 - ESS model Equations (5-3) to (5-6).
 - Energy cost saving Equations (5-10) to (5-12).
 - For ($n = 1$), the model computes the optimal solution based on the RTG crane demand prediction and initial data.
 - b. Find the optimal signal for ($n + 1$), Equation (5-9), and apply the control to the system.
 - c. Update the forecast model for time step ($n + 1$) to N by regenerating the forecast load profile with the new observation and update the other system variables.
 - d. Set $n = n + 1$,
 5. An optimal solution is achieved for the electrified RTG crane system model with ESS for the specific day.
 6. Repeat all steps for the next day.
-

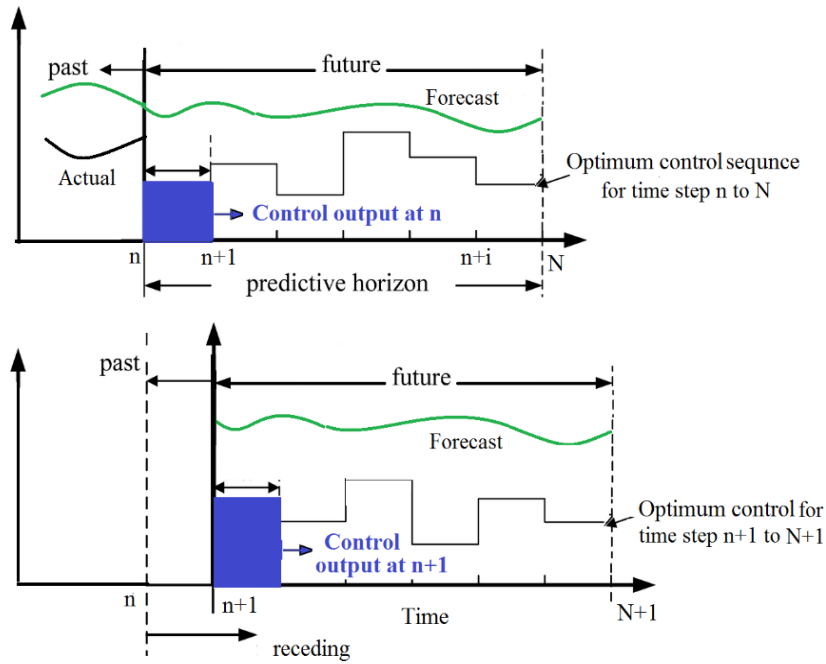


Figure 5-6: A simple illustration of the receding horizon used in MPC.

5.4 Optimal Energy Management Controller.

The optimal energy management controller can be designed for multiple objectives compared to the set-point algorithm and find optimal solutions to control the designed model. In this section, the objective of the optimal controller is to minimise peak demand and energy costs similar to the MPC controller, as described by Equation (5-9). The optimal controller in this section uses the peak shaving techniques to achieve the minimum cost and reduce peak demand by shifting demand from a high electricity price half hourly time period to a low-price half hourly time period, as presented in Equation (5-12). The peak shifting achieves the optimal solution by finding the optimal ESS output values which minimises a cost function. The ESS output is determined by using Equation (5-9) under constraint Equations (5-10) and (5-11). The optimal energy management controller in this section is designed as described in Algorithm 5-2. Furthermore, unlike the MPC controller in previous section, the proposed optimal management control here uses a fixed, half hourly electrified RTG crane demand forecast profile for one day-ahead, i.e. no updating the control or forecast

In general, the receding horizon controllers require an updating forecast demand profile and optimal calculations every time step to create rolling ESS optimal operation schedule.

Therefore, the receding horizon requires more effort to tune and higher computational cost compared to the set-point and optimal energy management controller presented in this section. Furthermore, the receding horizon and the optimal energy management controllers are not affected by choice of reference values similar to the set-point controller. Due to the limited work done on using optimal algorithms for electrical RTG crane applications and in particular the electrical cost saving and peak demand reduction, the optimal management controller in this section aims to provide an optimal controller based on load forecasts without any updating process during the day time as way to compare the rolling effect in the control. In addition, this optimal controller is used in Chapter 7 with full future knowledge similar to the literature [36] [103] to examine the maximum possible energy storage performance compared with all controllers developed in this thesis.

Algorithm 5-2: Basic concept of optimal energy management controller for RTG crane system with ESS.

1. Determine the control objective and constraints.
 2. Initialise: the crane, forecast data and ESS data.
 3. At $n= 1$
 - a. Solve optimal Equation (5-9),
subject to:
 - RTG crane model Equation (5-2).
 - ESS model Equations (5-3) to (5-6).
 - Energy cost saving Equations (5-10) to (5-12).
 - From ($n = 1$ to $N=48$), the model computes the optimal solution based on the RTG crane demand prediction and initial data.
 - b. Find the optimal signal and apply it to the system at every time step.
 4. An optimal solution is achieved for the electrified RTG crane model with ESS for the specific day.
 5. Repeat all steps for the next day.
-

5.5 Results and Discussion

The proposed set-point, MPC and optimal energy management controllers in this chapter were applied to a network of electrified RTG cranes equipped with an ESS. In this section, we will discuss the results from the proposed control algorithms. First, the results of the prediction model are presented; then, the proposed MPC and optimal energy management controllers are tested under a specific case study and compared to set-point controller. In this section, the receding horizon evaluation for the MPC controller is also considered. Finally, economic results of using the ESS in a network of cranes is introduced.

5.5.1 RTG Crane Prediction Demand Results.

As previously mentioned, the forecast data is created using an ANN prediction model as described in Chapter 4. For the optimal energy management controller, a half hourly forecast profile for day ahead has been used. The forecast data and model are updated only every 24 hours (daily updating). For the MPC controller, we modified the forecast model to update every time step by using the forecast error data. These modifications help to reduce the impact of the forecast error on the model predictive control (MPC). The forecast model in this chapter has used the actual demand and forecast error for each time step to recalculate and update the forecast demand for the following 24 hours, the forecast model is designed to:

- Firstly, forecast the half hourly electrified RTG crane demand for 24 hour ahead and generate a forecast load profile over $n + 48$.
- Secondly, calculate the forecast error at time n .
- Thirdly, regenerate the forecast load profile at each time step n for a day ahead $n+48$ by using the new observation and actual measurements at time n , where the ANN forecast is rerun with the new observation.

To assess the forecast accuracy the MAPE is used in this chapter. Firstly, the forecast models' profiles are generated for the five days of test data and compared to the crane actual demand, as presented in Figure 5-7. The overall daily MAPE for each forecast is presented in Table 5-1. A comparison of the ANN models of the cranes demand shows that the MAPE scores of the ANN model with time step updating is better than the fixed model over the testing period, as depicted in Table 5-1 and Figure 5-7. For illustration, on the first day the MAPE decreased to 13.6% from 18.8%. The minimum MAPE reduction was on Day 2 with MAPE reduced by 2.8%. The variation in the MAPE results in Table 5-1 is related to the high crane demand volatility and missing the peak points. In addition, Figure 5-8 presents the average daily MAPE for the proposed ANN for model with different time updating. By updating every half hour, the forecast process improves the average MAPE by 28.55% compared to daily updating. The MAPE has only improved by less than 4% for the time step updating from 16 to 48 half-hours. This is mean that updated information and forecast error correction can help increase the forecast model accuracy.

Table 5-1: The daily MAPE for the ANN prediction models.

| | With one-time step updating | Daily updating |
|-------|-----------------------------|----------------|
| Day 1 | 13.6% | 18.8% |
| Day 2 | 13.1% | 15.9% |
| Day 3 | 8.1% | 11.7% |
| Day 4 | 20.6% | 30.8% |
| Day 5 | 15.9% | 22.6% |

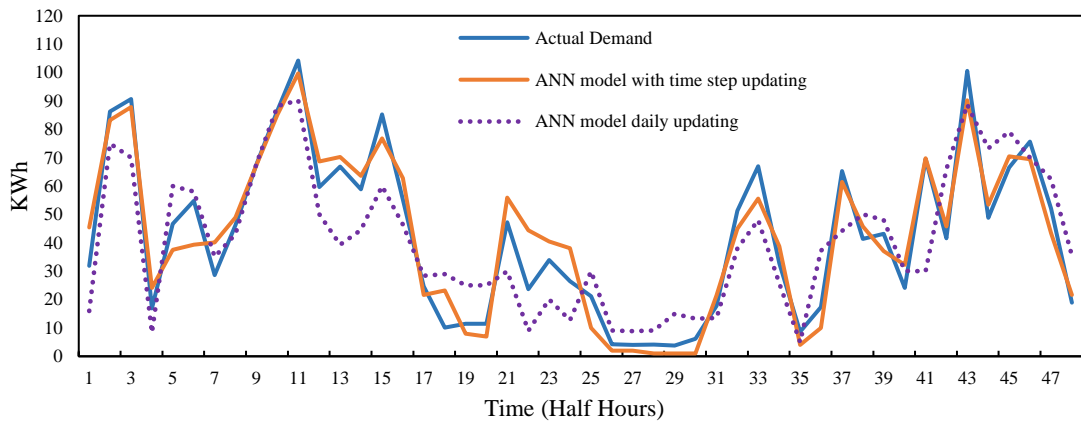


Figure 5-7: Results of ANN forecasts for the cranes demand for the first day of the testing period.

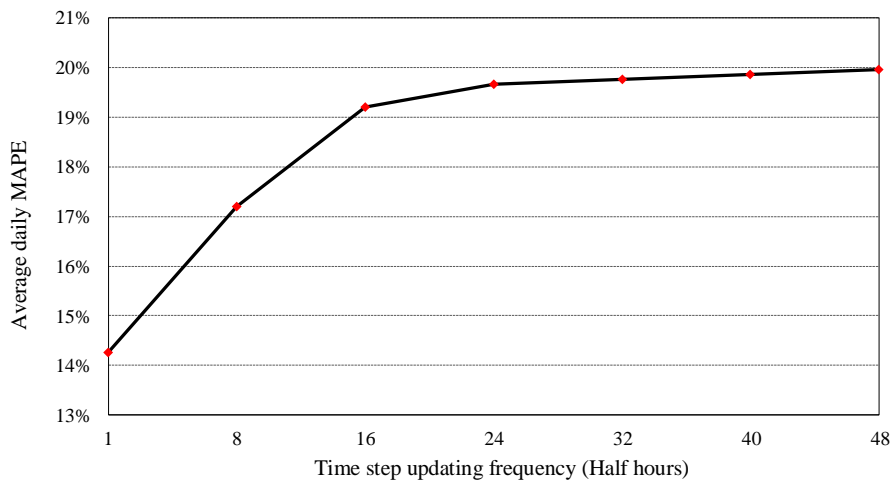


Figure 5-8: Results of rolling ANN forecast model with different time step updating for the data and forecast model.

5.5.2 Case Study: a specific network of crane operation example.

The set-point, MPC and optimal energy management controllers are implemented in the network of electrified RTG cranes equipped with an ESS, as presented in Sections 5.3 and 5.4. Two months of collected data for the network of electrified cranes demand was considered and divided into 56 days of historical data and 5 days of testing data, as described in Section 5.1.2. During the prediction demand model development, 20% of the historical data is used as validation data and 80% as training data, as described in Chapter 4 (see section 4.1) [80] [107]. To run the ESS model and present the performance of the various control strategies compared to the set-point controller, the following parameters in Table 5-2 were used in this example. This case study is not a focused on the ESS efficiency, and the transmission power line loss is neglected. The SoC and the changing rates of the ESS constraints, in this example, are similar to those used in the literature [33] [44] [48]. The ESS size and parameters for a network of RTG cranes are further investigated in Chapter 7.

Table 5-2: ESS parameters used in the case study.

| Parameter | Value |
|------------------------------------|---------------|
| $\Delta E^{\min}, \Delta E^{\max}$ | ± 150 kWh |
| SoC^{\min} | 0 kWh |
| SoC^{\max} | 150 kWh |

Simulation results for this specific case study showing the comparison between MPC, optimal energy management system and Set-point strategies are shown in Figure 5-9. The optimal energy control strategies, which use prediction data to create a charging and discharging trajectory based on the electricity price rate and the ESS constraint equations, help to reduce the risk of generating new peak points while charging the ESS. In the literature, using *a priori* data is used to determine the set-point is around 30-40% of the peak demand [7] [33]. In this case study, the set-point value was set at 38.5% of the greatest peak demand of crane network based on the historical load data. During the set-point control process, we considered the variation of the electricity price as an input parameter similar to the MPC and optimal management controllers to charge and discharge the ESS during the low and high electricity price period, respectively.

A comparison of the results for the three control strategies (set-point, MPC and optimal energy management) based on the average over the testing period of the peak reduction are presented in Table 5-3 and Figure 5-9. The MPC outperforms the standard controller (set-point control) and optimal energy management system and improves the peak demand reduction by 26.3% and 11.4%, respectively. The peak demand reduction accomplished in this work will help to reduce the stress on the port electrical infrastructure and reduce electricity bills. The set-point controller works without any future knowledge about the demand, which will increase the possibility of operating the ESS when it unnecessary and fail to reduce the significant peak points during the day. Furthermore, the results show that the optimal control algorithms based on load forecasting outperforms the benchmark controller (set-point). The MPC controller takes into account all interactions between the system variables after every time step and effects the output variables and improves the results compared to the optimal energy management system. Typically, the storage control technique for cost saving and peak reduction, will depend on the accuracy of the forecast profile and the actual demand volatility. A detailed comparison analysis and evaluation for the optimal controllers will be presented in Chapter 7 in line with the different forecast accuracies.

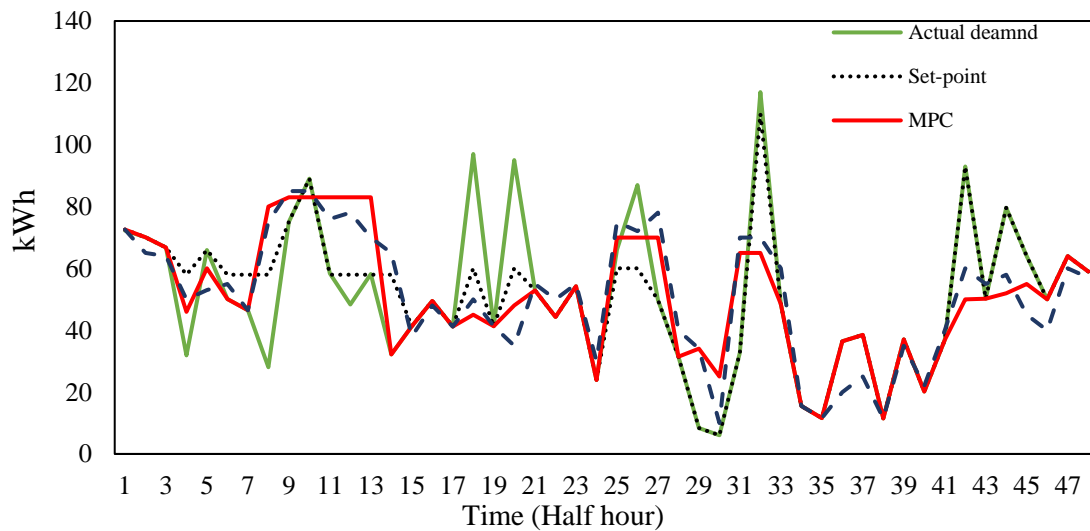


Figure 5-9: A specific example presenting the actual demand, and the results demand after implementing the set-point controller, the MPC and the optimal energy management controller for the substation demand in a network of RTG cranes for the given data set (Day 4 of testing period data).

Table 5-3: The percentage of peak reduction for the crane study in this chapter.

| Controller | Percentage of demand reduction |
|----------------------------------|--------------------------------|
| Set-point | 23.9% |
| Optimal energy management system | 27.1% |
| MPC | 30.2% |

5.5.3 Prediction Horizon Evolution

As discussed in Section 5.3, the horizon size is an important parameter required in the receding horizon algorithms. The MPC controller predicts the output of the model behaviour over a number of time steps into the future, this period is called the prediction horizon, h . This h value describes the future visibility, where the controller aims to achieve the desired response for the outputs. This section aims to compare the performance of the ESS model with the horizon size. Figure 5-10 presents the percentage of peak demand reduction for the MPC model as a function of horizon size. As expected the percentage of peak demand reduction increases as the horizon size increases. The RTG crane demand is highly volatile without a clear pattern or trend over the day, as discussed previously in Chapter 4. Peak points are distributed over the day, and it is reasonable that the potential peak demand reduction increases with the horizon window length. Furthermore, the peak demand reduction slightly increases within 2% when the horizon window increases more than 18 hours for this example.

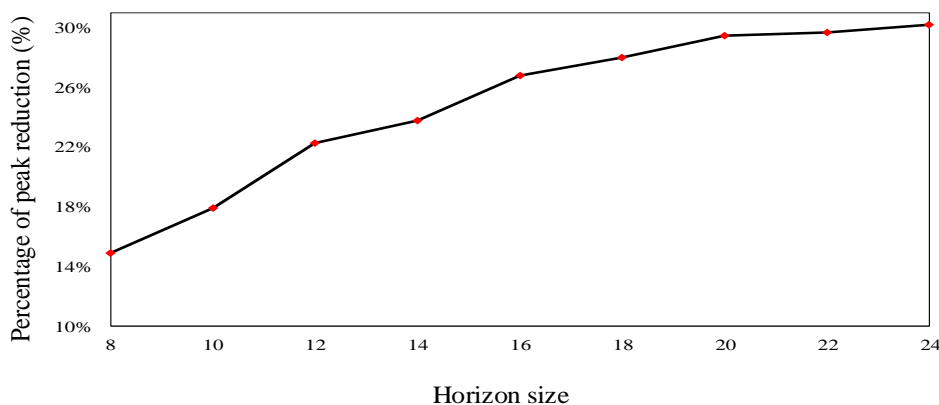


Figure 5-10: The percentage of peak demand reduction by MPC with different horizon window sizes.

In this work, the energy price parameter at Port of Felixstowe (PoF), will require a horizon size equal to 24 hours (48 half hours) to utilise the deviation of electricity energy price over a full day time. Since the peak demand can occur at any time of the day without any obvious patterns, as seen in Figures 3-8 and 3-11 in Chapter 3, a horizon size equal to 24 hours is required to determine the significant daily peaks. Therefore, for the set of data presented in this chapter, the horizon window size of 24 hours (48 half hours) will be applied to operate the MPC model. The updated information in each horizon and 24 hours window size increases the likelihood of successful peak reduction over each 24 hour period and allows the ESS to deal with peaks that are distributed over the beginning or end of the 24 hours period. In addition, this horizon window helps to capture the night peak in the early morning, which can allow the ESS to charge during the low demand period and avoid sudden increases in the demand. The prediction horizon has been considered in several energy saving studies, to cover the full day period to achieve the best performance [28] [49]. Holjevac et al. developed an optimal control strategy based on MPC controller for microgrid network with day ahead prediction horizon and half hour data resolution [51] and concluded that the increase in data resolution will increase the computational cost which may require a reduction in the prediction horizon. Figure 5-10 shows that a small horizon window, increases the possibility of reducing non-critical peak demand. For example, for a peak load within 2 or 4 hours of the current time may not be a critical peak within the full day horizon size and it will lead to unnecessary operation of the ESS. Therefore, using too a small horizon window will not achieve the maximum possible peak reduction. On the other hand, the large horizon window will introduce more computational cost but will allow the ESS controller to plan ahead for the larger peaks [33] [51].

In this work, the half hourly RTG cranes electric demand has been used to generate the results. In general, the cranes demand behaviour on the electrical distribution network changes at a sub-second resolution. Therefore, in practice the actual performance of the ESS control algorithms will be likely reduced. However, a higher resolution model will introduce more computational cost in the forecast and control algorithms due to the large window size. It is expected that sea ports will have standard smart meters with half hourly resolution for electricity billing purposes, hence practical predictions will likely remain with this resolution. For the ESS topology, the resolution of the demand profiles is likely to be dependent on the main role and aim of the ESS. For instance, an ESS being used to reduce voltage fluctuation as

a voltage supporter device will require higher resolution demand profile, where the small voltage deviation can have a high impact on the distribution network. On the other hand, an ESS being used for electricity cost and peak demand reduction, similar to our case, will only require lower resolution data as the peak demand will have less impact on the thermal constraints of the distribution network, where the distribution network infrastructure (cables and substation) are able to work outside the operating specifications for a short period. Furthermore, the electricity bills are normally calculated based at a relatively low resolution (half or one hour). The resolution of the RTG cranes demand profiles used are expected to have a significant effect on the performance of the ESS control algorithm.

5.5.4 Economic Results.

In this chapter, the procedures presented aimed to create a substantial reduction in the peak demand for the electrified RTG crane network by taking into account the electricity price. This section will present the basic economic results and introduce the annual cost savings for the proposed ESS control strategies. The proposed control strategies aim to charge the ESS with the maximal rate during the period with the lowest electricity tariff rate. The electricity energy tariff at the Port of Felixstowe, UK is 90 £/MWh for the day time and 60 £/MWh for night time, as described in Section 5.3. According to data provided by technical staff at the Port of Felixstowe and the energy cost analysis of an RTG crane [19], the annual electrical energy cost for a network of two RTG cranes is around £20,442 . Table 5-4 presents the annual electricity energy cost saving for the proposed control strategies presented in this chapter. The percentage of annual cost saving is calculated based on the daily substation average energy demand [19], the electricity tariff price, and the average daily shifted energy. The MPC controller can achieve annual electricity bill savings of around 7.26% with improvement by 32.7% and 10.3% compared to set-point and optimal management controllers, respectively. Although MPC produces the best energy cost saving and peak reduction, it is the most computationally expensive and has high precision requirements for designing and controlling the energy storage system compared to a set-point controller. On the other hand, the set-point controller is inexpensive and widely used in industrial applications and energy storage systems. However, the ESS enables a reduction in the peak demand on the electrical infrastructure (substation and cables), which introduces extra economic and technical benefits not considered in these costings.

Table 5-4: The percentage of annual energy cost saving for the annual electricity bill.

| Controller | Percentage of cost saving |
|---------------------------|----------------------------------|
| Set-point | 5.47% |
| MPC | 7.26% |
| Optimal energy management | 6.58% |

5.6 Summary

Due to the highly volatile nature of RTG crane demand, it is more difficult to accurately forecast compared to MV network, (which has a smoother demand) or the LV network demand (which has strong daily and seasonality correlation). This increases the complexity and challenges of controlling an ESS in a network of RTG cranes. Therefore, the situation requires more advanced control systems than conventional control algorithms to improve the ESS performance. The ESS in this work aims to minimise a port's electricity energy costs and achieve the maximum peak reduction in the crane network. The MPC strategy has been developed in this chapter to improve the performance by minimising the electricity energy bill and peak demand. The proposed optimal controllers utilize a load forecast without relying on perfect forecasts or accurate demand estimates in contrast to the literature, which employ perfect forecasts without considering the impact of forecast error.

In this chapter, three control strategies have been developed to generate the optimum plan for the ESS. Firstly, a set-point controller is developed as a common ESS control algorithm. Further, an MPC controller with a rolling forecast model is designed to generate a rolling energy device operation plan over a specific horizon size. Finally, an optimal energy management system has been developed to solve the energy optimisation problem using a fixed day ahead estimate of the demand. The optimisation algorithms in this chapter were tested to establish their appropriateness for electrified RTG cranes with ESS control by comparison on a data set that have been collected over different RTG crane operation days. It was found that the proposed MPC controller outperformed the optimal energy management and set-point controllers in terms of the peak reduction percentage. Additionally, the receding horizon control algorithms had significant economical benefits on reducing the electricity bills. In receding horizon controllers, the selection of the window size is an important parameter to

increase the control model's performance. The analysis of window size for the MPC shows the optimal control model required a 24-hour window size. The novelty of the MPC developed in this chapter for the network of RTG cranes connected to an energy storage device, helped to decrease the electricity energy costs and achieve maximum possible peak reduction, unlike the conventional controllers and limited optimal models [7] [42], which neglect the forecast algorithm as inputs to improve the ESS efficiency.

Chapter 6: Stochastic Model Predictive Control for electrified RTG cranes.

The previous chapter presented the benefit of developing a receding horizon control algorithm (MPC) for an ESS in a network of cranes. The high uncertainty in the demand profile have a significant impact on MPC energy storage control algorithms [28] [49]. The current literature in energy saving for LV network applications and microgrids has begun to investigate the benefits of treating the demand as a stochastic element by developing stochastic control methods in order to increase the efficiency performance of ESS in the distribution networks. For example, Rowe et al. [33] developed a Stochastic Model Predictive Control (SMPC) based on a scenario tree that presents possible future operation scenarios for ESS in an LV distribution network. However, the study only targeted the peak demand reduction, without considering the energy costs. In [33], to select the probability of future demand and develop the ESS plan, only the historical demand is used. D. Zhu, and G. Hug [52] presented a SMPC for microgrid system by developing a decomposition technique for the operation scenarios of renewable energy (wind generation), the ESS and the generation system and solve it as several subproblems. However, where the demand profile of customers is assumed to be deterministic over the horizon, ignoring the forecast demand uncertainty in the system. An electrified RTG crane demand profile has highly stochastic and less predictable behaviour compared to other low voltage loads. Challenges in developing accurate crane demand forecasts make it substantially more difficult to control the ESS and increase the energy systems' efficiency by using the actual prediction data. This chapter will present a Stochastic Model Predictive Control (SMPC) controller based on a Dynamic Programming (DP) technique and an empirical mean algorithm to reduce the effect of the high volatility of demand and increase the energy cost savings and peak reduction compared to the MPC and set-point controllers presented in Chapter 5. Furthermore, Chapter 6 includes a stochastic demand prediction model to improve the control of the ESS. The SMPC performance is then compared to the benchmark controllers performance.

Stochastic optimisation techniques are a special subset of mathematical programming algorithms that evaluate objective function problems under uncertainty [33]. Stochastic energy management controllers solved via DP have been used effectively to increase energy saving in buildings [53] [54], microgrid applications [55] [56] and electric vehicles [59] [132] [133]. The research literature has shown that a stochastic optimal controller can be beneficial for increasing energy cost savings in LV networks; therefore, SMPC aims to add uncertainty terms into the demand prediction of an MPC algorithm, and find the optimal ESS operation mode. A SMPC strategy for a network of electrified RTG cranes system with an ESS located on the side of the substation to feed a single crane or more could be of great interest worldwide. Furthermore, this could help sea ports to reduce the electricity energy costs and carbon emissions.

Aiming to fill the gap in the literature, this work describes and compares the SMPC, to an optimal energy management system and a set-point controller. Therefore, this chapter has key novel contributions: firstly, the electrified RTG crane demand is predicted by using a stochastic prediction model to facilitate the SMPC. Secondly, unlike previous studies with standard control algorithms and MPC, an SMPC controller that treats the high volatile demand behaviour and uncertainty terms in the RTG crane demand prediction to increase energy cost savings and peak reduction is presented in this chapter. The remainder of this chapter is organised as follows: Section 6.1 presents and illustrates the methodology of the SMPC controller. Section 6.2 presents a set of results including the RTG crane prediction demand results, and the proposed controllers through a specific case study. In addition, the State of Charge (SoC) evolution, numerical issues of the DP and the economic results of using ESS are also investigated. Finally, the conclusion is presented in Section 6.3.

6.1 Stochastic Model Predictive Control.

In the previous chapter, the RTG cranes control problem is formulated as optimisation problem with receding horizon (MPC). However, in reality the crane demand is naturally stochastic due to the highly volatile behaviour of crane operators. Stochastic optimal energy management is required to effectively minimise the energy costs and increase the peak demand reduction by dealing with the high uncertainties in the RTG cranes demand. This study presents a stochastic model predictive control (SMPC) problem, solved via a Dynamic Programming (DP) and empirical mean tool. The outline scheme of the SMPC strategy for the energy storage

system (ESS) for the network of RTG cranes is shown in Figure 6-1. As discussed in the literature review, for volatile demand it is essential to study the demand as a stochastic process in order to effectively control the ESS. Furthermore, generally stochastic optimisation models do not use a receding horizon in order to simplify the ESS operation. However, using a receding horizon can have a large positive impact on the ESS control performance, and is an ideal candidate to optimally control the ESS connected to a network of RTG cranes. In this section, a forecast model based on a combined Monte Carlo and ARIMAX (MC-ARIMAX) procedure is developed to generate the future crane demand scenarios. Then, a SMPC model is developed to minimise the energy costs and peak demand. This procedure is summarised in Figure 6-1.

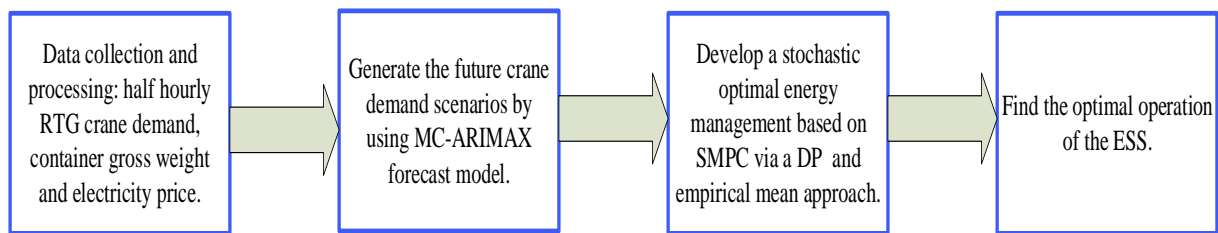


Figure 6-1: General schematic of the stochastic optimal energy management procedure implemented.

6.1.1 Energy Prediction Model Based on an ARIMAX and Monte Carlo Method.

In order to develop the energy control model, a future energy profile must be estimated. The ARIMAX and ANN forecast models have been previously used in Chapter 4 to forecast the demand for a single RTG crane. In order to generate a number of future crane demand scenarios, a Monte Carlo ARIMAX method is developed. The forecast task can be accomplished autonomously, prior to designing the energy storage control strategy. As discussed in Chapter 4, the ARIMAX (p, d, q) is a time series forecast method utilising the historical load data as a function of time, Equation (4-1), [66] [67]. Here, an ARIMAX (1,0,2) forecast model is used to generate a rolling demand forecast with independent exogenous variables, namely, the container gross weight variable. The ARIMAX model parameters (1,0,2) have been selected based on the analysis in Section 4.2.2 using the BIC calculations and the PACF and ACF plots.

In this section, the container gross weight variable is used as a stochastic input variable term to generate the forecast model scenarios. The unpredictability of the crane operator behaviour increases the stochastic nature of the RTG crane demand, as the crane operator

decides the container movement paths on the port platform. This situation leads to less predictable demand for the same container weight. Figure 4-6, in Chapter 4, shows the crane demand variation for different container weights, for example, the crane demand for container gross weight (149 tons) was between 7.7 kWh to 19.9 kWh, which equals 158% range in the demand for the same container weight. In this research, to minimise the impact of this variation, we develop a stochastic prediction system based on a Monte Carlo ARIMAX (MC-ARIMAX) method.

Stochastic forecast using a Monte Carlo ARIMAX (MC-ARIMAX) model

Monte Carlo is a computational algorithm which uses repeated random sampling to solve problems by modelling the range of possible scenarios [58] [59]. The electrified RTG crane demand considered here is uncertain and volatile. To account for this, we have modified the ARIMAX forecast model from Chapter 4, by including a Monte Carlo sampling step to generate a range of potential forecast scenarios. We sample the demand variation behaviour based on the historical distribution of demand based on container weight and then feed these samples into the ARIMAX. The basic steps for using the Monte Carlo method to generate a number of paths through the ARIMAX model are summarised as follows:

- Identify the problem variables and specify the presample data. In this work, the training data set has been used as the presample data.
- Specify the empirical joint distribution of the electrified RTG crane demand and container gross weight.
- Generate stochastic samples from the joint distribution of the container weight and crane demand.
- Use the ARIMAX (1,0,2) model, to forecast and simulated stochastic samples to obtain the output responses.

For sampling the crane demand from the probability empirical distribution, the 2D histogram with 100 bins for the container weight and the crane demand data set has been used, as displayed in Figure 6-2. The histogram plot displays the joint probability distribution for the container gross weight and crane demand. The Monte Carlo simulation provides the uncertainty results in line with the expected average results and it may capture a range of scenarios through the simulation iterations [134] [135] [136].

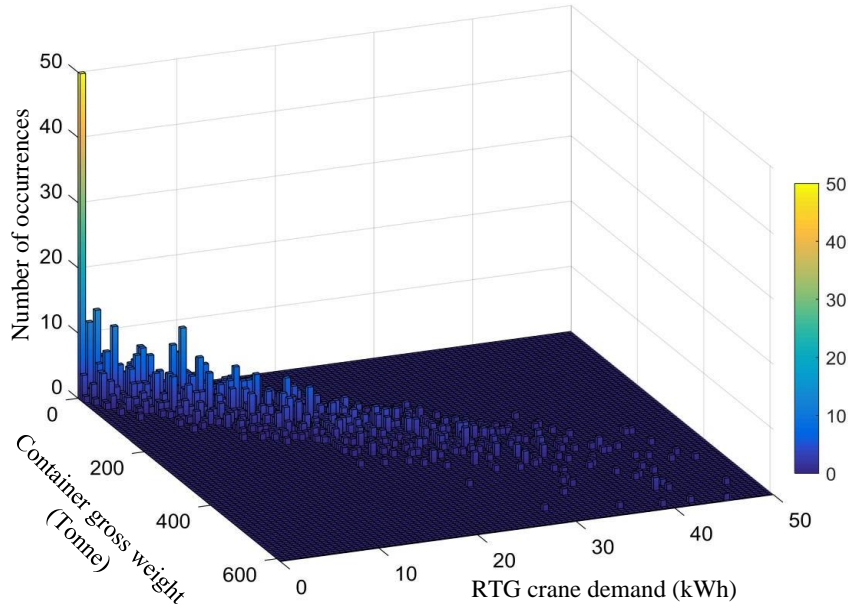


Figure 6-2: Illustration of the empirical distribution of the electrified RTG crane demand and container gross weight data via a 2D histogram.

6.2 Stochastic Model Predictive Control.

Dynamic Programming (DP) is a powerful approach for solving different types of optimisation problems [137] [138], which include constraints for both state and control variables. The DP method was first applied for Bellman’s dynamic programming algorithm to obtain the minimum value of a cost-to-go function by using backwards calculations [58] [138]. Generally, the DP optimisation technique is efficient, not influenced by the nature of the problem and finds the optimum solution for the control process under the model constraints [139]. In dynamic programming, the whole control process is divided into a series of optimisation problems and solved backwards to allow DP to achieve the minimum value of the cost function by controlling decisions at each discrete time point [58] [138]. In general, it is difficult to find the optimal input as a function of state for every time step, n , due to the large dimension of the problem [166]. Due to the computation difficulties, this chapter presents an alternative solution by computing the empirical mean of the cost function in order to approximate the DP problem [137] [140].

The future RTG crane demand profile for day k , \hat{L}_k , is modelled as a stochastic variable by generating M profiles, future demand profiles using the MC-ARIMAX forecast model, where

$m \in \{1, \dots, M\}$ and n is the half hourly period of the day ($n \in \{1, 2, \dots, N = 48\}$) defined by:

$$\hat{L}_k^m = (\hat{L}_k^m(1), \dots, \hat{L}_k^m(N))^T \in \mathbb{R}^N, \quad (6-2)$$

The SMPC method aims to create an energy storage control policy to minimise the maximum total demand over all M future scenarios for the periods n, \dots, N using the empirical mean for the cost function, in other words find:

$$\Delta E^*(n, n+1, n+2, \dots, N) = \arg \min_{\Delta E(n:N)} \frac{1}{M} \sum_{m=1}^M J(\hat{L}_k^m, \Delta E, n). \quad (6-3)$$

The aim here is to find the charged or discharged energy, ΔE , that minimises the cost function, subject to the ESS model constraints, as presented in Equations (5-4) to (5-7) in Chapter 5, with cost function J at time ℓ , $n \leq \ell < N$ defined as:

$$J(\hat{L}_k^m, \Delta E, \ell) := \max_{s \geq \ell} \{(\hat{L}_k^m(s) + \Delta E(s))^2\}, \quad (6-4)$$

where s is the variable describing the future time steps of the day ($\ell, \ell+1, \ell+2, \dots, N-1$). The DP model solves the problem by first minimising the cost function at the end of the day from $N=48$ backward to the n^{th} time step, by first finding the optimal storage plan, ΔE , for the subproblem at (N) from Equation (6-3) as follows:

$$J^*_{(N)} = \frac{1}{M} \sum_{m=1}^M J(\hat{L}_k^m, \Delta E, N), \quad (6-5)$$

and then iteratively solving at time ℓ , given $\ell+1$, until $\ell = n$ (backward calculation) via:

$$J^*_{(\ell)} = \frac{1}{M} \sum_{m=1}^M \max \{(\hat{L}_k^m(\ell) + \Delta E(\ell))^2\} + J^*_{(\ell+1)}. \quad (6-6)$$

In Equations (6-5) and (6-6), we find the charging and discharging energy in the ESS, ΔE , that minimise the cost function. The main idea of using the DP is the ESS control policy at each point equals the minimum over all paths in the search space from ℓ to $\ell+1$. In the SMPC controller model procedures, the final chosen ESS control policy at $n \in \{1, 2, \dots, N\}$ is then specified as: $\pi^*(n) = (\Delta E^*(n), \Delta E^*(n+1), \dots, \Delta E^*(N))^T$. The SMPC control model is updated to take account of each new observation e.g $n+1$. In addition, reduction in the energy cost of the network of cranes is achieved by finding the optimal operation of the ESS based on the time-of-use electricity price. The electricity tariff from 07:00 until midnight is higher than the period

of tariff during the rest of the day so it is beneficial to use the tariff changes to minimise the cost, as described in Chapter 5 for MPC model. The SMPC controller is designed to make sure that the ESS is fully charged during the low tariff period and discharged during the high tariff period. This also helps to reduce the cost of the DP calculation over the full day. The electricity tariff details for the Port of Felixstowe, UK are described in Section 6.3 through a specific case study. The SMPC has been used, in this work, to control the ESS as outlined and summarised in Table 6-1. In addition, for the proposed SMPC model, the DP is developed to find π^* by searching over a number of storage profiles constrained by a fixed discretization of search space [58] [138]. This will be investigated in Section 6.3 by evaluating the SMPC model performance with different increment values. The DP algorithm is described in more detail in Appendix C.

Table 6-1: The SMPC controller model procedures.

| Steps | Description |
|-------|--------------------------------------------------------------------------------------------------------------------------------------------------------------------------------------------------------------------------------------------------------------------------------------------------------------------------------------------------------------------------------------------------------------------------------------------------------------------------------------------------------------------------------------------------------------------------------------------------------------------------------------------------------------------------------------------------------------------------------------------------------------------------------------------------------------------------------------------------------------------------------------------------------------------------------------------------------------------------------------------------------------------------------------------------------------------------------------------------------------------------------------------------|
| 1 | Determine the control objective and constraints. |
| 2 | Initialise: the crane, forecast data and ESS data. |
| 3 | For $n = 1$ to N (daily demand operation), do <ol style="list-style-type: none"> a. Generate a number of the future crane demand profiles based on the MC-ARIMAX prediction model for when the previous n states of day are known, this is taken into account by step e. b. Solve the optimal Equation (6-3) for all demand scenarios from N to n using Equations (6-5) and (6-4). <p style="margin-left: 20px;">Subject to:</p> <ul style="list-style-type: none"> • Equations (5-3) to (5-6). • Energy cost saving Equations (5-10) to (5-12). • For ($n = 1$), the model computes the optimal solution based on the RTG crane demand prediction and initial data. c. From step b apply the ESS optimal control operation at time $n+1$ for one step. d. Update the prediction demand scenarios model and storage control policy to take in account new observation at time point $n+1$. e. Repeat steps with $n = n+1$, stop when $n = N$. |
| 4 | An optimal solution is achieved for the electrified RTG crane system model with ESS for the specific day. |
| 5 | Repeat all steps for the next day. |

6.3 Results and Discussion

The proposed SMPC controller was applied to a network of electrified RTG cranes equipped with an ESS. First, the results of the prediction model are presented; then, the proposed SMPC controller is tested under a specific case study. Throughout this section, the peak demand reduction of the SMPC controller is compared to set-point and optimal energy management controllers used in the literature (also see Chapter 5). The State of Charge (SoC) evaluation over the relevant day and numerical issues of the DP are also considered. Finally, economic results of using the ESS in a network of cranes are introduced.

The electrical demand and container gross weight data of two electrified RTG cranes were collected between 1st of March and 30th of April 2017. The collected data is divided into two sets: (1) a training data with 56 days of collected data (2) Testing set with 5 days of collected data. In particular, we analysed the real RTG crane demands over two months.

6.3.1 Network of RTG Cranes Prediction Demand Results.

The aim of developing an MC-ARIMAX forecast model is to capture the stochastic RTG crane demand behaviour by generating a number of future demand scenarios to feed the ESS control model. This section presents the MC-ARIMAX forecast results in comparison to the ARIMAX and ANN models. In order to compare the MC-ARIMAX prediction model with other results in the literature, the MAPE, as a common measure used in the literature, has been used. Firstly, the forecast models' profiles are generated for the five days of the test data and compared to the crane actual demand, as illustrated for one day in Figure 6-3. In addition, the overall daily MAPE for each forecast model is calculated in Table 6-2. A comparison of the MC-ARIMAX, ARIMAX and ANN models of the cranes demand shows that the MAPE scores of the MC-ARIMAX model with the average demand scenario, are better than the other prediction models over the testing period, as depicted in Table 6-2 and Figure 6-3. The results show, for the given data, that the hybrid model slightly improves the forecast performance and reduces the forecast error, especially when the ANN forecast model has a relatively large forecast error (MAPE). For illustration, on the first day, the MAPE decreased to 13.3% from 18.2% and 13.6% for the ARIMAX and ANN models, respectively. The variation in the MAPE results in Table 6-2 are related to the high crane demand volatility and poor forecasts of the peak points.

Table 6-2: The daily MAPE for the cranes demand forecast models: ANN, ARIMAX and MC-ARIMAX prediction models.

| | ANN | ARIMAX | ARIMAX-Monte Carlo |
|-------|-------|--------|--------------------|
| Day 1 | 13.6% | 18.2% | 13.3% |
| Day 2 | 13.1% | 14.7% | 10.8% |
| Day 3 | 8.1% | 9.8% | 7.9% |
| Day 4 | 20.6% | 24.5% | 18.8% |
| Day 5 | 15.9% | 18.9% | 12.4% |

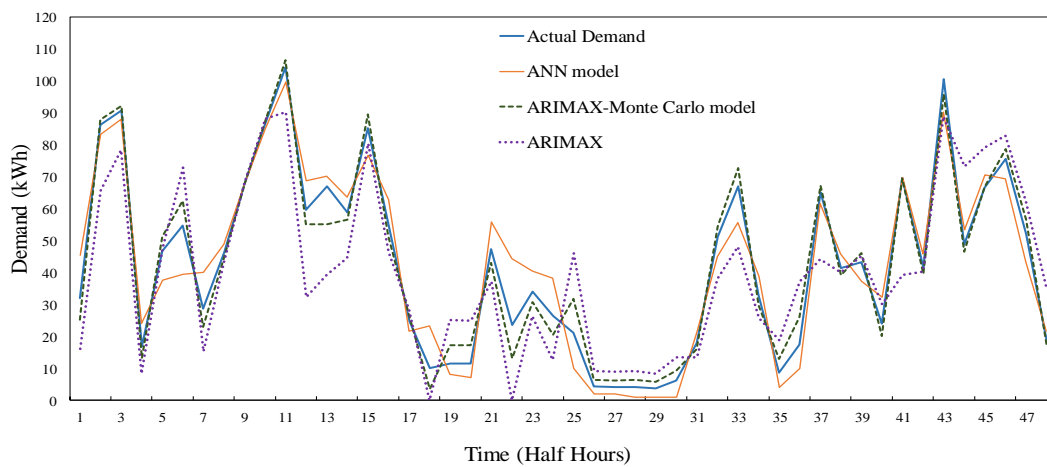


Figure 6-3: Results of MC-ARIMAX (average), ARIMAX and ANN models for the cranes demand for the first day of the testing period.

From Figure 6-3, the ARIMAX model misses peaks more than the other forecast models and it tends to underestimate the crane demand. The ANN forecast model tends to overestimate compared to ARIMAX. In Figure 6-4, the MC-ARIMAX demand predictions around the actual demand value are presented. The scenarios demand profiles are shown in red lines with small deviations around the actual demand line for each time step. The prediction updates minimise the forecast error after each time step to follow the actual demand, as shown in Figure 6-4. The half hourly time step updating forecast process decrease the average MAPE by 10.3% compared to daily updating, as seen in Figure 6-5. The MAPE only increases by 3% for the time step updating from 8 to 48 half-hours. For the MC-ARIMAX model, generates a number of demand scenarios over a long time period without updating the forecast model increases the probability of forecasting the demand inaccurately.

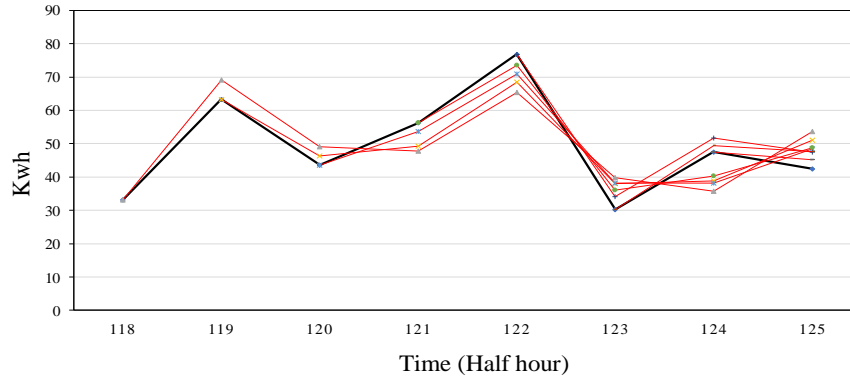


Figure 6-4: Example of the MC-ARIMAX forecast model (red lines) with actual demand (black line).

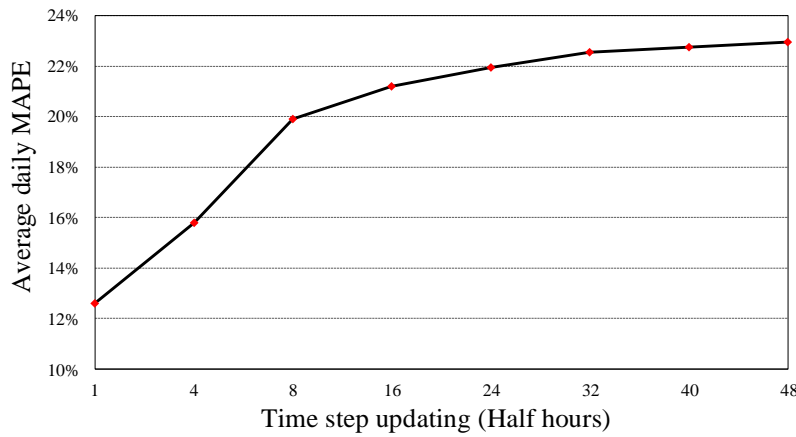


Figure 6-5: Results of rolling MC-ARIMAX (average), with different updating rates.

6.3.2 Case Study: a specific network of crane operation example.

The SMPC controller is implemented in the electrified RTG crane network equipped with an ESS, as presented in Sections 6.2. Table 6-3 presents the main model parameters for the ESS. These parameters are used in this case study to show and present the performance of the SMPC strategy performance compared to the set-point and optimal energy management system across the testing period (5 days). The increment of the SoC discretised value, was set equal to 0.5 and the number of demand scenarios generated by MC-ARIMAX is chosen to be 10, to provide a good balance between the performance and computational costs, as presented in Appendix D. Furthermore, the set-point value was set at 38.5% of the greatest peak demand seen in the historical crane demand data. This section does not focus on the ESS efficiency and hence neglects the transmission power line loss. The ESS efficiency is not the focus of this particular work. In this case study, the ESS size (150 kWh for two RTG cranes) is determined in kWh term based on the literature [150] [151] [152]. The following chapter, Section 7.2.1, will

present more details and a comparison between different ESS sizes. However, it was assumed that the ESS can be fully charged and discharged within half hour time. This introduces a peak reduction that is mainly related to a high power level up to 300 kW. The reduction in the power level of ESS, which also mean a slower charging for the ESS, can lead to less peak reduction due to the power limitation. In addition, the following chapter will present a detailed comparison between the receding horizon algorithms (SMPC and MPC) by using different forecast profiles (accurate and inaccurate). Chapter 7 will investigate the proposed ESS controllers performance based on different forecast profiles and the ESS location.

Table 6-3: The energy storage system parameters.

| Parameter | Value |
|------------------------------------|---------------|
| $\Delta E^{\min}, \Delta E^{\max}$ | ± 150 kWh |
| SoC ^{min} | 0 kWh |
| SoC ^{max} | 150 kWh |

Simulation results for this specific case study and the comparison between the SMPC, the optimal energy management and the set-point strategies are shown in Figure 6-6. The SMPC and optimal energy management system strategies use prediction data, and this help to reduce the risk of generating new peak points while optimally charging the ESS. A comparison of those three control strategies over the testing period of the peak reduction is presented in Table 6-4. The SMPC with 32.6% peak reduction outperforms both the benchmark controller (set-point control) and optimal management system. The SMPC shows an improvement in the percentage of peak demand reduction by 36.4% and 20.3% compared to the set-point control and the optimal management system, respectively. The set-point controller compared to the SMPC and the optimal management system is designed to work without any future knowledge about the demand, which will increase the possibility of unnecessary operation for the ESS and then fail to reduce the significant peak points during the day. The SMPC controller takes into account the uncertainty in forecast demand and updates the system variables after every time step to improve the results compared to the optimal energy management system. Typically, the storage control technique for cost saving and peak reduction, depends on the accuracy of the forecast profile and the actual demand volatility. The result shows the SMPC controller in this example is better able to deal with the larger forecast uncertainty and highly volatile

demand compared to the optimal energy management system and the set-point controller. The peak demand reduction accomplished in this work will reduce the stress on the port electrical infrastructure and reduce electricity bills.

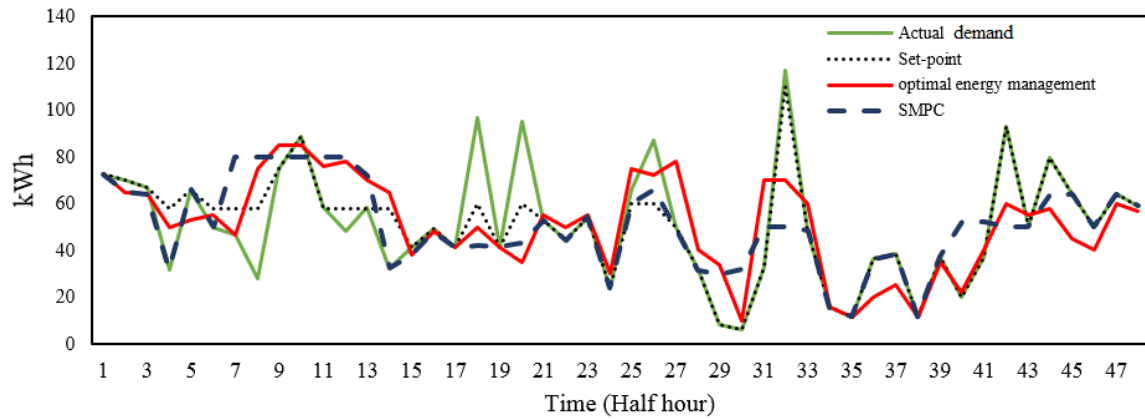


Figure 6-6: A specific example of the results presents the actual demand, and demand profiles from the set-point controller, the optimal management system and the SMPC for the cranes network for the given data set (Day 4 of testing period).

Table 6-4: The average percentage of demand reduction for a specific example over the 5 day testing period.

| Controller | Percentage of demand reduction |
|---------------------------|--------------------------------|
| Set-point | 23.9% |
| Optimal management system | 27.1% |
| SMPC | 32.6% |

The results in Figure 6-7 shows the distribution of percentage daily peak demand reduction, achieved by using the set-point, the optimal energy management and the SMPC controllers. SMPC outperforms the set-point and optimal energy management controllers with median percentage peak reduction of around 33.6%. As the box plot distributions for set-point controller overlap slightly with the optimal energy management system, it shows that the optimal controller performance is significantly affected by the high forecast error. The SMPC and optimal controllers show a better peak demand reduction performance for the days that have more accurate forecast profiles, as presented in Table 6-2. The SMPC as a receding

horizon controller has an advantage due to the process of updating the forecast model information, allowing an increase in the forecast accuracy and the likelihood of successful significant peak reduction over the full day. Chapter 7 will investigate the ESS performance for all proposed controllers in this thesis based on different forecast profiles to present the impact of the forecast error.

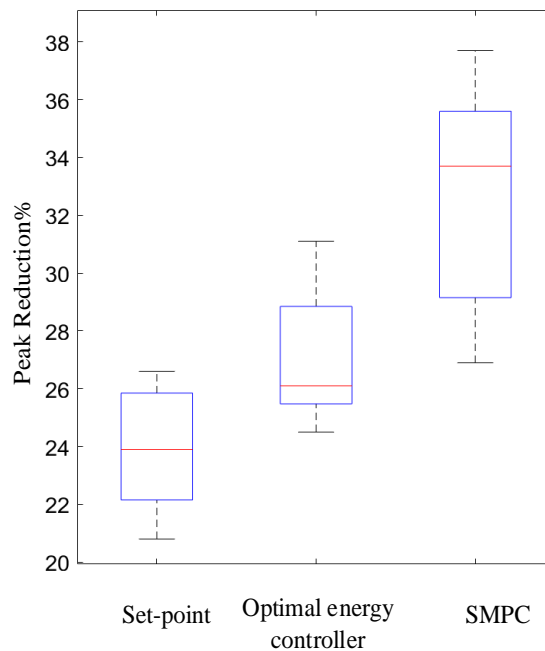


Figure 6-7: Box plot of the daily peak demand reduction achieved by the set-point, the optimal energy management and the SMPC controllers over the testing time period.

6.3.3 State of Charge (SoC) Evolution.

In this section, the SoC variation for the energy storage device controlled by SMPC is presented. Figure 6-8 displays the actual demand for the substation demand with and without energy storage for a particular day (day 5 of testing period data) with corresponding SoC of the ESS, as shown in Figure 6-9. In this example, the average daily substation demand for the two RTG cranes was 48.1 kWh. Figure 6-8 shows that the SMPC controller successfully smooths the highly volatile demands. The SoC evolution, as shown in Figure 6-9, shows that the ESS obtained the SoC^{\max} limit during the lower electricity tariff, before 07:00 (14 half hours), and discharged during the high electricity tariff period when the SoC reached a value near the SoC^{\min} boundary. Due to the electricity tariff constraint to achieve the maximum cost saving, the ESS was not able to reduce the peak demand much more at the half hour number 14. The

SoC evolution shows that the controller model can charge and discharge the storage device during the same electricity tariff period in order to minimise the peak demand, as shown in Figure 6-9, for the half hours between 12 and 35.

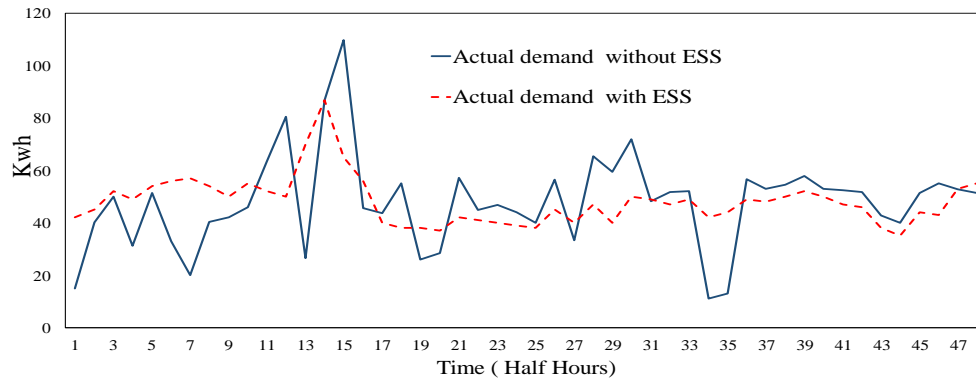


Figure 6-8: The network of RTG cranes demand profile with and without ESS (for day 5 of test set).

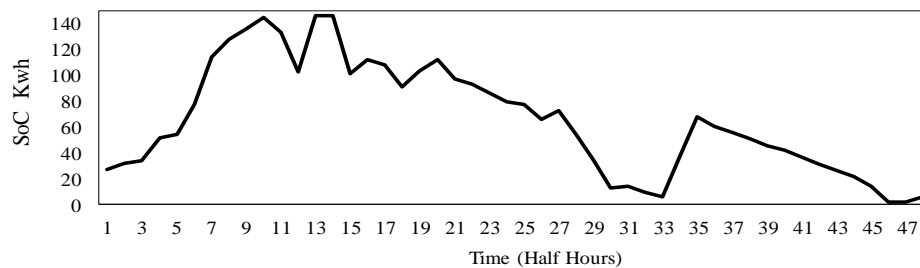


Figure 6-9: The State of Charge (SoC) of the ESS throughout the day (day 5 of test set).

6.3.4 Numerical Issues of the DP for State of Charge (SoC)

During the interpolation process in the DP model, the actual SoC value may not match with the nodes of the SoC grid in the DP model. This is mainly related to the size of the increment of the discretised value (discretised resolution) of the SoC (ΔC). Figure 6-10 shows the percentage peak reduction from applying the SMPC management on the cranes network equipped with an ESS as function of ΔC . Figure 6-10 shows that the percentage peak reduction increases as the discretised value ΔC decreases, and it stabilise after ΔC is sufficiently small. The percentage peak reduction is not significantly increased beyond $\Delta C = 0.5$ and the SMPC can be seen to converge to a maximum possible peak reduction at approximately $\Delta C = 0.5$. Therefore, for the set of data presented, a discretised value of 0.5 is used for all simulations using the SMPC controller. Furthermore, setting the discretised value too large, above 4, will

mean the ESS will achieve a very low possible peak reduction due to the coarse search space for the DP. The large discretised values increase the error compared to the optimal ESS operation decision. This is a consequence of the fact that the final SoC for the ESS is accumulating energy that could have been used for peak reduction or cost savings during the day period. In contrast, having too small a discretised value under $\Delta C = 0.5$ increases the computational costs of the control.

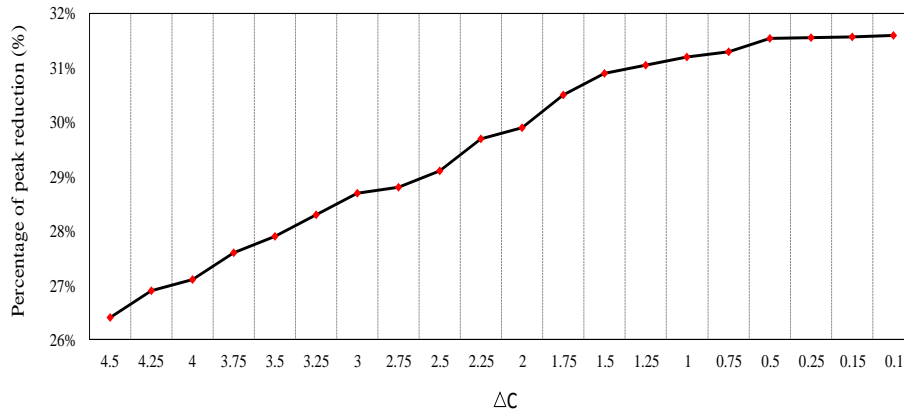


Figure 6-10: The percentage of peak demand reduction resulting from the SMPC energy management controller based on a DP solution for different SoC search space resolutions (ΔC).

6.3.5 Economic Results.

In this section, the economic implications of the study are considered and analysed. A primary economic analysis has been carried out to investigate the commercial benefits of the ESS in a network of RTG cranes based on the SMPC storage control strategy. There is a wide range of energy storage technologies that can be used in power system networks in order to increase energy cost savings and reduce peak demand. As discussed in Chapter 2, for a battery storage device, lithium-ion or NiCd batteries, have been used widely in ports and LV applications. For example, in the Vieira et al. study [41], a lithium-ion batteries system is used to store, and discharge energy based on the mismatch between the PV generation and the residential buildings energy consumptions. The objective of the ESS control model is to reduce the energy bill by minimising the power flows between the residential building and the LV network. The analysis results of the proposed management strategy, in [41], show that the power flow between the grid and householder reduced by 76% with an 84% reduction in the energy bill. The economic assessment shows that the proposed ESS solution can be cost-

effective in this case where the price of the batteries system is under 166£/kWh.

The stochastic control model procedures presented aimed to create substantial reduction in the peak demand of the network of electrified RTG cranes considering the electricity price. The SMPC controller aimed to charge the ESS with a maximal rate during the low demand period when the electricity tariff rate is lower. The electricity energy tariff at the Port of Felixstowe, UK described in Section 5.5.4, has been used to generate the economic results in this section. Table 6-5 shows that the SMPC controller can achieve an annual electrical energy cost savings of around 7.98% and improve the percentage of cost saving by 45.8% and 21.2% compared to the set-point and optimal management controllers, respectively. The set-point controller has the worst performance for reducing peaks and cost saving in this example but is easy to implement and it is widely used in industrial applications and energy storage systems. The SMPC has the maximum energy cost saving and peak reduction compared to the benchmarks, but it has the most computationally expensive and high precision requirements for designing and controlling the ESS.

Table 6-5: The percentage of annual energy cost saving to the annual electricity bill.

| Controller | Percentage of cost saving |
|---------------------------|----------------------------------|
| Set-point | 5.47% |
| Optimal management system | 6.58% |
| SMPC | 7.98% |

A primary economic analysis has been carried out to investigate the commercial benefits of the EES in the network of RTG cranes. Firstly, the main capital cost of the ESS technologies is presented in Table 6-6 based on the required ESS specifications given in Table 6-3. The techno-economic parameters for the ESS have been obtained from [141] to [146], which provide the recent and future prices of the ESS technologies. A battery energy storage system [144] [145] [146] currently has an average cost of 200 \$/kWh (140£/ kWh), and the ESS efficiency has been reported by [142] [144] to be around 90–95%. However, forecast results for the battery costs shows that the prices are expected to reduce to under 150\$/kWh (105£/ kWh) within the next 10 years [141] [142] [143]. These parameters are summarised in Table 6-6.

Table 6-6: The main techno-economic parameters for an ESS.

| Techno-economic parameters | Value |
|----------------------------|------------|
| Efficiency | 90%-95% . |
| Lifetime | 20 years. |
| Estimated cost | 140€/ kWh. |

In Table 6-7, a comparison analysis of the energy cost savings are introduced. The viability analysis includes: the annual cost savings, Internal Rate of Return (IRR), Net Present Value (NPV), and payback period. The results have been calculated using the EES parameters and a discount rate equal to 3% [147] [148]. The NPV is defined as:

$$NPV = \sum_{t=1}^T \frac{C_t}{(1+r)^t} - C_i, \quad (6-6)$$

where C_t is the net cash flow during the period t , C_i is the investment cost, r is the discount rate and T is the period of the project. In general, the NPV is a financial technique used in capital budgeting to determine the current value of all future cash flows for the initial capital investment and then establish if the project is profitable or not. The positive value of NPV indicates that the project is more likely to be profitable where the income of the investment exceeds the anticipated costs. In addition, the IRR is a financial method that aims to calculate the discounted cash flow rate of return. This method is applied to evaluate the attractiveness of the investment. The project is expected to be profitable, if the IRR value exceeds the required discount rate for the project. The IRR value is calculated as the discount rate value that produces an NPV value equal to zero.

The results in Table 6-7 indicate that the SMPC controller option is potentially economically profitable with a payback period of less than 15 years. The IRR is greater than 3% with a positive NPV value. The SMPC strategy is the most profitable option compared to the optimal energy management system and the set-point control, and is economically profitable with an IRR of over 4%. In addition, the economic benefits of using ESS with SMPC will become more substantial with the number of cranes at the port. The viability results analysis also shows that the optimal energy management and set-point options can only be profitable in the case when the discount rate is neglected.

Table 6-7: The ESS scenarios viability results

| | Annual cost saving (K £) | NPV (K £) | IRR (%) | Payback period (years) |
|---------------------------|-----------------------------|--------------|-------------|---------------------------|
| Set-point | 1.12 | -4.3 | 0.62 | 18.7 |
| Optimal management system | 1.34 | -0.9 | 2.45 | 15.6 |
| SMPC | 1.63 | 3.3 | 4.61 | 12.8 |

6.4 Summary

This chapter covers the gaps in the existing literature concerning the impact of the stochastic demand behaviour on potential peak demand reduction and electricity costs for a network of cranes with an ESS. When comparing the RTG crane demand to the smoother MV and LV demand profiles, controlling an ESS for a network of RTG cranes is challenging, due to the stochastic nature and high uncertainty levels in the crane demand. The load forecast is a significant tool to improve the storage control performance. Therefore, we utilize and compare three forecasting approaches, namely, MC-ARIMAX, ANN and ARIMAX, to estimate this demand. Results demonstrate that, for the given data, the hybrid prediction model is the most effective at estimating the demand by simulating a number of scenarios for the predicted demand.

Furthermore, a Stochastic Model Predictive Control (SMPC) controller has been developed to better cope with the crane demand volatility and hence improve the ESS performance. The SMPC controller is based on a DP technique for optimizing the ESS control over the generated forecast scenarios. The DP is employed to solve the energy optimisation problem through a backwards calculation, to find the optimal control over a discrete SoC grid. The performance of the proposed energy storage control strategies in this chapter is modified by using separate electricity pricing restrictions and prediction model output. In particular, the proposed SMPC controller outperformed the optimal energy management and the set-point controllers based on the peak reduction percentage. Additionally, the economic viability results were presented, showing that the SMPC control option is the most profitable compared to other control options shown in this chapter. This chapter has shown the advantage of including uncertainty within the control algorithm for the energy storage device. We can now compare all the developed control methods in the next chapter.

Chapter 7: Analysis and Comparison of ESS

Control Strategies

The previous chapters, Chapters 5 and 6, developed and tested MPC and SMPC algorithms for controlling an ESS in a network of RTG cranes. This chapter extends the results and introduces a comparison analysis of the energy storage control strategies proposed in this thesis. The comparison in this section investigates the stability and robustness of the proposed controllers by using the same data sets to test the proposed ESS controllers. The comparison analysis in this chapter is divided in two main components:

- Potential optimality and cost saving: the peak demand reduction and cost saving for the proposed controllers has been compared in two sections.
 - Firstly, Section 7.1 presents and evaluates the results of the SMPC and MPC controllers with different forecast profile sets compared to two benchmarking techniques, the set-point controller and the optimal controller based on perfect load forecast. Two types of forecast data sets from accurate and inaccurate forecast models, have been used to evaluate the proposed optimal controllers and understand the impact of forecast errors on the energy storage control algorithms. In addition, the ESS control model has been evaluated on larger data sets than used in Chapters 5 and 6.
 - In the subsequent section, Section 7.2, a comparison analysis for different ESS location scenarios is conducted to give sea ports an initial indicator regarding the possible location of ESS in line with a primary economic analysis. The ESS location scenarios for the network of multiple RTG cranes is a novel contribution of this chapter, since no studies consider a central ESS which feeds more than a single electrified crane or investigate different ESS location scenarios on the network.
- Complexity and computational cost: Section 7.3 will analyse the previous section's results and take into consideration the main parameters and characteristics of the

proposed controllers in this thesis. This analysis aims to present an initial indicator regarding the complexity of a practical implementation of the proposed control systems.

7.1 Analysis of Energy Storage Control Strategies

The primary objectives of using an energy storage in a network of RTG cranes are the reduction of peak demand and energy costs. In this section, the peak reduction and energy costs savings results are compared. Comparison evaluation of the performance of ESS will be determined by the following configurations:

- An ESS using benchmarks control strategies, as previously discussed in Section 5.2: First a set-point controller and second an optimal control model with perfect load forecast. This type of control revolves around employing a perfect forecast with full knowledge of what the system will do over the control period.
- An ideal ESS model based on set-point controller with infinite energy capacity; no limitations or constraints are imposed on the ESS in order to provide the greatest possible peak demand reduction. In this model, the set-point value will be the average half hourly demand on the day.
- Energy storage using the MPC and SMPC controllers, as described in Chapters 5 and 6, respectively. In order to maximise the benefits of using the ESS, the receding horizon control algorithms allow the use of the real time data to update the forecast model and optimise the ESS control decisions.

7.1.1 A Comparison Analysis for Optimal Controllers Based on Load Forecast Profile Accuracy.

The MPC and SMPC controllers require a forecast demand profile to determine the appropriate control for the ESS; Table 7-1 presents the errors for the forecast models that have been used to implement the ESS control models. We are interested in how the forecast error can affect the performance of the ESS. As discussed in the literature, an ESS control for LV network applications has typically been presented using perfect forecast models [38] [97] or forecasts with relatively small errors (between 10% to 15%) [45] [46]. Therefore, in this section, two types of forecast models, accurate and inaccurate, have been used to evaluate the proposed optimal controllers and understand the impact of forecast errors on the energy storage

control algorithms:

- Accurate forecasts: the future demand estimates are generated by using the most accurate forecast model, as presented in chapter 4, which only estimates the number of crane moves $X_2(n)$, while assuming the container gross weight, $X_1(n)$, is known in advance. This forecast has errors between 8% and 24% (from Tables 6-2 and 4-7).
- Inaccurate forecasts: the future demand estimates are generated by using an inaccurate forecast model that does not include the exogenous variable data. These give a MAPE between 21% and 39% (indicated by Table 4-7, and it generated by 5 days testing period).

The forecast models, in Table 7-1, are described in Chapter 4. In this section, the two months of collected data for the network of electrified crane demand are considered and divided into 56 days of historical data and 5 days of testing data, similar to Chapters 5 and 6. In the inaccurate forecast models, only the historical data has been used to generate the prediction profiles without requiring any of the external variables data ($X_1(n)$ and $X_2(n)$). In order to use the forecast models in this section with MPC and SMPC controller, the forecast models are designed to regenerate the forecast load profile at each time step n up to a day ahead, $n+48$, by using the forecast error and actual measurements at each new time n , where the forecast model is rerun with the new observation. The forecast model output from this step will be used to operate the receding horizon controllers. The forecast results, in Table 5-1, show, that the rolling forecast models which update the model every time step significantly reduced the forecast error. In Table 7-1, the MAPE decreased to 14.2% for the ANN model (Model B.2) from 28.3% for Model (A) and to 17.2% for model (C.2) from 30.1% for the ARIMA model (Model F).

Table 7-1: The average peak demand reduction for the ESS controllers with average forecast errors.

| ESS control model | Accurate forecast model | MAPE | Peak reduction% | Inaccurate forecast model | MAPE | Peak reduction% |
|-------------------|-------------------------|-------|-----------------|---------------------------|-------|-----------------|
| MPC | ANN (Model B.2) | 14.2% | 30.2% | ANN (Model A) | 28.3% | 20.2% |
| SMPC | ARIMAX (Model C.2) | 17.2% | 32.6% | ARIMA (Model F) | 30.1% | 24.2% |

The test data from Chapters 5 and 6 and the main parameters of ESS in Table 6-3 have been used to operate the ESS on a network of RTG crane. The optimal controllers (MPC and SMPC) are implemented using accurate and inaccurate forecast model as shown in Table 7-1. Due to the highly stochastic nature of the crane demand and forecast errors, the ESS is unable to achieve the highest peak reduction compared to the optimal controller with perfect future demand knowledge, as seen in Figure 7-1. The SMPC outperforms all controllers except for the control model which has perfect forecasts. The receding horizon controllers with the rolling forecast model improves the performance of the ESS compared to a set-point controller, if an accurate forecast is used. In the proposed controllers with the accurate forecast models, the percentage of peak reduction, as presented in Figure 7-1 for the data given, show that the SMPC improves the performance of the ESS by increasing the peak demand reduction compared to using an inaccurate forecast. The SMPC controller achieved a 32.6% peak demand reduction compared to 30.2% for MPC, 23.9% for set-point and 36.1% for the optimal controller with a perfect load forecast. Furthermore, the ideal ESS model with infinite capacity and no limitations, where this method basically produces a flat profile, reached a highest possible peak reduction of 64.8%.

The ESS control algorithms results, shown in Figure 7-1 and Table 7-1, demonstrate that the accurate forecast models are essential for optimal controllers to maximise the energy storage performance and increase the peak demand reduction. For illustration, the percentage of peak reduction decreased to 20.2% from 30.2% for MPC and to 24.2% from 32.6% for the SMPC, when using inaccurate versus accurate forecasts respectively. While using an inaccurate forecast model for running the optimal controllers, the SMPC controller outperformed the MPC and set-point control algorithms. The stochastic algorithms allow the control model to implement an ESS plan based on a number of demand profile scenarios, which minimises the impact of the high demand volatility. Figure 7-2 presents the relationship between the forecast errors and potential peak reduction for the SMPC over the testing data period. These results show that more accurate forecasts are directly related to greater peak reductions. The forecast accuracy is a significant term and driver for potential peak reduction for optimal controllers and is more likely to achieve a high peak reduction when utilizing a more accurate forecast [149]. However, the more accurate forecast do not always guarantee the greatest peak reduction, as seen in Figure 7-2. The forecast error could be concentrated at the peak period

rather than distributed over the day. In general, the peak demand reduction accomplished in this study will help to reduce the stress on the port's electrical infrastructure and reduce electricity bills.

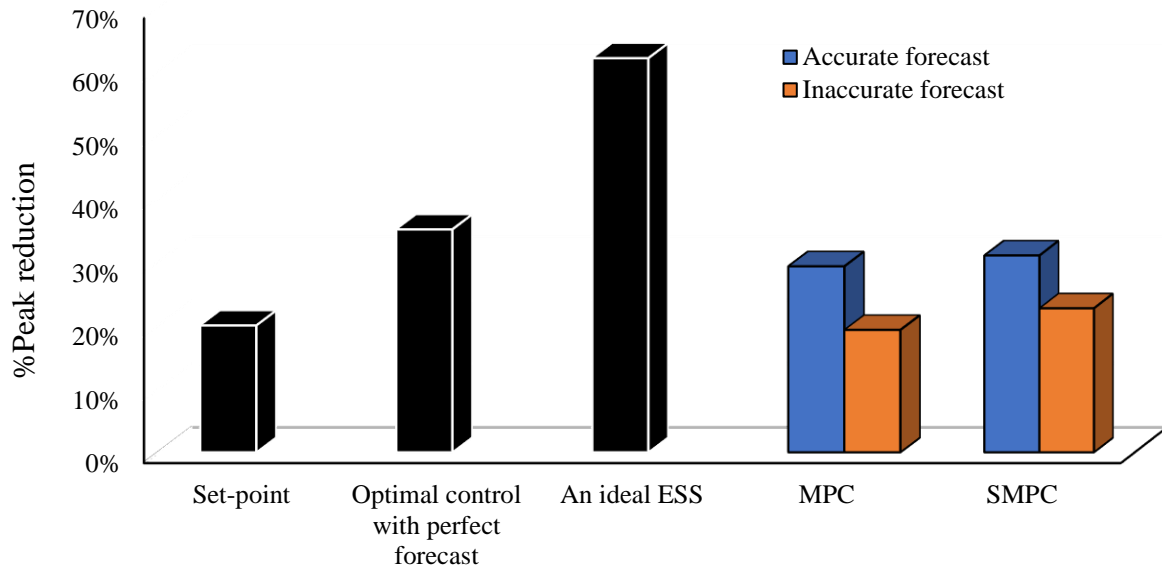


Figure 7-1: The average percentage of peak reduction for a specific case study.

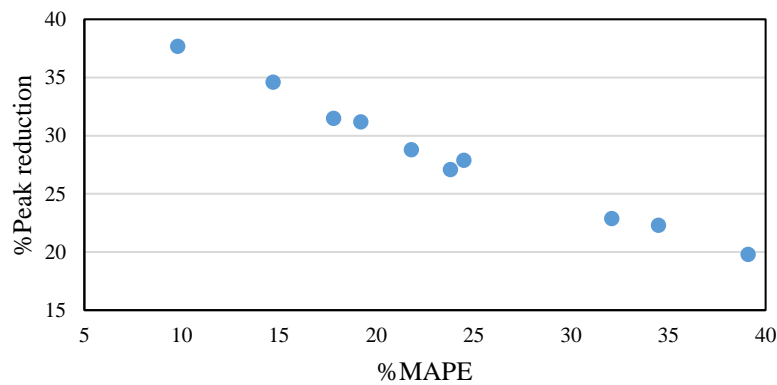


Figure 7-2: The relationship between MAPE and the percentage of daily peak reduction for the SMPC controller.

The cost function aimed to reduce energy costs and create substantial reduction in the peak demand of the network of electrified RTG cranes using the electrical energy costs term and demand shaving strategy. The electricity energy tariff and the annual electricity energy cost when using accurately forecasts are presented in Chapters 5 and 6 for MPC and SMPC. Table

7-2 collates all the annual electricity energy cost saving for the proposed control strategies. The stochastic controller, SMPC, with accurate forecasts can achieve annual electricity bill savings of around 7.9%, near the maximum possible energy cost savings of 8.01%. The energy cost saving results, in Table 7-2, show, that the accurate forecasts improved the energy storage performance and increased the energy cost savings compared to the control models with inaccurate forecasts with an improvement of 19% on average. For example, the percentage of annual electric energy cost saving increased to 7.26% from 5.88% for MPC and to 7.98% from 6.69% for SMPC. Furthermore, the reduction of the peak demand on the electrical infrastructure (substation and cables), introduces extra economic and technical benefits. Further economic analysis for different ESS location scenarios are introduced in Section 7.2.

Table 7-2: The percentage of annual electric energy cost saving to the annual electricity energy bill.

| Controller | Percentage of cost saving | | |
|------------------------------------------|-------------------------------|----------|------------|
| | No forecast/ perfect forecast | Accurate | Inaccurate |
| Set-point | 5.47 | - | - |
| Optimal controller with perfect forecast | 8.01 | - | - |
| MPC | - | 7.26% | 5.88% |
| SMPC | - | 7.98% | 6.96% |

As presented in Figure 7-1, all proposed optimal controllers which have an accurate forecast outperform the benchmark, set-point controller. Due to the highly stochastic demand behaviour and the peak demand distributed over the 24 hours a day, the set-point controller usually depletes the stored energy quickly at insignificant peak points. The substation is then forced to feed the network of cranes rather than utilize the ESS. The resulting improvement for optimal controllers is due to the penalty's for high energy costs at peak demand. Furthermore, the MPC and SMPC models allow for the minimisation of the maximum demand during the single electricity tariff period which helps to increase the peak reduction even more. The MPC and SMPC controllers, with rolling forecast and control models will also increase the robustness of the controllers by better reacting to the most recent demand changes. In the following subsection, new data sets from accurate forecast models were used to evaluate the proposed controller performance.

7.1.2 Results and Discussion for ESS Controllers

In this section, larger data sets of 12 days from two testing periods (period 1 and period 3, as presented in Chapter 4) have been used to evaluate the proposed controllers over two different time periods and test the transferability of the model trained on one crane to other cranes with the same specifications. As the substation only feeds a single RTG crane model in this section, the storage size has been reduced to 75 kWh for this specific example. The results for the set-point, optimal energy management, MPC and SMPC controllers are shown in Figure 7-3, with each box plot showing the distribution of daily peak reductions. The SMPC outperforms all other controllers on average with a median peak reduction of around 33%. As seen in Figure 7-3, the box plot of set-point controller overlap with other optimal controllers when the forecast error is high. The optimal controllers show a better performance for the days that have the more accurate forecast profiles. In receding horizon controllers, MPC and SMPC, the updated information of the demand model (the rolling load forecast) increases the amount of peak reduction over the full day time compared to the set-point controller or the optimal management system. The percentage of annual electricity energy cost savings is presented in Table 7-3. The receding horizon controllers, MPC and SMPC, outperform the setpoint and optimal energy management systems giving an annual electricity bill saving of 7.15% and 7.92%, respectively. The receding horizon controllers show an average improvement by 18.8% in energy cost savings compared to the optimal management system.

Table 7-3: The percentage of annual electric energy cost saving to the annual electricity energy bill.

| Controller | Percentage of cost saving |
|---------------------------|---------------------------|
| Set-point | 5.29% |
| Optimal management system | 6.41% |
| MPC | 7.15% |
| SMPC | 7.92% |

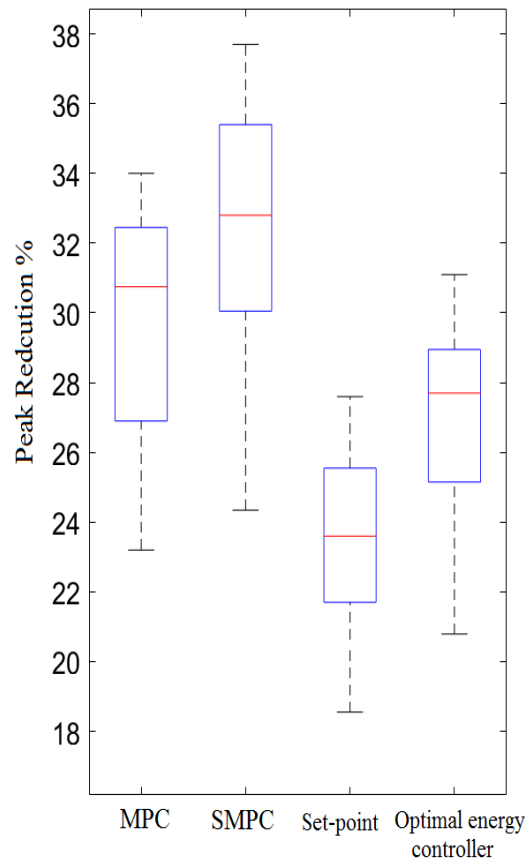


Figure 7-3: Box plot of the daily peak demand reduction achieved by MPC, SMPC, optimal management system and set-point controllers over two test data sets.

7.2 A Comparison Analysis for Different ESS Location Scenarios.

Multiple RTG crane location scenarios are considered in this chapter, since no other studies have considered a central ESS feeding more than a single electrified crane. This section presents a comparison analysis for different ESS location scenarios to give sea ports an initial indicator regarding the possible optimal locations for the ESS. The Single Line Diagram (SLD) of the network of electrified RTG cranes, Figure 7-4, shows a schematic for the actual electrical cranes connection for the Port of Felixstowe, UK. In the SLD, two electrified RTG cranes are fed from the same step-down transformer. This offers a number of possible locations for an ESS. The two scenarios investigated are as follows:

- Scenario 1: Two ESSs, ESS (1) and ESS (2), located on the low voltage side of each individual crane serves each crane separately. This scenario has been chosen to

evaluate a novel optimal controller with the ESS located in a similar position as considered in the literature [7] [16] [42]. This scenario can help to reduce peak demand, and thermal constraint problems on the cables and connections located at the end of the feeder. The ESS located next to the crane can also help support voltage problems with minimum losses [33].

- Scenario 2: A central ESS located on the low voltage side of the distribution substation to supply power to both RTG cranes. Unlike the literature that have studied and analysed the energy saving for a single RTG crane, this scenario has been chosen to investigate the benefits of using a central ESS to feed more than a single crane, motivated by using a central storage device in a low voltage network for residential customers [33]. This scenario aims to create greater costs and peak demand reductions compared to scenario 1. The ESS location close to the substation can give extra support to the secondary substation and mitigate operational constraints which will help to resolve the thermal issue in this zone.

Overall, there is a significant relationship between the ESS location and voltage and thermal problems in the LV network, but it will also depend on the demand behaviour, the role of using ESS and the ESS specifications. By controlling the ESS effectively, the performance of ESS on the network can be improved. In this thesis, voltage and current performance based on an ESS location have not been studied, the analysis of location scenarios will focus on peak reduction and energy cost saving performance to give initial indications about the possible ESS locations at the port.

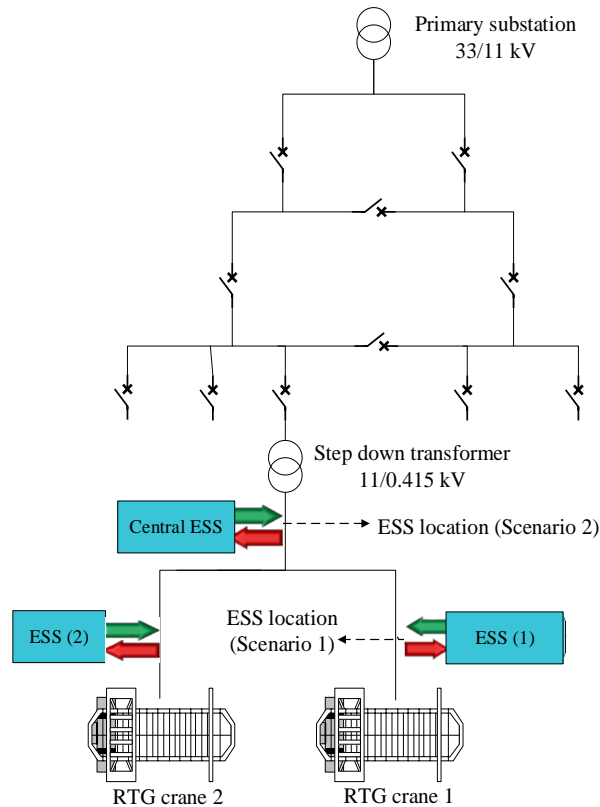


Figure 7-4: Single line diagram of network of electrified RTG cranes at the Port of Felixstowe, UK with different ESS location scenarios.

7.2.1 Peak Demand Reduction: a specific example

The ESS control strategies have been developed in the previous chapters for the network of electrified RTG cranes equipped with an ESS based on scenario 2, as shown in Figure 7-4. Here scenario 1 is also investigated. Table 7-4 presents the main parameters of the ESSs for each scenario to operate the network of RTG cranes. These parameters are used in this case study to show and evaluate the performance of the proposed control strategies performance with an accurate forecast compared to the set-point controller across the testing period (5 days) for different ESS location scenarios.

The electrified RTG used in this work has been retrofitted to be powered by the distribution power network at the port via a conductor bar, manufactured by Vahle (Germany). To minimise the gas emission and reduce the operation costs compared to diesel RTG crane, Vahle introduces two electrified systems. The first model is a hybrid RTG crane that included a battery system (80 kWh) and generator to supply the required power during the longer moving distance. The second model is a fully electrified RTG crane connected to the electrical power

network with a battery energy storage device (up to 120 kWh) to allow peak shifting or to supply crane power for a few hours independently from the grid [150] [151]. Hong-lei et al. developed a lithium battery energy system with capacity 128 kWh and SoC from 0% to 100% for a hybrid operation RTG crane [152]. In [16], the author determined the necessary battery energy storage size requested to operate the RTG crane for up to two hours is 124 -165 kWh. The ESS size proposed by Vahle, [16] and [152] for a single RTG crane is between 10% to 20% of the maximum daily RTG crane energy demand over an 8 day period [19]. In this chapter, the ESS size was chosen between the above reference values (approximately 11.5% of the maximum daily demand). The ESS size of ESS in literature [150] [151] [152] was chosen based on the kWh term. This introduces a high power level up to 300 kW for the 150 kWh storage size where the ESS can be fully charged and discharged within half hour time. The reduction in the power level which also mean a slower charging for the ESS can lead to lower peak reduction due to the power limitation. In general, a small ESS size increases the possibility of missing critical peak demand due to the energy storage limitations. In contrast, having a larger energy storage device, will increase the capital cost and it will be computationally more expensive to operate the optimal storage controller. To investigate the impact of the ESS size for a network of cranes, the ESS operation under scenario 2 (option 2) with 0.75 of the ESS sizes in the first option in scenario 2 is presented in this section. Due to the high volatile nature of demand, randomly distributed peak locations, electricity tariffs with the ESS systems potentially playing multiple roles, it is expected a large ESS would be required. In this work, we neglect the transmission power line loss and the overall ESS efficiency as 0.9 of the ESS size is only considered.

Table 7-4: The energy storage system parameters.

| ESS Location scenario | $\Delta E^{\min}, \Delta E^{\max}$ | SoC ^{min} | SoC ^{max} |
|---------------------------------------|------------------------------------|--------------------|--------------------|
| scenario 1 | | | |
| Each of the two ESS units (1) and (2) | ± 95 kWh | 10 kWh | 95 kWh |
| Scenario 2 | | | |
| ESS – option 1 | ± 180 kWh | 10 kWh | 180 kWh |
| ESS- option 2 | ± 135 kWh | 10 kWh | 135 kWh |

A comparison of three control strategies (set-point, MPC and SMPC) based on the average peak reduction values over the testing period are presented in Table 7-5. The SMPC outperformed all the other controller in all ESS scenarios. The percentage of peak reduction shows that the SMPC improves the ESS performance achieving a 31.2%, compared to 22.9% and 29.3% peak demand reduction for the set-point and the MPC controllers, respectively, for scenario 1. The SMPC controller achieves a peak reduction of 32.8% compared to 30.3% and 23.8% for the MPC and the set-point controllers, respectively, for scenario 2 (option 1). In scenario 2 (option 2), the SMPC technique improves the percentage of peak reduction by 28.4% and 6.3% compared to the set-point control and the MPC, respectively. The ESS operation under scenario 2 (option 2), where the ESS size is less than the ESS size of scenario 2 (option 1) by 25%, achieves a reasonable and favourable peak reduction of 23.5% compared to 32.8 % in scenario 2 (option 1) for the SMPC controller and 23.8% for the set-point controller. Despite the decrease in ESS size for scenario 2 (option 2), this could help reduce the capital and operation cost of the ESS with minimal loss in peak demand reduction capability.

Table 7-5: The percentage of peak demand reduction results for a specific case study.

| ESS Location scenario | Set-point | MPC | SMPC |
|-----------------------|-----------|-------|-------|
| scenario 1 | | | |
| Two ESS (1) and (2) | 22.9% | 29.3% | 31.2% |
| Scenario 2 | | | |
| One ESS (option 1) | 23.8% | 30.3% | 32.8% |
| One ESS (option 2) | 18.3% | 22.1% | 23.5% |

7.2.2 State of Charge (SoC) Evolution.

In this section, we consider the parameters of the ESS in scenario 2 (option 1). Figure 7-5(a) displays the actual demand on the substation with and without the ESS for a particular day (day 5 of testing period data) with the corresponding SoC of the ESS, in Figure 7-5(b). The example shows that the SMPC controller smooths the highly volatile demands. The SoC evolution, as shown in Figure 7-5(b), shows that the ESS achieved the SoC^{\max} limit during the lower electricity tariff, before 07:00 (14 half hours) taking into account the ESS efficiency of 0.9, and discharged during the high electricity tariff period where the SoC reached a value near the SoC^{\min} limit, 10 kWh. The SoC evolution shows that the controller model can charge

and discharge the storage device during the specified electricity tariff periods in order to minimise the peak demand, as shown in Figure 7-5(a) for the 12th and 29th half hours.

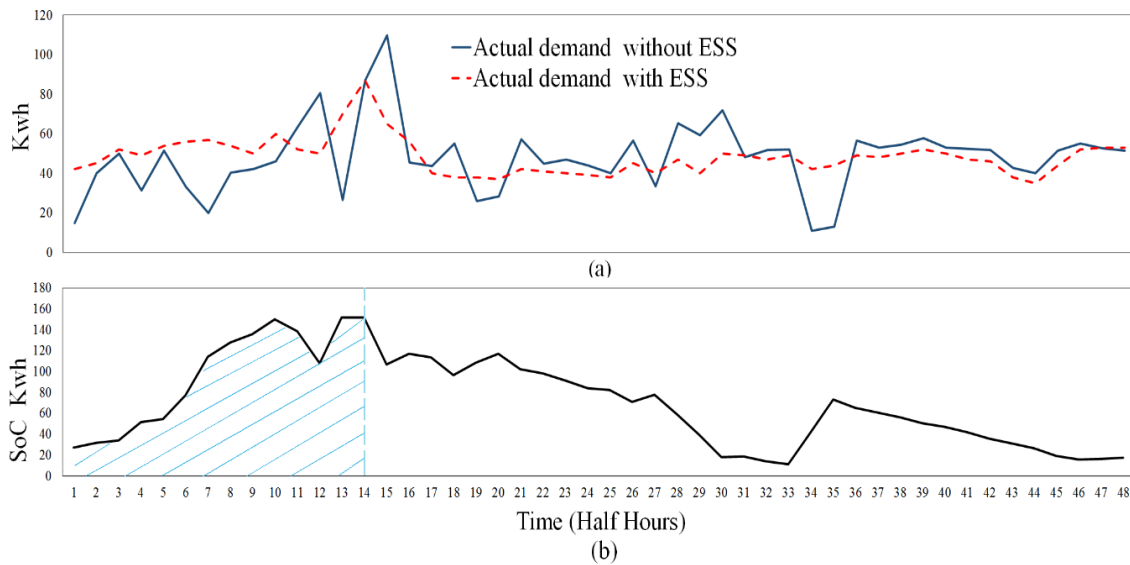


Figure 7-5: (a) The network of RTG cranes demand profile with and without an Energy storage System (for day 5 of test set); (b) The State of Charge (SoC) of the ESS throughout the day (day 5 of test set) with shade area for the low tariff period.

7.2.3 Economic Analysis.

In this section, the economic implications of the study are considered and analysed. A primary economic analysis has been carried out to investigate the commercial benefits of the ESS based on the location scenario and electricity tariff. There are a wide range of energy storage technologies that can be used in power system networks in order to increase the energy cost saving and reduce peak demand, as discussed in Chapter 2. Firstly, the main capital cost of ESS technologies have already been presented in Section 6.3.5 and Table 6-6 using a current average price of 200 \$/kWh (140 £/kWh) [144] [145] [146] and future expected price under 150 \$/kWh (105£/kWh) within the next 10 years [141] [142]. In this section, the SoC^{min} and ESS efficiency has been modified from 0 kWh and 100%, respectively, as in Section 6.3.5 to 10 kWh and 90%, respectively, to present the effect of efficiency and losses on the cost. Hence, the overall price for the ESS will have increased compared to Section 6.3.5. Figure 7-6 presents the annual electricity energy cost savings for this chapter proposed control strategies. The percentage of annual cost saving is calculated based on the average daily substation demand [19], the electricity tariff price and the average daily shifted energy. For example, the SMPC

controller can achieve an annual electricity bill saving of around 7.87%, 7.99% and 5.84% for scenario 1, scenario 2 (option 1) and scenario 2 (option 2), respectively. In scenario 1, the ESS location near the cranes allows a reduction in the required capacity rating of the electrical infrastructure (substation and cables), an extra economic and technical benefit compared to scenario 2. In contrast, the central ESS, scenario 2, will require the full capacity rating of the substation and the cables to deliver the expected crane demand.

Additionally, Table 7-6 shows a comparison analysis for the energy cost saving for the ESS location scenarios, as presented in Table 7-4. The viability analysis includes: the annual cost saving, Internal Rate of Return (IRR), Net Present Value (NPV), as described by Equation (6-6), and the payback period. The results have been calculated using the ESS parameters shown in Table 5-6 and a discount rate equal to 3% [147] [148]. The results indicate that the SMPC controller option is the most economically profitable with a payback period of just over 15 years, an IRR greater than 3% and a positive NPV value for ESS scenario 2 (option 1). The payback period for the SMPC and MPC controller options are less than 18 years for all ESS scenarios. The SMPC strategy is the most profitable option compared to the MPC and set-point (S.P) control for all ESS options and is economically profitable with an IRR of up to 3.3% due to the highest annual cost saving. The viability results analysis also shows that the SMPC control option can be cost-effective for all ESS scenarios in the cases when the price of batteries systems are under 140 £/kWh and an IRR equal to 2%. In general, the increase in the overall capital cost of an ESS in this section compared to Section 6.3.5, due to changes in energy efficiency and SOC^{min} terms, reduces the economic feasibility for the MPC and the set-point control strategies, for the data given. However, the MPC controller can be profitable in the cases where the discount rate is neglected. The Port of Felixstowe handles and operates more than 4 million twenty-foot container equivalent units (TEUs) every year, by running 85 RTG cranes continuously, it is only non-operational for maintenance, and work up to 24 hours daily with two work shifts for 362 days a year [22]. This introduces a large energy consumption at port and also a significant energy cost saving scenario by using a central ESS to feed a greater number of cranes similar to option 2.

Table 7-6: The ESS viability results for the different control strategies and all ESS location scenarios.

| | Annual cost saving (K £) | | | NPV (K £) | | | IRR (%) | | | Payback period (years) | | |
|--------------------------|--------------------------|------|------|-----------|------|------------|---------|-----|------------|------------------------|------|-------------|
| | S.P | MPC | SMPC | S.P | MPC | SMPC | S.P | MPC | SMPC | S.P | MPC | SMPC |
| Scenario 1 | 1.08 | 1.52 | 1.64 | -9.9 | -3.5 | -2.0 | -1.9 | 1.5 | 2.2 | 24.6 | 17.5 | 16.2 |
| Scenario 2 (option 1) | 1.15 | 1.59 | 1.68 | -8.0 | -0.6 | 0.8 | -0.8 | 2.7 | 3.3 | 21.9 | 15.8 | 15.1 |
| Scenario 2 (option 2) | 0.95 | 1.10 | 1.20 | -4.7 | -1.8 | -0.3 | 0.1 | 1.9 | 2.8 | 19.8 | 17.1 | 15.8 |

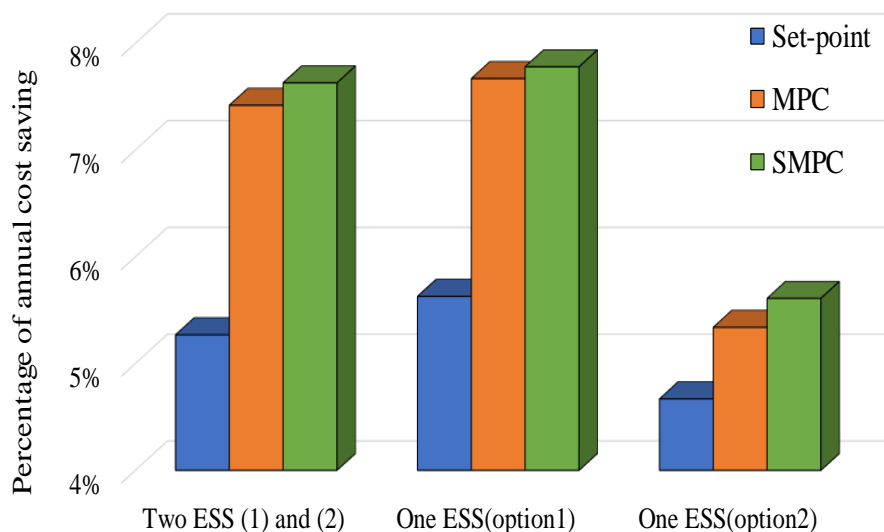


Figure 7-6: The percentage of annual electric energy cost saving for different controller algorithms for a network of electrified RTG cranes equipped with an ESS.

7.3 A Comparison of the ESS Control Strategies

The ESS control strategies results, in the previous section, present and compare the potential benefits of each storage control algorithm in terms of energy costs and peak demand. In this section, other criteria will be analysed, that relate to the main characteristics of the control model and the sensitivity with respect to model parameters and crane demand behaviour. In addition, to compare the proposed ESS controllers in this thesis, the difficulties of design and implementation of these controllers are presented.

7.3.1 *Set-point Controllers*

Section 5.2.2 presented and described how the set-point controller is developed to reduce the peak demand for a network of RTG cranes connected to an ESS. The set-point controller compares the network demand measurement to a reference demand value to decide when to charge and discharge the storage device. When the crane demand is under the reference demand point, the storage will start charging and when the demand is above the reference value, the ESS will discharge and result in reduction in demand. In the ESS performance results, in Section 7.1, the set-point control strategy showed a peak reduction equal to 23.8%. This result means the set-point controller has the lowest performance compared to the other proposed optimal controllers, in this case the optimal controllers using an accurate forecast model (with forecast errors up to MAPE 17%). The set-point controller works without any future knowledge about the demand, which will increase the possibility of operating the ESS when it is unnecessary and thus fail to reduce the significant peak points during the day. The situation changed when inaccurate forecast models were used, where the set-point controller outperformed both the MPC and optimal energy management controller. This is mainly because the set-point controller does not rely on the future demand knowledge unlike the other proposed receding horizon controllers, especially with forecasts errors up to a MAPE of 30%. These results emphasise the importance of having an accurate forecast to implement an optimal ESS controller.

The reference value, as the main parameter, in a set-point controller is typically specified based on the historical data or the network constraints. In a specific case study, discussed in Section 5.5.2, two set-points were used (30 kWh and 40 kWh), to show the impact of selecting the set-point value on the peak demand. The example results show that the ESS can achieve peak reduction by 15% and 23% for the set-points (30 kWh and 40 kWh), respectively. The method in both scenarios showed a peak demand reduction, but any variation in reference demand has a large effect on this control model performance. Thus, the set-point control strategy for the network of cranes is highly susceptible to variations in control parameters and the crane demand behaviour. The demand reference value needs to be calculated and readjusted to the crane and its activity, especially with the considerable impact of the human factor on demand and the highly volatile demand behaviour. This increases the difficulties of tuning this control model, due to the extreme sensitivity in choosing a reference value.

Another aspect is the on-line computational costs of the controller. The set-point controller is widely used in industry, energy and crane applications, and there is no problem running this controller with the on-line measurement and hence no heavy computational effort is required. The limitation of the set-point controller can be avoided by increasing the complexity of this control system. The next subsection presents the optimal controller based on load forecasting, which masks the complexity under a simple choice of the cost function.

7.3.2 Optimal Controllers Based on Load Forecasting

The literature shows the significance of forecasting the LV demand to improve the energy performance on the electrical distribution network through the optimal and receding horizon controllers of an ESS. The receding horizon control algorithms allow use of the updated forecast and network model data for each time step to generate the ESS control decisions. In general, these controllers aim to increase the benefits by using a specific cost function. The rolling forecast models can update the control process and thus minimise the impact of the forecast error and crane demand behaviour on the storage performance. The forecast model, presented in Chapter 4, provides the future estimates of the crane demand, which the optimal controller uses to pre-calculate the ESS operation trajectory. The results of the MPC and SMPC control strategies show increased energy cost savings and peak demand reduction, compared to set-point control. The receding horizon is an important parameter required in the MPC and SMPC algorithms. The large horizon size increases the computational cost, but also increases the possibility of reducing the main peak demands which occur later in the day. On the other hand, the small horizon window has less computational cost but will increase the possibility of using the control on reducing the non-critical peak load over the day time. The horizon size for the receding horizon controller was investigated in Chapter 5.

Furthermore, to treat the highly stochastic crane demand behaviour and uncertainty in the forecasts, an SMPC solved via dynamic programming was developed. The DP is a powerful tool to solve different types of optimisation and find a global solution. A stochastic optimisation controller based on DP was used effectively to solve the energy optimisation problem. The size of the increment of the discretised value (discretised resolution) in the interpolation process is the primary parameter required in the DP model. The discretised value for the SMPC controller has been investigated in Section 6.3 and it showed that that the percentage peak reduction increases as the discretised value decreases, stabilising after it is sufficiently small (0.5). The

receding horizon controller requires an updating forecast demand profile and optimal calculations every time step to create a rolling ESS optimal operation schedule. Therefore, the receding horizon requires more effort to tune compared to the set-point control. In addition, the receding horizon controllers require more technical skills and training processes to implement compared to set-point control, which is widely used and tested in port energy saving applications. However, the MPC and SMPC controllers are not as sensitive or determined by choice of reference values compared to the set-point controller. The receding horizon controller is nowadays widely used in smart grids and energy applications. Generally, the cost function for energy, peak demand and costs in a real application is usually pre-defined and commonly known. The receding horizon controller uses the updated forecast profiles, the new network of crane's model data and the ESS constraints for each time step in the cost function, to generate the optimal ESS operation schedule. These variables require a calculation process with a higher computational cost compared to the set-point control. Furthermore, the SMPC needs more effort for tuning and higher computational cost compared to the MPC. On the other hand, the updated data process for the crane, ESS and load forecast models in MPC and SMPC controller give an improved reduction in the significant peaks over the full day horizon. The extra information that becomes available in each horizon helps to improve the controllers and forecast model performance and increase the peak reduction due to the forecast error correction. The receding horizon controllers through the load forecasts capture the evening or late peaks over the 24 hours period, which allows the ESS to charge during low demand period and avoid creating sudden increase demand. In this thesis, the MPC investigated in Chapter 5 as main controller, due to is less complex and computationally less expensive compared to the SMPC, and therefore it can be more easily incorporated into business.

7.3.3 A Comparison Summary

A summary table of the main advantages and disadvantages of the proposed control strategies in this thesis, taking into consideration the characteristics of each controller discussed in this chapter, is presented in Table 7-7.

Table 7-7: A comparison for the advantages and disadvantages of each control technique.

| Control model | Advantages | Disadvantages |
|---------------|------------------------------------------------------------------------------------------------------------------------------------------------------------------------------------------------------------------------------------------------------------------------------------------------------------------------------------------------------|------------------------------------------------------------------------------------------------------------------------------------------------------------------------------------------------------------------------------------------------------------------------------------------------------------------------------------------|
| Set-point | <ul style="list-style-type: none"> • Easy to develop and implement. • Widely used in industry and port applications. • Low complexity. | <ul style="list-style-type: none"> • Very sensitive to changes in the parameters (set-point value). • Limited, as decided without any future knowledge. |
| MPC | <ul style="list-style-type: none"> • MPC is a closed loop, which minimises the impact of the forecast error on the performance. • Widely used in energy applications. • Best peak reduction and energy cost saving compared to optimal and set-point controllers, in case an accurate forecast model has been used. | <ul style="list-style-type: none"> • Requires rolling forecast model. • Requires new model information at every time step. • High computational cost. • Requires technical skills and training to implement the model. |
| SMPC | <ul style="list-style-type: none"> • Best peak reduction and energy cost saving compared to benchmark and MPC controllers. • SMPC is a closed loop, which minimises the impact of forecast error on the performance. | <ul style="list-style-type: none"> • High computational cost. • Requires rolling forecast model. • Requires new model information at every time step. • Requires a long tuning process. • Not easy to design and requires comprehensive knowledge of the system and demand behaviour. |

7.4 Summary

In this chapter, the analysis and comparison of the optimal control strategies proposed in this thesis have been presented. Different forecast data scenarios were used to evaluate the stability and robustness of the proposed controllers. Energy cost savings and peak demand reduction were calculated to present the performance of each control strategy. The MPC and SMPC controllers showed improvements over the standard control algorithm, the set-point controller. This improvement relies on the forecast model's accuracy, where it is a significant term to increase the potential peak reduction in optimal controllers and generally, more likely to have good peak reduction with more accurate forecasts [149]. Furthermore, each of the proposed control strategies has a number of advantages and drawbacks which were also discussed.

The performance of the ESS has been compared based on this specification and characteristics of the proposed control strategies. The set-point controller was too sensitive to the reference value compared to other control methods that were sensitive to the cost function and accuracy of the forecast profile. Overall, the SMPC outperforms other controllers and shows the best performance in terms of energy costs and peak reduction. The performance of the ESS for

different location scenarios and the economic implications of the study were considered and analysed, since no studies consider a central ESS which feeds more than a single electrified crane. The SMPC controller option was thus shown to be a potentially economically viable solution for peak demand reduction with much better performance compared to all other methods considered.

Chapter 8: Conclusions

This thesis has investigated and studied the control of energy storage systems on a network of RTG cranes to optimise energy cost savings and peak demand reduction based on load forecasting. This thesis as a whole includes several contributions to the knowledge and the literature in area of forecasting and ESS controlling for RTG cranes network. This chapter will collate the findings and contribution of this research to the problem statement that was presented in Chapter 1. This chapter, Chapter 8, is divided into four sections as follows: Section 8.1 presents the summary of the main finding of this research. Then, Section 8.2 presents the contributions to knowledge. Finally, Section 8.3 and 8.4 present and discuss the limitations of the research and future work.

8.1 Summary of the Thesis and Main Findings.

This thesis began by introducing the background of the research and describing the motivation behind this work. This work attempted to solve the problem statement, presented in Chapter 1, which can be summarised as follows:

- The research aimed to study and investigate how the ESS on the network of RTG cranes should be controlled, to reduce the electricity energy costs and achieve the maximum peak demand reduction.
- In order to control the ESS in port applications, it is essential to better understand the port network and the RTG crane energy demand behavior. To this end, this thesis studied the correlation between the current time demand, historical demand and different exogenous variables. This understanding is vital for operating power suppliers in the distribution network to reduce the energy costs and peak demand.
- This thesis aimed to predict the RTG crane demand and then investigate how the demand forecasts can help to improve the performance of the ESS controllers.
- In order to maximise the potential benefits of using ESS in a network of RTG cranes, minimise the unnecessary storage device monitoring, and treat the volatility and stochastic demand behaviour, the thesis investigated and studied different optimal

energy management strategies based on load forecasting for a network of RTG cranes equipped with an ESS.

The literature review, in Chapter 2, showed that the research into RTG cranes focussed on using conventional control strategies such as set-point control, to store recovered potential energy and regenerate it during the lifting of containers to increase energy savings and reduce gas emissions. It is clear from the literature that diesel cranes are the primary focus, and there have been no studies on energy saving for networks of electrified RTG crane using optimal power management strategies. The literature review showed the significance of predicting the demand accurately to achieve a higher ESS performance in LV applications. Chapter 3 introduced and investigated the electrical demand characteristics of the network of RTG cranes and studied the correlation in the time series of crane demand and with different exogenous variables. The understanding of the demand behaviour is vital for developing accurate load forecast models and ESS control algorithms. The analysis of the network of electrified RTG crane's demand to investigate the demand characteristics form the contribution to knowledge presented in Section 1.6, contribution I.

Chapter 4 implemented and tested a number of models to forecast the RTG crane day-ahead demand. Given the RTG crane demand series and the exogenous variables analysis in Chapter 3, Chapter 4 examined different input parameters options for the forecast model to increase the prediction accuracy. The results showed, there are a number of challenges facing load forecasting of RTG cranes. These challenges can be attributed to the fact there are no clear seasonality trends. The outliers to the linear relationship between the exogenous variable and crane demand were presented and explained by the unpredictability of human and highly volatile demand behaviour. The results of the evaluation methods of each forecast model showed that the ANN model which assumes there is knowledge of the exogenous variables in advance outperforms all other models. Furthermore, the results of the analysis showed that it is not recommended to estimate both exogenous variables in the forecast models. Moreover, the prediction models achieve an acceptable performance when estimating only one exogenous variable with more positive significant impact on forecast performance by using the accurate container gross weight. The results analysis in Chapters 4 show that understanding and forecasting the RTG crane energy demand behaviour, will provide ports with a key tool for the estimation of any financial or technical risk that may occur in the future resulting from demand

inconsistency and the electrification process for RTG cranes. It is important to note, until now there have been no studies that have discussed the prediction of RTG cranes' electric demand on the distribution network. This forms the contribution to knowledge, presented in Section 1.6, contributions II.

Motivated by the limited studies on using different optimisation methods and the lack of studies on using load forecasting to estimate the peak demand, this research presented novel optimal energy management strategies using forecasted electrified RTG crane demand profiles to control the ESS. The MPC and SMPC were developed in Chapters 5 and 6 in order to maximise the benefits of using the forecast demand profile. The objective function in previous controllers aimed to minimise the electric energy cost and increase peak demand reduction, considering the electricity price and the volatility behaviour of the crane demand. Furthermore, Chapter 5 presented benchmark control technique for ESS modelling on the network of RTG cranes. The set-point algorithm is used as a standard and common controller and is introduced in Chapter 5 as a benchmark control algorithm. The results showed that load forecasting help to improve the control performance compared to the set-point control.

As discussed in the literature review, forecast error and uncertainty have a significant impact on MPC energy storage control algorithms [28] [46] [49]. Due to the highly volatile and less predictable behaviour of RTG crane demand and high level of uncertainty in forecast error, the Stochastic MPC controller in Chapter 6 was developed. The SMPC controller attempted to take into account the crane demand volatility and thus improve the ESS performance. In this chapter, the SMPC controller was implemented via a Dynamic Programming (DP) algorithm to solve the energy optimisation problem through a backwards calculation. The SMPC algorithm, presented in Chapter 6, outperformed each of the comparable control techniques developed, in this thesis, for an ESS in a network of cranes. The results in Chapters 5 and 6 are the contribution to knowledge presented in Section 1.6, contribution III.

This thesis showed that the ESS control algorithms can be improved by considering the future demand impact on present time control decisions. The research, in Chapter 7, presented a detailed analysis and comparison of the optimal control strategies by using different forecast data scenarios to evaluate the stability and robustness of the proposed controllers. Furthermore, Chapter 7 presented an optimal control method with perfect future knowledge and an ideal ESS

model based on set-point control as a benchmark control technique for the ESS on a network of RTG cranes. The results of the MPC and SMPC controllers showed improvements over the standard control algorithm. This improvement relies on the forecast model's accuracy. Unlike the control strategies in the literature that only focused on energy saving at a single crane, this research investigated using optimal controllers based on load forecasting to decrease the electricity bills and peak demand for a network of two RTG cranes connected to a central ESS. The performance of the ESS for different location scenarios and the economic implications of the study were considered and analysed. The SMPC and MPC controller options are potentially economically viable and achieve the highest peak reduction compared to the set-point and optimal energy management controller.

8.2 Contributions to Knowledge

The literature review, Chapter 2, presented the past and current literature on the control techniques of an ESS in an LV distribution networks and RTG crane systems, to support the research problem statement in Section 1.4. Through the literature evaluation, a number of the gaps in the literature were identified, which required further investigation, and which could be beneficial for the industry sector, ports, and the research community. This thesis aimed to fill the gap in the literature in several novel aspects that are summarised as follows:

- I. This research has provided an analysis of the network of electrified RTG cranes demand under a real operation time period and has identified the correlations in the historical demand and the exogenous variables. This analysis has helped to fill the gap and lack of understanding of the network of RTG cranes energy demand behaviour. It can also be used as a tool to develop power generation strategies, reduce the environmental effects of gas emissions, peak demand problems, and energy costs.
- II. This research has provided an approach to estimating the exogenous variables (number of crane moves and container gross weight). This estimation has used to examine the impact of the exogenous variables estimation on the forecast model's performance. An accurate forecast is a practical solution for energy management system problems such as load shedding, peak demand, and electrical infrastructure development by improving the understanding of load behaviour. In addition, the research has presented a novel use of forecast models to generate future demand profiles for an electrified RTG crane and network of electrified RTG cranes

(substation demand) for one-day ahead. The prediction demand model is a key role in LV network planning and energy markets. Unlike the low voltage demand application, the electrified RTG crane demand behaviour is highly volatile and less predictable due to the effect of human actions (crane driver) on the crane demand, and the lack of clear seasonality or patterns. Further discussion and clarification of this can be found in Chapter 3.

- III. A Model Predictive Controller (MPC) and Stochastic MPC for network of RTG cranes connected to energy storage device were presented in Chapters 5 and 6, respectively. Unlike controllers found in the literature review, e.g. set-point controls that tend to consider only a single RTG crane system and neglect the forecast algorithm as inputs to improve the ESS efficiency, this research presented a receding horizon controller aims to decrease the electricity energy costs and achieve maximum possible peak reduction. This model was successful by taking into account the highly volatile demand behaviour and uncertainty in the crane demand. For example, the SMPC shows an improvement in the percentage of peak demand reduction by 36.4% and 20.3% compared to the set-point control and the optimal management system, respectively. The performance results, in Chapters 5, 6 and 7, show that the performance of proposed control algorithms is dependent on the forecast model accuracy and the horizon window size. On a specific example the Stochastic MPC algorithm, presented in Chapter 7, outperforms both the set-point and the MPC controllers.
- IV. The energy storage performance is investigated for a network of two RTG cranes at different location scenarios to give sea ports an initial indicator regarding the possible location of an ESS in line with economic evaluation analysis, unlike the studies in the literature review, which have often only investigated the energy savings in a single RTG crane system.

8.3 Limitations of the Research

The presented research, has a number of limitation, which are discussed further here. Firstly, the energy storage model is relatively simple and has been modelled without taking into account the efficiency and the realistic non-linear behaviour of the storage system. This simplicity limits the scope of this work when simulating the ESS control strategies for an actual

storage device. However, this limitation is in line with similar works in the literature for LV network application and diesel RTG crane demand where simpler energy storage topologies are used (see sections 2.2, 5.1.1 and 7.2).

Secondly, the performance evaluation results for the control strategies are driven by the given demand data used throughout the project. In addition, the forecast models and demand analysis section can not fully evaluate the annual seasonality of the crane demand due to the lack of annual data. Therefore, these results and the analysed data sets are limited by the data collected. However, the number of simulations generated in this thesis for different forecast profile scenarios including the varying characteristics of the crane demand covered for normal operation days in different time periods have been shown to be valid for two different cranes demand data sets. Furthermore, due to the non-smooth behaviour of the RTG crane demand and the lack of seasonality or trends over the time series, the long time series data is expected to have negligible effect on the forecast and ESS control results presented. In this thesis, the testing period 17 days data allows us to evaluate the ESS controllers over three different time periods and test the transferability of the model trained on one crane to other cranes with the same specifications

The results are limited by the lack of detailed distribution electrical network model parameters such as the thermal constraints of the network cables. Simulating the ESS control strategies in preparation for the deployment of a realistic distribution network model, will allow a greater understanding of the relationship between the voltage and current of the network and the peak demand. As discussed in Section 1.2.3, the ESS can play different roles on the power network to support the conventional network and postpone or reject the need for electrical infrastructure reinforcement and one of them is the voltage and frequency control. The limitations of the thesis presented in this section form the basis of the future work discussed in the following section.

8.4 Future Work

Based on the limitations, presented in the previous section, and experience gained, this section contains potential future research steps:

- **Energy storage system:** Throughout this work, a simple ESS model has been used, as presented in Section 5.1. This storage model is similar to research in the literature on

LV network applications and RTG crane system where simpler energy storage topologies have been used (see section 2.2). In this ESS, There are a number of assumptions that could be reconsidered. For instance, the efficiency of the energy storage device in the real world is not 100% due to energy losses and leakage, as a result it would be worth including the losses terms in Equation (5-3). In addition to the leakage, the energy output of the ESS is affected by the external temperature. Also, in an actual ESS, the SoC has a linear charging relationship between 10% and 90% of SoC, where it requires a longer time to empty or charge the remaining 10% of the storage capacity. Therefore future simulations will need to incorporate this information provided by the management system. The future work for an actual energy storage model requires a more detailed information such as optimal ESS size, efficiency, leakage and temperature limitations, and future control algorithms will need to include such information from the storage management system. These requirements could be added as new constraints for the optimisation problem, and the simulation results could be compared to the original model used in this thesis. This comparison could help to understand the impact and the necessity of the extra details of the ESS.

- **Distribution Network Model:** Integrating the control strategies presented in this work to investigate the impact of the models on voltage, current and other electrical network parameters requires a more accurate network model. The accurate network model will allow the study into the impact of the storage device and control algorithms on the network equipment. Also, it will allow the Active Front End (AFE) converter to be incorporated into the network model, AFE is expected to have a significant impact on the energy saving performance of the network through the bi-directional capabilities to regenerate the energy recovered into the network. This future work will be important before the proposed controllers can be applied to the actual network system.
- **Forecasts:** the forecast demand profiles were used in both the MPC and SMPC controllers, as discussed in Chapters 5 and 6. Currently, ANN and ARIMA forecasts have been developed to be incorporated into the ESS control strategies by generating a future half hourly demand profile for up to a day ahead. The future work will target the forecasting of the power of the RTG crane system for the real-time duty cycle with higher resolution data, using the forecast models presented in this thesis. This future work will provide the necessary information to study the ESS control algorithms

performance with actual energy storage device and network models, as previously discussed.

- **Higher resolution data:** This work has presented and tested control algorithms on half hourly data. The half hourly RTG crane's electric demand represents the average demand over the half-hour period. In general, the cranes demand behaviour on the electrical distribution network changes at a sub-second resolution. The high resolution of the RTG cranes demand profiles used is expected to have a significant effect on the performance of the ESS control algorithm. The high data resolution will include a larger number of time steps within the same window size in the real-time algorithms, which will introduce more computational costs in the forecast and control algorithms. Furthermore, it is expected that sea ports will have smart meters with half hourly resolution for electricity billing purposes, therefore without additional costs for high-resolution substation monitoring, the prediction will remain at a half hourly resolution. In this thesis, the energy price parameter at the Port of Felixstowe (PoF), will require a horizon size equal to 24 hours (48 half hours) to utilise the deviation of electricity energy price over a full day. Since the peak demand can occur at any time of the day, a horizon size equal to 24 hours is required to determine the significant daily peaks. For the ESS topology, the resolution of the demand profiles is likely to be dependent on the main role and aim of the ESS. For instance, an ESS used to reduce voltage fluctuations will require a higher resolution demand profile, since the small voltage deviation can have a high impact on the distribution network. On the other hand, an ESS used for electricity costs and peak demand reduction, similar to our case, will use lower resolution data as the peak demand will have less impact on the thermal constraints of the distribution network, where the distribution network infrastructure (cables and substation) can work outside the operating specifications for a longer period. Furthermore, electricity bills are typically calculated based on a low resolution (half or one hour).

References

- [1] World Shipping Council, “Trade Statistics,” [Online]. Available: <http://www.worldshipping.org/about-the-industry/global-trade/trade-statistics>. Accessed 2 5 2017.
- [2] World Shipping Council, “Ports,” [Online]. Available: <http://www.worldshipping.org/about-the-industry/global-trade/ports>. Accessed 2 5 2017.
- [3] International Maritime Organisation, “Statistical Resources-UNCTAD Review of Maritime Transport,” [Online]. Available: http://unctad.org/en/PublicationsLibrary/rmt2016_en.pdf. Accessed 2 5 2017.
- [4] H. Yu, Y. Ge, J. Chen, L. Luo, C. Tan and D. Liu, “CO₂ emission evaluation of yard tractors during loading at container terminals,” *Transportation Reserch Part D*, vol. 53, pp. 17-36, 2017.
- [5] J. Mach, E. Proano, and K. Brown, “Impacts of electric rubber-tired gantries on green port performance,” *Research in Transportation Business & Management*, vol. 8, pp 67-76, 2013.
- [6] Trans-European Transport Network, “Report on Port Container Terminals Energy Profile,” *Green Cranes*, 2013. [Online]. Available: <http://www.greencranes.eu/M2Report.pdf>.
- [7] S. Pietrosanti, W. Holderbaum and V. Becerra, “Optimal Power Management Strategy for Energy Storage with Stochastic Loads,” *Energies*, vol. 9, 175, 2016.
- [8] Kalmar Industries, “E-One2,” *Cargotech, Tampere*. [Online]. Available: <https://www.kalmargloal.com/equipment/rtg-cranes/>. Accessed 15 5 2017.
- [9] Control Techniques, “Control Techniques RIS.GA. System,” Emerson Industrial Automation, 2008.
- [10] Port of Felixstowe, “The Port of Felixstowe commissions greener electric rubber tyred gantry cranes 2014,”. [Online]. Available: <https://www.portoffelixstowe.co.uk/press/news-archive/the-port-of-felixstowe-commissions-greener-electric-rubber-tyred-gantry-cranes/>. Accessed 2 8 2018.

-
- [11] H. Ibrahim, A. Ilinca and J. Perron, “Energy storage systems characteristics and comparisons,” *Renewable and Sustainable Energy Reviews*, vol 12, issue 5, pp 1221–1250, 2008.
- [12] H. Ibrahim, A. Ilinca and J. Perron, “Comparison and Analysis of Different Energy Storage Technologies Based on their Performance Index,” in *IEEE Canada Electrical Power Conference*, Montreal, 2007.
- [13] S. M. Lukic, J. Cao, R. C. Bansal, F. Rodriguez and A. Emadi, “Energy Storage Systems for Automotive Applications,” *IEEE Transactions on Industrial Electronics*, vol. 55, no. 6, pp. 2258-2267, 2008.
- [14] X. Luo, J. Wang, M. Dooner and J. Clarke, “Overview of current development in electrical energy storage technologies and the application potential in power system operation,” *Applied Energy*, vol 137, pp 511–536, 2015.
- [15] B. P. Roberts and C. Sandberg, “The role of energy storage in development of smart grids,” *Proceedings of the IEEE*, vol. 99, no. 6, pp. 1139-1144, 2011.
- [16] W. Niu, X. Huang, F. Yuan, N. Schofield, L. Xu, J. Chu and W. GU, “Sizing of Energy System of a Hybrid Lithium Battery RTG Crane,” *IEEE Trans. Power Electron*, vol 32, pp 7837-7844, 2017.
- [17] N. Zhao, N. Schofield, W. Niu, “Energy Storage System for a Port Crane Hybrid Power-Train,” *IEEE Trans. Transp. Electrification*, vol 2, pp 480-492, 2016.
- [18] M. Antonelli, M. Ceraolo, U. Desideri, G. Lutzemberger, and L. Sani, “Hybridization of Rubber Tired Gantry (RTG) Cranes,” *J. Energy Storage*, vol 12, 186–195, 2017.
- [19] V. Papaioannou, S. Pietrosanti, W. Holderbaum, V. Becerra, R. Mayer, “Analysis of Energy Usage for RTG Cranes,” *Energy*, vol 125, pp 337–344, 2017.
- [20] Port of Felixstowe, Hutchisonport portf Felixstowe [Online]. Available: <https://www.portoffelixstowe.co.uk/#/about>. Accessed 2 5 2018.
- [21] J. Monios, “Port governance in the UK: Planning without policy,” *Research in Transportation Business & Management*, vol. 22, pp. 78-88, 2017.
-

-
- [22] Port of Felixstowe, "Ship2shore magazine No 29," [Online]. Available: <https://www.portoffelixstowe.co.uk/press/>. Accessed 20 1 2018.
- [23] S. Gyamfi, S. Krumdieck, and T. Urmee, "Residential peak electricity demand response highlights of some behavioural issues," *Renewable and Sustainable Energy Reviews*, vol. 25, pp. 71–77, 2013.
- [24] H. Saadat, "Power System Analysis," Third Edition. PSA publishing. ISBN: 978-09845438-0-9, 2010.
- [25] Z. Sun, L. Li, M. Fernandez and J. Wang, "Inventory control for peak electricity demand reduction of manufacturing systems considering the trade-off between production loss and energy savings," *Journal of Cleaner Production*, vol. 82, pp. 84–93, 2014.
- [26] L. Zhang, Z. Li, C. Wu, and S. Ren, "Online Electricity Cost Saving Algorithms for Co-Location Data Centers," *IEEE Journal On Selected Areas In Communications*, vol. 33, no. 12, 2015.
- [27] L. Nicholls, S. Strengers, "Peak demand and the 'family peak' period in Australia: Understanding practice (in) flexibility in households with children," *Energy Research and Social Science*, vol. 9, pp. 116–124, 2015.
- [28] Y. Zhang, B. Liu, T. Zhang, and B. Guo, "An Intelligent Control Strategy of Battery Energy Storage System for Microgrid Energy Management under Forecast Uncertainties." *International Journal of Electrochemical Science*, vol. 9, 2014.
- [29] A. Masoum, S. Deilami, P. Moses, M. Masoum, and A. Abu-Siada, "Smart load management of plug-in electric vehicles in distribution and residential networks with charging stations for peak shaving and loss minimisation considering voltage regulation," *IET Generation, Transmission and Distribution*, doi: 10.1049/iet-gtd.2010.0574, ISSN 1751-8687, 2010.
- [30] P. Cottone, S. Gaglio, L. Re, and M. Ortolani, "User activity recognition for energy saving in smart homes," *Pervasive and Mobile Computing*, vol 16, pp. 156–170, 2015.
- [31] J. Widen, and E. Wackelgard, "A high-resolution stochastic model of domestic activity patterns and electricity demand," *Applied Energy*. vol. 87, pp. 1880–1892, 2010.
-

-
- [32] Y. Strengers, "Peak electricity demand and social practice theories: Reframing the role of change agents in the energy sector," *Energy Policy*, vol. 44, pp. 226–234, 2012.
- [33] M. Rowe, T. Yunusov, S. Haben, W. Holderbaum, and B. T. Potter, "The Real-Time Optimisation of DNO Owned Storage Devices on the LV Network for Peak Reduction," *Energies*, vol. 7(6), pp. 3537–3560, 2014.
- [34] S. Kim, and S. Sul, "Control of Rubber Tyred Gantry Crane With Energy Storage Based on Supercapacitor Bank," *IEEE Transactions On Power Electronics*, vol. 21, no. 5, 2006.
- [35] M. Flynn, P. McMullen, and O. Solis, "Saving energy using flywheels," *IEEE Industry Applications Magazine*, vol. 14, issue: 6, 2008.
- [36] H. Hellendoorn, S. Mulder, and B. Schutter, "Hybrid Control of Container Cranes," *IFAC Proceedings Volumes*, vol. 44, pp. 9697–9702, 2011.
- [37] A. Hassan, L. Cipcigan, and N. Jenkins, "Optimal battery storage operation for PV systems with tariff incentives," *Applied Energy*, vol. 203, pp. 422-441, 2017.
- [38] A. Pena-Bello, M. Burer, M. Patel, and D. Parra, "Optimizing PV and grid charging in combined applications to improve the profitability of residential batteries," *Journal of Energy Storage*, vol. 13, pp. 58-72, 2017.
- [39] X. Wu, X. Hu, S. Moura, X. Yin, and V. Pickert, "Stochastic control of smart home energy management with plug-in electric vehicle battery energy storage and photovoltaic array," *Journal of Power Sources*, vol. 333, pp. 203-212, 2016.
- [40] Y. Riesen, C. Ballif, and N. Wyrsh, "Control algorithm for a residential photovoltaic system with storage," *Applied Energy*, vol. 202, pp. 78-87, 2017.
- [41] F. Vieira, P. Moura, and A. Almeida, "Energy storage system for self-consumption of photovoltaic energy in residential zero energy buildings," *Renewable Energy*, vol. 103, pp. 308-320, 2017.
- [42] F. Mohamed, and H. Koivo, "Online management genetic algorithms of microgrid for residential application," *Energy Conversion and Management*, vol. 64, pp. 562-568, 2012.
-

-
- [43] C. Hu, S. Luo, Z. Li, X. Wang, and L. Sun, "Energy Coordinative Optimization of Wind-Storage-Load Microgrids Based on Short-Term Prediction," *Energies*, vol. 8, pp. 1505-1528, 2015.
- [44] F. Garcia-Torres, L. Valverde, and C. Bordons, "Optimal Load Sharing of Hydrogen-Based Microgrids With Hybrid Storage Using Model-Predictive Control," *IEEE Transactions On Industrial Electronics*, vol. 63, No. 8, 2016.
- [45] S. Oh, S. Chae, J. Neely, J. Baek, and M. Cook, "Efficient Model Predictive Control Strategies for Resource Management in an Islanded Microgrid," *Energies*, vol. 10, 2017.
- [46] Z. Ji, X. Huang, C. Xu, and H. Sun, "Accelerated Model Predictive Control for Electric Vehicle Integrated Microgrid Energy Management: A Hybrid Robust and Stochastic Approach," *Energies*, vol. 9, 973, 2016.
- [47] M. Xiong, F. Gao, K. Liu, S. Chen, and J. Dong, "Optimal Real-Time Scheduling for Hybrid Energy Storage Systems and Wind Farms Based on Model Predictive Control," *Energies*, vol. 8, pp. 8020–8051, 2015.
- [48] D. Halamay, M. Antonishen, K. Lajoie, A. Bostrom, and T. Brekken, "Improving Wind Farm Dispatchability Using Model Predictive Control for Optimal Operation of Grid-Scale Energy Storage," *Energies*, vol. 7, pp. 5847–5862, 2014.
- [49] M. Maasoumy, M. Razmara, M. Shahbakhti, and A. Vincentelli, "Handling model uncertainty in model predictive control for energy efficient buildings," *Energy and Building*, vol. 77, pp. 377–392, 2014.
- [50] X. Wang, A. Palazoglu, and N. El-Farra, "Operational optimization and demand response of hybrid renewable energy systems," *Applied Energy*, vol. 143, pp. 324-335, 2015.
- [51] N. Holjevac, T. Capuder, N. Zhang, I. Kuzle, and C. Kang, "Corrective receding horizon scheduling of flexible distributed multi-energy microgrids," *Applied Energy*, vol. 207, pp. 176-194, 2017.
- [52] D. Zhu, and G. Hug, "Decomposed Stochastic Model Predictive Control for Optimal Dispatch of Storage and Generation," *IEEE Transactions on smart grid*, vol. 5, pp. 2044-2053, 2014.
-

-
- [53] B. Favre, and B. Peuportier, "Application of dynamic programming to study load shifting in building," *Energy and Buildings*, vol. 82, pp. 57-64, 2014.
- [54] K. Deng, Y. Sun, S. Li, Y. Lu, J. Brouwer, P. Mehta, M. Zhou, and A. Chakraborty, "Model predictive control of central chiller plant with thermal energy storage via dynamic programming and mixed-integer linear programming," *IEEE transaction on automation science and engineering*, vol.12, 2, 2015.
- [55] Z. Feng, W. Niu, C. Cheng, and X. Wu, "Optimization of hydropower system operation by uniform dynamic programming for dimensionality reduction," *Energy*, vol. 134, pp. 718-730, 2017.
- [56] Q. Wei, G. Shi, R. Song, and Y. Liu, "Adaptive dynamic programming -based optimal control scheme for energy storage systems with solar renewable energy," *IEEE transaction on industrial electronics*, vol. 64, 7, 2017.
- [57] Z. Song, H. Hofmann, J. Li, X. Han, and M. Ouyang, "Optimization for a hybrid energy storage system in electric vehicles using dynamic programming approach," *Applied Energy*, vol. 139, pp.151-162, 2015 .
- [58] S. Xie, H. He, and J. Peng, "An energy management strategy based on stochastic model predictive control for plug-in hybrid electric buses," *Applied Energy*, vol.196, pp. 279-288, 2017.
- [59] H. He, M. Yan, C. Sun, J. Peng, M. Li, and H. Jia, "Predictive air-conditioner control for electric buses with passenger amount variation forecast," *Applied Energy*, <http://dx.doi.org/10.1016/j.apenergy.2017.08.181>.
- [60] C. Lee, and C. Ko, "Short-Term Load Forecasting Using Adaptive Annealing Learning Algorithm Based Reinforcement Neural Network," *Energies*, doi:10.3390/en9120987, 2016.
- [61] G. Aneiros, J. Vilar, and P. Raña, "Short-term forecast of daily curves of electricity demand and price," *International Journal of Electrical Power and Energy Systems*. vol 80, pp 96–108, 2016.
-

-
- [62] G. Papaioannou , C. Dikaiakos, A. Dramountanis, and P. Papaioannou, “Analysis and Modeling for Short- to Medium-Term Load Forecasting Using a Hybrid Manifold Learning Principal Component Model and Comparison with Classical Statistical Models (SARIMAX, Exponential Smoothing) and Artificial Intelligence Models (ANN, SVM): The Case of Greek Electricity Market,” *Energies*, doi:10.3390/en9080635 , 2016.
- [63] N. Huang, G. Lu and D. Xu, “A Permutation Importance-Based Feature Selection Method for Short-Term Electricity Load Forecasting Using Random Forest,” *Energies*, doi:10.3390/en9100767, 2016.
- [64] A. Pektas, and H. Cigizoglu, “ANN hybrid model versus ARIMA and ARIMAX models of runoff coefficient,” *Journal of Hydrology*. vol 500, pp 21–36, 2013.
- [65] S. Chadsuthi, M. Modchang, Y. Lenbury, S. Iamsirithaworn and W. Triampo, “Modeling seasonal leptospirosis transmission and its association with rainfall and temperature in Thailand using time-series and ARIMAX analyses,” *Asian Pacific Journal of Tropical Medicine*. vol 5, pp 539-546, 2012.
- [66] C . Bennett, R. Stewart, and J. Lu, “Autoregressive with Exogenous Variables and Neural Network Short-Term Load Forecast Models for Residential Low Voltage Distribution Networks,” *Energies*. doi:10.3390/en7052938, 2014
- [67] S. Barak, and S. Sadegh, “Forecasting energy consumption using ensemble ARIMA–ANFIS hybrid algorithm,” *International Journal of Electrical Power and Energy Systems*, vol 82, pp 92–104, 2016.
- [68] H. Cui, and X. Peng, “Short-term city electrical load forecasting with considering temperature effects: An improved ARIMAX model,” *Mathematical problems in engineering*, vol 2015, Article ID 589374, 2015.
- [69] S. Feuerriegel, S. Riedlinger, and D. Neumann, “Predictive Analytics for Electricity Prices Using Feed-ins From Renewables,” *Twenty Second European Conference on Information Systems*. ISBN 978-0-9915567-0-0, June 9-11, 2014.
- [70] M. Sun, , J. Li, C. Gao, and D. Han, “Identifying regime shifts in the US electricity market based on price fluctuations,” *Energy Policy*, vol 194, pp 658–666, 2017.
-

-
- [71] M. Amini, A. Kargarian, and O. Karabasoglu, “ARIMA-based decoupled time series forecasting of electric vehicle charging demand for stochastic power system operation,” *Electric Power Systems Research*. vol 140, pp 378–390, 2016.
- [72] B. Yogarajah, C. Elankumaran, and R. Vigneswaran, “Application of ARIMAX Model for Forecasting Paddy Production in Trincomalee District in Sri Lanka,” *3rd International Conference at the South Eastern University of Sri Lanka*, July 2013.
- [73] P. Box, M. Jenkins, and C. Reinsel,. “Time Series Analysis: Forecasting and Control,” Third Edition, Englewood Cliffs, NJ: Prentice Hall, pp.197-199 1994.
- [74] C. Lee, and B. Lin, “Application of Hybrid Quantum Tabu Search with Support Vector Regression (SVR) for Load Forecasting,” *Energies*. doi:10.3390/en9110873, 2016.
- [75] P. Duan, K. Xie, T. Guo, and X. Huang, “Short-Term Load Forecasting for Electric Power Systems Using the PSO-SVR and FCM Clustering Techniques,” *Energies*, doi:10.3390/en4010173, 2011.
- [76] X. Yan, and N. Chowdhury, “Mid-term electricity market clearing price forecasting utilizing hybrid support vector machine and auto-regressive moving average with external input,” *International Journal of Electrical Power and Energy Systems*, vol 63, pp 64–70, 2014.
- [77] N. Amjadi, and F. Keynia, “A New Neural Network Approach to Short Term Load Forecasting of Electrical Power Systems,” *Energies*, doi:10.3390/en4030488, 2011.
- [78] L. Hernandez, C. Baladrón, J. Aguiar, B. Carro, A. Sanchez-Esguevillas, and J. Lloret, “Short-Term Load Forecasting for Microgrids Based on Artificial Neural Networks,” *Energies*. pp 1385-1408; doi:10.3390/en6031385, 2013.
- [79] A. Jalalkamali, M. Moradi, and N. Moradi, “Application of several artificial intelligence models and ARIMAX model for forecasting drought using the Standardized Precipitation Index,” *International Journal of Environmental Science and Technology*. vol 12, pp 1201–1210, 2015.

-
- [80] D. Montgomery, C. Jennings, and M. Kulahchi, "Introduction to Time Series Analysis and Forecasting -III," Published by John Wiley and Sons, New Jersey. Published simultaneously in Canada. ISBN 978-0-4 71-65397-4, 2014
- [81] M. Cerjan, M. Matijaš, and M. Delimar, "Dynamic Hybrid Model for Short- Term Electricity Price Forecasting," *Energies*. doi:10.3390/en7053304, 2014.
- [82] Y. Liang, D. Niu, M. Ye, and W. Hong, "Short-Term Load Forecasting Based on Wavelet Transform and Least Squares Support Vector Machine Optimized by Improved Cuckoo Search," *Energies*. doi:10.3390/en9100827, 2016.
- [83] H. Alfares, and M. Nazeeruddin, "Electric load forecasting: literature survey and of methods," *International Journal of Systems Science*. vol 33,pp 23-34, 2002.
- [84] J. Taylor, L. Menezes, and P. McSharry, "A comparison of univariate methods for forecasting electricity demand up to a day ahead," *International Journal of Forecasting*, doi:10.1016/j.ijforecast.2005.06.006, 2006.
- [85] C. Deb, F. Zhang, J. Yang, S. Lee, and K.Shah "A review on time series forecasting techniques for building energy consumption," *Renewable and Sustainable Energy Reviews*, vol. 74, pp. 902-924, 2017.
- [86] C. Bennett, R. Stewart, and J. Lu, "Forecasting low voltage distribution network demand profiles using a pattern recognition based expert system," *Energy*, vol 67, pp 200–212, 2014.
- [87] N. Amjady, and F. Keynia, "A New Neural Network Approach to Short Term Load Forecasting of Electrical Power Systems," *Energies* . doi:10.3390/en4030488, 2011.
- [88] S. Yuan, A. Kocaman, and V. Modi, "ABenefits of forecasting and energy storage in isolated grids with large wind penetration e The case of Sao Vicente," *Renewable Energy*, vol 105, pp 167-174, 2017.
- [89] A. Klingler, and L. Teichtmann, "Impacts of a forecast-based operation strategy for grid-connected PV storage systems on profitability and the energy system," *Solar Energy*, vol 158, pp 861-868, 2017.
-

-
- [90] M. Hossain, S. Mekhilef, M. Danesh, L. Olatomiwa and S. Shamshirband, "Application of extreme learning machine for short term output power forecasting of three grid-connected PV systems," *Journal of Cleaner Production*, vol 167, pp 395-405, 2017.
- [91] R. Bi, L. Wang and M. Ding, "An ANN-based Approach for Forecasting the Power Output of Photovoltaic System," in *Procedia Environmental Sciences*, pp 1308-1315, 2011.
- [92] P. Bacher, H. Madsen and H. Nielsen, "Online short-term solar power forecasting," *Solar Energy*, vol 83, pp 1772-1783, 2009.
- [93] S. Feuerriegel, S. Riedlinger and D. Neumann, "Predictive Analytics For Electricity Prices Using Feed-ins From Renewables," in *Proceedings of the European Conference on Information Systems (ECIS)*, 2014.
- [94] F. Oldewurtel, A. Parisio, C. Jones, D. Gyalistras, M. Gwerder, V. Stauch, B. Lehmann, and M. Morari, "Use of model predictive control and weather forecasts for energy efficient building climate control," *Energy and Buildings*, vol. 45, pp. 15-27, 2012.
- [95] T. Hilliard, L. Swan, M. Kavacic, Z. Qin and P. Lingras, "Development of a whole building model predictive control strategy for a LEED silver community college," *Energy and Buildings*, vol. 111, pp. 224-232, 2016.
- [96] M. Labidi, J. Eynard, O. Faugeroux, S. Grieu, "A new strategy based on power demand forecasting to the management of multi-energy district boilers equipped with hot water tanks," *Applied Thermal Engineering*, vol 113, pp 1366-1380, 2017.
- [97] Y. Zhang, T. Zhang, R. Wang, Y. Liu and B. Guo, "Optimal operation of a smart residential microgrid based on model predictive control by considering uncertainties and storage impacts," *Solar Energy*, vol. 122, pp. 1052-1065, 2015.
- [98] Y. Chae, R. Horesh, Y. Hwang and Y. Lee, "Artificial neural network model for forecasting sub-hourly electricity usage in commercial buildings," *Energy and Buildings*, vol 111, pp. 184-194, 2016.
- [99] J. Grant, M. Eltoukhy, and S. Asfour, "Short-Term Electrical Peak Demand Forecasting in a Large Government Building Using Artificial Neural Networks," *Energies*, doi:10.3390/en7041935, 2014.
-

-
- [100] C. Deb, L. Eang, J. Yang, and M. Santamouris, "Forecasting diurnal cooling energy load for institutional buildings using Artificial Neural Networks," *Energy and Buildings*, vol. 121, pp. 284–297, 2016.
- [101] Z. Liu, Q. Wu, A. Nielsen and Y. Wang, "Day-Ahead Energy Planning with 100% Electric Vehicle Penetration in the Nordic Region by 2050," *Energies*, vol. 7, pp. 1733-1749; doi:10.3390/en7031733, 2014.
- [102] E. Galván-López, T. Curran, J. McDermott and P. Carroll, "Design of an autonomous intelligent Demand-Side Management system using stochastic optimisation evolutionary algorithms," *Neurocomputing.*, vol. 170, pp. 270-285, 2015.
- [103] M. Alonso, H. Amaris, J. Germain and J. Galan, "Optimal Charging Scheduling of Electric Vehicles in Smart Grids by Heuristic Algorithms," *Energies*, vol. 7, pp. 2449-2475; doi:10.3390/en7042449, 2014.
- [104] M. Arias, and S. Bae, "Electric vehicle charging demand forecasting model based on big data technologies," *Applied Energy*, vol. 183, pp. 237-339, 2016.
- [105] M. Majidpour, C. Qiuand, P. Chu, H. Pota, and R. Gadh, "Forecasting the EV charging load based on customer profile or station measurement?," *Applied Energy*, vol. 163, pp. 134-141, 2016.
- [106] A. Poghosyan, D. Greetham, S. Haben, and T. Lee, "Long term individual load forecast under different electrical vehicles uptake scenarios," *Applied Energy*, vol. 157, pp. 699-709, 2015.
- [107] R. Hyndman, and G. Athanasopoulos, "Forecasting: principles and practice," [Online]. Available: <https://www.otexts.org/fpp>. ISBN 978-0-9875071-0-5 ,printed edition 2014.
- [108] Y. Jiang, X. Chen, K. Yu, and Y. Liao, "Short-term wind power forecasting using hybrid method based on enhanced boosting algorithm," *Journal of Modern Power System and Clean Energy*, vol. 5, pp. 126-133, 2017.
- [109] W. Hu, Y. Min, Y. Zhou, and Q. Lu, "Wind power forecasting errors modelling approach considering temporal and spatial dependence," *Journal of Modern Power System and Clean Energy*, vol. 5, pp. 489-498, 2017.
-

-
- [110] H. Liu, H. Tian, and Y. Li, "Comparison of two new ARIMA-ANN and ARIMA-Kalman hybrid methods for wind speed prediction," *Applied Energy*, vol. 98, pp. 415-424, 2012.
- [111] B. Amrouche, and X. Pivert, "Artificial neural network based daily local forecasting for global solar radiation," *Applied Energy*, vol. 130, pp. 333-341, 2014.
- [112] H. Torr , "Electricity futures prices: some evidence on forecast power at Nord pool," *Journal of Energy Markets*, vol. 2, pp. 3-25, 2009.
- [113] R. Mushtaq, "Augmented Dickey Fuller Test," *SSRN Journals*, electronic copy available at:<http://ssrn.com/abstract=1911068>, 2011.
- [114] S. Kolassa, "Combining exponential smoothing forecasts using Akaike weights," *International Journal of Forecasting*, vol. 27, pp. 238-251, 2011.
- [115] W. Holderbaum, "Application of Neural Network to Hybrid Systems With Binary Inputs," *IEEE Transactions on Neural Networks*, vol. 18, 2007.
- [116] S. Ryu, J. Noh, and H. Kim, "Deep Neural Network Based Demand Side Short Term Load Forecasting," *Energies*, doi:10.3390/en10010003, 2017.
- [117] G. L pez, and J. Tovar-Pescador, "Selection of input parameters to model direct solar irradiance by using artificial neural networks," *Energy*, vol. 30, pp. 1675-1684, 2005
- [118] W. Kramer, "Fractional integration and the augmented Dickey–Fuller Test," *Economics Letters*, vol. 61, pp. 269-272, 1998.
- [119] F. Wang, , Z. Mi, , S. Su, and H. Zhao, "Short-Term Solar Irradiance Forecasting Model Based on Artificial Neural Network Using Statistical Feature Parameters," *Energies*, p.p 1355-1370, doi:10.3390/en5051355, 2012.
- [120] S. Kalogirou, "Applications of artificial neural-networks for energy systems," *Applied Energy*, vol. 67, p.p 17-35, 2000.
- [121] L. Kaastra, and M. Boyd, "Designing a neural network for forecasting financial and economic series," *Neurocomputing*, vol. 10, p.p 215-236, 1996
-

-
- [122] L. Hernandez, C. Baladrón, J. Aguiar, L. Calavia, B. Carro, A. Sanchez-Esguevillas, and J. Lloret, "Artificial Neural Network for Short-Term Load Forecasting in Distribution Systems," *Energies*, pp.1576-1598; doi:10.3390/en7031576, 2014.
- [123] L. Hernandez, C. Baladrón, J. Aguiar, L. Calavia, B. Carro, A. Sanchez-Esguevillas, and J. Lloret, "Experimental Analysis of the Input Variables' Relevance to Forecast Next Day's Aggregated Electric Demand Using Neural Networks," *Energies*, pp. 2927-2948; doi:10.3390/en6062927, 2013.
- [124] F. Ziel, and B. Liu, "Lasso estimation for GEFCom2014 probabilistic electric load forecasting," *International journal of forecasting*, vol.32, pp. 1029-1037, 2016.
- [125] J. Munkhammara, J. Widna, and J. Rydnb, "On a probability distribution model combining household power consumption, electric vehicle home-charging and photo-voltaic power production," *Applied Energy*, vol.142, pp. 135-143, 2015.
- [126] UN Faq (2018) Verification of the gross mass of packed containers by sea. [Online]. Available: <https://www.gov.uk/government/publications/>. Accessed 10 March 2018.
- [127] International Maritime Organization (2018) SOLAS container mass verification requirements. [Online]. Available: <http://www.imo.org/en/MediaCentre/HotTopics/container>, Accessed 10 March 2018
- [128] R. McNown, and M. Wallace, "Cointegration Tests of the Monetary Exchange Rate Model for Three High-Inflation Economies," *Journal of Money*, vol. 26, pp. 396-411, 1994.
- [129] T. Nguyen, H. Yoo, and H. Kim, "Application of Model Predictive Control to BESS for Microgrid Control," *Energies* 2015, 8, 8798–8813, doi:10.3390/em8088798.
- [130] M. Moradzadeh, R. Boel, and L. Vandeveld, "Anticipating and Coordinating Voltage Control for Interconnected Power Systems," *Energies* 2014, 7, 1027–1047, doi:10.3390/en7021027.
- [131] J. Hu, and K. Cheng, "Predictive Control of Power Electronics Converters in Renewable Energy Systems," *Energies* 2017, 10, 515, doi:10.3390/en10040515.

-
- [132] L. Li, S. You, C. Yang, B. Yan, J. Song, and Z. Chen, "Driving-behavior-aware stochastic model predictive control for plug-in hybrid electric buses," *Applied Energy*, vol.162, pp. 868-879, 2016.
- [133] X. Wang, H. He, F. Sun, and J. Zhang, "Application Study on the Dynamic Programming Algorithm for Energy Management of Plug-in Hybrid Electric Vehicles," *Energies*, vol.8, pp. 3225-3244, 2015.
- [134] R. Dufo-López, E. Pérez-Cebollada, J. Bernal-Agustín, and I. Ignacio Martínez-Ruiz, "Optimisation of energy supply at off-grid healthcare facilities using Monte Carlo simulation," *Energy Conversion and Management*, vol.113, pp. 321-330, 2016.
- [135] J. Jung, Y. Cho, D. Cheng, A. Onen, R. Arghandeh, M. Dilek, and R. Broadwater, "Monte Carlo analysis of Plug-in Hybrid Vehicles and Distributed Energy Resource growth with residential energy storage in Michigan," *Applied Energy*, vol.108, pp. 3218-235, 2013.
- [136] L. Mendo, and J. Hernando, "A simple sequential stopping rule for Monte Carlo simulation," *IEEE Transaction Communication*, vol.54, pp. 231-241, 2016.
- [137] T. Nguyen, H. Yoo, and H. Kim, "Analyzing the Impacts of System Parameters on MPC-Based Frequency Control for a Stand-Alone Microgrid," *Energies* 2017, 10, 417, doi:10.3390/en10040417.
- [137] I. Batina, A. Stoorvogel, and S. Weiland, "Stochastic disturbance rejection in model predictive control by randomized algorithms," *The American control conference IEEE*, Arlington, USA, 2001.
- [138] O. Sundstrom, and L. Guzzella, "A generic dynamic programming Matlab function," *In: 2009 IEEE control applications, (CCA) & intelligent control, (ISIC), IEEE*, 2009. pp. 1625–1630.
- [139] V. Marano, G. Rizzo, and F. Tiano, "Application of dynamic programming to the optimal management of a hybrid power plant with wind turbines, photovoltaic panels and compressed air energy storage," *Applied Energy*, vol. 97, pp. 849-859, 2012.

-
- [140] A. Hooshmand, M. Poursaeidi, J. Mohammadpour, and H. Malki, "Grigoriads Stochastic model predictive control method for microgrid management," *Innovative Smart Grid Technologies (ISGT), IEEE PES*, Washington, DC, USA, 2012.
- [141] H. Yu, "A prospective economic assessment of residential PV self-consumption with batteries and its systemic effects: The French case in 2030," *Energy Policy*, vol. 113, pp. 673-687, 2018.
- [142] World energy council. World energy resources E-storage 2016. https://www.worldenergy.org/wp-content/uploads/2017/03/WEResources_E-storage_2016.pdf.
- [143] K. Gur, D. Chatzikyriakou, C. Baschet, and M. Salomon, "The reuse of electrified vehicle batteries as a means of integrating renewable energy into the European electricity grid: A policy and market analysis," *Energy Policy*, vol. 113, pp. 535-545, 2018.
- [144] Park, and P. Lappas, "Evaluating demand charge reduction for commercial-scale solar PV coupled with battery storage," *Renewable Energy*, vol. 108, pp. 523-532, 2017.
- [145] Y. Ru, J. Kleissl, and S. Martinez, "Storage size determination for grid-connected photovoltaic systems," *IEEE Transactions on Sustainable Energy*, vol. 4, pp. 68-81, 2013.
- [146] T. Hoff, R. Perez, and R. Margolis, "Maximizing the value of customer-sited PV systems using storage and controls," *Solar Energy*, vol. 81, pp. 940-945, 2007.
- [147] J. Steinbach, and D. Staniaszek,, "Discount rates in energy system analysis.," *Building Performance institute Europe BPIE*, 2015. Available online:http://bpie.eu/uploads/lib/document/attachment/142/Discount_rates_in_energy_systemdiscussion_paper_2015_ISI_BPIE.pdf
- [148] L. Abadie, "Valuation of Long-Term Investments in Energy Assets under Uncertainty," *Energies* 2009, 2, 738-768; doi:10.3390/en20300738.
- [149] T. Yunusov, S. Haben, T. Lee, F. Ziel, W. Holderbaum and B. Potter, "Evaluating the effectiveness of storage control in reducing peak demand on low voltage feeders," *CIREN* 2017, Galsgow, UK, PP. 1-5.
- [150] Vahle, "Port Technology" [Online]. Available: <https://www.vahleinc.com/porttechnology.html>, Accessed 25 5 2017.
-

-
- [151] Vahle, "Electrification of RTG cranes," [Online]. Available:https://vahle.com/fileadmin/user_upload/pdf/Broschueren/englisch/VAHLE_Port_eRTG.pdf.
- [152] W. Hong-lei, D. Wei, and C. Jain-Xin, "The Danamic Power Control Technology for the High Power Lithium Battery Hybrid Rubber-Tired Gantry (RTG) Crane," *IEEE Transactions on Industrial Electroinic* 2019, vol. 66, pp.132-140.
- [153] R. Godina, E. Roderigues, E. Pouresmaeil, J. Matias and J. Catalao, "Model predicitive control home energy management and optimization strategy with demand response," *Applied sciences* 2018, 8, doi:10.3390/app8030408.
- [154] J. Garriga and M. Soroush, "Model predicitive control tuning methods: Areview," *Industrial and engineering chemistry reserch* 2010, 49, pp 3505-3515
- [155] P. Jensen and J. Bard, "Dynamic programming models," *In Operations Research: Models and Methods*, Wiley, United state 2002, https://www.me.utexas.edu/~jensen/ORMM/instruction/pdf_supplements/dynamic_prog/dp_models.pdf
- [156] IME "Multimetering" [Online]. Available: <http://www.imeitaly.com/docs/NT680.pdf>.
- [157] I. Harrison, S. Pietrosanti, A. Luque, R. Mayer and W. Holderbaum, "Recording and analysing measurements from an RTG crane," *Measurment* 2018, 125, pp 284-293

Appendix A

Network of RTG cranes measurement system

The network of RTG cranes measurement system described in this section has been used in order to collect the required data to understand the RTG crane demand behaviour and find the correlation between the crane demand and the external variables such as container gross weight. This understanding is used to develop an accurate forecast model and investigate the benefits of using an ESS for a network of cranes.

Figure 7-4 presents the SLD for a network of electrified RTG cranes at the Port of Felixstowe, UK. The RTG cranes are connected to (11 KV/415V, 1.6 MVA) substation. The circuit breaker at low voltage side of substation, 415 V, is set at 1600 A. To measure the energy at each crane, the cranes at the Port of Felixstowe are installed with Nemo 96 HD meters, as seen in Figure A-1. The Nemo meters were programmed to give demand data at half hourly time resolution for monitoring and billing purposes. Furthermore, the metering system at the 11 KV side of the substation was not available. The metering system is connected via a Profibus to the port database that also provide the number of cranes moves and container gross weight through a vehicle booking system which is available with a date and half hour slot as part of the new SOLAS regulations [126] [127] for verified container weight.



Figure A- 1: Nemo 96 HD meter system [156].

In addition, the Port of Felixstowe agreed to upgrade the instrumentation system at a single RTG crane. The upgrading measurement system is to understand the power flow within the crane system and provide more information regarding power factor and the power dissipated in the dump resistor. This data helped to validate the RTG crane data (demand, container weight and number of moves) and understand the energy flow within the crane, as presented in Chapter 3. Figure A-2 presents the installed measurement system on the RTG crane. The new installed measurement system recorded the crane data via a Beckhoff and Programming Logic Computer (PLC) [157]. The line diagram of the Beckhoff PLC measurement system is displayed in Figure A-3, this system handles the information based on the following components[157]:

- The power measurement card, Beckhoff (EL3403), records the voltage, current and power factor on the three-phase side of the crane.
- The Beckhoff (EL3008) records the voltage and current data on the DC side of the crane.
- The Profibus interface between the Beckhoff and the RTG PLC system records the number of crane variables i.e spreader position, the container gross weight and time.
- The Beckhoff PLC is connected via an Ethernet cable to the Westermo router which allows the port to collect the data remotely.

The collected data is stored in the internal memory of the PLC for 6 hours as a Comma Separated Variable (CSV) file, due to the large size of the data and amount of files. Once each file is written, it is transferred to an external memory device, in this case a USB memory storage. The data file is then compressed into a ZIP file.

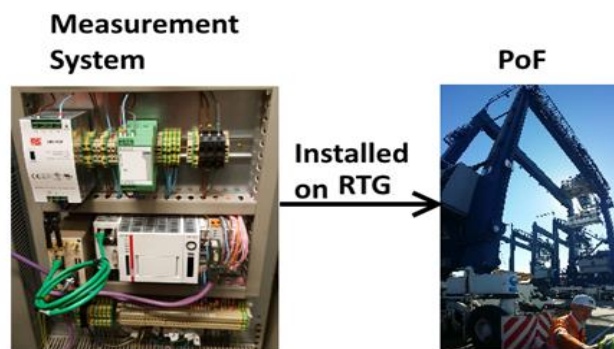


Figure A- 2: The RTG crane measurement system [157].

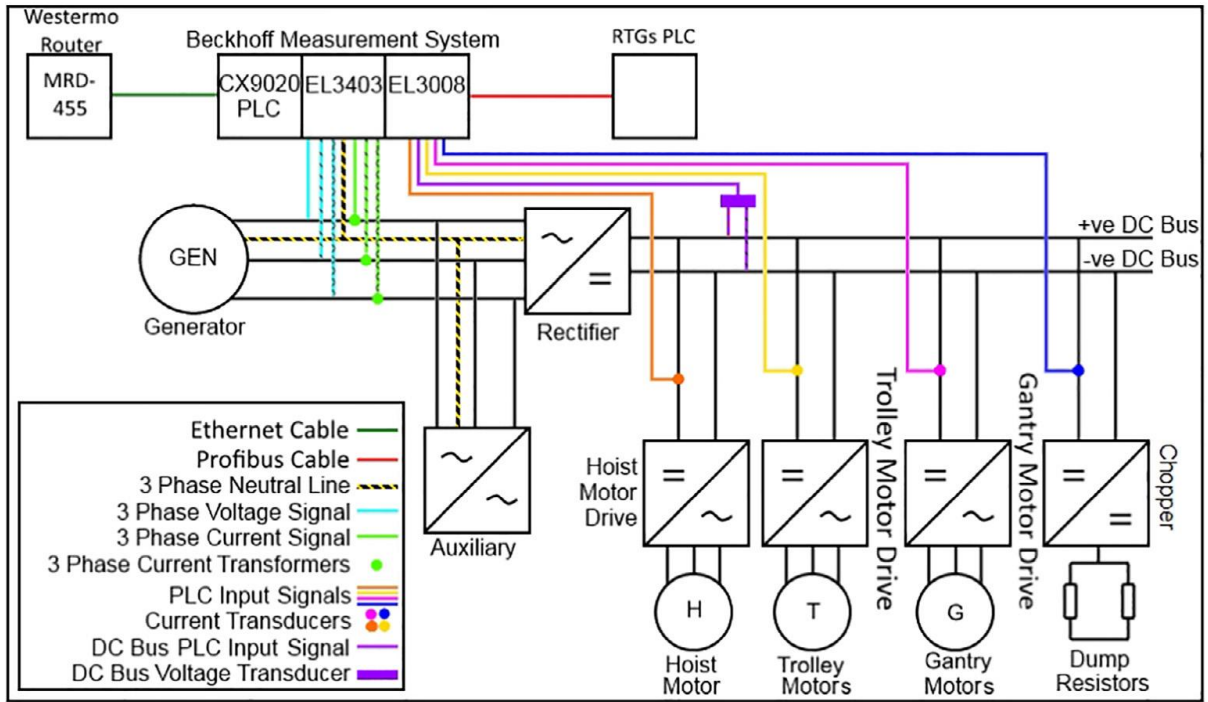


Figure A- 3:Line diagram of the RTG crane measurement system [157].

Appendix B

Model Predictive Control (MPC)

This appendix aims to give an introduction to Model Predictive Controller (MPC) as discussed and described in the literature [47] [153][154]. MPC, also known as receding horizon control, is an advanced and general control approach that involves repeatedly solving an optimisation problem while satisfying a set of constraints and operating conditions over a moving time horizon to determine the optimal control action. There are a several formulations and variations of the MPC algorithms have been developed in wide range of applications such as energy, robotics and food processing due to a number of advantages, summarised as follow:

- MPC can handle Multi Input Multi Output (MIMO) systems by taking into account all interactions between the system variables that effect the output variables.
- MPC controller has a preview capability as a predictive controller, which helps to improve the control performance compared to more conventional techniques.
- MPC can handle constraints, which help to operate the model safely within normal or real conditions. The ability to incorporate constraints can help to increase the output quantity or quality by safely running the model close to the constraints, which in many cases is often cost effective.

Figure B-1 shows the control loop of a common MPC controller. In this simple form of MPC, the reference input, $r(k)$, is the point that needs to be regulated, therefore the error at time k , $e(k)$, is defined as $e(k) = r(k) - y(k)$. In general, MPC consists of a plant model and optimiser. The MPC uses the plant model to predict the future plant output through solving an optimisation problem in order to generate an optimal control, $u(k)$, that make sure the plant output, $y(k)$, tracks the reference point $r(k)$. The model output at time k , $y(k)$, is estimated by $\hat{y}(k)$ by using the previous time data. Figure B-2 presents the basic concepts of the MPC, which tries to minimise the error between the reference point trajectory and predicted output data path by solving the optimisation problem under the model constraints at time step k over a predefined prediction horizon (p). Based on the applied control at the first step and new system measurements, the MPC controller will repeat the same procedure at $k+1$ under a receding

horizon. Furthermore, over the control horizon, m , the set of control actions leads to the predicted system output. In general, increasing the control horizon can improve the prediction output performance but at the cost of increasing complexity and computations.

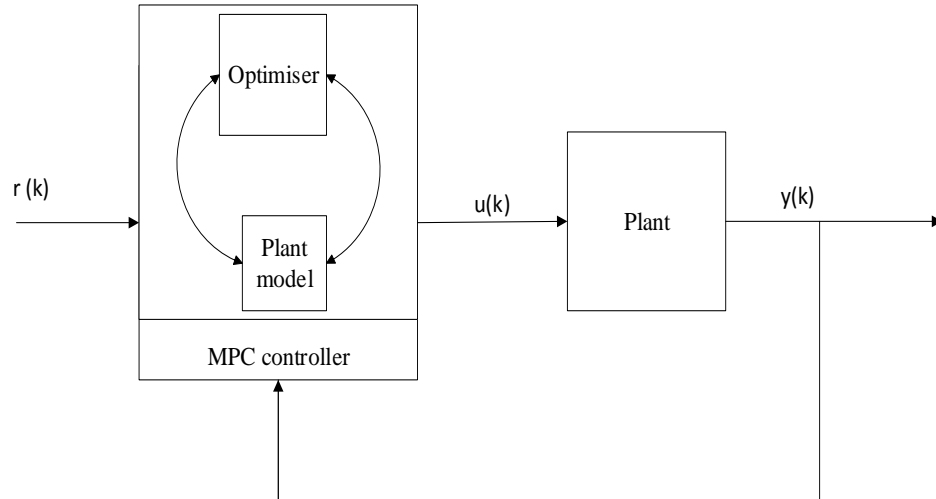


Figure B- 1:Simple control loop for MPC.

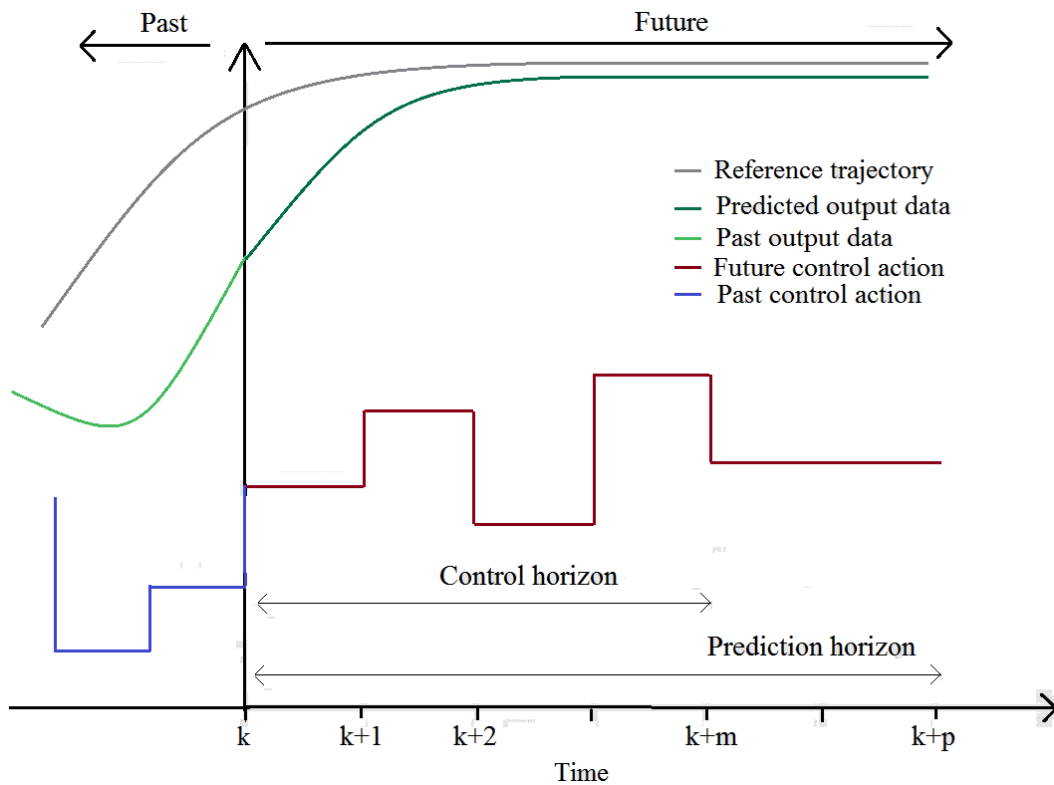


Figure B- 2:Basic concept schematic for the MPC controller.

From Figures B-1 and B-2, the MPC controller process can be summarised by the following steps:

- At each time step k , the output response of the plant is predicted over p time steps ahead. The prediction value, \hat{y} , is calculated dependent on the historical information and the planned control sequence over the next m steps ahead.
- The planned control moves, $\Delta\hat{u}$, are calculated from minimising a cost function. The quadratic cost function has been widely used in the literature, where it's easy to solve and has useful theoretical properties. Generally, the MPC controller is designed using a cost function that penalises deviation of a given reference point trajectory. However, nowadays the MPC is becoming more used as general receding horizon approach that aims to minimise the disturbance impact in the model through solving the optimisation problem and updating the model data at every time step based on future estimation. In this appendix, the basic and common MPC model is presented. The cost function incorporates the $\Delta\hat{u}$ and the error value which is the difference between the future reference trajectory and \hat{y} . The estimated output is $\hat{y}(k+p|k)$, where the double indices $(k+p|k)$ presents the prediction at time k for p time steps ahead. The MPC controller aims to find the $\Delta\hat{u}$ over the control horizon, m , where $\Delta\hat{u}(k|k) = \hat{u}(k|k) - u(k-1)$, where $u(k-1)$ is the previous control action. However, only the first planned control move is typically applied to the process, $u(k) = \hat{u}(k|k)$, where $u(k)$ is the actual control applied at time k .
- The prediction output is corrected at the next time step by using the current measured values and the new control moves. The above steps are repeated as receding horizon process, where the prediction horizon, p , stays the same length, sliding along by one-time step.

MPC controller: problem statement.

This section introduces a simple MPC algorithm based on a linear discrete time prediction model as discussed and described in the literature [33] [153][154]. A common and basic state space model is introduced by Equation (B-1) and is used to describe the MPC algorithm.

$$x(k+1) = Ax(k) + Bu(k) \quad (\text{B-1})$$

$$y(k) = Cx(k) + Du(k) + w(k) \quad (\text{B-2})$$

where $x(k) \in \mathbb{R}^{N_p}$ is the state vector at time k , $u(k) \in \mathbb{R}^{N_m}$ is the vector of control variables, $y(k) \in \mathbb{R}^{N_p}$ is the output, $w(k) \in \mathbb{R}^{N_w}$ is the disturbance vector and A, B, C, D are the matrices defining the state-space model. For more convenience, in this section, we will assume $D = 0$.

The discrete models are one step ahead models, where given a data at time k will help to determine data at $k+1$. The output of the next time step, $y(k+1)$:

$$y(k+1) = Cx(k+1) + w(k+1) \quad (\text{B-3})$$

By using $x(k+1) = Ax(k) + Bu(k)$ assuming there no changes in disturbance term, $w(k+1) = w(k)$, the $y(k+1)$ can be written:

$$y(k+1) = CAx(k) + CBu(k) + w(k) \quad (\text{B-4})$$

This process will be used recursively to find a p -step ahead prediction. The state space prediction can be written:

$$\begin{aligned} x(k+p|k) = & A^p x(k) + A^{p-1} B u(k|k) + A^{p-2} B u(k+1|k) + \dots \\ & \dots + A B u(k+p-2|k) + B u(k+p-1|k) \end{aligned} \quad (\text{B-5})$$

where $x(k+p|k)$ is the p step ahead prediction for x at time k , $x(k)$ is a state value and all u terms are decision variables that need to be determined. Similarly, the output y can be described as follow:

$$y(k+p|k) = Cx(k+p|k) + w(k) \quad (\text{B-6})$$

$$\begin{aligned} y(k+p|k) = & CA^p x(k) + C(A^{p-1} B u(k|k) + A^{p-2} B u(k+1|k) + \dots \\ & \dots + A B u(k+p-2|k) + B u(k+p-1|k)) + w(k) \end{aligned} \quad (\text{B-7})$$

In Equation (B-7), the terms $CA^p x(k)$ and $w(k)$ are known based on current or past measurement data and the rest of the equation need to be determined based on the future input choices. The MPC controller aims to determine the unknown inputs by solving an optimisation function to make sure that the overall prediction is satisfactory. The quadratic performance indices are widely used in the literature and the most common indices within energy and smart grid applications, where it has a unique minimum, penalises the larger deviation heavily compared to smaller deviation, smooth and robust control. The cost function J in Equation (B-

8) aims to present a simple form of performance indices for manipulated outputs and it penalises two parts. Firstly, the cost function penalises the error vector between the output and reference point trajectory, $e(k) = r(k) - y(k)$, at each step across the prediction horizon. The second part of Equation (B-8), $\Delta u^2(k)$, aims to penalise the deviations of the manipulated vector. Equation (B-8), Z and H are used as weighting vectors in order to allow J to penalise the previous two parts at certain levels.

$$J = \sum_{i=1}^p Z e^2(k+i) + \sum_{i=0}^{p-1} H \Delta u^2(k+i). \quad (\text{B-8})$$

Finally, the MPC controller aims to find the control policy based on Equation (B-8) to minimise the distance between the predicted value and reference trajectory, which usually is the perfect model, and the rate change of the manipulated value. These steps are repeated at every step $k + 1$ by using the updated data and the final chosen control policy can be specified as: $\hat{\pi}(k) = (\Delta \hat{u}(k), \Delta \hat{u}(k+1), \dots, \Delta \hat{u}(m))^T$.

Appendix C

Dynamic programming

Appendix C introduces and discusses the basic concept of Dynamic programming (DP) as described in the literature [55] [133] [155]. DP is a numerical algorithm based on an optimality principle was developed by Richard Bellman in the 1950s and is often called “Bellman’s principle of optimality. The DP method transforms complex optimisation problems into a sequence of several smaller problems that are easier to solve. Once all the subproblems have been solved, the overall problem can be optimised. The DP approach has been widely used and applied in industrial applications such as energy and smart grid due to the number of advantages, summarised as follows:

- The DP framework can be employed to solve different type of problems and is easily generalised to many applications.
- DP is a powerful approach for finding the global optimum solution, due to its exhaustive search process.
- DP has the ability to include and handle constraints for both state and control variables within the cost function. This ability can help to increase the output quantity or quality by safely running the model close to the constraints, which is often cost effective.

Generally, the DP technique is efficient in solving complicated constrained optimization problems, not influenced by the nature of the problem and guaranteed to find the global optimum solution for a discrete grid if given sufficient time. In dynamic programming, the control process starts by dividing the complicated optimisation problem into a series of subproblems or multi stages that will be sequentially solved one stage at a time. This process will be used recursively to find a global optimal solution in the state space by solving each subproblem as an ordinary optimisation problem, which will help to define the characteristics of the next subproblem in the sequence. In DP, the exhaustive search increases computational costs and requires a lot of memory space to store all subproblem solutions until finding the final solution. The computational costs and memory increases exponentially with the problem

dimension. However, in order to avoid this problem, DP is adapted in this thesis to solve optimisation problems with few variables.

Implementing DP.

The DP approach is described by two main components: the states and the decisions. The states provide the information required to assess the consequences of the current decision upon future actions. The decisions are actions that change the states from the current state to another through a predefined process. These state movements in the discrete time format are governed by state-transition equation which can be written as:

$$x_{k+1} = f(x_k, \Delta u_k), \quad (C-1)$$

where $F(\cdot)$ is a transition function, x_k is the state variable and Δu_k is the control action at step k . Generally, the DP aims to find the optimal control or decisions sequence for the optimisation problem, given by Equation (C-2) which consists of an objective function, with system model constraints.

$$J = \sum_{k=1}^N Q(x_k, \Delta u_k), \quad (C-2)$$

subject to model constraints, for example:

$$\left. \begin{array}{l} x^{\min} \leq x_k \leq x^{\max} \\ \Delta u^{\min} \leq \Delta u_k \leq \Delta u^{\max} \end{array} \right\} \quad \forall k. \quad (C-3)$$

$$(C-4)$$

where N is the total number of steps and Q is the cost function. The DP works to determine the optimal control sequences to minimise or maximise the cost function. In dynamic programming, the whole control process is divided into a series of optimisation problems and backwards calculations are used to allow DP to achieve the minimum or maximum value of the cost function by controlling policies at all discrete points. Thus the accumulated cost, $J_k^*(x_k)$, at state x_k can be described by firstly the cost $Q(x_k, \Delta u_k)$ occurring due to apply action u_k and secondly the remaining cost J_{k+1} which consider all outcomes in the subsequent steps $k+1, k+2, \dots, N$. The subproblems for all steps from N to $k=1$ can be described as follow for a representative example:

-
- End calculation for the subproblem at step N:

$$J_N^*(x_N) = \min_{\Delta u} \{Q(x_N, \Delta u_N)\} \quad (C-5)$$

- Intermediate calculation for k step, where $1 \leq k < N$, is:

$$J_k^*(x_k) = \min_{\Delta u} \{Q(x_k, \Delta u_k) + J_{k+1}^*(x_{k+1})\} \quad (C-6)$$

where $J_k^*(x_k)$ is the optimal cost function at state energy variable x_k at step k and x_{k+1} is the state variable at step, k+1, when the control action, Δu_k , is applied to state variable x_k , at step k based on Equation (C-1). Then the optimal control at every step are obtained and the final chosen control policy is specified as: $\pi_k^* = (\Delta u_k^*, \Delta u_{k+1}^*, \dots, \Delta u_N^*)^T$.

Appendix D

SMPC and the computational effort

The results of the SMPC controller from Chapter 6 must be considered in relation to the computational effort of the controller. This will illustrate the ability to apply the model in practice in order to determine the control model parameters. Furthermore, the computational cost (total duration) of the model simulation can be significant when the model is designed for a daily optimisation cycle and the control process needs to be completed at every time step. The total computational cost of the SMPC depends on the number of forecast scenarios as presented in Table D-1. In daily optimisation with half hourly time step updating, each computational step for the model need to be finished in approximately less than 30 sec, which for 48-time step will sum up to 25 minutes, Equation D-1 [51].

$$t_{\text{tot}} = N t_s + t_d, \quad (\text{D-1})$$

where t_{tot} is the total duration of time for the simulation, t_s is the time for each step, N the number of the time steps during the day ($N=48$) and t_d is the time duration for data cycling ($t_d = 2$ minutes). The SMPC model with 5 and 10 demand future scenarios is finished within the required time duration frame (≤ 25 minutes). The average of the total time duration is 10.8 and 18.8 minutes for the SMPC model with 5 and 10 demand future scenarios options, respectively. There are a few simulations that exceed the time limit (30 sec) for the 10 demand future scenarios case with maximum time (33 sec). However, the sum up of time for this case was 28.4 minutes which is still within the half hour time. The SMPC with the option of 15 demand future scenarios exceed the total duration limit and requires on average 30.8 minutes. Therefore, the number of demand future scenarios chosen was 10 for the SMPC in Chapter 6, where the model simulated within the time frame and included the highest possible number of future demand scenarios. The model was run on PC Windows 8.1 with Intel(R) i5-4590 @ 3.3GHz processor with 8 GB RAM. However, the faster computer will reduce the computational time and improve the practicality of implementing the model.

Table D- 1: The computational effort for SMPC.

| Number of forecast demand scenarios | Average simulation duration (sec) | Maximum simulation duration (sec) |
|------------------------------------------------|----------------------------------------------|----------------------------------------------|
| 5 | 11 | 25 |
| 10 | 21 | 33 |
| 15 | 36 | 49 |